UNIVERSITY OF Southampton

University of Southampton Research Repository
ePrints Soton

Copyright © and Moral Rights for this thesis are retained by the author and/or other copyright owners. A copy can be downloaded for personal non-commercial research or study, without prior permission or charge. This thesis cannot be reproduced or quoted extensively from without first obtaining permission in writing from the copyright holder/s. The content must not be changed in any way or sold commercially in any format or medium without the formal permission of the copyright holders.

When referring to this work, full bibliographic details including the author, title, awarding institution and date of the thesis must be given e.g.

AUTHOR (year of submission) "Full thesis title", University of Southampton, name of the University School or Department, PhD Thesis, pagination

http://eprints.soton.ac.uk

UNIVERSITY OF SOUTHAMPTON

FACULTY OF MEDICINE

School of Medicine

Role of microRNA-155 in dendritic cells and macrophages

MiR-155 directly targets PU.1 and IL13Rα1

by

Rocio Teresa Martinez-Nunez

Thesis for the degree of Doctor of Philosophy

October 2010

UNIVERSITY OF SOUTHAMPTON

ABSTRACT

FACULTY OF MEDICINE

SCHOOL OF MEDICINE

Doctor of Philosophy

ROLE OF MICRORNA-155 IN DENDRITIC CELLS AND MACROPHAGES

by Rocio Teresa Martinez-Nunez

In search of genes differentially expressed between M1 (pro-Th_1 or pro-inflammatory) and M2 (pro-Th_2 or pro-tolerogenic) macrophages, BIC (microRNA 155 hosting gene) was found up regulated under inflammatory conditions. MicroRNAs are non coding RNAs of ~22nt in length that inhibit gene expression upon pairing to the 3'UTR (UnTranslated Region) of target mRNAs. *In silico* analysis predicted two pro-Th_2 targets for miR-155: PU.1 and IL13Rα1. PU.1 is a transcription factor essential in myelopoiesis and dendritic cells (DCs) that favours a Th_2 profiling; moreover, PU.1 had been shown to regulate the transcription of DC-SIGN (Dendritic Cell- Specific ICAM-3-Grabbing Non-integrin 1) which is a pathogen receptor expressed in DCs controlled by Th_2 stimuli. IL13Rα1 is the chain receptor for the Th_2 cytokine IL-13, which promotes M2 differentiation. Pro-Th_1 stimuli cause maturation of DCs, cells that orchestrate the immune response between Th_1 and Th_2 profiles; moreover, Th_1 stimuli cause classical (M1) macrophages activation versus an alternative (M2) one. My hypothesis was that miR-155 contributes to the pro-Th_1 profile by down regulating pro-Th_2 factors. MiR-155 was found up regulated during DC maturation and both PU.1 and IL13Rα1 were demonstrated as direct targets of miR-155. Employing a developed monocytic cell line which harbors a miR-155 transgene under the control of a Tet-On system (THP1-155 cells), both PU.1 and IL13Rα1 were shown to be down regulated following miR-155 induction in these cells. Moreover, THP1-155 cells showed that DC-SIGN transcription is regulated by miR-155 levels through PU.1 targeting, and that IL-13 signalling cascade through STAT6 transcription factor was down regulated when miR-155 was over expressed. Using Anti-miR-155 transfections in DCs, miR-155 was shown to modulate not only DC-SIGN expression, but also DC pathogen binding ability. Using the same technique in macrophages, miR-155 was shown to modulate IL13Rα1 and STAT6 activation, and to regulate the expression of IL-13/STAT6 dependent genes. Therefore, miR-155 contributes to the pro-Th_1 profile by down regulating pro-Th_2 factors, acting as a pro-Th_1/anti-Th_2 modulator in myeloid cells under inflammatory conditions.

Table of contents

List of figures

List of tables

Acknowledgments

I guess I am thinking what everyone else does at this point: finally, here it is. It would not have been possible without support and helpful criticism which involved many laughs and sometimes, tears. But it is done.

I would like to thank my friend Tilman. Thank you so much. I do not know even where to start. Thank you for giving me the opportunity to feel science; for sharing thoughts, for believing in me, for teaching me, for helping me all this way, a way that involved changing country... Both Madrid and Southampton have been two great lessons. Thank you. You were right (as usual): you do not have to be ruthless to compete and to be one of the best in science. You have to resist and you have to fight back. And you give the best example of those. That watch that stopped will start again now. And who knows where or when it might fall again… It feels like an honor to work and share science with you. But above all, the honor is being your friend. You are part of my family. Thank you.

Thank you to my family. Thank you for understanding me and for being always there. For so many talks that made distance be nothing. Mosqueteros, you know I fell for science… and here it is the beginning.

Thank you, Laura. I think destiny made a decision some time ago, something like 7 years ago? And I am just so happy he did so. Science chipped in 4 years ago in Milano. Thank you for being always in here and there. For being so brave, caring and helping me so much. Claudia, thanks for your friendship and for beign so determined, teaching us the best lesson: if you really want something, you go for it.

Cosmica, you earned your feathers! Thank you for taking care of me… It is a pleasure to discuss science and life with you. I feel deeply grateful and honored. You and Tom deserve the best. Like someone said “we will fight back”. And we will win.

David, thank you so much. For everything. Everything. So many conversations, coffees with chocolate, laughs, advices, sharing thoughts and honesty. And thesis revision… even with the hangman, thank you very much for all your help. For your time.

You have been always there, in the shadow, helping and guiding, supporting and being a friend. Most of all, thanks for your friendship. I will always remember all this. Thank you so much.

And thanks to my true colleagues in Level E! I think we make a good team. It is a pleasure to share the lab with you and to be surrounded by good people that want to help and make good science. Please keep being a team. Jane, thank you for your support and guidance, it is a pleasure and honor to discuss things with you. Thank you very much.

Special thanks to my group, JunkRNA Team. Thanks Victor for sharing the path. Thank you Mirella… lab is just fun! I am so grateful we kidnapped you. And that I can bother you with whatever doubts expecting (and getting) a great answer. Fethi, thank you so much for teaching me lots, thank you for considering my opinions, thank you for contributing to this work (I even enjoy flow cytometry thanks to you) and thank you for helping me always. You make a great contribution in the lab. And this thesis would not have been possible without you.

Thank you also to Prof. Hywel Morgan and his group: Dr. Sam Birtwell and Dr.Marta Lombardini were extremely helpful for building the microfluidic device. It would not have been possible without them. Thanks. Marta, you contributed to more than enjoying experiments. Thank you for being the way you are, thank you for our teas, for sharing thoughts, worries, laughs, and for being a true friend.

Thanks to my friends in Spain. This is the reason why I am away, but as many times we have said, true friendship follows us wherever we are. Thank you for teaching me that, and thank you for understanding me.

Dad and David, you three are and will be always with me. You are in this thesis. Mum is also here. This is for you all.

To those who chase their dreams and not fear living them

To TheFour Mosqueteros

Abbreviations

3'UTR: 3' UnTranslated Region

AAMϕ: Alternatively Activated Macrophage

CAMϕ: Clasically Activated Macrophage

CD: Cluster of Differentiation

cDC: Conventional dendritic cell

cDNA: Copy DNA

C/EBP β: Ccaat Enhancer Binding Protein beta

DC: Dendritic cell

DC-SIGN: Dendritic Cell -Specific Intercellular adhesion molecule-3-Grabbing Non-integrin 1

γIFN: gamma interferon

G-CSF: Granulocyte Colony Stimulating Factor

GM-CSF: Granulocyte-Macrophage Colony Stimulating Factor

IL-1, 4, IL-5, IL-10, IL-13: Interleukins 1 4, 5, 10,13 respectively

IL13RA1: Interleukin 13 Receptor alpha 1 (mRNA or gene)

IL13Rα1: Interleukin 13 Receptor alpha 1 (protein)

IL-4: Interleukin 4

LPS: bacterial LipoPolySacharide

miR: MicroRNA

miRNA: MicroRNA

moDC: Monocyte derived dendritic cell

mRNA: messenger RNA

Mϕ: Macrophage

NF-κB: Nuclear Factor Kappa B

PAMP: Pathogen-Associated Molecular Pattern

PCR: Polymerase Chain Reaction

pDC: plasmacytoid dendritic cell

piRNA: Piwi-interacting RNA

PKC: Protein Kinase C

PRR: Pattern Recognition Receptors

P-STAT6: Phosphorylated Signal Transducer and Activator of Transcription 6

PU.1: transcription factor encoded in SPI1 gene

qPCR: Quantitative (or Real Time) PCR

RT : Reverse Transcription

RT-qPCR: Reverse Transcription and Quantitative Polymerase Chain Reaction

siRNA: Small-interference RNA

STAT6: Signal Transducer and Activator of Transcription 6

TLR: Toll Like Receptor

TNF-α: Tumor Necrosis Factor alpha

1 Chapter 1: Introduction

1.1 The immune system

1.1.1 Overview

The immune system is the host's system in charge of defence and self balance. Its task is to keep the organism in a healthy state and fight against foreign (pathogens) and self destructive (cancer cells) components. Defence mechanisms are present in primitive organisms such as bacteria (in the form of enzymes); they have also evolved into networks of different tissues and cell types in more complex organisms. Its phylogeny extents from plants, nematodes, invertebrates and mammals; all share some conserved genes along the phylogeny (for example NFκB or some pathogen receptor encoding genes) (Murphy et al., 2008). Thus, studying the immune system and its regulation is essential to understanding health and disease and how an organism can interact with its surroundings.

The immune system in mammals has several components such as skin, mucosae, blood and lymphatic system; it also includes different cell types distributed in different tissues such as microglia in the nervous system or Kupfer cells in the liver. Classically, immunity has been divided into two main types of response: innate and adaptive. The innate response is the first and immediate response against pathogens; it is nonspecific and does not lead to long lasting immunity. Nevertheless, it is essential as a first barrier and often sufficient to overcome infection. Examples of cells in charge of this response are macrophages or neutrophils. Adaptive immunity has a specific repertoire of cells (mainly lymphocytic) and antibodies against the pathogens encountered. Thus, it is pathogen-specific and in many cases results in the so called "immunological memory", which gives lifelong protection against reinfection with the same pathogen (Kindt et al., 2007; Murphy et al., 2008). Adaptive immune responses depend on the pathogen encountered and the microenvironment resulting from the interaction between innate cells (first barrier) and the given infectious agent.

All these cell types and structures need to be in continuous activation and deactivation to exert an effective and balanced response. Thus, immunity is accomplished by a system that requires fine equilibrium, in which inflammation and resolution may be seen as two plates in the scales of homeostasis.

A simplified representation of the immune response against a given pathogen is shown in Figure 1. Upon pathogen encounter and pathocytosis, dendritic cells (DCs) and macrophages (Mϕs) process the foreign structures and migrate to the lymphoid organs; there they will present the antigens (structures recognized and responded by the adaptive system) to the effector cells- lymphocytes (T and B cells). After encountering an antigen, B cells proliferate and differentiate into plasma cells, specialized in the production of antibodies. T cells that are activated by antigen presenting cells (APCs) (DCs, Mϕs and B cells) proliferate and differentiate into one of several types of effector T cells (cytotoxic, helper o regulatory cells). T helper cells, or Th cells, activate and modulate other immune cells classically driving the immune respone into either Th_1 or Th_2 responses. In addition to these populations, other T cells known to date include Th_{17}, Th_9, regulatory T cells (T_{regs}) and follicular T cells (T_f) (Dardalhon et al., 2008; Harrington et al., 2005; Veldhoen et al., 2008; Wan, 2010). T helper cell phenotypes have been show to be plastic and different populations of Th cells seem to influence each other (Peck and Mellins, 2010; Wan, 2010). Th_{17} cells, induced by interleukin 23 (IL-23) and characterized by the production of interleukin 17 (IL-17), have been mainly related to inflammatory autoimmune disease and extracellular pathogens (Langrish et al., 2005; Lombardi et al., 2009). T_{regs} are T cells that develop either in the thymus (naturally occurring T_{regs} or nT_{regs}) or induced (iT_{reg}) by TGF-β from naïve T cells following TCR stimulation, and are involved in immune suppression and homeostasis (Wan, 2010). Th_9 cells have only been recently described, as a subset of T cells related to Th_2 that express high amounts of IL-9, mainly involved in allergy (Soroosh and Doherty, 2009). DCs induce the differentiation of naïve T cells into these subsets by secreting different cytokines upon selected TLR stimulation. IL-12 induces Th_1 diffferentiation (Trinchieri, 2003), IL-4 promotes Th_2 cells activation, IL-10 and/or TGF-β induce T_{reg} development, IL-1β, IL-6, IL-23 and/or TGF-β induce the differentiation of Th_{17} cells, whilst IL-4 and TGF-β promote Th_9 differentiation (Acosta-Rodriguez et al., 2007; Dardalhon et al., 2008; Lombardi et al., 2009). DCs therefore elicit

one or other type of T cell response following pathogen sensing by secreting different pools of cytokines that will determine the microenvironment for T cell differentiation.

Th_1/Th_2 responses are a better known model involving an active role for dendritic cells and macrophages (Murphy et al., 2008). Indeed, macrophages show a spectrum of activation that relates to these two types of responses (Gordon and Taylor, 2005; Mantovani et al., 2004; Mosser and Edwards, 2008; Stout and Suttles, 2004) so the immune response will be simplified to this Th_1/Th_2 model hence forth.

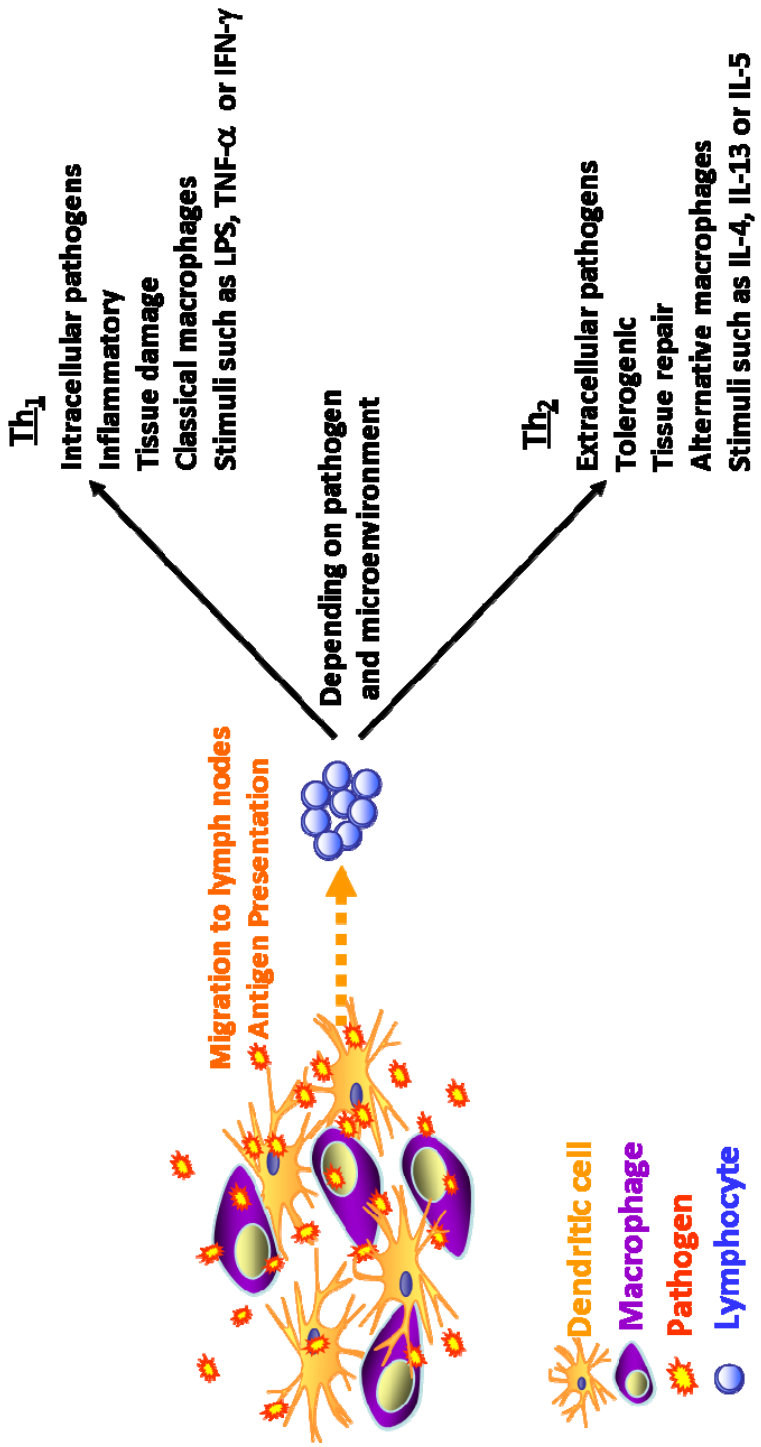

Figure 1 Overview of the immune response. Dendritic cells and macrophages sample peripheral tissues; upon binding of pathogens, dendritic cells migrate to the lymph nodes where they will present antigens to the lymphocytes. These lymphocytes will then proliferate and activate into two main types, Th_1 and Th_2, depending on the pathogen encountered (intra or extracellular) and microenvironment (e.g. TNF-α or IL-4) around them. Initials: IFN-γ: interferon-gamma; LPS: bacterial LipoPolysacharide; TNF-α: Tumor Necrosis Factor alpha: IL-4, IL-13, IL-5: Interleukins 4, 13 and 5 respectively.

1.1.2 Dendritic cells

Paul Langerhans first visualized dendritic cells in skin (Langerhans Cells) in the nineteenth century (Langerhans, 1868). However, it was not until 1973 that Ralph M. Steinman and Zanvil A.Cohn coined the term “dendritic cells” for the description of a new type of cell. They were identified in murine peripheral lymphoid organs and showed distinctive morphological features such as cytoplasmic processes-dendrites, which gave them their name (Steinman and Cohn, 1973).

Dendritic cells are antigen-presenting-cells that arise from either myeloid or lymphoid precursors (Doulatov et al., 2010; Geissmann et al., 2010). They are classified into different subsets depending on their original localization, falling into two main categories: conventional DCs (cDCs) and plasmacytoid DCs (pDCs). cDCs can be divided into different subcategories depending on their origin, localization and surface marker expression. Many of them reside in the skin, for instance, Langerhans cells. During inflammatory processes monocytes can migrate into the dermal layer and give rise to DCs (monocyte-derived DCs or moDCs). Both Langerhans cells and moDCs are referred as “immature” DCs and their main ability is capturing pathogens, displaying a low T cell stimulatory capability. pDCs are the major source of IFN production; they circulate in the blood and migrate to lymphoid organs following stimulation. However, chronic inflammation has been shown to induce recruitment of pDCs to non-lymphoid tissues (Buckwalter and Albert, 2009a) suggesting the importance of their balanced activation. Both pDC and cDC populations complement each other for pathogen sensing as shown by the expression of different TLR (Toll Like Receptor) repertoires. cDCs in the blood express all TLRs except for TLR9, and pDCs express TLR1, 6, 7, 9 and 10 (Buckwalter and Albert, 2009b). Studies in mice have shown that PU.1 dose is important for the development of DCs, and that its expression differs between cDCs and pDC populations. It is highly expressed by cDCs and low in pDCs (Back et al., 2005; Nutt et al., 2005). Recent studies in mice have broadened the picture of DC populations and suggest that peripheral tissues are populated by distinct types of DCs: lymphoid tissue SIRPα^- CD8$^+$ DCs and the related SIRPα^- CD103$^+$ DCs in nonlymphoid tissues; and SIRPα^+ CD8$^-$ DCs in lymphoid tissue together with nonlymphoid tissue SIRPα^+ CD103$^-$DCs. Thus, the DC

picture is a much more complex network than previously thought, and it is yet to be revealed how/if all this populations relate to those found in humans.

Despite these different types of cells are present throughout the organism, they all share common features such as morphology (with the typical dendrites), high expression of MHC (Major Histocompatibility Complex) I and II, intermediate-high expression of costimulatory molecules, motility, and the hallmark of the DC family: maturation.

Maturation is the process by which DCs undergo a switch from immature tissue samplers and residents (iDCs) into mature immunostimulators for the T cells they will activate (Kindt et al., 2007). Immature DCs have been described as "sentinels" in peripheral tissues that sample their surroundings capturing the antigens that will be presented to T cells by mature DCs in lymphoid organs. Antigens in direct contact with T cells are ignored because they are not processed by DCs and presented together with co-stimulatory signals; those that are captured and presented by APCs stimulate T cells due to these secondary signals from APCs which are required to activate T cells and causes them to proliferate (Murphy et al., 2008). Therefore, DCs are the interface between foreign and tissue antigens and T cells, playing a key role in cell-mediated (adaptive) immunity (Lanzavecchia and Sallusto, 2001).

Figure 2 shows a representation of the principal features of DC maturation. Immature DCs in peripheral tissues are characterized by the presence of low levels of Major Histocompatibility Complex class II (MHC-II) molecules that recycle constantly, highly endocytic activity and low levels of co-stimulatory molecules such as Cluster of Differentiation 83 and 86 (CD83 and CD86) (Banchereau and Steinman, 1998; Wallet et al., 2005). This phenotype allows them to function as searchers and sensors.

Upon antigen recognition, DCs mature and change their phenotype; they stop the uptake of antigens and migrate to T cell compartments, where they exert their antigen-presenting function. Maturing DCs undergo through a series of changes that include the loss of endocytic activity, up regulation and redistribution of co-stimulatory molecules (Cella et al., 1997) while migrating towards the lymphoid organs. Antigens are loaded into MHC molecules and presented together with co-stimulatory molecules to T cells in

the “immunological synapse”; in this synapse TCRs (T Cell Receptors), MHC and co-stimulatory molecules congregate in a ring area surrounded by adhesion molecules such as LFA-1 and its main counter receptor ICAM-1 (Bromley et al., 2001; Lanzavecchia and Sallusto, 2001). The formation of the immunological synapse is key in order to activate naïve T cells, and it has been hypothesised that the duration of the immune synapse plays a key role in polarising T cells towards a Th_1 or Th_2 response, that it also dependent on the cytokine milieu (Lanzavecchia and Sallusto, 2001; Wallet et al., 2005). T cells will differentiate into different subsets (Th_1, Th_2 and others) depending on the pathogens captured by DCs and the microenvironment. Th_1 cells release interferon-gamma (IFN-γ) stimulating macrophages to fight intracellular microbes; they promote an inflammatory response and relate to the innate branch of immunity. Th_2 cells secrete interleukins-4, 5 and 13 (IL-4, IL-5 and IL-13, respectively), inducing responses against extracellular pathogens; they are more related to fibrosis, angiogenesis and humoral (antibody production) responses. Correct sensing of pathogens is therefore key in regulating an appropriate immune response that will result in the clearance of pathogens and resolution of inflammation, restoring the balance of the immune system after damage (Geijtenbeek and Gringhuis, 2009).

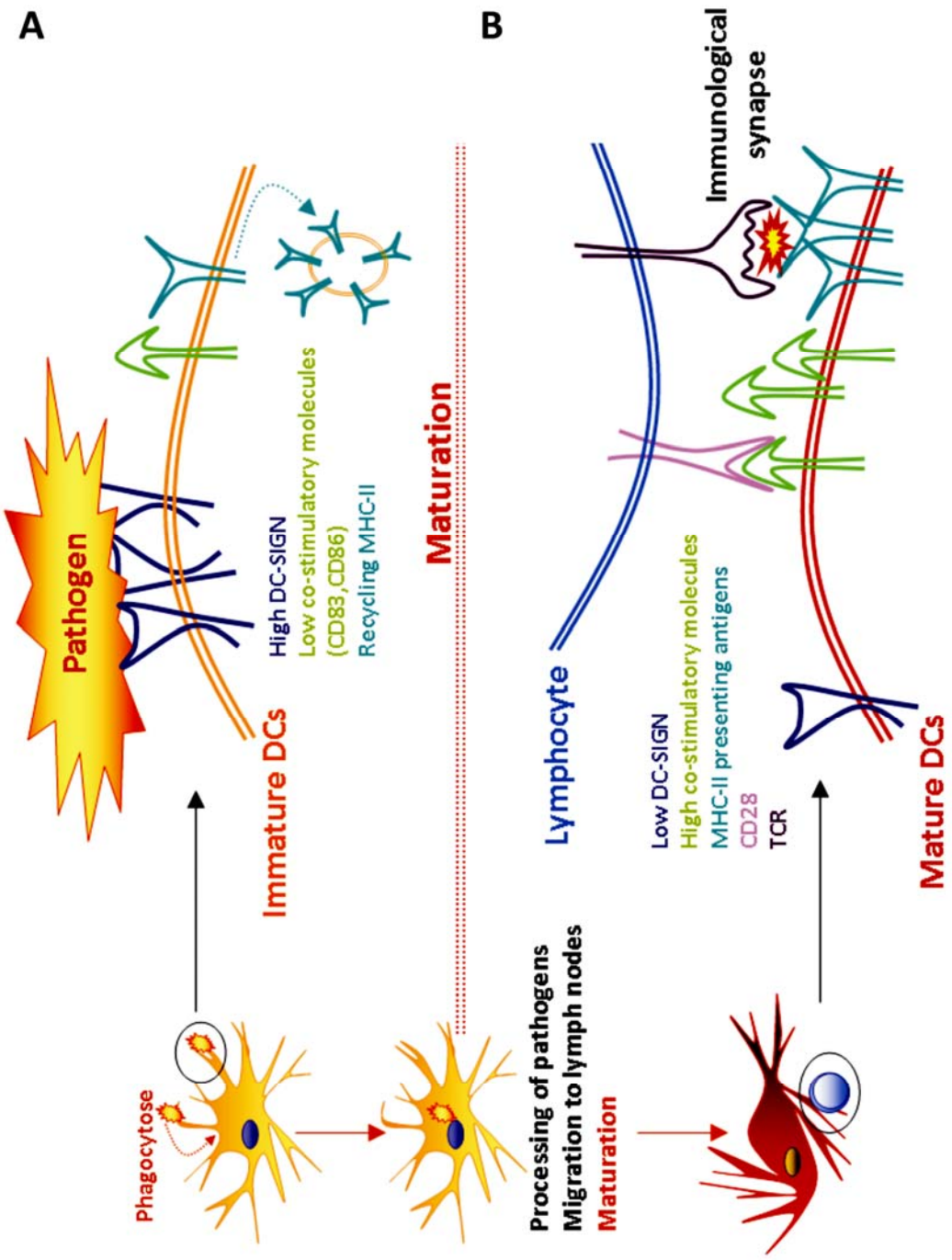

Figure 2. Dendritic cell maturation. *A*: immature DCs (membrane respresented by double orange line) are characterized by high phagocytic ability and display high pathogen receptors like DC-SIGN, low co-stimulatory molecules (e.g. CD86), recycling MHC-II and TLRs. Maturation: upon antigen capture (phagocytosis), DCs migrate towards lymphoid organs while processing of pathogens, becoming mature DCs. *B*: In lymphoid organs, mature DCs (membrane represented by double red line) present the antigens inside MHC molecules to lymphocytes while stimulating them in the immunological synapse. Lymphocytes (blue double line) will sense pathogens via TCRs and get activated through binding of co-stimulatory molecules (e.g. CD28 binds to CD86). Initials: DC-SIGN (Dendritic Cell Specific Intercellular adhesion molecule-3 Grabbing Non-integrin), TLR (Toll-Like Receptor).

DCs may also be mediators in tolerance: immature DCs may capture antigens from dying cells and mature, migrating to lymphoid tissues and presenting these antigens to self-reactive T cells, inducing self-tolerance. It has been suggested that these "tolerogenic DCs" present self-antigens to T cells but do not express inflammatory mediators, therefore inducing tolerance rather than inflammation. In the case of CD4 T cells this may result in the generation of T_{regs} whilst in the case of cytotoxic CD8 T cells the absence of co-stimulatory signals may be the cause of self-tolerance induction (Buckwalter and Albert, 2009a).

Therefore, by directing the immune system towards either inflammation or tolerance, dendritic cells orchestrate an efficient and appropriate immune response leading to pathogen clearance. Unbalanced responses underlie pathologies such as allergies, auto-immune disesases or exacerbated-inflammatory diseases (e.g. asthma, colitis, psoriasis). Thus, regulation of DCs towards a balanced immune response (Th_1,/Th_2) is central in the control of the immune system and key in health and disease.

1.1.3 Macrophages

Macrophages were first recognized and described by Elie Metchnikoff in 1905. He observed that phagocytic mononuclear cells from animals resistant to certain bacterial infections were more skilled at killing those and other pathogens, initiating the concept of "macrophage activation" (Gordon and Martinez, 2010; Metchnikoff, 1905).

Mϕs arise from circulating monocytes following recruitment to different tissues due to inflammation or they act as homeostatic regulators in the steady state. (Mosser and Edwards, 2008). In the tissues they acquire different profiles depending on the microenvironment. Macrophages provide a defence barrier serving as potent phagocytes in the innate response and also as antigen presenting cells in the adaptive branch of the immune system. Thus, like DCs, they act at the interface between innate and adaptive immunity (Murphy et al., 2008) being key cells in the communication between external stimuli and immune responses.

Macrophages are usually classified into two main types represented in Figure 3: M1 (classically activated) and M2 (alternatively activated) macrophages (Martinez et al., 2009) analogous with T-cell terminology. M1 macrophages show a more inflammatory profile; they are specialized in the defence against intracellular pathogens and promote inflammation and tissue damage upon stimulation with pro-inflammatory stimuli such as IFN-γ or bacterial LipoPolySacharide (LPS) (Martinez et al., 2009; Mosser and Edwards, 2008). In contrast, alternatively activated macrophages (M2 or pro-Th_2 following T cell terminology) are induced by a broader range of stimuli such as glucocorticoids or IL-10 although the most frequently described M2 type are Mϕs generated in the presence of interleukin 4 (IL-4) or interleukin 13 IL-13 (Martinez et al., 2009). M2 macrophages are specialized in the defence against extracellular pathogens (e.g. helminthes, nematodes or protozoa); they promote tissue repair and inflammation resolution enhancing tissue remodelling and fibrosis (Borowski et al., 2008; Munitz et al., 2008). Moreover, M2 Mϕs exert their effects mainly by promoting a humoral response from B cells (Martinez et al., 2009). Although some studies have raised doubts about their ability as effector cells in immune defence (Mosser and Edwards, 2008), it has been shown that alternatively

activated macrophages are necessary in the host defence against parasites and helminthes (Anthony et al., 2006; Zhao et al., 2008).

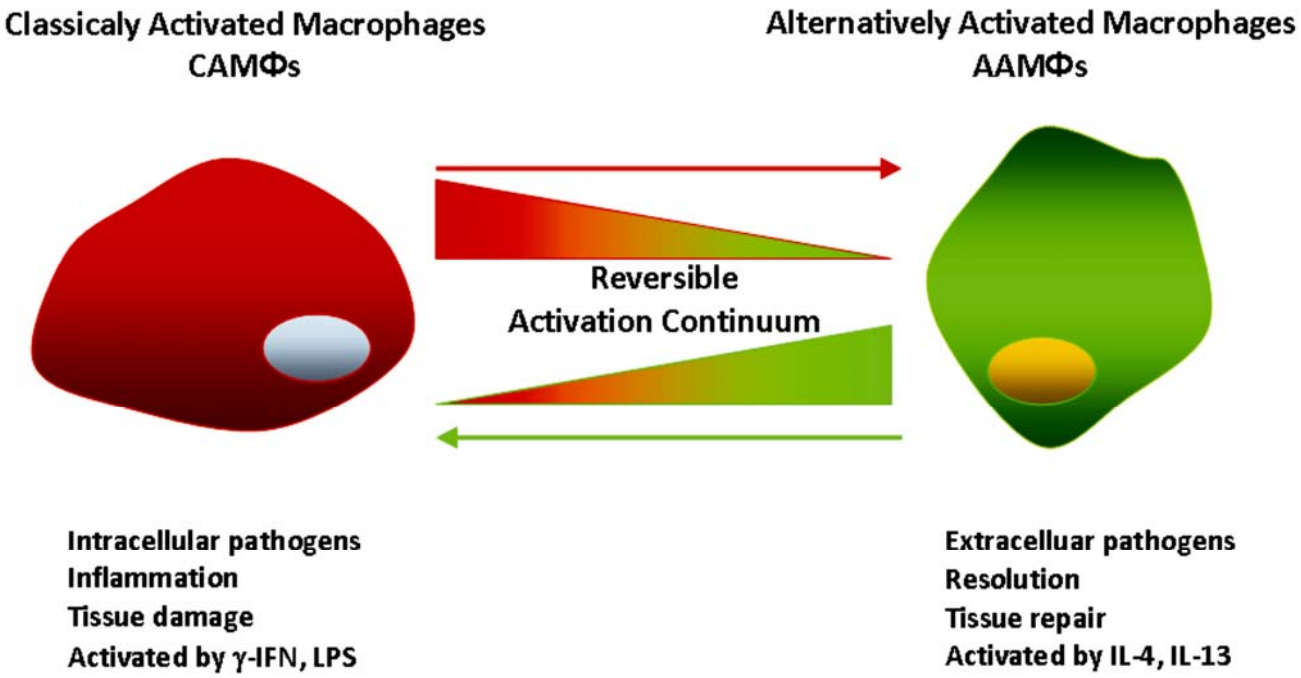

Figure 3 Schematic representation of macrophage activation. Macrophages show two main activation types: Classicaly Activated Macrophages (CAMϕs in red) and Alternatively Activated Macrophages (AAMϕs in green). CAMϕs are driven by γ-IFN or LPS and specialized in the defence against intracellular pathogens, causing inflammation with tissue damage. AAMϕs are driven by IL-4 or IL-13, specialized in the defence against extracellular pathogens and repair damaged tissue. These two types are reversible; macrophages show a broad spectrum of activation status between them (as shown by the color-graded triangles).

An important characteristic of macrophages is their plasticity and heterogeneity. They have the capability to reverse their phenotype and reprogram their characteristics depending on the requirements and microenvironment. Thus, they balance their behaviour between the M1/pro-inflammation and M2/pro-resolution phenotypes displaying a wide spectrum of activities (Porcheray et al., 2005; Stout and Suttles, 2004). Their equilibrated regulation is key to develop an effective immune response and to maintain a healthy/homeostatic status. As an example, exacerbated M2 responses (in line with exacerbated Th_2 responses) are related to different pathologies such as allergies, asthma or inflammatory bowel disease (Brusselle et al., 1994; Fuss and Strober, 2008a; Martinez et al., 2009; Wills-Karp, 2004). This M1/M2 model has been suggested

as two poles of many intermediate states that are needed to respond effectively and resolve inflammation efficiently (Mosser and Edwards, 2008)

The most studied M2 Mϕs are those generated in the presence of IL-4 or IL-13 (Martinez et al., 2009). Together with IL-4, IL-13 is a Th_2 type cytokine that drives and modulates the immune response. Firstly described as a Th_1 down regulator (Minty et al., 1993), its role as an active immune mediator has been described and distinguished from those of IL-4 by several studies mainly using mice and knock-out models (Hogan et al., 1997; Kolodsick et al., 2004; Punnonen et al., 1993; Ramalingam et al., 2008b). Although both IL-4 and IL-13 trigger a pro-Th_2 environment, they are non redundant cytokines, as demonstrated by several lines of evidence. For example, IL13 induces IgG_4 and IgE production independent of IL-4, and knock out mice for IL-13 and IL-4 studies showed a critical role for IL-13 in the immune response to *Nippostrongylus brasiliensis*, pathogen that elicits Th_2 responses (Punnonen et al., 1993; Wynn, 2003). Interleukin 13 is a key cytokine in the defence against gastrointestinal nematodes and plays a central role in some diseases such as asthma (Wills-Karp, 2004; Wynn, 2003).

These different and many profiles displayed by Mϕs and the required activation status of DCs are likely to be tightly controlled and mechanistically related. One possible mechanism of gene regulation is that exerted by microRNAs: small non coding RNAs that modulate and tune the expression of several genes at the same time by pairing to their target RNAs. Therefore, in these equilibrated systems microRNAs seem ideal candidates to regulate both DC and Mϕ biology.

1.2 MicroRNAs

MicroRNAs (miRNAs) are small non-coding RNAs of approximately 22nt in length that inhibit gene expression by pairing to the 3' UnTranslated Region (3'UTR) of their target mRNAs (Bartel, 2004). MiRNAs belong to a class of small non coding RNAs together with short-interfering RNAs (siRNAs) and Piwi-RNAs (piRNAs); all of them share inhibitory functions and belong to the RNA interference (RNAi) pathway (Carthew and Sontheimer, 2009) .

The term RNA interference (RNAi) was firstly used by Christian E. Rocheleau in 1997, (Rocheleau et al., 1997) Naturally occurring anti-sense RNA functions were firstly observed in bacterial control of replication (Polisky, 1988) and later in eukaryotes, inhibitory functions of transgenes were first observed in plants (Napoli et al., 1990; van der Krol et al., 1990). This type of gene regulation was induced in plants by transfection of complementary DNA constructs in cells and it was known as Post Transcriptional Gene Silencing (PTGS) (Beclin et al., 1998; Vaucheret et al., 1998) and quelling in fungi (Romano and Macino, 1992).

The first members of the RNAi family, small interference RNAs (siRNAs), were discovered by Andrew J. Hamilton and David C. Baulcombe as a mechanism of viral defence in plants (Hamilton and Baulcombe, 1999); later siRNAs were subsequently shown to be effective in mammalian cells (Elbashir et al., 2001). MicroRNAs were initially observed in *C.elegans* as small regulators of development and they were characterized by complementarity to their regulated mRNAs (Lee et al., 1993), athough the term "microRNA" was first used several years later (Lagos-Quintana et al., 2001; Lee and Ambros, 2001).

Both siRNAs and miRNAs are derived from double-stranded RNAs and are found in many eukaryotes. Piwi-interacting RNAs (piRNAs) seem to be more restricted to animal germ lines and derive from single-stranded precursors, but there is relatively poor understanding of them (Carthew and Sontheimer, 2009).

There have been several differences reported between siRNAs and miRNAs which can be summarized in three main points (Carthew and Sontheimer, 2009):

- siRNAs derive from RNA duplexes or long hairpins while miRNAs derive from short hairpins created by self-folded transcripts.

- siRNAs promote mRNA cleavage following perfect pairing to target RNAs. MiRNAs block the translation of imperfectly-matched targets and mRNA degradation also occurs (Baek et al., 2008; Selbach et al., 2008).

- siRNAs were first thought to be a defence against foreign nucleic acids, such as transposons, viruses or transgenes, while miRNAs were described as regulators of endogenous genes.

- siRNAs act against specific genes whilst microRNAs exert their action in a broader range of target genes (Baek et al., 2008; Selbach et al., 2008).

It is however clear that the criteria that defines the distinction between siRNAs and miRNAs is changing. MiRNAs have been described as part of the host defence against viruses (Pedersen et al., 2007) and the evidence for microRNAs exerting their inhibitory functions via mRNA degradation in addition to translational inhibition are increasing (Baek et al., 2008; Guo et al., 2010; Selbach et al., 2008). Moreover, enhancement of translation has also been reported to be part of microRNA action for some microRNAs such as miR-223 (Buchan and Parker, 2007); TNF-α mRNA translation has been shown to be promoted through AU-rich elements in its 3'UTR recruiting Ago-2 (Vasudevan and Steitz, 2007), and miR-10a binding to the 5'UTR of ribosomal protein mRNAs and promoting their translation under starvation (Orom et al., 2008). In addition, microRNAs have been shown to enhance transcription through binding to 5'UTR complementary sites (Place et al., 2008). All this evidence broadens the picture of microRNA regulatory actions and show a more widespread function of microRNAs than initially suggested (Bartel, 2004). As microRNAs have been more extensively described and are known for their inhibitory action, sections 1.2.2 and 1.2.3 will only relate to this miRNA function.

1.2.1 MicroRNA biogenesis

MiRNAs arise from genome encoded precursors that fold into imperfect hairpin structures, pri-miRNAs. Figure 4 shows a schematic representation of microRNA biogenesis. Pri-miRNAs can be transcribed from independent genes that may include more than one miRNA (a poly-cistronic cluster of miRNAs) (Lagos-Quintana et al., 2001; Lee et al., 2002). They can also derive from intronic sequences in protein-coding genes transcribed by the RNA Polymerase II (termed mirtrons) (Ruby et al., 2007). Recently it was shown that miRNAs can be also harboured in other types of genomic sequence such as small nucleolar RNAs (He et al., 2008; Saraiya and Wang, 2008) or long non-coding RNAs (He et al., 2008). Pri-miRNAs vary in length depending on the genes they have arisen from : clusters of five microRNAs have shown transcripts of approximately 800 bp; clusters of three miRNAs have shown precursors of 400 bp and single miRNAs precursors of more than 300 bp (Lee et al., 2002)..

A typical animal pri-miRNA consists of an imperfectly paired stem of 33 bp with a terminal loop and flanking segments (Bartel, 2004). Pri-miRNAs are bound by Drosha-DGCR8 complexes (Han et al., 2004; Lee et al., 2003) and processed into ≈ 70nt pre-miRNAs (see Figure 4). In the case of miRNAs included in other RNA species (such as mirtrons), these are excised during the splicing of the mRNA in which they are located skipping this first step of miRNA biogenesis.

The generation of mature single stranded microRNAs and their effects depend on two protein families: Dicer proteins, to release them from their precursors (Bernstein et al., 2001) reviewed in (Carmell and Hannon, 2004) and Argonaute (Ago) proteins to enable them to function as single stranded RNA molecules when loaded in RNA-induced silencing complexes (RISCs) (Chendrimada et al., 2005; Liu et al., 2004) reviewed in (Hutvagner and Simard, 2008).

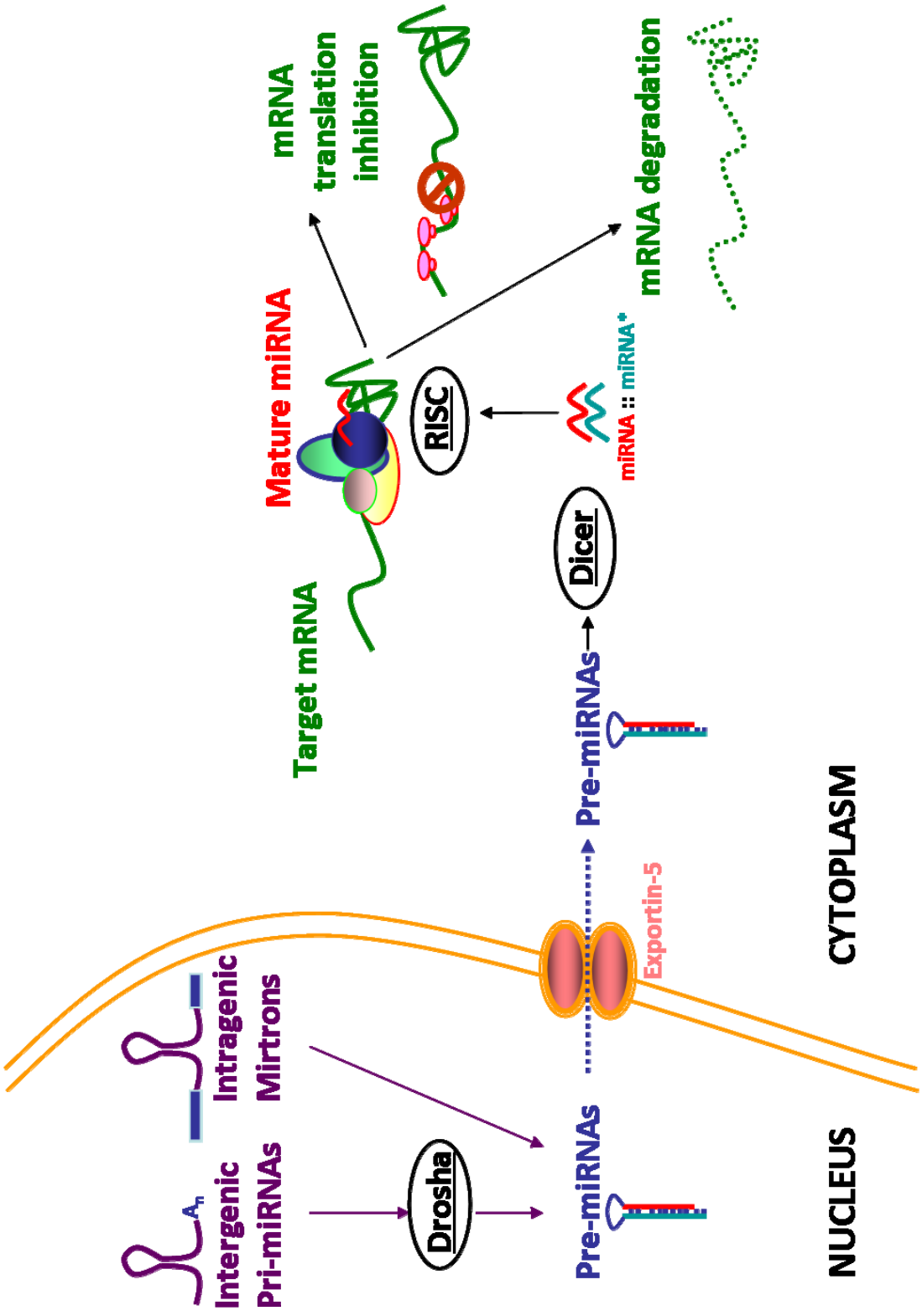

Figure 4 MicroRNA biogenesis. Pri-miRNAs are processed by Drosha into pre-miRNAs, which are then transported to the cytoplasm through Exportin-5. In the cytoplasm, pre-miRNAs are processed by Dicer, which generates double stranded miRNA::miRNA* duplexes. The mature miRNA (in red) is loaded into the RISC complex, where it will exert inhibitory function on the target mRNA: mRNA inhibition of translation or mRNA degradation.

Pre-miRNAs are bound by Exportin5 in the nuclear membrane and exported by a Ran-GTP mechanism to the cytoplasm (Bohnsack et al., 2004; Yi et al., 2003). In the cytoplasm, Dicer-TRBP (the human immunodeficiency virus Transactivating response RNA-Binding Protein) complexes bind to the double-stranded pre-miRNAs (Chendrimada et al., 2005), generating mature miRNA::miRNA* duplexes of about 22nt. Eventually, the leading strand (the mature miRNA) is loaded into the miRISCs and guides Argonaute proteins to their target mRNAs (Eulalio et al., 2008). It is worth noting that a dsRNA (miRNA*:miRNA) molecule is generated from the pre-miRNA. In this dsRNA molecule, the leading strand or miRNA is preferentially incorporated into the RISC complex, while the other strand, miRNA* (called miRNA species) tends to be degraded. This has been related to differences in their stability and affinity to be loaded in the RISC complex (Khvorova et al., 2003; Schwarz et al., 2003). However, some targeting roles have been described for this miRNA*strand, which has been shown to be conserved between several species (Okamura et al., 2008) and led to their inclusion in the microRNA prediction databases.

1.2.2 Mechanisms of miRNA action

MiRNAs have been reported to exert their function mainly by blocking translation and to a lesser extent by cleaving target mRNAs (Filipowicz et al., 2008). Target mRNA cleavage has been recently supported by polyribosome profiling experiments that showed miRNA action relates to levels of degradation of their targeted mRNAs (Guo et al., 2010) in addition to previous proteome global analysis (Baek et al., 2008; Selbach et al., 2008).

MiRNAs in miRISCs direct the action of Argonaute proteins towards their targeted mRNAs upon 3'UTR pairing. They exert post transcriptional inhibitory action by four different mechanisms: i) inhibiting translation initiation (Humphreys et al., 2005; Pillai et al., 2005), ii) inhibiting translation elongation (Seggerson et al., 2002), iii) causing ribosome drop-off (premature translation termination) and iv) protein cotranslational degradation (Nottrott et al., 2006). In addition, miRNA can cause the degradation of their target mRNAs (Bagga et al., 2005; Guo et al., 2010) or sequester the targeted mRNAs in foci called P bodies in which the translation machinery is excluded (Parker and Sheth, 2007).

All these mechanisms lead to a reduction in the protein output from a target mRNA. However, several questions remain unanswered: is this a single mechanism (rather than four) with four different outcomes? And, are some observations (P bodies for example) a consequence rather than a cause of mRNA inhibition? (Eulalio et al., 2008).

1.2.3 MiRNA-target interactions

After a mature miRNA strand is loaded in the RISC complex, RISC binds to the microRNA target mRNA. The target specifity of microRNAs is given by the “seed region”: nucleotides in positions 2- 7 at its 5´ end. The seed region pairs to the complementary site in the targeted 3´UTR by Watson-Crick interactions (GC, AU- G: guanosine, C: cytosine, A: adenine, U: uracil) and directs the RISC action (Bartel, 2004). Importantly, G:U “wobble” interactions are permitted in the pairing. MiRNA:target binding depends on the sequence complementarity between the 3’UTR of the target mRNA and the mature miRNA and also on the miRNA site accessibility and structure of the targeted mRNA (Kertesz et al., 2007b).

Typically the matching occurs between the seed region of the microRNA and 6 to 8 nucleotides (and sometimes one or two extra bases) that reside in 3´UTR of its target. Figure 5 illustrates the types of the seed pairing between microRNAs and the targeted 3´UTR (adapted from (Bartel, 2009; Shin et al., 2010)). Canonical sites are composed of 7 or 8 nucleotides pairing, although 6 nucleotides pairing can also occur but seems to be less efficient. Supplementary sites at the 3´ of the miRNA enhance binding efficiency and might include non Watson-Crick interactions (G:U wobbles) (Bartel, 2004; Varani and McClain, 2000). Recently a new class of miRNA target sites has been described and termed “centered sites” that show 11-12 contiguous base pairing to the center of the miRNA (Shin et al., 2010).

In summary and based on the terminology by (Grimson et al., 2007; Shin et al., 2010), microRNA sites are (see Fig.5):

- 6mer: pairing to nucleotides 7-2 of the microRNA;

- 7mer-m8: pairing to nucleotides 2 to 8 of miRNA;

- 7mer-A1: pairing to nucleotides 2 to 8 plus adenosine opposite to nucleotide 1 of miRNA;

- 8mer: pairing to nucleotides 8 to 2 plus adenosine opposite to nucleotide 1 of miRNA;

- centered sites: pair to the center of the microRNA

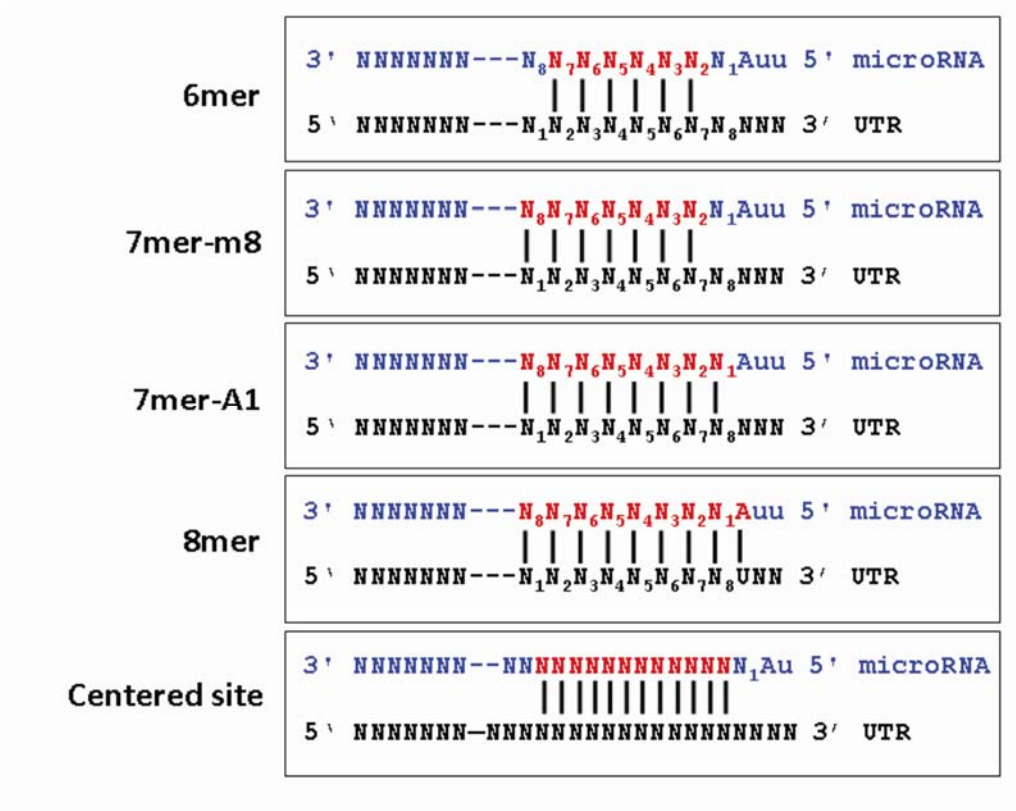

Figure 5 Different types of pairing between miRNA and the target mRNA. MicroRNA (in blue) pairs to the 3'UTR of the target gene (in black). Red sequence shows the paired nucleotides of the microRNA to the 3'UTR that determine the type of miRNA pairing. No additional base pairings are shown to simplify the figure (like G:U wobble pairs or complementary pairing nucleotides at the 3' of the microRNA). N: nucleotide.

Studies investigating genome sequencing and cross species sequence conservation have predicted that more than half of the coding-genome is regulated by miRNAs from (Bartel, 2009). Many models have been developed to predict miRNA-target interactions. These are useful predictions that need to be confirmed experimentally. Target-microRNA interactions are predicted upon three main parameters: Watson-Crick complementarity in the seed region, conservation across species and accessibility-secondary structure of the targeted UTR (Bartel, 2009). Target site context has also been considered to be important, as the same site for a given miRNA is differentially recognized depending on the flanking 3´UTR context (Didiano and Hobert, 2008),. Thus, the interaction between miRNAs and their predicted targets is determined not only by the predicted binding site of miRNA-target, but also by the molecular context of this

region. Evolutionary conservation occurs mainly in sites of predicted targets co-expressed with their regulatory miRNAs; this observation suggests that miRNA::target interactions are more than a mere base-pairing and that they have co-evolved together (Bartel, 2009).

Cellular compartmentalisation may add another layer of regulation to the miRNA network. P bodies are regions in the cytoplasm in which many molecules involved in mRNA turn over are present (Parker and Sheth, 2007). In these foci, miRNAs, Argonaute proteins and target mRNAs co-localise (Eulalio et al., 2007). However, their role in miRNA biology is unclear. Some studies have shown that miRNA pathways are not affected when P-bodies are not detectable suggesting that their presence is a consequence of miRNA action rather than a cause (Humphreys et al., 2005; Pillai et al., 2005). They may function as a reserve of miRNA and/or their targets, allowing cells to respond quicker to stimuli that require immediate action (Parker and Sheth, 2007).

1.2.4 MicroRNA 155

MiR-155 is the microRNA encoded in BIC (B-cell Integration Cluster) gene (or MIR155HG, miR-155 hosting gene) located in chromosome 21 (21q21.3) between positions 26934457 and 26947480 (Kluiver et al., 2005) (see Fig.6). BIC transcript has 1421 base pairs and two exons; the mature microRNA, miR-155, is located in the second exon between positions 25868163 and 25868227.

This gene was mentioned for the first time in 1989, when Clurman and Hayward described c-bic as a novel locus for the integration of the avian leucosis virus in B-cell lymphomas and characterized it as a proto-oncogene (Clurman and Hayward, 1989). Eight years later it was hypothesised that BIC harboured a non coding RNA rather than coding for a protein (Tam et al., 1997). However, it was not until 2001 that BIC was described as a human non-coding RNA gene (Tam, 2001) . Publications after that date were generally restricted to its function in B-cell lymphomas and its characterization mainly in Hodgkin and Burkitt lymphomas (Eis et al., 2005; Kluiver et al., 2005; Metzler et al., 2004; van den Berg et al., 2003).

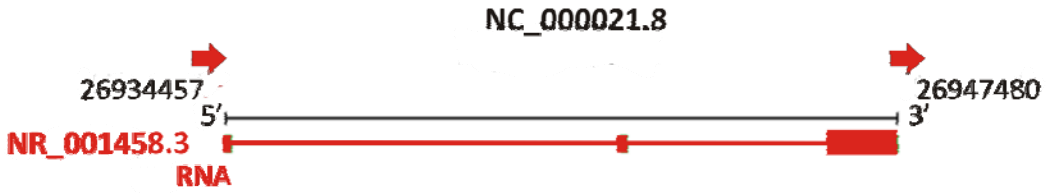

Figure 6. BIC gene. Representation of BIC or MIR155HG; numbers 26934457 and 26947480 in black show the chromosome positions that encompass this gene in 21q21.3. NC_000021.8 is the accession number; NR_001458.3 refers to the RNA accession number.

BIC and miR-155 expression ratios have been shown to differ suggesting possible regulation in the pathway from BIC to miR-155 (Eis et al., 2005). In 2007, Kluiver et al. described the regulation of BIC and miR-155 in different cell lines, concluding that NF-κB (Nuclear Factor Kappa B) and PKC (Protein Kinase C) are involved in the transcription of BIC, whereas mature miR-155 requires an additional step (blocked in Burkitt lymphoma cells) that remains unknown (Kluiver et al., 2007). New publications arose addressing this issue showing that miR-155 is processed in Burkitt lymphomas (Zhang et al., 2008). Recently, the maturation of miR-155 in murine macrophages has been shown to depend

on the KH-type splicing regulatory protein (KSRP), an RNA binding protein involved in splicing that promotes maturation of miR-155 precursors when macrophages are stimulated with LPS (Ruggiero et al., 2009).

The first validated target of miR-155 was the human angiotensin II type 1 receptor (Martin et al., 2006). It was O´Conell and colleagues who described for the first time the role of miR-155 in the inflammatory response in mice (O'Connell et al., 2007). Murine macrophages showed up regulation of miR-155 when stimulated with several pro inflammatory stimuli (pro-Th_1 or pro-M1 macrophages stimuli): polyriboinosinic:polyribocytidylic acid, LPS and interferons, the latter requiring TNF-α autocrine signaling. Only four months later, two independent groups developed two different miR-155 knock-out mice (Rodriguez et al., 2007; Thai et al., 2007); these mice showed abnormal immune function with defective B and T cells and aberrant antigen presenting cells. Moreover, these mice showed an imbalance of the T cell population with a trend towards Th_2 differentiation (Thai, Calado et al. 2007). MiR-155 has been reported to be controlled by Foxp3 and to be important for the development of T_{regs} in mice (Kohlhaas et al., 2009). This supports a role for miR-155 in the development of a healthy immune response.

MiR-155 has also been implicated in other aspects of the inflammatory response. MiR-155 has also been implicated in acute inflammatory response in mice through C/EBP β and G-CSF (Worm et al., 2009) and in the inflammatory response induced by *Helicobacter pylori* (Xiao et al., 2009). MiR-155 has also been shown to be required for an appropriate production of IgG_1 antibodies through PU.1 in murine B cells (Vigorito et al., 2007). Only recently the role of miR-155 in dendritic cell biology was described (Ceppi et al., 2009) showing that miR-155 is involved in the TLR/IL-1 pathway in LPS matured monocyte-derived dendritic cells (moDCs) via TAB2 targeting.

Therefore, microRNA-155 regulates the immune system and its activation in different cells and environments. Its involvement in the inflammatory response positions miRNA-155 as an ideal candidate in DC maturation and to regulate the inflammatory status of Mϕs.

1.3 Hypothesis

MicroRNA 155 targets specific genes in dendritic cells and monocytes that regulate their immune activation and function.

1.4 Aims

Aim 1. To determine possible targets of miR-155 by bioinformatics' analysis of putative binding sequences.

Aim 2. To select from the putative targets those genes relevant to dendritic cell and monocyte biology.

Aim 3. To validate the selected targets *in vitro*.

Aim 4. To demonstrate their biological significance in DCs and Mϕs.

2 Chapter 2: Materials and methods

2.1 List of materials used

2.1.1 Equipment

7900HT Fast Real-Time PCR System (#4329001, Applied Biosystems, California, USA)

BD FACSAria™ or a BD FACSCalibur™ cytometers (BD Biosciences)

DNA Engine TETRAD™ 2 Peltier Thermal Cycler (#TA001175, Esco Technologies, Inc., USA)

EVG620 mask aligner (EV Group, Optimim Services, Liandysul, UK)

Hemocytometer (#MNK-420-010N, Fisher Scientific UK Ltd, Leicestershire, UK)

Mini-PROTEAN Tetra Cell (#165-8002, Bio-Rad, California, USA)

Nanodrop (Fisher Scientific UK Ltd, Leicestershire, UK)

STS Pegasus DRIE plasma etcher (STS, Sumitomo Precision Products Co. Ltd., Japan)

Thermo Scientific Heraeus FRESCO 17 Centrifuge (#CFH-203-010K, Fisher Scientific UK Ltd, Leicestershire, UK)

XCell SureLock® Mini-Cell and XCell II™ Blot Module Kit CE Mark (#EI0002, Invitrogen Ltd, Paisley, UK)

2.1.2 List of reagents

100 BP DNA LADDER 250 UG (#MW-0302-04, Eurogentec Ltd., Hampshire, UK)

30% Acrylamide/Bis Solution 29:1 (#161-0157, Bio-Rad)

Agarose (#BPE 1356-100 C4, Thermo Fisher Scientific Inc, Leicestershire, UK)

Albumin from bovine serum ≥98% (BSA) (#A7906-100G, SIGMA-ALDRICH COMPANY LTD., Dorset, UK)

Aminoallyl-UTP - OYSTER-656 (#NU-821-656, Bioquote Limited, York, UK)

Ammonium persulfate (APS) (##161-0700, Bio-Rad, California, USA)

Anti α-Tubulin (AA12) (#sc-58667, Santa Cruz Biotechnology Inc., Heidelberg, Germany)

Anti beta Actin antibody - Loading Control (ab8227, Abcam plc., Cambridge, UK)

Anti β-Tubulin (H-235) (#sc-9104, Santa Cruz Biotechnology Inc., Heidelberg, Germany)

Anti DC-SIGN (H-200): sc-20081 (Santa Cruz Biotechnology, Inc., Heidelberg, Germany)

Anti IL-13Rα1 (sc-25849, Santa Cruz Biotechnology Inc., Heidelberg, Germany)

Anti-miR™ miRNA Inhibitors—hsa-155 (#AM17000, Ambion, Texas, USA)

Anti-miR™ miRNA Inhibitors—Negative Control #1 (#AM17010, Ambion, Warrington, UK)

Anti Phospho STAT6 (#9361, Cell Signalling Technology- New England Biolabs (UK) Ltd., Hertfordshire, UK)

Anti STAT6 (#9362, Cell Signalling Technology- New England Biolabs (UK) Ltd., Hertfordshire, UK)

AZ® 400K Developer 1:4 (MicroChemicals GMBH, Ulm, Germany)

AZ® 9260 thick film photoresist (MicroChemicals GMBH, Ulm, Germany)

BCA Protein Assay Kit (#23225, Thermo Fisher Scientific Inc, Leicestershire, UK)

Beta-Mercaptoethanol (#6250, SIGMA-ALDRICH COMPANY LTD., Dorset, UK)

Boric acid (#B/3800/53 C9, Thermo Fisher Scientific Inc, Leicestershire, UK

Bromophenol blue (#114405-25G, SIGMA-ALDRICH COMPANY LTD., Dorset, UK)

CD14 magnetic beads (#130-050-201, Miltenyi Biotech, Germany)

cOmplete Protease Inhibitor Cocktail Tablets (#0469312400, Roche Products Ltd., Hertfordshire, UK)

D-MEM Media - GlutaMAX™-I (#61965-059, GIBCO®, Invitrogen Ltd., Paisley, UK)

Doxycycline hyclate ≥98% (TLC) (#D9891-5G, Fluka, SIGMA-ALDRICH COMPANY LTD., Dorset,UK)

Dual-Luciferase Reporter Assay System (#E1910, Promega UK Ltd, Hampshire, UK)

EDTA Disodium Salt (#D/0700/53 C30, Thermo Fisher Scientific Inc, Leicestershire, UK

Fetal Bovine Serum, Certified (#16000-044, GIBCO®, Invitrogen Ltd., Paisley, UK)

Ficoll-Paque™ PLUS (#17-1440-03, GE Healthcare)

FITC using FluoroTag™ FITC Conjugation Kit (SIGMA-ALDRICH COMPANY LTD., Dorset,UK)

Foetal Bovine Serum (Heat Inactivated) (#10108-165, Life Technologies LTD, Paisley, UK)

Genopure Plasmid Maxi Kit (#03143422001, Roche Products Ltd., Hertfordshire, UK)

Glycerol (#G/0650/08 C35, Thermo Fisher Scientific Inc, Leicestershire, UK)

Glycine (#G/0800/60 C40, Thermo Fisher Scientific Inc, Leicestershire, UK)

Glycogen 20mg (#10901393001, Roche Products Ltd., Hertfordshire, UK)

H_2DCFDA, (H_2-DFC, DFC) (#D-399, Invitrogen Ltd., Paisley, UK)

High Capacity cDNA Reverse Transcription Kit (#4374967, Applied Biosystems, USA, California)

hsa-miR-155 miRCURY™ LNA microRNA Power Inhibitor, 5 nmol, ready to label (#426839-00, Exiqon, Vedbaek, Denmark)

IGEPAL CA-630 (#I7771-50ML, SIGMA-ALDRICH COMPANY LTD., Dorset, UK)

Immobilon polyvinylidene difluoride membrane (#IPVH00010, Millipore Ltd.., Watford, UK)

LB Agar (#L2897 SIGMA-ALDRICH COMPANY LTD., Dorset, UK)

LB Broth (#L3022 SIGMA-ALDRICH COMPANY LTD., Dorset, UK)

LS Columns (#130-042-401, Miltenyi Biotech, Germany)

Luminol ≥97% (HPLC) (#A8511, SIGMA-ALDRICH COMPANY LTD., Dorset, UK)

MACS® MultiStand (#130-042-303, Miltenyi Biotech, Germany)

microRNA Power Antisense Control A (#199020-00, Exiqon,)

Midi-MACSTM separator (#130-042-301, Miltenyi Biotech, Germany)

mini Quick Spin RNA Columns (#11814427001, Roche Products Ltd., Hertfordshire, UK)

NaCl for molecular biology (#71376-1KG, SIGMA-ALDRICH COMPANY LTD., Dorset, UK)

N,N,N',N'-Tetramethylethylenediamine (TEMED) (##161-0801, Bio-Rad, California, USA)

NuPAGE® MOPS SDS Running Buffer (for Bis-Tris Gels only) (20x) (#NP0001, Invitrogen Ltd, Paisley, UK)

NuPAGE® Novex 4-12% Bis-Tris Gel 1.0 mm, 10 well (#NP0321BOX, Invitrogen Ltd, Paisley, UK)

NuPAGE® Novex 4-12% Bis-Tris Gel 1.0 mm, 15 well (#NP0323BOX, Invitrogen Ltd, Paisley, UK)

Oligofectamine Transfection Reagent (SKU#12252-011, Invitrogen Ltd, Paisley, UK)

One Shot Mach1 T1 Phage-Resistant Chemically Competent E.coli (#C8620-03, Invitrogen Ltd, Paisley, UK)

Opti-MEM® I Reduced-Serum Medium (1X), liquid (#31985-062, GIBCO ®)

PBS tablets (#18912-014, GIBCO ®, Invitrogen Ltd, Paisley, UK)

p-Coumaric acid ≥98.0% (HPLC) (#C9008, SIGMA-ALDRICH COMPANY LTD., Dorset, UK)

Pefablock SC (#11585916001, Roche Products Ltd., Hertfordshire, UK)

Pfu DNA Polymerase 100U (#M7741, Promega UK Ltd, Hampshire, UK)

Polybrene (#L107689, SIGMA-ALDRICH COMPANY LTD., Dorset, UK)

Polyclonal Goat Anti-Rabbit Immunoglobulin HRP conjugated (#P0448, Dako UK Ltd., Cambridgeshire, UK)

Propidium iodide (#81845-25MG, SIGMA-ALDRICH COMPANY LTD., Dorset, UK)

PU.1 (Spi-1) (T-21) (#sc-352, Santa Cruz Biotechnology, Inc., Heidelberg, Germany)

QIAquick Gel Extraction Kit (#28704, Qiagen, Sussex, UK)

QIAquick PCR Purification Kit (#28104, Qiagen, Sussex, UK)

Recombinant human IL-13 (#213-IL-005, R&D Systems Europe Ltd., Oxfordshire, UK)

Restriction enzymes used were purchased from New England Biolabs (Herts, UK)

rh GM-CSF (#11343127, Immunotools, Germany)

rh IL-4 (#11340047, Immunotools, Germany)

RPMI Medium 1640 - GlutaMAX™-I (#72400-054, GIBCO®, Invitrogen Ltd, Paisley, UK)

SmartLadder (#MW-1700-10, Eurogentec Ltd., Hampshire, UK)

Sodium azide (#S2002-100G, SIGMA-ALDRICH COMPANY LTD., Dorset, UK)

Sodium dodecyl sulphate (#S/5200/53 C107, Thermo Fisher Scientific Inc, Leicestershire, UK)

Spectra™ Multicolor Broad Range Protein Ladder Lot 34744 (#SM1841, Fermentas,)

SuperFect Transfection Reagent (#301305, Qiagen, Sussex, UK)

SYLGARD® 182 silicone elastomer kit (Seneffe, Belgium)

Syringe pumps (UB microfluidics)

T7 RNA Polymerase (#10881767001, Roche Products Ltd., Hertfordshire, UK)

TaqMan® Universal PCR Master Mix, No AmpErase® UNG (#4364341, Applied Biosystems, USA, California)

tert-Butyl hydroperoxide solution (#19990 SIGMA-ALDRICH COMPANY LTD., Dorset, UK)

TOPO® TA Cloning® Kit (#K450001, Invitrogen Ltd, Paisley, UK)

TOPO® TA Cloning® Kit (with pCR®2.1-TOPO®) with One Shot Mach1™-T1R Chemically Competent E. coli and PureLink™ Quick Plasmid Miniprep Kit (SKU# K4510-22, Invitrogen Ltd, Paisley, UK)

TransIT®-LT1 Transfection Reagent (#MIR 2300, Mirus Bio LLC, USA)

TRI Reagent Solution (#AM9738, Applied Biosystems, Warrington, UK)

Tris Base Ultra Pure (#BPE152-1 C131, Thermo Fisher Scientific Inc, Leicestershire, UK)

Tris hydrochloride 1M pH 7.5 (#BPE1757-500, Thermo Fisher Scientific Inc, Leicestershire, UK)

TRIzol (#15596-018, Invitrogen Ltd, Paisley, UK)

Tween 20, Molecular Grade: 500ml (#41116134, Promega UK Ltd, Hampshire, UK)

Ultrapure DNAse⁄RNAse-Free distilled water (#10977035, Invitrogen Ltd., Paisley, UK)

Ultrapure LPS from Escherichia coli 0111:B4 (# tlrl-pelps, InvivoGen).

2.1.3 Buffer recipes

For cell biology:

FACS Blocking solution: 1%BSA, 0.1% sodium azide, 10%FBS in PBS

FACS solution: 0.01% sodium azide and 1% BSA in PBS

MACS BUFFER: 1% BSA, 0.1% sodium azide in PBS

Binding Buffer (20mM Tris pH7.5, 150mM NaCl, 1mM CaCl2, 2mN MgCl2 and 1% BSA)

For DNA

CES 5x: 0,54M betaine, 1.34mM DTT, 1.34% DMSO and 11mg/ml BSA

Tris Acetate EDTA (TAE) 50x: 240g Tris Base, 57.1ml Glacial acetic acid, 100ml 0.5M EDTA

For protein work and Western Blotting:

Lysis buffer: NP-40 1% in water (add protein inhibitors at the moment of use)

5x SDS-loading buffer: 10% SDS, 50% glycerol, 0.25M Tris-HCl pH 6.8, 0.01% bromophenol blue

Blocking solution: TBS-T 5% non fat milk

Enhanced Chemiluminescence (ECL) solution: 1:1 mix of Solutions A and B, and add H_2O_2 (0.02% final)

- Solution A (100mL): 1ml 250mM luminol, 0,44ml 90mM p-Coumaric acid, 10mL Tris-HCl 1M pH 7,5

- Solution B (100mL): 10mL 10mL Tris-HCl 1M pH 7.5

Running buffer electrophoresis (for 1l): 14 g Glycine, 3g Tris-Base, 20%SDS

Transfer buffer (for 1l): 11,25 g Glycine, 2,25 g Tris-Base, 20% methanol

TBS-T: 20mM Tris-Cl, pH 7,4; 12,5 mM NaCl, 0,05% or 0.1% Tween 20

2.2 Cell culture

All cell culture was performed under regular culture conditions (37°C and 5%CO_2) in antibiotic free media (except in the cases of doxycycline treatment). "Complete medium" refers to the addition of 10% foetal bovine serum (FBS). When using FBS not commercially heat inactivated, inactivation of the complement system was achieved by incubation at 56°C during 30min before adding it to the different media.

2.2.1 Cell lines.

THP-1 cells. This cell line was kindly provided by Dr.Christopher Pickard (ATCC number TIB-202™). It was maintained in RPMI complete medium at a cell density of 5-7·10^5 cells/mL.

THP1-155 cells. This cell line was cultured in RPMI complete medium at a cell density of 5-7·10^5 cells/ml. In miR-155 up regulation experiments with doxycycline treatment, cell density was maintained between 3 and 5 10^5 cells/mL over the course of doxycycline treatment (5 days). Cells were kept during the time course diluting them half the volume each day and retreating with doxycycline when needed.

When treated with IL-13 or IL-4, THP1-155 cells were starved over night and then stimulated with these cytokines. Starvation consisted in culturing cells in RPMI 0.5% FBS.

HEK293T (ATCC number CRL-11268™) and **HeLa** (ATCC number CCL-2™) cells were cultured in complete D-MEM medium and passed when confluent.

2.2.2 Monocyte derived dendritic cells

Monocyte derived dendritic cells (DCs). All dendritic cells used in this study were derived from monocytes. Monocytes were isolated from human peripheral blood mononuclear cells as previously described (Domínguez-Soto A et al., 2005). Peripheral Blood Mononuclear Cells (PBMCs) were separated from buffy coats by centrifugation in gradient density with Ficoll or Lymphoprep. Buffy coats were diluted in PBS at least by half before subjecting them to density gradient separation and pipetted on top of Ficoll (or Lymphoprep) in a ratio 1:4 (Ficoll: diluted buffy) approximately. These gradients were centrifuged at 2000 rpm 20min at room temperature with no centrifuge brake. The layer

of separated PBMCs was then removed using a serological pipette and washed 4-6 times in PBS to remove cell debris and platelets. Centrifugation during washes was performed as follows: 1st and 2nd wash at 1500 rpm 10min and the remaining washes at 1200 rpm 10 min. All washes were performed at room temperature. Washed PBMCs were then labelled using CD14 magnetic beads (Miltenyi) in MACS buffer (approximately 80µl MACS buffer+20µl CD14-beads per $100 \cdot 10^6$ PBMCs) at 4°C during 18min inside a 15ml facon tube. After labelling, cells were washed in MACS buffer and pelleted at 1200 rpm during 10min. $CD14^+$ cells (monocytic fraction) were separated by positive selection using magnetic LS MACS columns (Miltenyi) and the column was washed 4-6 times with MACS buffer to remove unlabelled cells. Isolated monocytes were then counted and cultured for 5–7 days at a cell density of $0.7\text{-}1 \cdot 10^6$cells/ml in RPMI 10% FBS with 500 units/ml of GM-CSF (Granulocyte-Macrophage Colony Stimulating Factor) and 250 units/ml of IL-4 in order to obtain immature DCs. Immature DCs were stimulated on day 5 of culture with 1µg/mL ultrapure LPS from Escherichia coli 0111:B4 and left 48h more to allow maturation. Cells were cultured on 6 well plates for RNA and protein expression analysis and on 96 well plates (U shape) for transfection experiments.

2.2.3 Macrophages

Monocytes were obtained using the same protocol described in 2.2.2 for obtaining dendritic cells. Isolated monocytes were plated at a cell density of 10^6 cells/ml onto 96 well plates (flat bottom) and maintained in RPMI 10% FBS supplemented with 500U/ml GM-CSF to allow macrophage differentiation.

2.3 Cloning

2.3.1 Vectors generated

pCDNA3.1.BIC: This vector harbors the coding region that contains microRNA 155. In order to clone it, the genomic region encompassing miR-155 in the BIC gene was amplified by PCR and cloned using TOPO TA Cloning Kit (Invitrogen) into pCR4 vector, clone named as pCR4_BIC (Fig.7, first vector represented on the left). The primers employed were BIC_FOR: CTC GAG TAT GCC TCA TCC TCT GAG TGC and BIC_REV: AAG CTT ACG AAG GTT GAA CAT CCC AGT GAC C, designed in order to clone the fragment including Xho I restriction site at its 5' end and Hind III at its 3' end. The annealing temperature used was 60°C. After checking by sequencing, this fragment was sub cloned from pCR4_BIC into XhoI/HindIII sites of pCDNA3.1 (-) multicloning site (Fig. 7). T4 DNA Ligase High Concentrated was used following manufacturer's instructions overnight at 16°C. Clones were checked by sequencing (Geneservice, Oxford- Appendix 1).

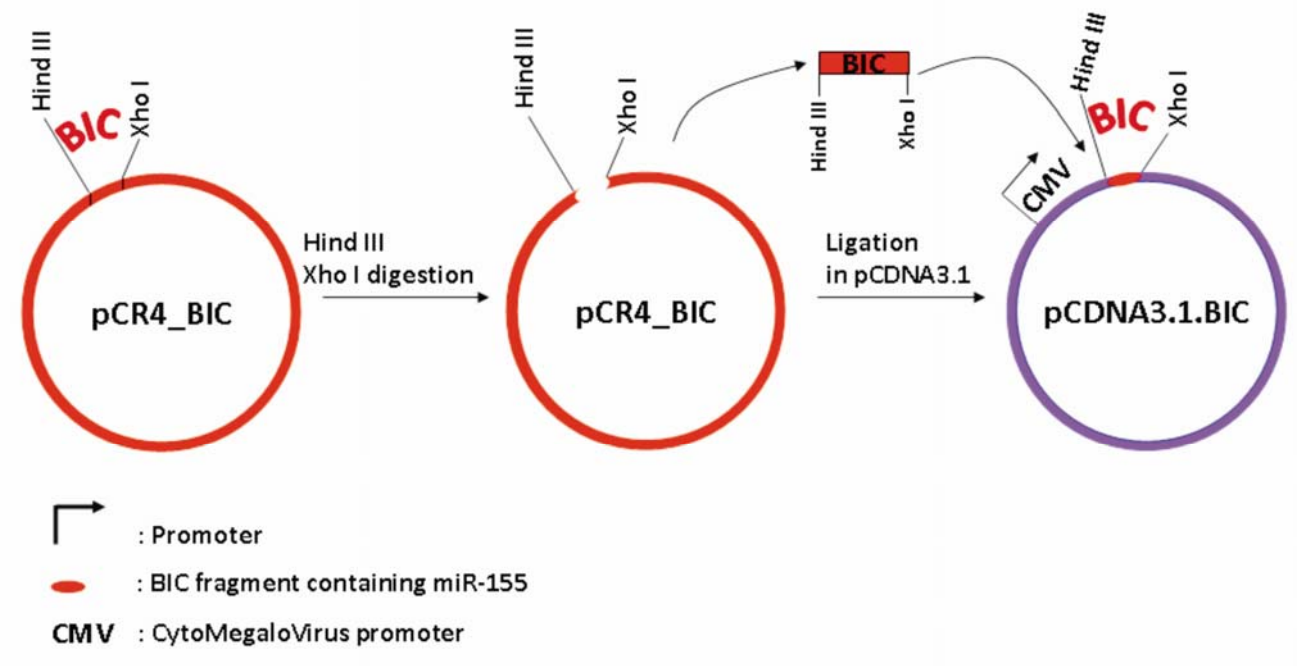

Figure 7 MiR-155 expression vector construct. The genomic region encompassing miR-155 (BIC in the figure) was cloned into pCR4 TOPO vector (first vector represented on the left, pCR4_BIC). pCR4_BIC was subsequently digested with Hind III/Xho I enzymes; the excised fragment was cloned into pCDNA3.1. empty vector constructing pCDNA3.1.BIC (vector represented on the right).

pSUPER_BIC: The same genomic fragment as above was amplified using the following primers: BIC_LENTI_FOR AAG CTT TAT GCC TCA TCC TCT GAG TGC and BIC_LENTI_REV: CTC GAG ACG CGT ACG AAG GTT GAA CAT CCC AGT GAC C. The forward primer includes a Hind III site at its 5' end, and the reverse primer a Mlu I site followed by a XhoI site at its 3' end. These restrictions sites were included for the subsequent cloning steps required to contruct the lentiviral vector pLENTI_BIC. BIC genomic fragment was amplified by PCR and cloned using TOPO TA Cloning Kit (Invitrogen) into pCR4 vector following manufacturer's recommendations. The resulting clone was called **pCR4_LENTIBIC** (Fig. 8, upper row, first represented vector on the left). A second cloning step was done subsequently in pSUPER between HindIII/XhoI sites (Fig. 8, upper row right). T4 DNA Ligase High Concentrated was used following manufacturer's instructions overnight at 16°C. The resulting construct was named **pSUPER_BIC**. This cloning step was required to excise the histone 1 (H1) promoter from **pSUPER_BIC** vector and clone it in the lentiviral pLVTHM vector afterwards. H1 promoter drives transcription from RNA Polymerase III, which is the cellular RNA Polymerase that transcribes small RNAs, tRNAs, 5S ribosomal RNA and U6 spliceosomal RNA. H1 promoter has been shown to be efficient for transcribing siRNA molecules (Brummelkamp et al., 2002; van de Wetering et al., 2003). RNA Polymerase II promoters (like the one present in pCDNA.3.1, CMV or CytoMegaloVirus promoter) have also been reported to efficiently transcribe microRNAs (Zeng et al., 2005). pLVTHM lentiviral vector was designed to drive the expression of the cloned transgene (siRNA usually) from the H1 promoter (Wiznerowicz and Trono, 2003). To keep its original structure, the subcloning steps were performed in such way that the H1 promoter was kept in the final construct **pLENTI_BIC**.

pLENTI_BIC: The fragment containing H1 promoter-BIC was removed form pSUPER_BIC digesting with EcoRI and MluI sites and subcloned into pLVTHM (Fig. 8 lower row). T4 DNA Ligase High Concentrated was used following manufacturer's instructions overnight at 16°C. This vector was named as **pLENTI_BIC** and it was the lentiviral vector used for creating THP1-155 cell line.

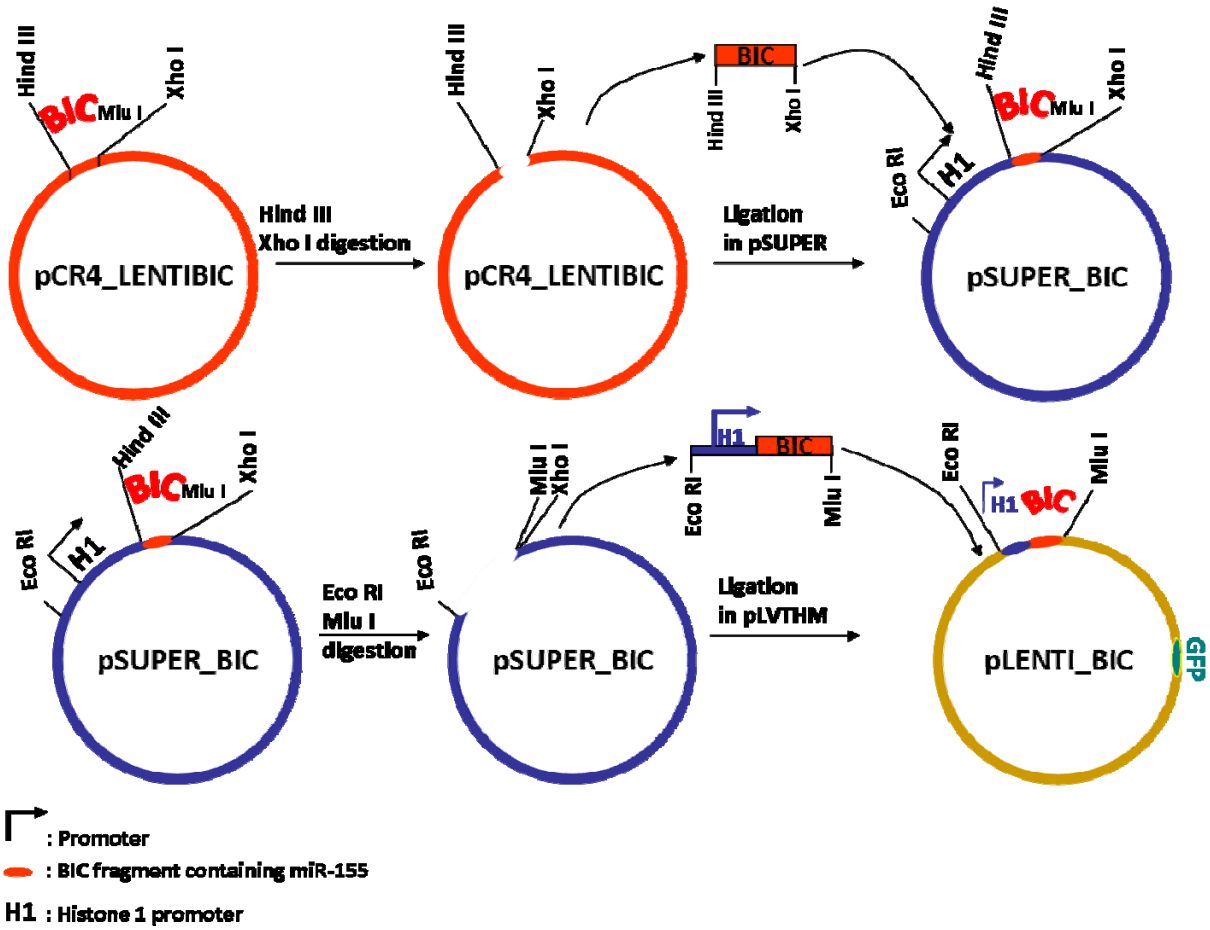

Figure 8 Cloning steps for constructing miR-155 lentiviral vector. Upper row: pCR4_LENTI_BIC harbours the genomic fragment form BIC gene containing a Hind III site at its 5'end and Mlu I+XhoI sites at its 3' end. After digestion with HindIII+XhoI, the excised fragment was subcloned into pSUPER constructing pSUPER_BIC. Lower row: pSUPER_BIC was digested with EcoRI+Mlu I enzymes; the resulting fragment including the histone 1 (H1) promoter and BIC was cloned into pLVTHM leading to the construction of pLENTI_BIC, lentiviral vector used for the generation of THP1-155 cells.

pRLTK_ 3´UTR_PU.1: The construction of this vector is summarized in Fig.9. The 3´UTR of PU.1 was amplified from genomic DNA by PCR following the protocol established by (Ralser et al., 2006) using primers 3´UTR_PU.1_FOR TCT AGA TAC GAC TTC AGC GGC GAA GTG CTG and 3´UTR_PU.1_REV_BamHI GGA TCC GGA TTG AGA ATA ACT TTA CTT G. The conditions for the PCR were modified due to the high GC content of this region (discussed in section 4.2.1). The protocol established by Ralser et al. includes the use of a solution called CES containing 0,54M betaine, 1.34mM DTT, 1.34% DMSO and 11mg/ml BSA (final concentrations). The volume used in the PCR reaction was 30µl and the amount of genomic DNA 50pg. Gradient PCR determined the optimal annealing temperature between 58 and 60 degrees. PCR conditions were as follows:

95°C 10min	
95°C 30secs	40 cycles
58°C to 60°C 30sec	
72°C 1min	
72°C 10min	
4°C until samples were collected and kept on ice	

The amplified region was cloned into pCR4 with TOPO TA Cloning Kit (Invitrogen) leading to **pCR4_3´UTR PU.1** (represented in Fig.9, left hand vector). Clones were checked by sequencing (Geneservice, Oxford-Appendix 2). **pCR4_3´UTR PU.1** was then digested with Xba I+Not I enzymes and the excised fragment subloned into the reporter vector pRLTK Basic (Promega). For the ligation step, T4 DNA Ligase High Concentrated (NEB) was used overnight at 16°C following manufacturer's instructions. The constructed vector was named **pRLTK_3'UTR_PU.1** (Fig.9, vector represented on the right side).

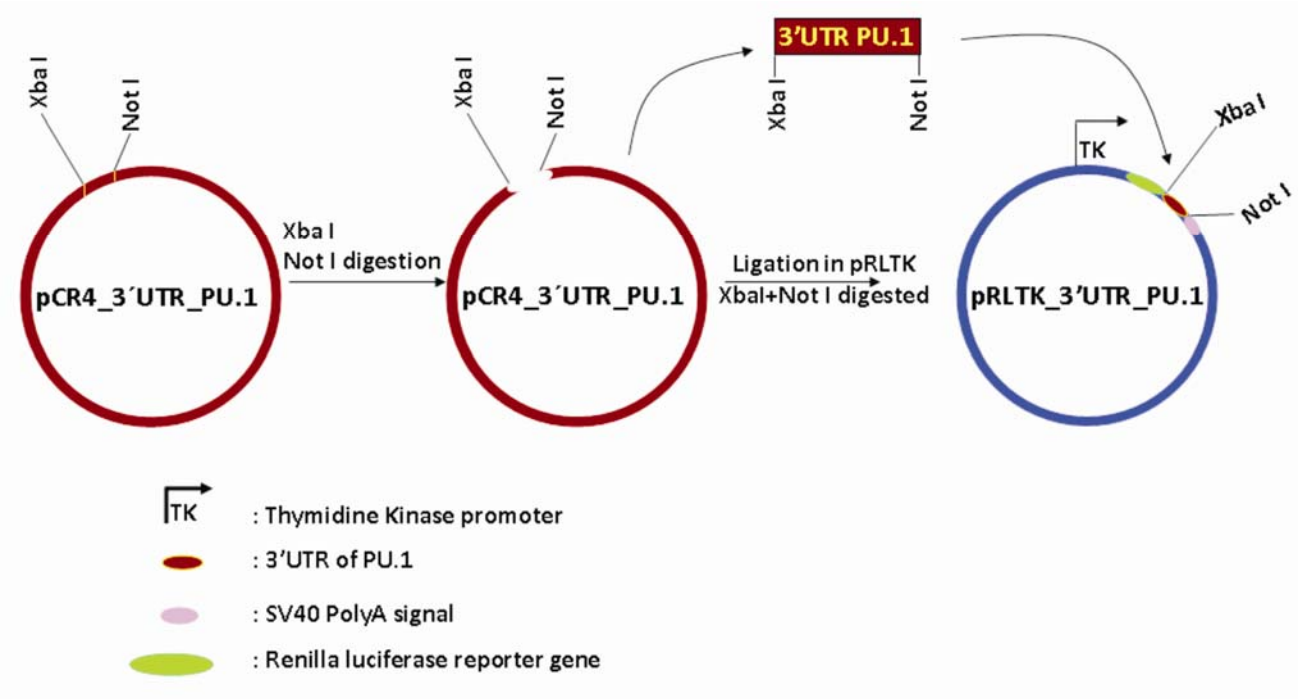

Figure 9 pRLTK_3'UTR_PU.1 reporter vector cloning steps. The 3'UTR of PU.1 was firstly cloned into pCR4 TOPO TA (left vector pCR4_3'UTR PU.1). It was then excised using Xba I/Not I enzymes and subsequently cloned into pRLTK (Promega) leading to pRLTK_3'UTR_PU.1 reporter vector. This was the reporter vector used in the luciferase assays testing miR-155 direct targeting of PU.1 3'UTR.

pRLTK_MUT_3´UTR_PU.1: this vector was generated by site directed mutagenesis on **pRLTK_3´UTR_PU1**. This vector was mutated in the putative miR-155 binding site (positions 45 to 51 of PU.1 3'UTR) using the following primers: 3´UTR_MUT_PU.1 FOR GCC TCC CCG CTG GCC TGA ATT CGA AGC CCT CGC CCG GCC CGG 3´UTR_MUT_PU.1 REV CCG GGC CGG GCG AGG GCT TCG AAT TCA GGC CAG CGG GGA GGC. Mutagenesis was done using the QuickChange© Site-Directed Mutagenesis Kit (Stratagene) following manufacturer's instructions. The predicted seed region of miR-155 was changed in the 3'UTR of PU.1 into an EcoRI site to easily check mutated clones.

The pair of PCR primers was designed following manufacturer's instructions:

- both primers contained the same mutation and primers annealed in opposite strands of the same sequence;

- primers length was between 25-45nt (42nt in this case);

- primers meting temperature (T_m) was greater than or equal to 78°C using the formula $T_m = 81.5 + 0.41(\%GC)-675/N - \%$ mismatch where "%GC" is the percentage of guanosine+cytosines in the primer and "N" is number of nucleotides in the primer;

- primers GC content must be at least 40%;

- primers should preferentially terminate in on or more G or C bases;

- primers should contain the desired mutation in the middle of the primer flanked by 10-15nt of correct sequence on each side.

pCDNA3.1_PU.1_3'UTR. This vector contains the full length cDNA PU.1 sequence. It was generated by cloning the 3'UTR fragment of PU.1 from **pCR4_3´UTR PU.1** into **pCDNA3.1_PU.1** (vector that codes for PU.1 and lacks the 3'UTR of PU.1; see 2.3.2). **pCR4_3´UTR PU.1** was digested with EcoRI to excise the 3'UTR of PU.1 and blunt ends were then generated using Klenow DNA polymerase. **pCDNA3.1_PU.1.** construct was linearized using Hind III and filled with Klenow polymerase to generate blunt ends. The linearized vector was subsequently dephosphorylated Alkaline Phosphatase Calf Intestinal (CIP) to avoid religation of undigested **pCDNA3.1_PU.1.** Each one of these digestion+filling steps was followed by heat inactivation of the enzymes and purification

of the fragments using QIAquick PCR Purification Kit (Qiagen). Ligation was performed using Quick Ligation™ Kit (NEB) 5 min at room temperature.

pRLTK_WT_IL13RA1_3'UTR: The steps for constructing this vector are summarized in Fig.10. The 3'UTR of IL13RA1 was amplified using 120ng of the plasmid clone HmiT009700-MT01 (Gene Copoeia) as template and the following primers: IL13RA1_3'UTR_FOR GGC TGT TAG GGG CAG TGG AG and IL13RA1_3'UTR_REV CAG AGC CTT GGC TGG CTG G. The PCR reaction included CES solution (0,54M betaine, 1.34mM DTT, 1.34% DMSO and 11mg/ml BSA) (Ralser et al., 2006). PCR reaction volume was 30µl; the PCR protocol was a "touch up" as follows:

95°C 7min	
95°C 40secs	40 cycles
58°C +0.2°C/cycle 30sec	
72°C 1min 20secs	
72°C 10min	
4°C until samples were collected and kept on ice	

The amplified product was cloned into pCR2.1 TOPO TA (Invitrogen) generating **pCR2.1._3'UTR_IL13RA1** (Fig.10, left hand vector) and checked by sequencing (Geneservice, Oxford-Appendix 3). The amplified fragment was excised from **pCR2.1_2'UTR_IL13RA1** with Bam HI/NotI enzymes and inserted into Not I linearized pRLTK (Promega) (Fig.10, right vector). In these cut+filling steps, both insert and vector were then subjected to blunt ending with Klenow DNA polymerase. Vector was dephosphorylated using CIP prior ligation of the insert. Both vector and insert were purified using QIAquick PCR Purification Kit (Qiagen) after digestion and filling to ensure the quality of DNA and eliminate possible enzymatic contaminations. Ligation was performed using Quick Ligation™ Kit (NEB) 5 min at room temperature to obtain **pRLTK _WT_IL13RA1_3'UTR** (right hand vector in Fig.10).

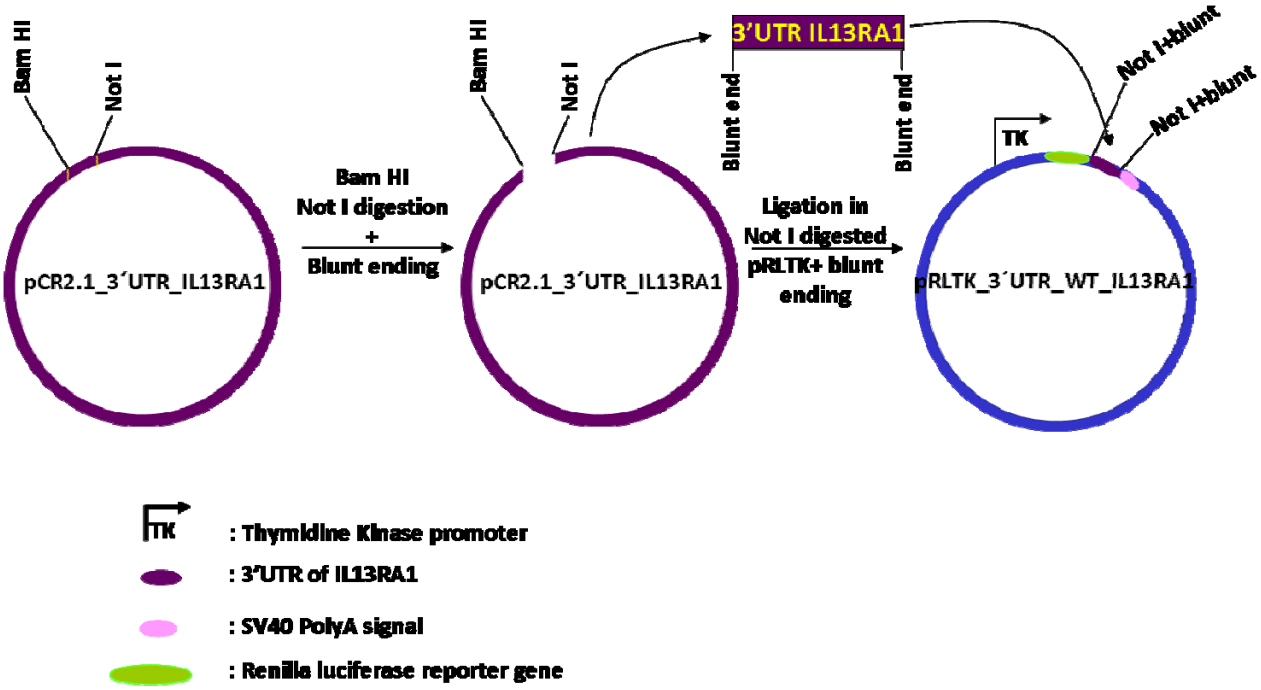

Figure 10 Cloning steps to obtain pRLTK_WT_3'UTR_IL13RA1. The fragment of IL13RA1 3'UTR containing both predicted binding sites for miR-155 was amplified by PCR and cloned into pCR2.1 TOPO TA (Invitrogen), clone named as pCR2.1_3'UTR_IL13RA1 (vector represented on the left). This fragment was then excised using Bam HI and Not I and filled with Klenow Polymerase. This insert was then cloned into Not I digested and subsequently blunt ended pRLTK (Promega) obtaining pRLTK_WT_3'UTR_IL13RA1.

pRLTK__MUT1_3´UTR_IL13RA1 and pRLTK__MUT2_3´UTR_IL13RA1. These clones were obtained by site directed mutagenesis of **pRLTK__WT_3´UTR_IL13RA1** using QuickChange Site Directed Mutagenesis (Stratagene) following manufacturer's instructions, as previously described for **pRLTK_MUT_3'UTR_PU.1** construction. MiR-155 was predicted to bind to two sites in the 3'UTR of IL13RA1 named Site1 and 2 hence forth. Mutation of Site 1 (positions 1049-1071 of IL13RA1 3'UTR) led to the construction of the reporter **pRLTK_MUT1_3´UTR_IL13RA1**. Primers employed were IL13RA1_3'UTR_MUT1_FOR CTG CTA CTC AAG TCG GTA CCA CTG TGT CTT TGG TTT GTG CTA GGC CCC and IL13RA1_3'UTR_MUT1_REV GGG GCC TAG CAC AAA CCA AAG ACA CAG TGG TAC CGA CTT GAG TAG CAG. Site 2 was predicted to map to positions 1399-1424 of IL13RA1 3'UTR; mutation of this site led to the construction of **pRLTK__MUT2_3´UTR_IL13RA1**. Primers employed were IL13RA1_3'UTR_MUT2_FOR CCA TGT GAG GGT TTT CAG GGC CGA TAT TTG TGC ATT TTC TAA ACA G and IL13RA1_3'UTR_MUT2_REV CTG TTT AGA AAA TGC ACA AAT ATC GGC CCT GAA AAC CCT CAC ATG G. Clones were checked by sequencing (Geneservice, Oxford).

Vectors generated in this study are listed in Table 1 and primers used in Table 2.

	Vector name	Clone	Vector function
miR-155	**pCR4_BIC**	BIC- pri-miR-155	Cloning
	pCDNA3.1.BIC	BIC- pri-miR-155	Expression
	pSUPER_BIC	BIC- pri-miR-155	Sub-cloning
	pCR4_LENTIBIC	BIC- pri-miR-155	Cloning
	pLENTI_BIC	BIC- pri-miR-155	Lentiviral expression
PU.1	**pCR4_3´UTR PU.1**	WT 3'UTR PU.1	Cloning
	pRLTK_3´UTR_PU.1	WT 3'UTR PU.1	Reporter
	pRLTK_MUT_3´UTR_PU.1	Mutant 3'UTR PU.1	Reporter
	pCDNA3.1_PU.1_3'UTR	Full length PU.1 protein	Expression
IL13RA1	**pCR2.1._3'UTR_IL13RA1**	WT 3'UTR IL13RA1	Cloning
	pRLTK _WT_IL13RA1_3'UTR	WT 3'UTR IL13RA1	Reporter
	pRLTK__MUT1_3´UTR_IL13RA1	Mutant1 3'UTR IL13RA1	Reporter
	pRLTK__MUT2_3´UTR_IL13RA1	Mutant2 3'UTR IL13RA1	Reporter

Table 1 List of vectors generated during this study. From left to right, first column shows the gene these constructs relate to. Second column shows the name of the vector; third column shows the cloned product and fourth column the function or use of the vector.

	Name	Sequence
miR-155	**BIC_FOR**	CTC GAG TAT GCC TCA TCC TCT GAG TGC
	BIC_REV	AAG CTT ACG AAG GTT GAA CAT CCC AGT GAC C
	BIC_LENTI_FOR	AAG CTT TAT GCC TCA TCC TCT GAG TGC
	BIC_LENTI_REV	CTC GAG ACG CGT ACG AAG GTT GAA CAT CCC AGT GAC C
3'UTR PU.1	**3´UTR_PU.1_FOR**	TCT AGA TAC GAC TTC AGC GGC GAA GTG CTG
	3´UTR_PU.1_REV_BamHI	GGA TCC GGA TTG AGA ATA ACT TTA CTT G
	3´UTR_MUT_PU.1 FOR	GCC TCC CCG CTG GCC TGA ATT CGA AGC CCT CGC CCG GCC CGG
	3´UTR_MUT_PU.1 REV	CCG GGC CGG GCG AGG GCT TCG AAT TCA GGC CAG CGG GGA GGC.
3'UTR IL13RA1	**IL13RA1_3'UTR_FOR**	GGC TGT TAG GGG CAG TGG AG
	IL13RA1_3'UTR_REV	CAG AGC CTT GGC TGG CTG G
	IL13RA1_3'UTR_MUT1_FOR	CTG CTA CTC AAG TCG GTA CCA CTG TGT CTT TGG TTT GTG CTA GGC CCC
	IL13RA1_3'UTR_MUT1_REV	GGG GCC TAG CAC AAA CCA AAG ACA CAG TGG TAC CGA CTT GAG TAG CAG
	IL13RA1_3'UTR_MUT2_FOR	CCA TGT GAG GGT TTT CAG GGC CGA TAT TTG TGC ATT TTC TAA ACA G
	IL13RA1_3'UTR_MUT2_REV	CTG TTT AGA AAA TGC ACA AAT ATC GGC CCT GAA AAC CCT CAC ATG G

Table 2 List of primers used in this study. From left to right, first column shows the the gene amplified by these primers; second column shows the name of the primer and third column the primer sequences.

2.3.2 Other vectors

Other vectors used in this study were either commercially purchased or provided by other groups:

Lentiviral system: **pPAX2**, **pMD2G** and **pLV/tTR_KRAB_Red** were kindly provided by Prof. Didier Trono (Ecole Polytechnique Fédérale de Lausanne, Switzerland). The viral envelope is encoded in **pPAX** and capsid proteins are transcribed from **pMD2G**. **tTR_KRAB_Red** encodes for dsRed reporter gene and for the KRAB repressor (see 2.4.1 and 3.5).

MiR-155 direct targeting of PU.1 and IL13RA1 3'UTRs: **pGL3 Control** (Promega) was used as normalizer in the transfections performed to determine the direct targeting of PU.1 and IL13RA1 3'UTRs by miR-155.

Promoter assays: **pCD209–468 pXP2** and **pCDNA3.1_PU.1** were kindly provided by Prof. Angel L. Corbi (Centro de Investigaciones Biologicas, Madrid, Spain); these constructs have been previously described elsewhere (Dominguez-Soto et al., 2005). **pCD209–468 pXP2** is a reporter vector that harbors a fragment of DC-SIGN promoter containing a PU.1 binding site at the 5' of a firefly luciferase reporter gene (thus, controlling its transcription in a PU.1 dependent manner). **pCDNA3.1_PU.1** is an expression vector for PU.1 protein that lacks the 3'UTR of PU.1. **pRLTK** (Promega) was used as normalizer in promoter assays

2.4 Lentiviral work: THP1-155 cell line generation

The lentiviral system used in this study was generated and described previously (Wiznerowicz, M. and D. Trono, 2003). This system consists on two different lentiviruses that share both the envelope and capside proteins and differ in the lentivirus genome (see 2.3.1. for **pLENTI_BIC** and 2.3.2 for the other vectors). The viral genome harbours the transgene that will be transduced in the host cell.

2.4.1 Viral stocks production

HEK293 T cells were used as packaging cells to generate viral stocks. HEK293 T cells were transfected with Superfect (Qiagen) following manufacturer´s instructions; plasmid DNA amounts employed were: 5µg of pLVTHM_BIC construct (or pLV/tTR_KRAB_Red when appropiate), 3.75µg of pPAX2 and 1.5µg of pMD2G vectors. Cell supernatants were collected 48h post transfection and centrifuged at 1500 rpm during 15min to pellet cell debris and also avoid possible cell cross-contamination. Centrifuged supernatant containing lentiviral particles was then added to THP-1 cells. Fresh medium was added to HEK 293 T cells and 24h later supernatants were again collected, centrifugued at 1500 rpm during 15min and used in a second infection of the cells.

2.4.2 THP-1 cells transduction protocol

THP-1 cells were doubly transduced in two different rounds of infection (of double infections as explained in 2.4.1) to generate the THP1-155 cell line. A first round of infection was done with pLENTI_BIC derived-viruses (two infection steps) to generate THP-1 cells stably harbouring this construct. pLENTI_BIC vector contained both the cloned miR-155 transgene (see 2.3.1) and a GFP marker under a Tet-On controlling system. Transduced cells were sorted by FACS using GFP as reporter gene. Sorted cells were then re-infected with pLV-tTR-KRAB containing-viral particles (second round of infection performed in two infection steps). This viral construct provides inducibility to the system as explained in 3.5. These cells were then sorted again constituting the inducible THP1-155 cell line.

Cells were plated onto 6 well plates at a cell density of 2.6-3·10^5 cells/ml and incubated with 8µg/ml of polybrene (SIGMA) 30 min at 37°C to enhance the efficiency of infection (Coelen et al., 1983). Supernatants from 48h post transfected HEK293T cells were added on THP-1 cells in a ratio of 1:1. Cells were then centrifuged at 2000rpm during 90 min at 37°C and incubated under normal conditions afterwards (37°C and 5%CO_2). Infection was repeated 24h later using supernatants of 72h post transfected HEK293 T cells following the same conditions except that no polybrene was added. Transduction efficiency was assesed 4 days after this second infection by flow cytometry and GFP positive cells were sorted.

Sorted cells were then infected following the same conditions and steps with lentiviral particles derived from pVL/tTR-KRAB plasmid. This vector harbors tTR-KRAB, a fusion protein in which KRAB module represses transcription of nearby promoters and tTR confers tetracycline inducibility (see section 3.5 and Fig.23). Both miR-155 and GFP genes harboured in pLENTI_BIC are transcribed from promoters with TR (Tetracycline Response) elements. Thus, in the presence of tTR-KRAB cells harbouring pLENTI_BIC phages become GFP negative. After the second transduction with pVL-tTR-KRAB-viruses, GFP negative cells were sorted. Because this population contained also non-infected GFP negative cells, doxycycline was added to the medium to select only miR-155-GFP containing cells. After culturing cells in the presence of doxycycline during one week, a third sorting round was then performed to purify only GFP-miR-155 positive cells, population that constituted the THP-1 155 cell line.

2.5 Dual Luciferase system

The Dual Luciferase Reporter (DLR) system is an *in vitro* tool to determine the translational effects of non-protein coding sequences. It consists on two different reporter genes, Renilla and Firefly luciferase, in which one is used as reporter and the other as normalizer. These genes code for enzymes that catalyze the conversion of different substrates in a chemical reaction that leads to the emission of light of different wavelengths (represented in Fig.11). To assay promoter activity (like that exerted by transcriptional factors) sequences are cloned at the 5' end of the reporter gene, which translation will depend on the transcriptional activity of the promoter. To assay post transcriptional regulation (like that exerted by microRNAs), sequences are cloned at the 3'end of the reporter leading to post transcriptional control of the reporter gene. In both cases, translational effects are measured as light emission readout captured by a luminometer.

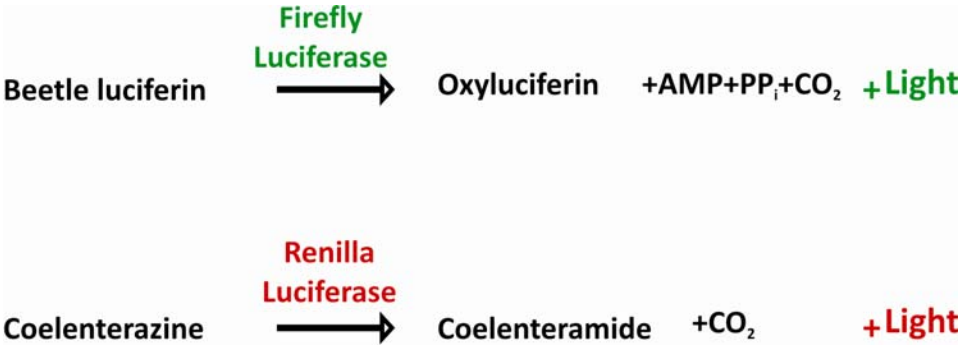

Figure 11 Dual Luciferase Reporter enzymatic reactions. Firefly Luciferase (upper reaction, in green) and Renilla Luciferase (lower reaction, in red) are two enzymes that can be both used as reporter and normalizer genes. These enzymes catalyze the conversion of different substrates (beetle luciferin and colenterazine, respectively) with the emission of light of different wavelengths, represented as green and red colors. These different light emissions are captured by a luminometer and serve as readout of the enzyme quantity in each of the reactions.

Dual-Luciferase Reporter Assay System (Promega) was used to determine the direct targeting of PU.1 and IL13RA1 3'UTRs by miR-155. These 3'UTRs were cloned into pRLTK (Promega) at the 3' end of the reporter Renilla luciferase (explained in sectior 2.3.1.) constituting pRLTK_3'UTR_PU.1 and pRLTK_WT_3'UTR_IL13RA1, respectively. The assay is summarized in Figure 12. Renilla luciferase was used as reporter gene for assaying miR-155 effects and Firefly lucifearse (encoded in pGL3 Basic vector, see 2.3.2) was used as normalizer.

Figure 12 Luciferase system representation for miR-155 direct targeting of a given 3'UTR. Renilla luciferase reporter vector (up in blue) harbouring Renilla gene ("Renilla" in red) fused to the assayed 3'UTR ("3'UTR" in pink) is co-transfected with or without a miR-155 over expressing vector (indicated as "MiR-155" in green). The absence of miR-155 over expression (upper reaction) leads to a basal expression of the construct with the concomitant light emission in the luciferase enzymatic assay. The over expression of miR-155 (lower reaction) inhibits the expression of the Renilla construct leading to a decreased light emission in the luciferase enzymatic reaction.

The DLR system was also used for promoter assays (see 3.6.4) and it is summarized in Fig.13. The assayed promoter is cloned at the 5' end of the reporter gene and the light measured is readout of the reporter transcriptional activity. In this case Firefly luciferase was used as reporter gene and Renilla luciferase as normalizer

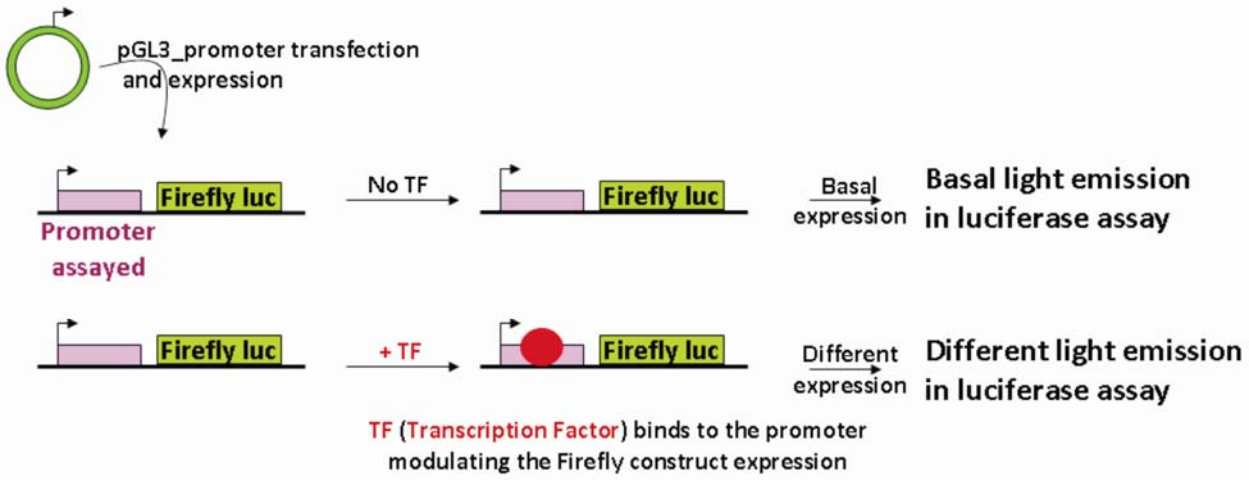

Figure 13 Luciferase system representation for promoter assays. The promoter assayed (in pink) is cloned at the 5' end of the reporter Firefly luciferase (Firefly luc, in green). The presence of a transcription factor (TF in red) modulates the transcriptional activity of the Firefly construct, which is measured as light emission captured by a luminometer.

2.6 Plasmid transfections

In all cases, plasmid DNA preparations were isolated and purified using Plasmid Maxi Kit (Qiagen) following manufacturer's instructions.

2.6.1 Direct targeting of PU.1 by miR-155

pRLTK, pRLTK_WT_3´UTR_PU1 or **pRLTK_MUT_3´UTR_PU1** plasmids were co-transfected with **pCDNA3.1.BIC** or **pCDNA3.1** empty vector into HeLa cells employing Superfect (Qiagen) following manufacturer's instructions. Normalization was done by co-transfection of pGL3 (Promega). Assays were measured employing the Dual-Glo kit (Promega). The experiments were performed three times in triplicates. Statistical differences were determined using Student's t test.

2.6.2 Direct targeting of IL13RA1 by miR-155

The constructs **pRLTK_WT_3´UTR_IL13RA1**, **pRLTK_MUT1_3´UTR_IL13RA1** or **pRLTK_MUT2_3´UTR_IL13RA1** were co-transfected with **pCDNA3.1.BIC** or **pCDNA3.1** empty vector into HeLa cells employing LT1 (Mirus) following manufacturer's instructions. Normalization was achieved by co-transfecting pGL3 (Promega). Assays were measured employing the Dual-Glo kit (Promega). Experiments were performed three times in triplicates. Statistical differences were determined using Student's t test and GraphPad Prism, Prism 5 version 5.00 for Windows software.

2.6.3 Promoter assays

These experiments were performed by Dr. Tilman Sanchez-Elsner (University of Southampton, UK). **pCD209–468 pXP2** harbours the proximal region of DC-SIGN promoter reported to be bound by PU.1 transcription factor (Dominguez-Soto et al., 2005). **pCDNA3.1-PU.1** encodes for PU.1 without 3'UTR (see 2.3.2). **pCDNA3.1_PU.1_3'UTR** construct is explained in 2.3.1. THP-1 155 cells were transfected using DEAE-dextran following standard procedures. pRLTK (Promega) was used as normalizer. Assays were measured employing the Dual-Glo kit (Promega). Experiments were repeated at least three times in triplicates. Statistical analysis was performed using student's t-test.

2.7 Anti-microRNA transfections

2.7.1 THP-1 and THP1-155 cells transfection

THP-1 or THP1-155 cells were seeded at $2.5 \cdot 10^5$ cells/mL onto 24well plates in RPMI serum free medium in a volume of 400μL/well. Preliminary experiments showed that higher cellular concentrations rendered lower transfection efficency and cell viability was reduced at lower concentrations.

The transfection protocol employed is summarized as follows:

1. Seed cells in serum free media.

1. Mix 2μl Oligofectamine + 3.7μl Opti-Mem◊ incubate 5min at room temperature.

2. Mix 40μl Optimem+ Anti-miRNA Inhibitors (Anti-155 or Control, 0.8μL of 50μM stock)◊ add the previous mixture of Oligofectamine/Opti-Mem◊ incubate 20min at room temperature◊ add on top of the cells.

3. Addition of 100 ul of RPMI 50%FBS to reach normal culture conditions (10%FBS) 3h post transfection.

Cells were collected at 24h and 48h post transfection; RNA was extracted using TRIzol (see 2.8) and subjected to analysis (see 2.9).

2.7.2 Dendritic Cells transfection

For the pathogen binding experiments, mature DCs (see 2.2.2) were transfected with 100 nM of Anti-miR-155 Inhibitor or Anti-miR Inhibitors—Negative Control # (Applied Biosystems), and 50 nM of Cy3-premiR-control-1 (Ambion) at day 5 of culture. Cy3 fluorescence was used in order to assess transfection efficiency by flow cytometry. These cells are transfected with no need of reagents/transfection techniques avoiding possible undesired effects of these. It is likely that they uptake the oligonucleotides by natural phagocytosis or passive diffusion. Cells were collected, counted and plated at a cell density of $1.5 \cdot 10^6$cells/ml in 96 round bottom well plates. Medium and cytokines were renewed and LPS and anti-miRNA probes were added. Binding assays and DC-SIGN surface expression were assayed 48h post transfection by flow cytometry (see 2.11.1). Transfection efficency was checked by qPCR detection of miR-155 (see 2.9.2).

2.7.3 Macrophages transfection

Following human monocyte isolation (see 2.2.2 and 2.2.3) cells were plated onto 96 well plate (flat bottom) in the presence of 500U/ml of GM-CSF (Immunotools) to induce macrophage differentiation. 100nM Anti-miR-155 Inhibitor or Anti-miR Inhibitors—Negative Control # (Applied Biosystems) were transfected in monocytes at day 0. 100nM Cy3-premiR-control-1 (Ambion) was used to check transfection efficency. As it happens with DCs, these cells are transfected by natural phagocytosis or passive diffusion. At day 3, some cells were collected and checked for miR-155 inhibition. 10ng/ml IL-13 was added or not to the cells and these were collected 24h post stimulation to check miR-155 effects on the IL-13 pathway.

2.8 RNA extraction

RNA samples were obtained using TRIzol (Invitrogen) and TRI Reagent Solution (Applied Biosystems), following manufacturer's instructions and modifying some of the steps. Briefly, after disrupting the cells with TRIzol or TRI Reagent Solution, samples were left 5 min at room temperature. 200 μl of chloroform per ml of TRIzol or TRI Reagent were added, vortexing samples for at least 15 secs and incubating them 5min at room temperature. Samples were then centrifuged at 13000 rpm in a bench minifuge at 4°C during 30 min in order to separate the organic and aqueus phases, the latter containing the RNA fraction. After taking the aqueus phase, RNA was precipitated in isopropanol (0.65 vols of isopropanol per vol TRIzol approximately) and glycogen (1mg/ml) during 10 min at room temperature followed by a minimum of 10 min at -80C. After centrifugation at 4°C at 13000rpm during 30 min, the pellet obtained was washed with chilled 75-80% ethanol (lower % could cause loss of small RNAs), left 15 min on ice and centrifugued at 13000rpm during 15min at 4°C. Ethanol was removed completelyand pellets were air dryed. RNA pellets were then resuspended in RNAse free water, and RNA concentration was determined using a Nanodrop.

2.9 Reverse Transcription and Real Time PCR analysis

2.9.1 Reverse Transcription

2.9.1.1 mRNA reverse transcription

RNA reverse transcription was performed using High Capacity cDNA Reverse Transcription Kit (Applied Biosystems) following manufacturer´s instructions. 400ng to 1μg of total RNA were used in the reverse transcription reaction, which was performed using Random Hexamer primers. The reverse transcription protocol employed was:

10min at 25°C
2h at 37°C
5min at 85°C
Hold at 4°C until samples were removed and kept on ice

After reverse transcription, Real Time PCR (Quantitative PCR or qPCR) was performed (2.9.2.1 and for protocol see 2.9.3).

2.9.1.2 MicroRNA Reverse Transcription

For the detection of microRNAs, 5ng of total RNA were used with High Capacity cDNA Reverse Transcription Kit (Applied Biosystems) with specific stem loop primers for miR-155, RNU6 or RNU44 from TaqMan® MicroRNA Assays (Applied Biosystems) following manufacturer's instructions.

Protocol for microRNA reverse transcription employed:

30 min at 16°C
30 min at 42°C
5min at 85°C
Hold at 4°C until samples were removed and kept on ice

After reverse transcription, Real Time PCR (Quantitative PCR or qPCR) was performed following manufacturer's instructions (2.9.2.2 and for protocol see 2.9.3).

2.9.2 Real Time PCR

2.9.2.1 mRNA Real Time PCR

Real Time PCR (Quantitative PCR or qPCR) for mRNA was performed following manufacturer's instructions using TaqMan® Universal PCR Master Mix, No AmpErase® UNG.

Two different probes were used: Perfect Probe and TaqMan. The difference in these probes relate to the structure of the detection probe: TaqMan probes are linear, Perfect Probe creates a stem loop. Both TaqMan and Perfect Probe detection probes and primers were designed to avoid intron amplification, thus excluding genomic contamination in the qPCR results. Detenction of DC-SIGN, PU.1 and ACTB1 in Chapter 3, and IL13RA1 and ACTB1 in Chapter 4 mRNA levels was done using PerfectProbe from PrimerDesign (Southampton SO15 0DJ). Genes assayed in Chapter 4 were detected using TaqMan® Gene Expression Assays (Applied Biosystems).

2.9.2.2 microRNA Real Time PCR

Real Time PCR for microRNAs was performed using TaqMan® Universal PCR Master Mix, No AmpErase® UNG following manufacturer's instructions. miR-155, RNU6 and RNU44 were detected using Applied Biosystems TaqMan® MicroRNA Assays following manufacturer's instructions.

2.9.2.3 Protocols for Real Time PCR

TaqMan:

95°C 8min

95°C 15secs
60°C 1min
} 40 cycles

Perfect Probe:

95°C 8min

95°C 15secs
50°C 30secs DATA COLLECTION
72°C 15 secs
} 40 cycles

Data collection and real time analysis enabled

72°C 10min

2.10 Western Blotting

Cells were lysed in NP-40 1%; 2mM Pefablock and 2 µg/ml aprotinin, leupeptin and pepstatin protease inhibitors were added in the moment of cell lysis. Alternatively, complete Protease Inhibitor Cocktail Tablets (Roche) were used.

Lysis was performed on ice during 15 min, and cell lysates were centrifuged at 13000 rpm in a top bench centrifuge at 4°C. Supernatants containing whole cell extracts were collected and quantified using the BCA Assay following manufacturer´s instructions. 30µg of cell lysates were mixed with 5x loading buffer (see 2.1.3) to a final concentration of 1x. Beta-Mercaptoethanol was added in a 1:50 ratio to ensure reducing conditions and samples were boiled during 5 min before subjected to SDS-PAGE.

For electrophoresis of the samples, two different systems were used. Chapter 3 results were obtained using Mini-PROTEAN Electrophoresis System and casting the gels using Acrylamide/Bis 29:1, N,N,N',N'-Tetramethylethylenediamine (TEMED) and ammonium persulfate (APS), all from Bio-Rad. Chapter 4 results were mainly obtained using precasted gels from Invitrogen: NuPAGE® Novex 4-12% Bis-Tris Gel 1.0 mm, 10 well and NuPAGE® Novex 4-12% Bis-Tris Gel 1.0 mm, 15 well, in the manufacturer's electrophoresis system XCell SureLock® Mini-Cell and XCell II™ Blot Module Kit CE Mark. The change in system did not affect the results, but the advantage of using pre-casted gels saves time and avoids possible inconveniences from casting the gels (leaking, time of polymerization, ease of use). Invitrogen system was only used in Chapter 4 and not 3 simply because of its availability.

Protein samples were then transferred onto an Immobilon polyvinylidene difluoride membrane during 90min at 100V and at 4°C. For blocking purposes, membrane incubation in TBS-T 5% non fat milk was carried for at least 1h at room temperature with the exception of memebranes for the detection of Phospho-STAT6 which were blocked in TBS 0.05% Tween 5% BSA.

Primary antibodies were incubated in different conditions, as follows:

- anti-βtubulin antibody was incubated in TBS 0.05% Tween 5% non fat milk during 1h at room temperature;

- anti-IL13RA1 antibody was incubated over night at 4ºC in TBS 0.1% Tween 5% non fat milk 0,1M NaCl;

- anti PU.1 primary antibody was incubated at 4°C over night in TBS containing 0.05% Tween and 5% non fat milk;

- anti-STAT-6 antibody was incubated over night in TBS 0.05% Tween 5% BSA at 4°C

- anti-Phospho-STAT6 antibody was incubated over night in TBS 0.05% Tween 5% BSA at 4°C

After washing the excess of primary antibody 3 times in TBS-0.05% Tween (or TBS-T 0.1% Tween in the case of anti-IL13Rα1), membranes were incubated 1h at room temperature with secondary antibody HRP conjugated anti rabbit (#P0448, DAKO) in TBS-0.05% Tween 5% non fat milk (or TBS-0.05% Tween 5%BSA in the case of detection of Phospho-STAT6)

The excess of secondary antibody was washed three times with TBS-0.05% Tween and protein detection was performed using the ECL (see 2.1.3).

Antibodies purchased from Santa Cruz Biotechnology, Inc. were α-PU.1 (sc-352); α-DC-SIGN (sc-20081), and α-IL13RA1 (sc-27861. As loading control it was used Anti beta Actin antibody - Loading Control (ab8227, abcam). Antibodies for STAT6 and Phospho-STAT6 were purchased from Cell Signalling Technology (#9362 and #9361, respectively).

2.11 Flow cytometry and microscopy analysis

2.11.1 DC-SIGN surface expression

Mature DCs were transfected with 50nM of anti-miR-155 or anti-Mir-Control as explained in 2.7.2. DC-SIGN surface expression was assayed 48h post transfection by flow cytometry. Staining of the cells was performed as follows:

- cells were blocked in FACS Blocking Solution (see 2.1.3.) 15 to 30min on ice;

- cells were then incubated with either 0.3 ng/ml APC-anti-DC-SIGN or APC IgG_{2a} isotype control during 1h on ice

- wash excess of unbound antibody using 10 volumes of cold PBS;

- cells were resuspended in FACS solution (see 2.1.3) and flow cytometry was performed.

Detection of APC fluorescence was performed in FL4 channel in a BD FACSAria™ Cell Sorting System (BD Biosciences) cytometer.

2.11.2 Pathogen binding assays

For the pathogen binding experiments mature DCs were transfected with 50nM of anti-miR-155 or anti-Mir-Control as explained in 2.7.2. Binding assays were assayed 48h post transfection.

2.11.2.1 Labelling of pathogens

C. albicans conidia were heat inactivated at 95°C during 20 minutes. After this, conidia were stained using propidium iodide (1mg/ml) during 1h at 4°C with shaking. Conidia were then washed with Binding Buffer (see 2.1.3) four times and counted with a hemocytometer.

gp120 protein (Trinity Biotech) was labelled with FITC using FluoroTag™ FITC Conjugation Kit (SIGMA) following manufacturer's instructions.

2.11.2.2 Pathogen binding assays

Pathogen binding assays were performed as follows:

- cells were collected and washed in binding buffer (see 2.1.3)

- cells were the incubated 30 min at 4°C in the presence of labelled *C.albicans* conidia were added in a 1:5 - 1:10 ratio

- for FITC-gp120 binding experiments, 1μg labelled FITC-gp120 was added and cells were incubated at 37°C during 20 min

- cells were washed with binding buffer twice and analyzed by flow cytometry in a BD FACSAria™ or a BD FACSCalibur cytometers (both from BD Biosciences).

2.11.3 Reactive Oxygen Species (ROS) detection

For the detection of ROS (Chapter 5), cells were monitored using a fluorescent microscope with a culture chamber at 37°C 5%CO_2. The excitation source and filters that were employed corresponded to those used for FITC.

In order to label the cells with ROS detector probe:

- cells were collected and washed with PBS;

- cells were resuspended at 10^6 cells/ml in PBS and incubated with OxyBURST® Green H2DCFDA in a dilution 1:1000 on ice during 30-40min. This is a cell-permeable indicator for reactive oxygen species that is not fluorescent until the acetate groups are removed by intracellular esterases and oxidation occurs within the cell

- positive control cells were incubated with 1:100 tert-Butyl hydroperoxide solution (TBHP)

- cells were washed in PBS and analyzed by fluorescent microscopy using Carl Zeiss Axio Vision software.

3 Chapter 3. Results: Role of miR-155 in dendritic cell pathogen binding ability

3.1 Introduction

Dendritic cells act at the interface between innate and adaptive immunity. In their immature state they recognise and bind to pathogens in peripheral tissues due to the expression of PRRs such as DC-SIGN. Upon binding of pathogens they undergo maturation while migrating to a lymphoid organ, where they will engage and activate lymphocytes. Maturation involves the down regulation of PRRs and up regulation of co-stimulatory molecules that will later allow lymphocyte activation (Fig.2). DCs present the sensed and processed pathogens in the form of antigens to the lymphocytes, which will then proliferate and develop the adaptive branch of the immune response in a pathogen-specific manner depending also on the microenvironment (Geijtenbeek and Gringhuis, 2009; Murphy et al., 2008). These adaptive immune responses can be classified into two main types, Th_1 or Th_2 (described in 1.1.1 and represented in Fig.1). Thus, to exert an effective immune response it is key that DCs sense and present pathogens correctly.

DC pathogen recognition relies primarily on DC surface receptors and membrane sensors such as DC-SIGN, a C-type (Calcium dependent) lectin present in immature DCs that is down regulated during DC maturation triggered by pro-inflammatory (pro-Th_1) stimuli like LPS (Geijtenbeek et al., 2000c; Steinman, 2001). Also known as CD209 (Cluster of Differentiation 209), DC-SIGN binds to a wide range of pathogens via mannose and fucose interactions. Mannose interactions include the ones with *Candida albicans* and the HIV glycoprotein gp120 (Cambi et al., 2003; Curtis et al., 1992). Besides, DC-SIGN also promotes transient adhesion with T cells trough ICAM-3 recognition, (Geijtenbeek, T.B. et al., 2000), DC transmigration across endothelium via ICAM2 interactions and neutrophil interaction via Mac-1 (Geijtenbeek, T. B.et al., 2000).

In myeloid cells, DC-SIGN transcription has been shown to be controlled by PU.1 (Dominguez-Soto et al., 2005). PU.1. dictates DC-SIGN basal levels and shows a parallel

expression during dendritic cell maturation (Serrano-Gomez et al., 2008). PU.1 is a key transcription factor in hematopoietic development, with an expression pattern restricted to B lymphoid, monocytic and granulocytic cells. PU.1 levels are tightly regulated during hematopoietic development in different lineages. It is required in a fine balance with MafB levels in order to determine a dendritic phenotype versus a macrophagic one (Bakri et al., 2005; Bharadwaj and Agrawal, 2007; Friedman, 2007). The low levels of PU.1 in PU.1 (-/-) cells achieved by the fusion of PU.1 to the estrogen receptor (PUER) and controlled by the addition of 4-hydroxy-tamoxifen (OHT) induced granulopoiesis while high levels primed monopoiesis (Laslo et al., 2006). The lack of one PU.1 allele has been shown to favour neutrophil development from embryonic stem cells (Friedman, 2007) and if PU.1 is expressed at 20% of its normal levels, monopoiesis loss is observed and granulopoiesis is preserved. Besides, PU.1 concentration has been reported to be critical for the development of B lymphocytes as compared with macrophages (DeKoter and Singh, 2000). Importantly, PU.1 has been described as a Th_2-type determining factor (Brunner et al., 2007; Chang et al., 2005a), being a key transcriptional factor in the establishment of a Th_2 phenotype.

Previous results in the lab (personal communication of Dr.T.Sanchez-Elsner) suggested a possible implication of BIC (MIR155 HG) in inflammatory (pro-Th_1) conditions in human macrophages, and shortly after miR-155 was shown to be involved in the inflammatory response of murine macrophages (O'Connell et al., 2007). Intriguingly, these stimuli can trigger DC maturation and bioinformatics' *in silico* tools predicted PU.1 as a putative target of miR-155.

3.2 Hypothesis and aims

3.2.1 Hypothesis

MiR-155 is up regulated during human dendritic cell maturation, leading to down regulation of DC-SIGN through direct targeting of PU.1 and modulating the pathogen binding ability of dendritic cells.

3.2.2 Aims

- To determine miR-155 and PU.1 expression during dendritic cell maturation

- To assay the direct binding of miR-155 to PU.1

- To create a cellular model in which miR-155 expression can be controlled and test miR-155 effects**.** Assay miR-155 effects in this model.

- To determine the effects of miR-155 in dendritic cell pathogen binding ability

3.3 MicroRNA 155 and PU.1 levels in dendritic cell maturation

3.3.1.1 Dendritic cell maturation phenotyping

Immature dendritic cells (iDCs) are present in peripheral tissues sampling their surroundings by PRRs such as DC-SIGN and binding of pathogens triggers DC maturation. Maturation involves a series of changes in DCs surface (Fig.2); typical features of maturation are the down regulation of DC-SIGN and up regulation of co-stimulatory molecules like CD83 or CD86 required for T-cell activation (Steinman, 2001). These phenotypical changes are in accordance with the different roles of DCs before and after maturation: from sensors and pathogen recognizers (immature DCs or iDCs) they become antigen presenting cells (mature DCs or mDCs).

Maturation can be mimicked *in vitro* by stimulating DCs with bacterial lipopolysacharide (LPS). iDCs (see section 2.2.2) were stimulated or not with 1μg/mL LPS and 48h later DC-SIGN, CD83 and CD86 surface expression was checked by flow cytometry. Figure 14 shows the flow cytometry profiles of immature DCs versus mature DCs. DC purity was checked by flow cytometry (data not shown). When comparing iDCs and mDCs, LPS triggered DC-SIGN down regulation whilst it promoted both CD83 and CD86 up regulation as shown by the numbers in upper right corners (mean fluorescence of the population). These flow cytometry profiles are the validation proof for the dendritic cell model and hypothesis, and starting point of work. It is shown one donor out of N>20. The shown flow cytometry profiles were provided by Dr.Fethi Louafi (University of Southampton, UK).

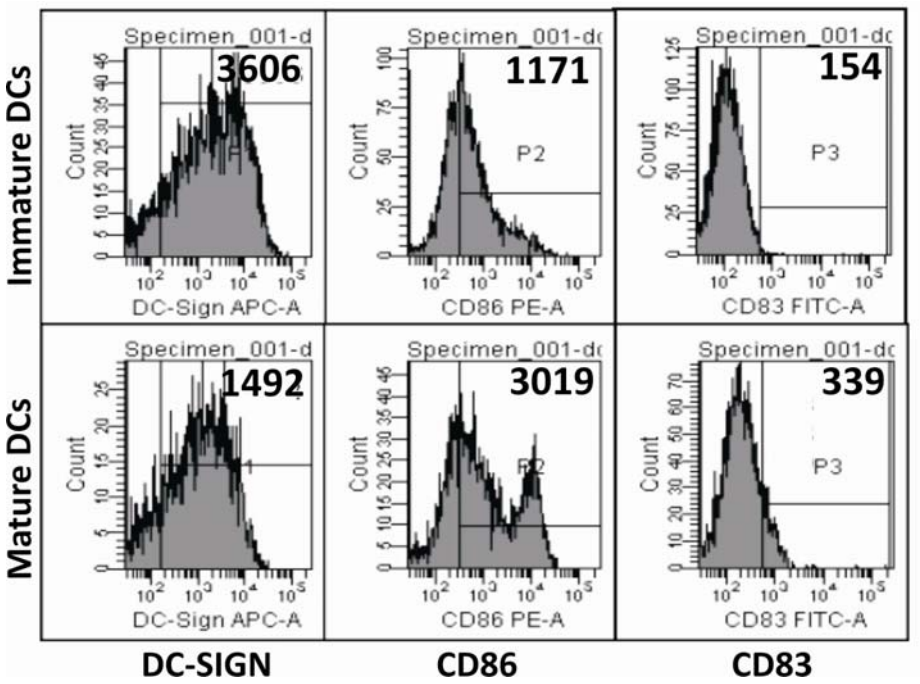

Figure 14 Flow cytometry profiles of maturing DCs. DCs were stimulated with LPS (lower row, Mature DCs) or not (upper row, Immature DCs) during 48h and analyzed by flow cytometry afterwards. DC-SIGN was down regulated whilst the co-stimulatory molecules CD86 and CD83 were up regulated as indicated by the population mean fluorescence numbers in the upper right corner of each plot. Left axis shows cell count and X axis shows fluorescence units (logaritmic scale).

Previous experiments in Dr.T.Sanchez-Elsner lab suggested a possible role of miR-155 in macrophages under inflammatory conditions. Shortly after, miR-155 was reported to be up regulated by LPS in murine macrophages (O'Connell et al., 2007). Several target databases and *in silico* tools predicted PU.1 as a candidate for miR-155 targeting (TargetScan, microCosm Targets, PITA, RNAHybrid). To test a possible link between PU.1 and miR-155 levels during dendritic cell maturation two objectives were assayed:

- Objective 1: Determination of miRNA-155 levels during dendritic cell maturation by specific reverse transcription followed by Real Time PCR.

- Objective 2: Determination of PU.1 protein and mRNA levels by Western Blotting and reverse transcription followed by Real Time PCR, respectively.

3.3.1.2 MiR-155 levels during DC maturation

Monocyte derived DCs were stimulated or not with 1μg/ml LPS (mDCs and iDCs, respectively) during the course of 48h. Levels of miR-155 were detected by specific

reverse transcription with stem loop primers followed by Real Time PCR (qPCR) amplification and quantification as described in section 2.9.1.2., 2.9.2.2. and 2.9.2.3. C_t (Cycle threshold) values of the qPCR for miR-155 oscillated between 27.5 (iDCs) and 20.5 (mDCs) approximately (Appendix 4). Results are shown in Fig.15: mir-155 levels augmented steadily during DC maturation, increasing up to 136 times 48h after LPS stimulation when compared to the basal levels (starting point of the time course)

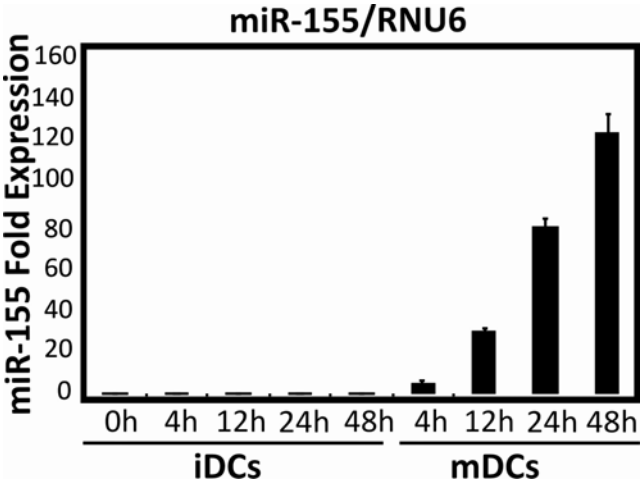

Figure 15 MiR-155 levels during dendritic cell maturation. DCs were incubated in the presence of LPS (mDCs) or not (iDCs) during 48h and mir-155 levels were detected at different time points (X axis) by specific reverse transcription followed by qPCR. RNU6 was used as house keeping gene. Mature DCs (mDCs) showed an up regulation of 136 times when compared to time 0. It is shown one experiment of a series of more than three.

3.3.1.3 PU.1 levels during dendritic cell maturation

Dendritic cells were subjected to maturation with LPS and PU.1 expression was analyzed at both protein and mRNA levels (Fig.16). Fig.16A shows a western blot for PU.1 protein (left panel) and its densitometry quantification (right panel). PU.1 protein expression dropped by 50% 48h post LPS treatment when compared to time 0 (starting point of the treatment). Fig.16B shows the results of the qPCR analysis for detecting PU.1 mRNA levels (see 2.8, 2.9.1.1, 2.9.2.1 and 2.9.2.3). PU.1 mRNA showed a decrease of 60% at 48h post stimulation. It is noticeable that PU.1 protein levels increased slightly in the case of immature DCs (iDCs) during the course of 48h while its mRNA levels remained almost constant under the same conditions. It is shown one experiment of a triplicate.

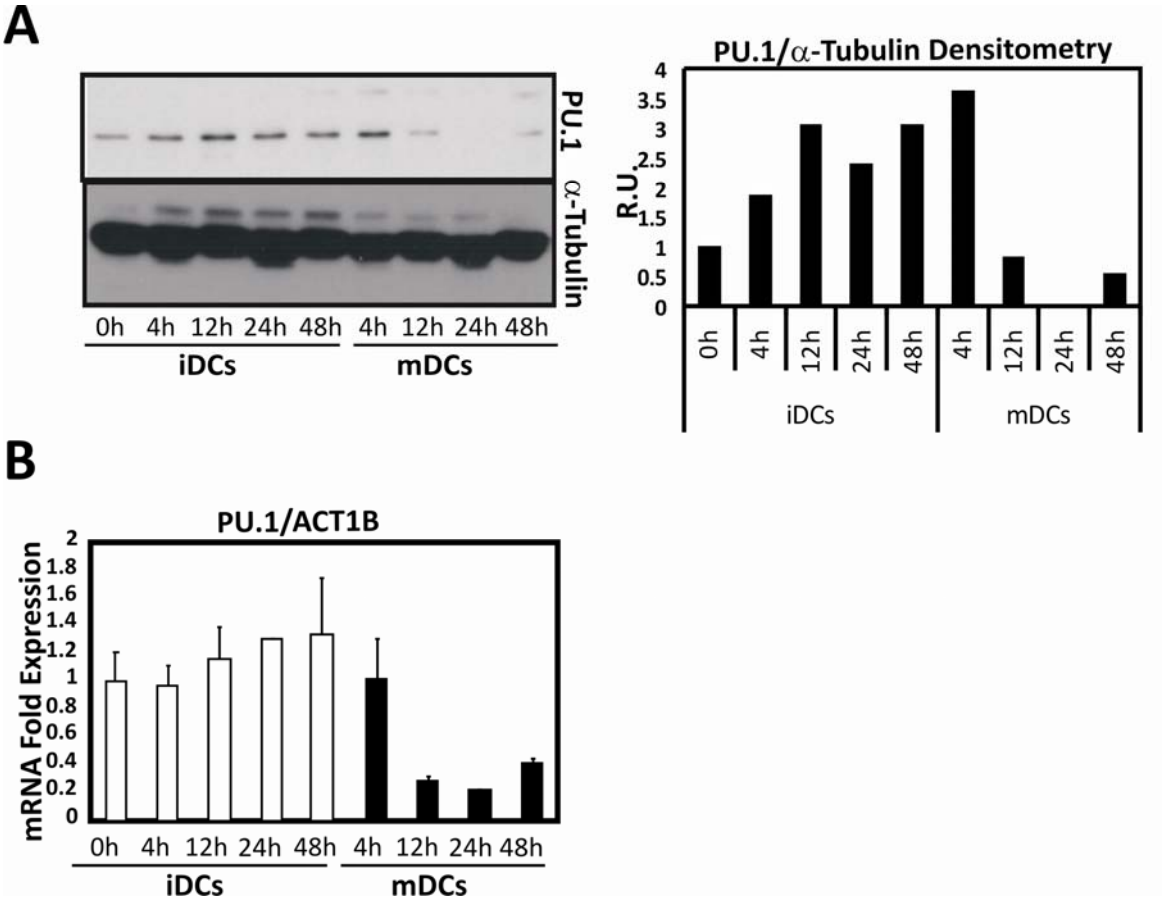

Figure 16 PU.1 levels during LPS-induced dendritic cell maturation. *A*: Left panel: Western blot of PU.1 protein during 48h of DC maturation time course. Immature DCs (iDCs) displayed higher levels than mature DCs (mDCs) as determined by densitometry (right panel). *B*: RT-qPCR analysis of PU.1 mRNA comparing immature DCs (iDCs) and mature DCs (mDCs). PU.1 mRNA levels dropped during DC maturation.

Thus, it was concluded that LPS triggers DC maturation during which DC-SIGN is down regulated (Fig.14), miR-155 is over expressed (Fig.15) and PU.1 protein and mRNA levels are diminished (Fig.16).

3.4 PU.1 is a direct target of miR-155

PU.1 was predicted as a putative target of miR-155; after observing the inverse correlation between miR-155 and PU.1 levels (Figs.15 and 16, respectively), the aim was to test the direct targeting of PU.1 3'UTR by miR-155. To assay this hypothesis several objectives were designed:

- Objective 1: Bioinformatics' analysis of PU.1 3'UTR::miR-155 interaction

- Objective 2: Cloning of PU.1 3´UTR in the reporter vector pRLTK. Site directed mutagenesis of the predicted binding site for miR-155.

- Objective 3: Co transfections of pRLTK-based reporter constructs with or without a miR-155 over expressing vector. Luminometry assays.

3.4.1 Bioinformatics' analysis of PU.1 3'UTR::miR-155 interaction

The first database used for the prediction of miR-155 targeting PU.1 was TargetScan 3.0 (June 2006 release). Other databases that were employed to analyze the possible interaction between miR-155 and the 3'UTR of PU.1 are listed in Table 3.

Database	miR-155 targets PU.1
TargetScan 5.1.	Yes
microRNA.org (January 2008)	No
microRNA.org (September 2008)	No
microCosm Targets	Yes
PITA	Yes
PicTar	No
Diana-microT 3.0	Yes

Table 3 MiR-155 predictions for PU.1 targeting amongst the different databases used

All these *in silico* tools are based on algorithms that predict the likelihood of binding between a given microRNA and a gene. This is achieved mainly by performing alignments between conserved 3'UTRs and miRNA sequences in search of Watson-Crick complementarity (John et al., 2006; Maragkakis et al., 2009). RNA secondary structure is also taken into account by some of them such as PITA algorithm, which relies on microRNA site accessibility modelling the thermodynamic stability of microRNA-target interaction (Hofacker, 2003; Kertesz et al., 2007).

3.4.1.1 TargetScan predictions

TargetScan 3.0 was the first prediction tool used for predicting miR-155 targeting of PU.1 3'UTR. MiR-155 was the only microRNA predicted to target the 3'UTR of PU.1; Fig.17 shows the predicted site for miR-155 in the 3'UTR of PU.1 that maps to nucleotides 45 to 51 of PU.1 3'UTR. Following the classification shown in Fig.5, miR-155 predicted site consists on a 8mer: an exact match to positions 2-8 of the mature miRNA (underlined in Fig.17) followed by an adenosine matching to nucleotide 1 of the mature miRNA.

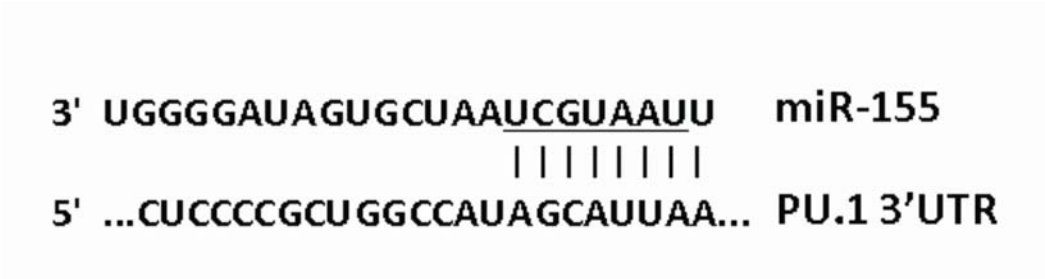

Figure 17 Predicted pairing between PU.1 3'UTR and miR-155 in TargetScan 5.1.

TargetScan 5.1 (last version) predicts miR-155 site as the only conserved one in the 3'UTR of PU.1 as shown in Figure 18. Other microRNAs are also predicted but those sites lack the conservation shown by miR-155.

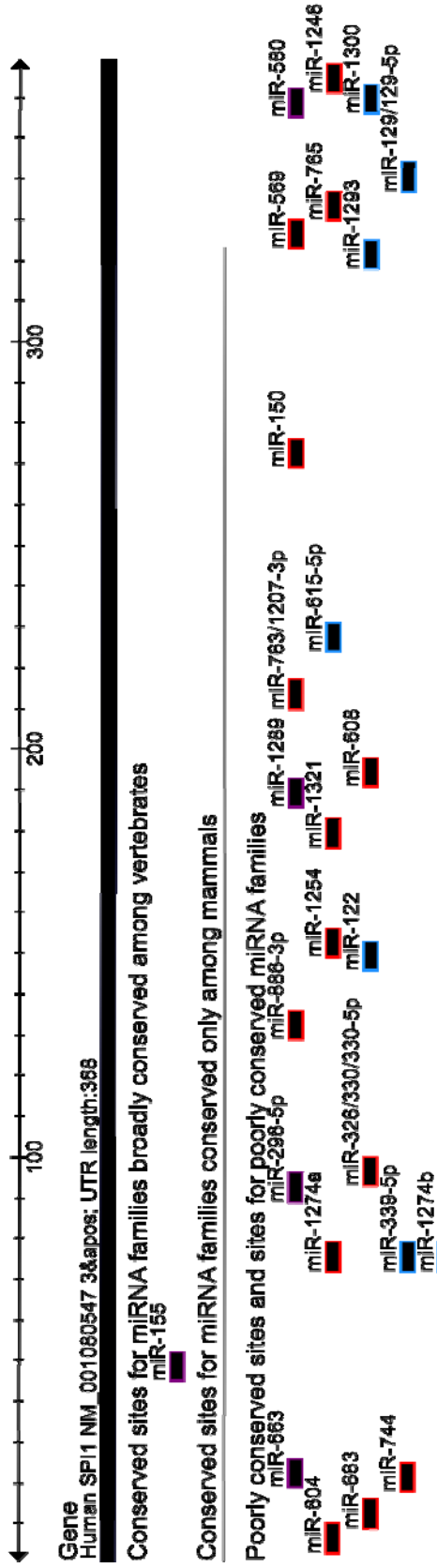

Figure 18 MicroRNAs predicted to bind to PU.1 3'UTR in TargetScan 5.1. MiR-155 is the only conserved site predicted as shown in the first row (Conserved sites for miRNA families broadly conserved amongst vertebrates). Image was downloaded from www.targetscan.org/vert_50 website.

3.4.1.2 miRanda,microCosm Targets, PITA, Diana-microT

miRanda, microCosm Targets, PITA and Diana-microT predicted the same site for miR-155 in PU.1 3'UTR. Figure 19 shows an example that corresponds to microCosm Targets web interface (source at http://www.ebi.ac.uk/enright-srv/microcosm/cgi-bin/targets/v5/search.pl). microCosm Targets predicts miR-155 site binding to the 3'UTR showing also additional base interactions in the 3' end of miR-155 between positions 32 and 53 of the 3'UTR of PU.1. The seed region of miR-155 binds to nucleotides 45-51 of the 3'UTR of PU.1.

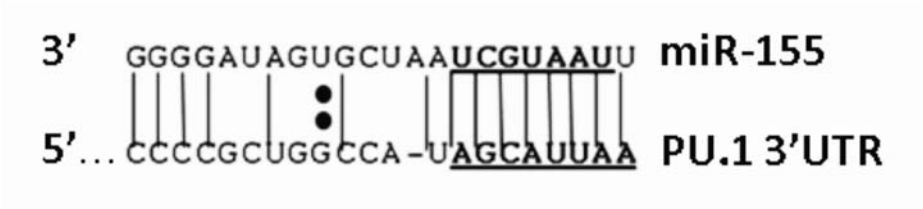

Figure 19 miR-155 predicted binding site in the 3'UTR by microCosm Targets. This in silico tool predicts additional base interactions between the 3' end of miR-155 and the 3'UTR of PU.1 MicroCosm Targets can be found at http://www.ebi.ac.uk/enright-srv/microcosm/cgi-bin/targets/v5/search.pl.

3.4.1.3 RNAHybrid

miR-155 predicted site in the 3'UTR of PU.1 is conserved amongst at least 7 species. During the course of this work miR-155 was shown to target PU.1 3'UTR in mice (Vigorito et al., 2007). microRNA::target interaction depends also on RNA secondary structure and site accessibility of the binding site. To test structural diferences in miR-155::PU.1 interaction between human and mouse, *in silico* structure analysis was performed. RNA folding of miR-155::3'UTR interaction was done using RNAHybrid (found at http://bibiserv.techfak.uni-bielefeld.de/rnahybrid/submission.html) (Rehmsmeier et al., 2004). It allows performing on line predictions for microRNA::target interaction. Fig. 20 shows the predicted secondary structures for miR-155::PU.1 3'UTR in human and mouse species. Despite the sites are conserved, the predicted RNA folding and energy released in the interaction is different between human (-26kcal/mol) and mouse (-24.2 kcal/mol). Higher energies mean more stability in the interaction. Thus, *in vitro* assays were required to confirm the prediction of human miR-155 binding to PU.1 3'UTR.

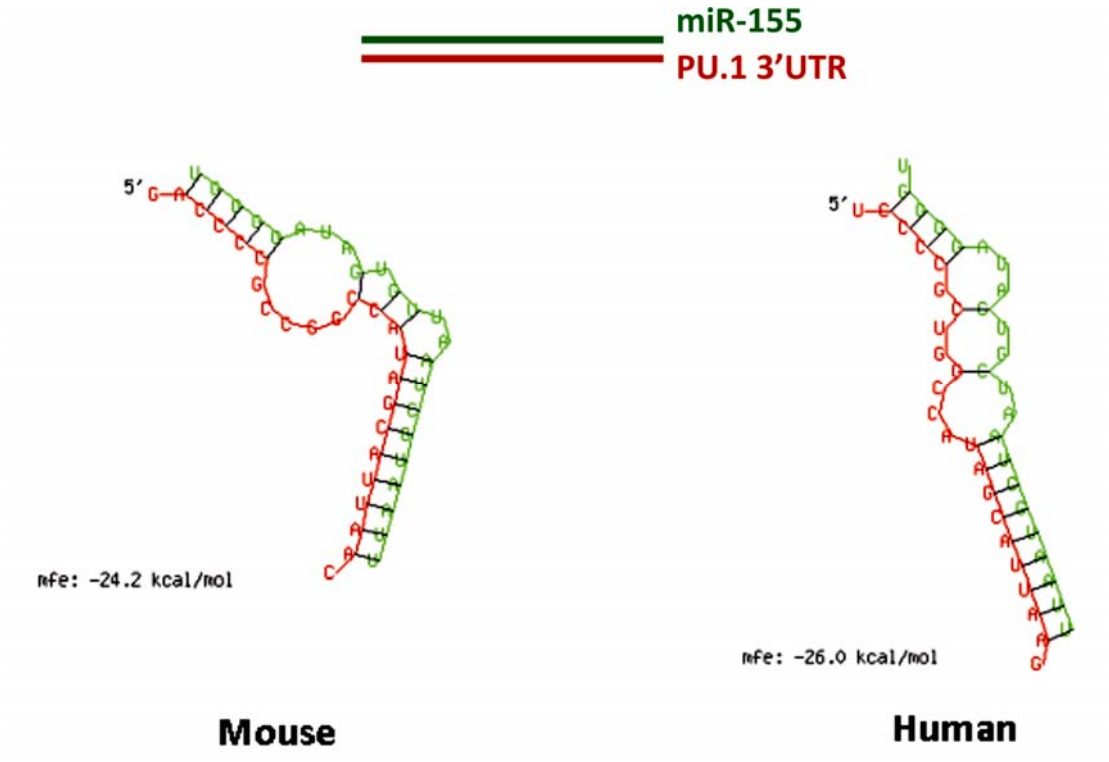

Figure 20 Predicted structure for miR-155::PU.1 3'UTR interaction in mouse and human. Red indicates the 3'UTR sequence that is predicted to interact with miR-155 (in green). Energies indicated are the predicted energy values released in each one of the interactions. Downloaded from RNAHybrid (http://bibiserv.techfak.uni-bielefeld.de/rnahybrid/submission.html)

3.4.2 Amplification of the 3'UTR of PU.1: cloning of pRLTK_3'UTR_PU.1

Dual luciferase assay (section 2.5) was performed to test the predicted direct binding of miR-155 to the 3'UTR of PU.1 as explained in Fig.12. This assay required cloning the 3'UTR of PU.1 at the 3' end of the Renilla luciferase reporter gene harboured in pRLTK vector (see section 2.3.1).

The 3'UTR of PU.1 was amplified from genomic DNA instead of cDNA; PU.1 mRNA was detected when using primers to amplify exonic sequences (Fig.16B); however, the 3'UTR of PU.1 was never detectable when amplifying it from cDNA. It was hypothesised that the 3'UTR high GC content (68%) made the reverse transcription reaction unable to produce cDNA from cytoplasmic mRNA and 50 pg of genomic DNA were used as PCR template instead.

PCR conditions were optimized following the protocol established by (Ralser et al., 2006). The 30µl PCR reaction included a solution called CES (for composition see section 2.1.3). These conditions make the concentration of DNA in the mixture higher and improves the PCR amplification (Ralser et al., 2006).

Gradient PCR was performed to establish the optimal annealing temperature which was calculated between 58 and 60 degrees (Fig.21). Figure 21 shows a gel picture of the amplified genomic region corresponding to the 3'UTR of PU.1. Left lanes 2 to 6 show that in the absence of CES solution the PCR reaction amplified unspecific bands, none of which correspond to the expected size (450nt approximately). Lanes 8 to 13 show the amplified products obtained when adding CES solution to the PCR mixture. Bands circled were the ones extracted, cloned and sequenced, corresponding to the 3'UTR of PU.1.

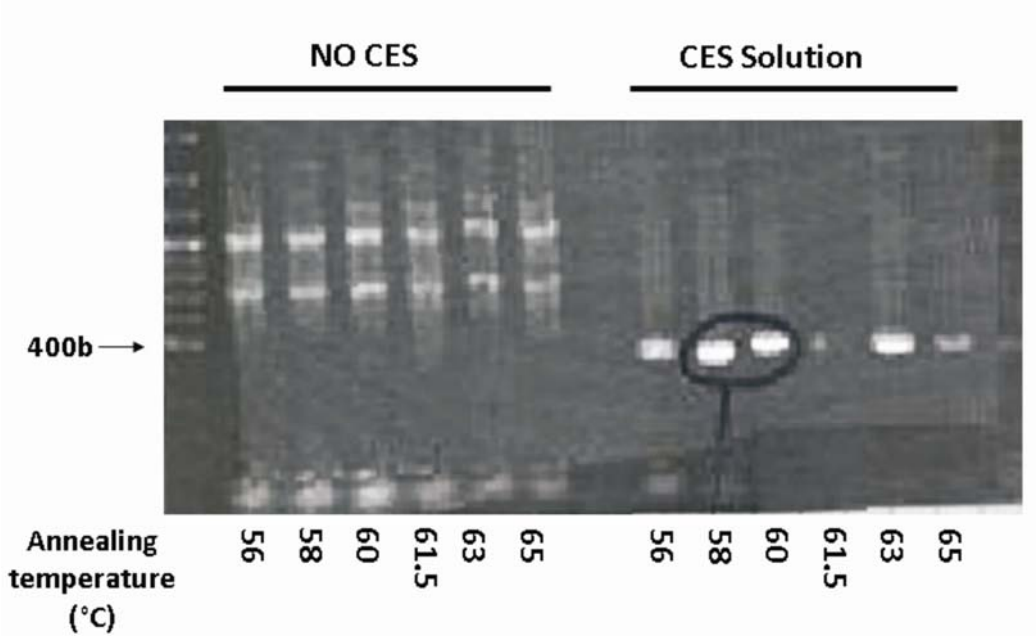

Figure 21 Agarose gel image corresponding to the amplification of PU.1 3'UTR by gradient PCR. Annealing temperatures tested in the PCR reaction are indicated below. First lane: Smart Ladder (Eurogentec). 2-6 left lanes: no CES (enhancer solution for high GC content sequences) was added. 8-13 lanes on the right correspond to the matched annealing temperatures with addition of CES solution. CES use in the PCR reaction was adopted from the protocol by (Ralser et al., 2006).

After several subcloning steps (see section 2.3.1 and Fig.9) the 3'UTR of PU.1 was cloned in pRLTK vector constructing **pRLTK_3´UTR_PU1.** This vector was then subjected to site directed mutagenesis (see section 2.3.1) to construct **pRLTK_MUT_3´UTR_PU.1**. for pin pointing the site of miR-155 targeting. This mutant version contains mismatches in the putative miR-155 binding site (positions 45-51 of the 3'UTR) as shown in Fig. 22A.

3.4.3 MiR-155 directly binds to the 3'UTR of PU.1

After cloning the 3'UTR of PU.1 and obtaining the wild type and mutant reporter versions **pRLTK_3´UTR_PU1** and **pRLTK_MUT_3´UTR_PU.1**, respectively, these constructs were assayed using Dual Luciferase Assay system as described in 2.5 and represented in Fig.12. The mutant version was designed and then specifity checked by employing RNAHybrid and PITA for miR-155 binding, which did not predict putative miR-155 sites.

Each reporter vector was co transfected with pCNA3.1_BIC (over expressing vector for miR-155) or with empty pCDNA3.1 as control into HeLa cells.

pRLTK empty vector (**pRLTK** in Fig.22B) was unaffected by the over expression of miR-155 as shown by the similar luciferase values when co transfecting pRLTK with control or miR-155 over expressing vectors. When the 3´UTR of PU.1 was included in the pRLTK vector (**WT** in Fig.22B) the co-transfection of miR-155 led to a drop of 85% in luciferase activity. Mutating the predicted pairing region for miR-155 (**MUT** in Fig.22B) rendered the construct unaffected by miR-155 over expression similarly to pRLTK empty vector. All transfections were normalized using pGL3 as the 3'UTR of this Firefly luciferase reporter gene is not affected by microRNA-155. Moreover, this normaliser is routinely used in this type of assays. Transfections were performed in triplicates and it is shown one of them.

Therefore, it was concluded that human PU.1 is a direct target of miR-155 and that the predicted binding sequence mapping to nucleotides 45-51 of the 3'UTR of PU.1 is essential for miR-155 activity.

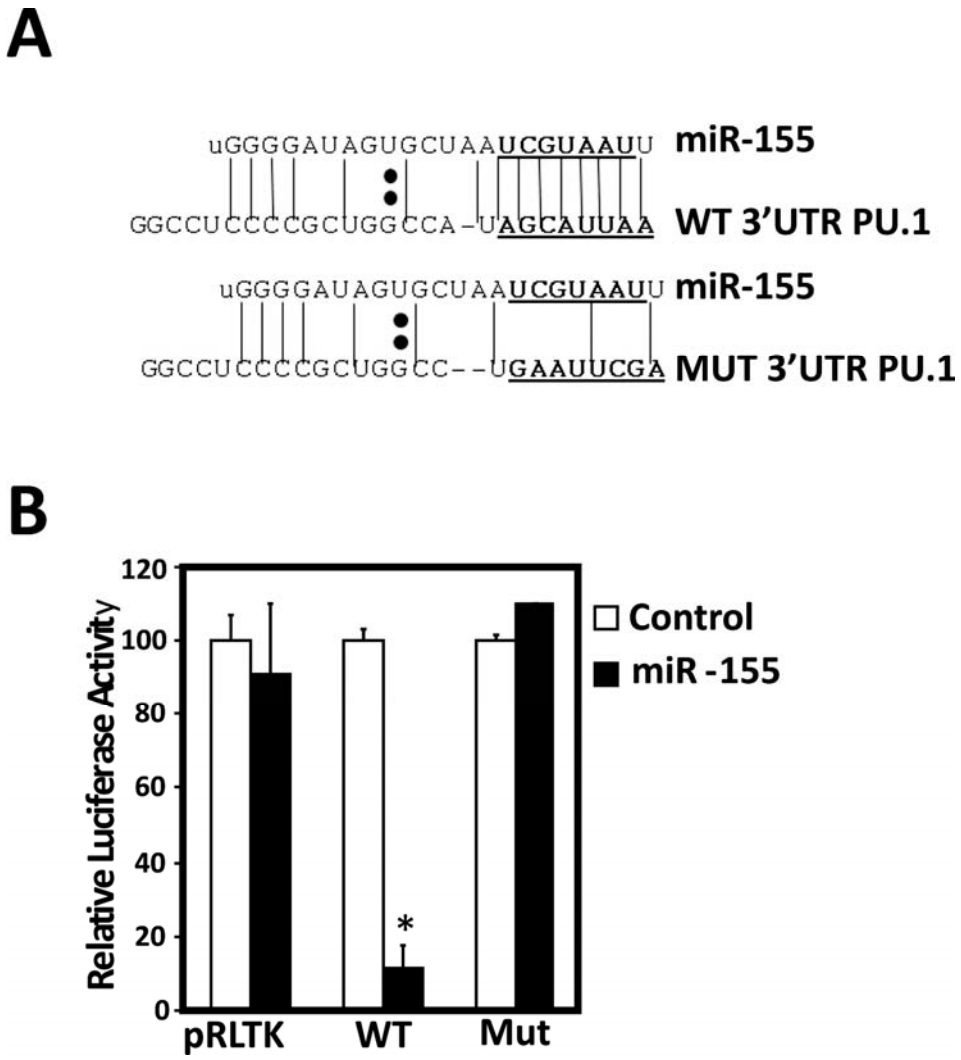

Figure 22 MiR-155 directly targets the 3'UTR of PU.1. *A*: predicted binding site for miR-155 in the 3'UTR of PU.1 and the generated mutant version between nucleotides 45-51 of PU.1 3'UTR. *B*: Luciferase assay for miR-155 action on the 3'UTR of PU.1. pRLTK: pRLTK empty vector; WT: pRLTK including the wild type 3'UTR of PU.1; MUT: pRLTK including the mutant version for miR-155 binding site on the 3'UTR of PU.1 as shown in A.

3.5 Generation of THP-1 155 cell line

MiR-155 was shown to be up regulated by LPS in DCs (Fig.15) which has also been reported to induce miR-155 expression in murine macrophages (O'Connell et al., 2007) and involved in the inflammtory response of human macrophages (personal communication of Dr.T.Sanchez-Elsner). LPS is a pro-inflammatory stimulus that triggers different pathways such as TLR4 and NFκB which in turn involve many other downstream targets. Thus, LPS exerts its effects on many targets at the same time (e.g. PU.1 and miR-155) that might or might not be directly interrelated. A cell line with controllable and titrable miR-155 expression was developed to analyze the effects of miR-155 over expression on its own and isolate it from other inflammatory pathways and events. The chosen cell model was THP-1 cell line due to several of its characteristics: i) it is of myelocytic origin as DCs and Mϕs are; ii) it is known to share characteristics with human DCs (Berges et al., 2005); iii) it is commonly used for obtaining Mϕ-like cells (Auwerx, 1991; Park et al., 2007) and, importantly, iv) they express PU.1.

The lentiviral system used in this study was generated and described by Wiznerowicz and Trono (Wiznerowicz, M. and D. Trono, 2003) and it is represented in Figure 23. This system consists on two different lentiviruses that share the envelope and capside proteins and differ in the lentivirus genome that is inserted in the host cell. The viral envelope is encoded in the plasmid pPAX and the capsid proteins are transcribed from pMD2G plasmid (see 2.3.2). The transduction protocol is detailed in 2.4.

Both pLENTI_BIC and pLV/tTR-KRAB-Red lentiviral vectors contain reporter genes that allow their monitoring by flow cytometry. pLENTI_BIC harbours pri-miR-155 and has a GFP marker gene transcribed from an independent promoter (EF-1α, Elongation Factor-1 alpha).

pLV/tTR-KRAB-Red harbours the tTR-KRAB fusion protein and DsRed2 protein. DsRed2 codes for a fluorescent marker that has an excitation wavelength of 563nm and an emission at 582nm. The flow cytometer used did not have the required laser to excite this fluorophore so it was not possible to use it as a marker for infected cells. This explains the infection protocol and the several rounds of sorting performed to obtain the

THP-1 155 cell line (see 2.4.2). tTR-KRAB is a fusion protein with two modules: tTR and KRAB. KRAB is a repressor of both Polymerase II and III transcriptional activity within a distance of 3Kb from its binding site. tTR (tetracycline TransRepressor) is a DNA binding domain which confers specifity to the repression resulting in a specific binding to tetO (tetracycline Operators) sequences. Thus, tTR-KRAB suppresses the transcription of tetO juxtaposed promoters. tTR confers not only specifity but also inducibility to the system because its binding to DNA is regulated by tetracycline or a derivative such as doxycycline (Doxy). When tetracycline (or Doxy) are added to the medium tTR-KRAB is then sequestered freeing the promoter and allowing gene expression to occur (Deuschle et al., 1995). This inducibility is necessary as the long-term over expression of the transgene could lead to changes in the overall behaviour of the system and possibly generate some undesired off-target effects.

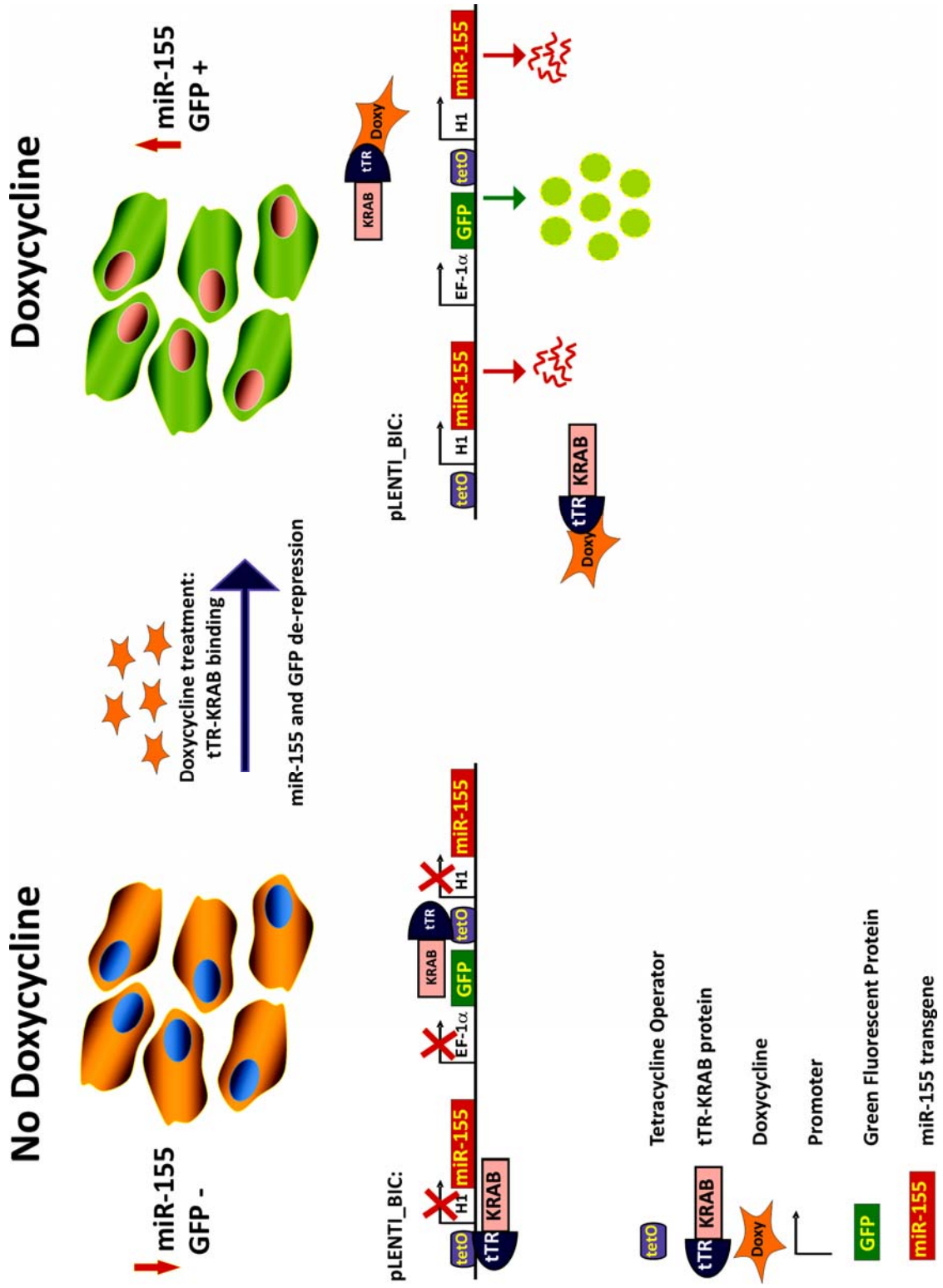

Figure 23 THP1-155 cells lentiviral system. THP-1 155 cells harbour pLENTI_BIC and pLV/tTR_KRAB_Red. pLENTI_BIC is a lentivirus that contains a miR-155 transgene and a GFP reporter. Both genes are constitutively repressed in a Tet On dependent manner (left side) due to tTR-KRAB protein (encoded in pLV/tTR_KRAB_Red) repression. Addition of doxycycline sequesters tTR-KRAB by binding to the tTR module, releasing promoters of both miR-155 and GFP which become transcriptionally active.

3.5.1 Validation of THP-1 155 cells

3.5.1.1 Flow cytometry analysis of THP1-155 cells

To validate the inducibility of the system, Doxycycline was added to the medium at different concentrations (0.25, 2.5 and 10 μg/mL) and GFP was monitored. The optimal concentration, 2.5μg/ml, was determined as the lowest one that showed earliest and strongest GFP expression. Figure 24 shows the flow cytometry profiles of cells treated with 2.5 μg/ml doxycycline over 96h; time points were taken every 24h and cells were monitored by flow cytometry. After 96h almost all cells (96% approximately) were GFP positive.

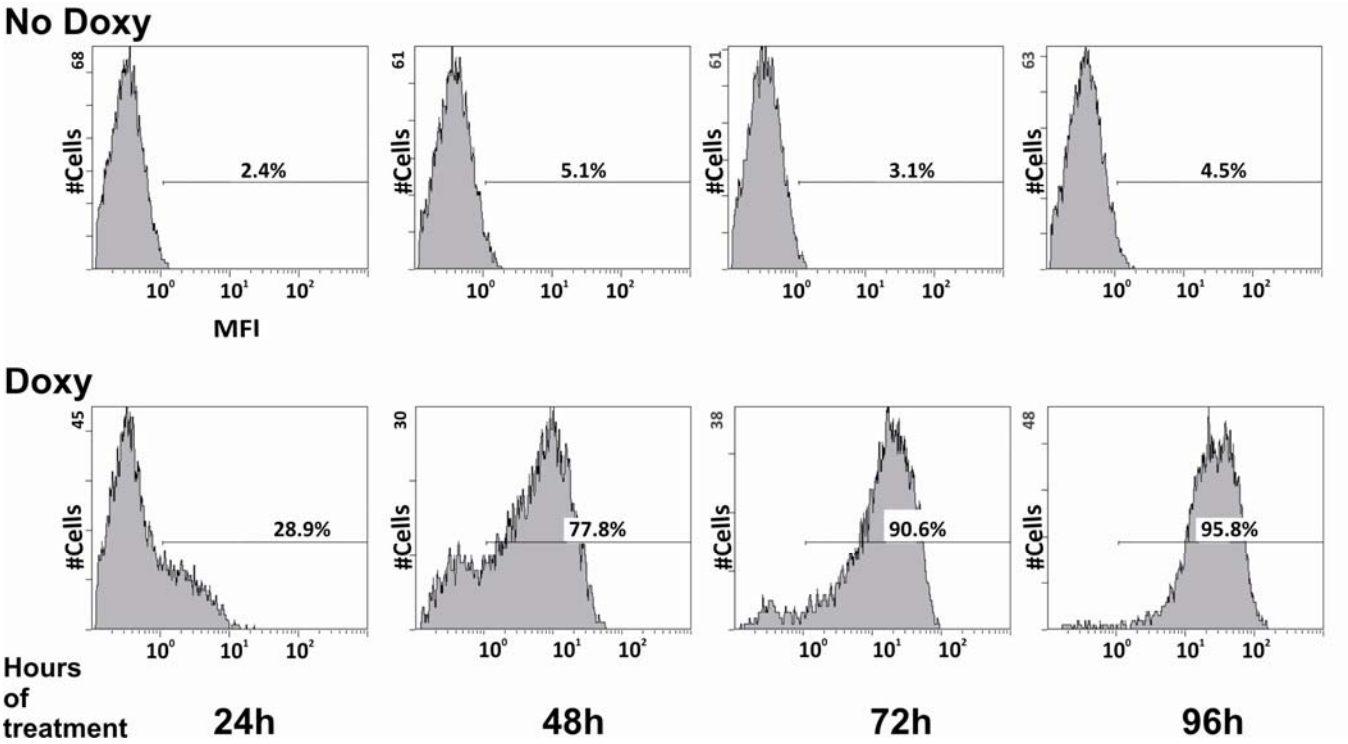

Figure 24 Flow cytometry profile of Doxycycline treated THP1-155 cells. Addition of Doxycycline to THP-1 155 cells during the course of 96h up regulated GFP expression reaching 95.8% of GFP positive cells after 5 days of treatment

Thus, it was established that the optimal timing for de-repression of THP-1 155 cell system was 96h and the chosen dose of doxycycline 2.5μg/mL.

3.5.1.2 miR-155 analysis of THP1-155 cells

The addition of doxycycline to THP-1 155 cells during 96h was sufficient to allow GFP de-repression of almost the whole population (Fig.24). To assay miR-155 de-repression THP1-155 cells were incubated with 2.5μg/mL during 96h and time points were taken each 24h. MiR-155 expression was analysed by specific RT-qPCR (see 2.8, 2.9.1.2., 2.9.2.2 and 2.9.2.3). Figure 25 shows that miR-155 over expression occurred steadily during the course of 96h of doxycycline treatment; after 96h THP1-155 cells an increase of eight times in miR-155 expression when compared to the start of the treatment. Untreated cells (**No Doxy** in Fig.25) showed no significant modification of miR-155 levels.

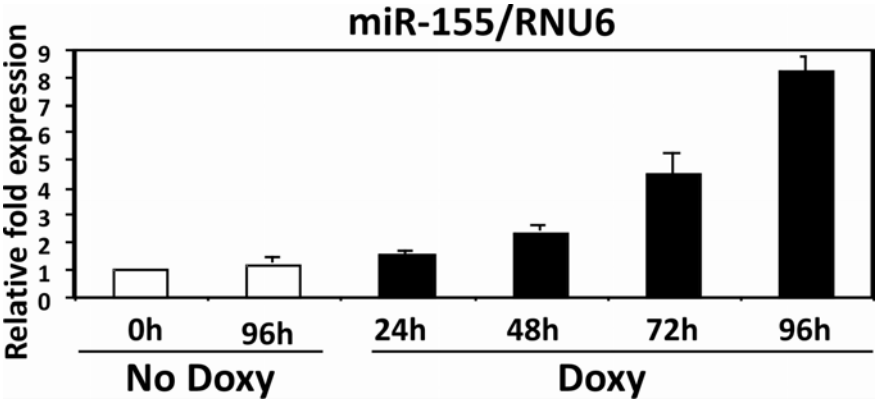

Figure 25. Mir-155 expression in doxycycline treated THP-1 155 cells. THP1-155 cells were treated with doxycycline (Doxy) or not (No Doxy) during 96; cells were taken every 24h and analyzed to detect miR-155 expression. Fold expression was calculated using the small nuclear RNA RNU6 as house keeping gene.

3.6 Determination of miR-155 effects on PU.1 and DC-SIGN in THP-1 155 cells

PU.1 was demonstrated to be directly bound by miR-155 (Fig. 22B) and it is a known transcriptional regulator of DC-SIGN (Dominguez-Soto et al., 2005). After validating the THP1-155 cell line (Figs.24 and 25), the effects of miR-155 up regulation in PU.1 and DC-SIGN expression were tested following these objectives:

- Objective 1: Determination of miR-155 up regulation effects on of PU.1 and DC-SIGN protein by western blotting. Analyze PU.1 and DC-SIGN mRNA expression by qRT-PCR.

- Objective 2: Analyze miR-155 regulation of DC-SIGN expression employing promoter assays.

- Objective 3: Checking the specifity of the system by transfecting THP1-155 cells with Anti-miR-155 oligonucleotides. Analysis of mRNA levels of PU.1 and DC-SIGN by qRT-PCR.

3.6.1 miR-155 effects on PU.1 expression

THP-1 155 cells were treated with doxycycline during 96h (which results in up regulation of miR-155 as shown in Fig. 25). Cells were taken every 24h and analyzed both protein and RNA levels by Western blotting (see 2.10) and RT-qPCR, respectively. Figure 26A shows that PU.1 protein levels dropped to 16.8% of the initial levels at the start of the treatment (time 0h) as determined by densitometry. Normalisation was done against α-tubulin. Analysis of RNA by RT-qPCR (see 2.8, 2.9.1.1, 2.9.2.1. and 2.9.2.3) determined that PU.1 mRNA levels remained almost constant during the same time course (Fig.26B). The results shown correspond to an experiment that was performed in triplicates.

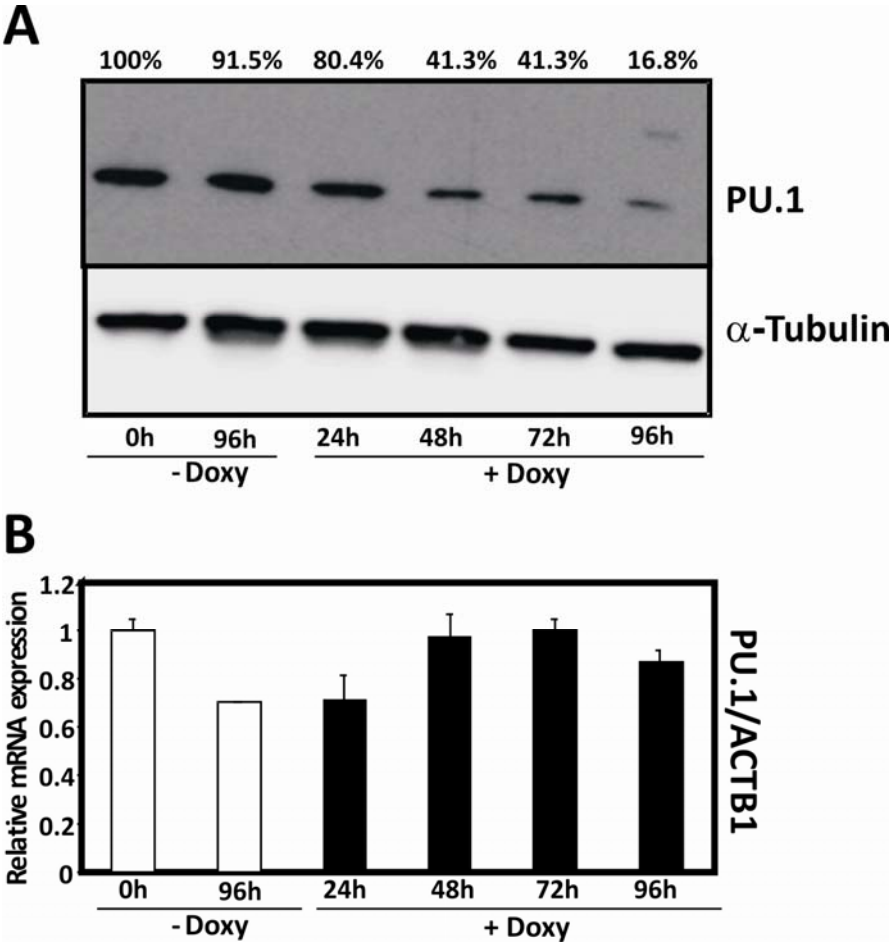

Figure 26 MiR-155 modulates PU.1 expression in THP1-155 cells. *A*: Western blot analysis of PU.1 protein in THP1-155 cells during 96h of doxycycline (Doxy) treatment. Densitometry values are shown on top of each lane compared to time 0 and normalized against α-Tubulin. B: RT-qPCR of PU.1 mRNA levels compared (α-actin) (ACTB1).

3.6.2 miR-155 effects on DC-SIGN expression

MiR-155 up regulation led to a decrease of PU.1 levels in THP-1 155 cells (Fig. 26). PU.1 controls the transcription of DC-SIGN in myeloid cells (Dominguez-Soto et al., 2005) and thus, it was hypothesised that miR-155 levels would have an effect on DC-SIGN expression. To test this, THP-1 155 cells were treated with doxycycline over 96h, time to release the repression from the whole cell population (Fig.24) and over express miR-155 (Fig.25). Cells were then maintained a further period of 48h with or without doxycycline and protein and RNA were analyzed every 24h by western blot (2.10) and RT-qPCR (see see 2.8, 2.9.1.1, 2.9.2.1. and 2.9.2.3), respectively. Both DC-SIGN protein and mRNA levels were down regulated in the presence higher levels of miR-155 (Figs.27A and B, upper panels **+Doxy**, respectively). PU.1 protein levels were down regulated when miR-155 levels were increased (**+Doxy**, middle panel in Fig.27A) while PU.1 mRNA levels remained constant (Fig.27B, lower panel). An experiment that was performed in triplicates is shown.

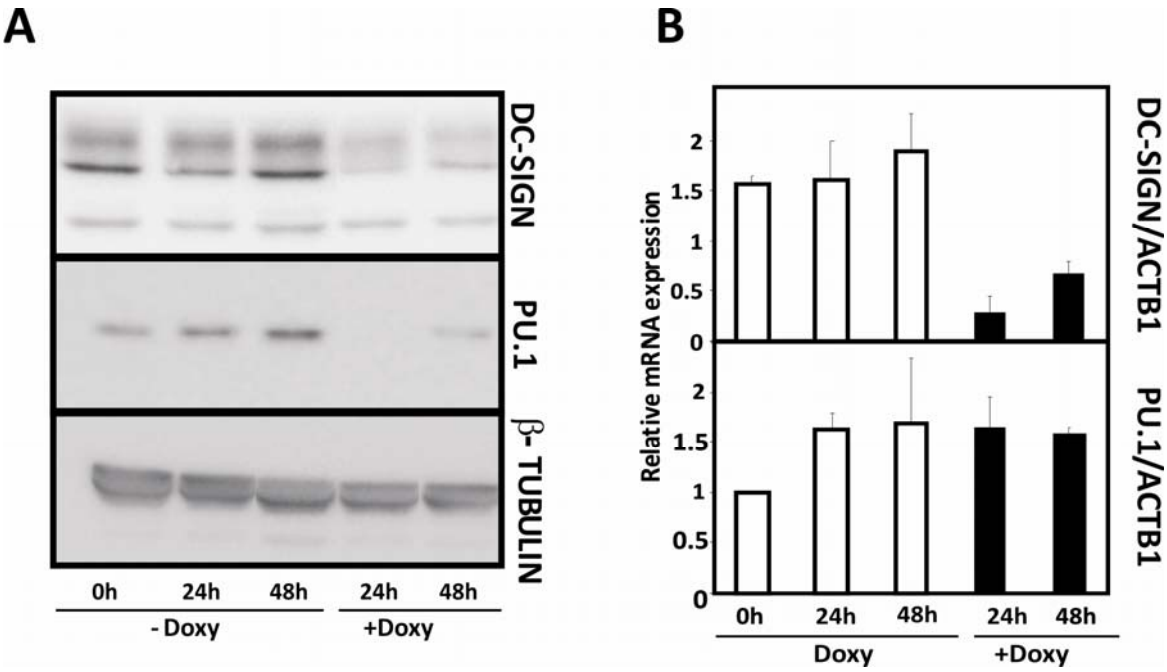

Figure 27 DC-SIGN and PU.1 expression in THP-1 155 cells. THP1-155 cells treated during 96h with Doxycycline (+Doxy) or not (-Doxy) were left an extra period of 48h with/without Doxy. *A*: Western Blot showing DC-SIGN and PU.1 protein levels (upper and middle panels, respectively). Normalisation was done against β-tubulin. *B*: RT-qPCR results of DC-SIGN and PU.1 mRNA levels (upper and lower panels, respectively) normalised against α-actin (ACTB1)

DC-SIGN surface expression was also analysed in THP1-155 cells by flow cytometry. Fig.28 shows the flow cytometry profiles of THP1-155 cells treated or not with doxycycline (**+Doxy** and **–Doxy**, respectively), that is, over expressing or not miR-155. MiR-155 over expression led to a reduction of DC-SIGN membrane levels of 65% as shown by the MFI (Mean Fluorescence Intensity).

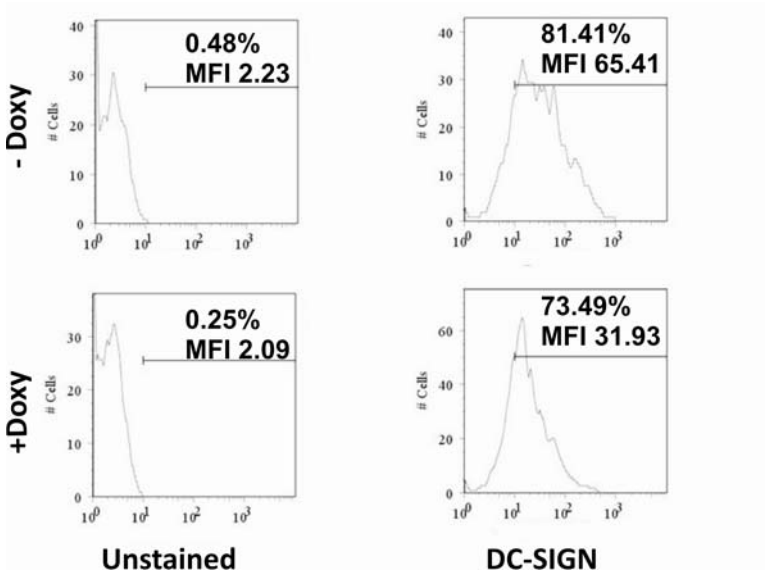

Figure 28 Flow cytometry profiles of DC-SIGN surface expression in THP1-155 cells. THP1-155 over expressing (+Doxy) or not (-Doxy) miR-155 were stained with anti-DC-SIGN fluorescent antibody and analyzed by flow cytometry. % indicates percentage of positive cells: MFI: Mean Fluorescence Intensity. Stained population was determined by comparison to unstained cells.

The results shown in Figs.26, 27 and 28 suggested that miR-155 regulates PU.1 expression post transcriptionally whilst it modulates transcriptional DC-SIGN activity, suggesting this regulation to be mediated via direct targeting of PU.1.

3.6.3 Specifity of miR-155 effects

In order to confirm the specificity of miR-155 effects on PU.1 and DC-SIGN expression a "reverse" approach was assayed by blocking miR-155. Anti-miR-155 inhibitor oligonucleotires (Ambion) were transfected into doxycycline treated THP1-155 cells (cells over expressing miR-155) (see 2.7.1). Transfection efficiency was firstly checked by flow cytometry using a Cy3 labelled Pre-miRNA probe (Fig.29A). Almost 90% of the population was transfected as shown by the percentage of positively labelled cells (Fig.29A right plot) when compared to unstained cells. Anti-miR-155 or Anti-miRNA-Control oligonucleotides were then transfected following the same protocol; 48h post transfection RNA was extracted from transfected cells and analyzed by RT-qPCR (see 2.8, 2.9.1.1., 2.9.2.1 and 2.9.2.3). Fig.29B shows that PU.1 mRNA levels were not affected by miR-155 inhibition (black bars). DC-SIGN mRNA levels were significantly increased up to 1.6 fold when Anti-miR-155 oligonucleotides were transfected (Fig. 29B right, black bar). Fold increase was calculated by comparing to Control-Anti-miRNA (Fig.29B white bars) and normalizing against α-actin (ACTB1 gene).

These results showed the reversibility of the THP1-155 cell system and confirmed the previous observations in Figs.26, 27 and 28: miR-155 modulates PU.1 expression at the post transcriptional level while it regulates DC-SIGN at the pre-transcriptional level.

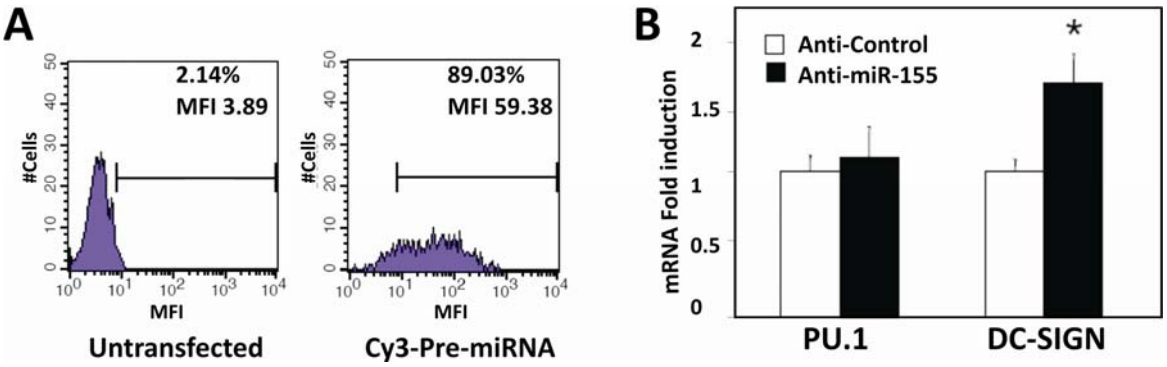

Figure 29 THP1-155 cells transfection with Anti-miRNA probes. *A*: Transfection efficency was checked transfecting Cy3-Pre-miRNA in THP-1 cells and monitored by flow cytometry (efficency approx. 89.03% of Cy3 positive cells). *B*: THP-1 155 cells were transfected with Anti-miR-155 probe or an Anti-miRNA-Control to prove specifity of miR-155 in PU.1 and DC-SIGN regulation at the mRNA level (right panel).

3.6.4 MiR-155 regulates DC-SIGN promoter activity by targeting PU.1

Previous results (Figs. 27 and 29) suggested that miR-155 modulates DC-SIGN expression at the pre-transcriptional level; moreover, DC-SIGN was not found amongst the putative targets for miR-155 in any of the *in silico* predictions. Given that PU.1 is a transcriptional activator of DC-SIGN expression (Dominguez-Soto et al., 2005) it was hypothesised that miR-155 affects the promoter activity of DC-SIGN in a PU.1-dependent manner.

In order to test this hypothesis promoter assays were performed based on the dual luciferase system (see 2.5 and Fig.13). Dr.Tilman Sanchez-Elsner performed these assays. The reporter vector used was **pCD209–468 pXP2** (see 2.3.2). This is a Firefly luciferase construct that reports for DC-SIGN transcriptional activity dependent on PU.1 as it harbours a fragment of DC-SIGN promoter previously shown to respond to PU.1 binding (Dominguez-Soto et al., 2005). Thus, the activity of the luciferase reporter gene depends mainly on the presence of PU.1 present in the cell. Normalisation was done against pRLTK.

THP1-155 cells were treated or not with doxycycline during 96h to allow miR-155 over expression or not, respectively (see Fig.25), and cells were then transfected with **pCD209–468 pXP2.** The bar graph in Figure 30 represents the results of these transfections. "Basal" shows that miR-155 over expressing cells (**+Doxy**, black bars) reported a significant reduction in DC-SIGN transcriptional activity dependent on PU.1. This result confirmed the previous observations in Figs. 27 and 29, demonstrating that miR-155 modulates DC-SIGN expression at the promoter level.

To determine the role of PU.1 in the miR-155-dependent reduction of DC-SIGN promoter activity, two additional experimental conditions were tested. In the first one (**+PU.1 No 3'UTR** in Fig.30) the reporter for DC-SIGN promoter was co-transfected with a plasmid encoding for PU.1 protein (**pCDNA3.1_PU.1**, see 2.3.2). This PU.1 construct harbours the cDNA of PU.1 protein with no 3'UTR sequence and thus, with no binding site for miR-155. Co-transfecting this PU.1 vector rescued completely the activity of the reporter for DC-SIGN promoter: miR-155 over expressing cells (**+Doxy**) –which have less PU.1- reported the same transcriptional activity as miR-155 non-over expressing cells

(**-Doxy**). The second experimental condition (**+PU.1 Complete** in Fig.30) was performed to determine whether the presence of the 3'UTR of PU.1 dictates miR-155 modulation of DC-SIGN transcriptional activity. It consisted on the co-transfection of DC-SIGN promoter reporter with a PU.1 construct containing the full length 3´UTR (**pCDNA3.1_PU.1_3'UTR**, see 2.3.1). **+PU.1 complete** in Fig.30 shows that this expression vector for PU.1 was not able to rescue the transcriptional activity of DC-SIGN showing a similar behaviour as the basal conditions (**Basal** in Fig.30). An experiment that was performed in triplicates is shown.

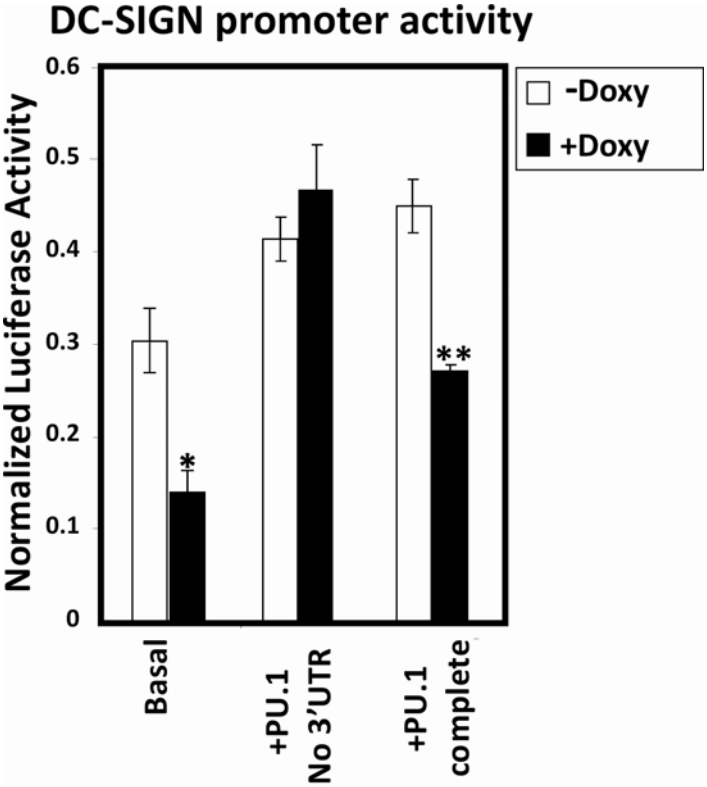

Figure 30 MiR-155 modulates DC-SIGN promoter activity. THP-1 155 cells over expressing miR-155 (+Doxy, black columns) or not (- Doxy, white columns) were transfected with a reporter construct harbouring a fragment of DC-SIGN promoter that binds to PU.1. "Basal" shows that Doxy treated cells reported less luciferase activity. "+PU.1 No 3'UTR" shows that the co-transfection of the DC-SIGN promoter reporter with a vector coding for PU.1 that lacks its 3´UTR (no binding site for miR-155) restored the luciferase values. "+PU.1 complete" shows that co-transfecting DC-SIGN reporter with a PU.1 expression vector containing its full lenght 3´UTR behaved similarly to the basal conditions. It is shown one experiment that was performed in triplicates. Normalisation was performed against Renilla luciferase (pRLTK)

Therefore, the hypothesis stated initially was demonstrated: miR-155 modulates the transcriptional activity of DC-SIGN by directly regulating PU.1 levels.

3.7 Role of miR-155 in dendritic cells pathogen binding ability

Previous results have shown that miR-155 augments during dendritic cell maturation (Fig.15) while DC-SIGN and PU.1 are down regulated (Figs.14 and 16, respectively); that PU.1 is a direct target of microRNA 155 (Fig.22B) and that miR-155 modulates DC-SIGN expression through PU.1 regulation (Figs.26 and 30).

DC-SIGN is a C-type lectin that binds to pathogens such as *Candida albicans* (Cambi et al., 2003)or HIV glycoprotein gp120 (Cambi et al., 2003; Geijtenbeek and van Kooyk, 2003) These data together with the previous results suggested that miR-155 can modulate the pathogen binding ability of dendritic cells through DC-SIGN modulation. In order to test this hypothesis two different objectives were planned:

- Objective 1: Transfection of Anti-miR-155 or Anti-miR-Control oligonucleotides in dendritic cells and validation by RT-qPCR.

- Objective 2: Assay Anti-miR-155/Control transfected DCs binding to gp120-FITC and labeled *Candida albicans* by flow cytometry.

3.7.1 Anti-microRNA transfection of dendritic cells

Dendritic cells show high phagocytic ability (Banchereau and Steinman, 1998; Kindt et al., 2007; Murphy et al., 2008; Steinman, 2001) so it was hypothesised that these cells might naturally uptake Anti-microRNA inhibitors with no need of transfection reagents and/or techniques such as electroporation.

To test the transfection efficency a Cy3 labelled Control-microRNA probe was initially transfected into DCs (see 2.2.2 for DC generation). Cells were incubated in the presence of 50nM Cy3-labelled oligonucleotides and checked 48h post transfection by flow cytometry. Fig.31A shows that cells were 100% positive when incubated in the presence of the Cy3 probe. Confocal microscopy experiments were carried out to test the cellular localization of the probe. These experiments confirmed that the probe was located inside the cytoplasm and not bound to the cell membrane. Confocal microscopy assays were done by Dr. Fethi Louafi (data not shown). Dendritic cells were then transfected with Anti-miR-155 (see section 2.7.2 for a detailed protocol) and miR-155 levels were checked by RT-qPCR (see see 2.8, 2.9.1.2., 2.9.2.2 and 2.9.2.3). Two doses (50nM and 500nM) of specific anti-miR-155 or control anti-miRNA oligonucleotides were employed initially to optimize the blocking efficency. miR-155 knock down was not detectable 24h post transfection (data not shown); Fig.31B shows the RT-qPCR results for miR-155 detection 48h after transfection. When compared to immature DCs (**iDCs** in Fig.31B) LPS triggered miR-155 up regulation with both doses of anti-miRNA transfection (**Control** in Fig.31B). LPS up regulation was reduced when transfecting the highest concentration of anti-microRNA control (**500nM Control**) when compared to the lowest one (**50nM Control**). It is possible that the highest ammount of oligonucleotides impaired the maturation of DCs, as the levels of miR-155 were similar when comparing transfections of 500nM of Control and 50nM of Anti-miR-155 oligonucleotides. 50nM dose of Anti-miR-155 was efficient in the blocking and to avoid possible undesired effects 50mM was chosen as the working dose.

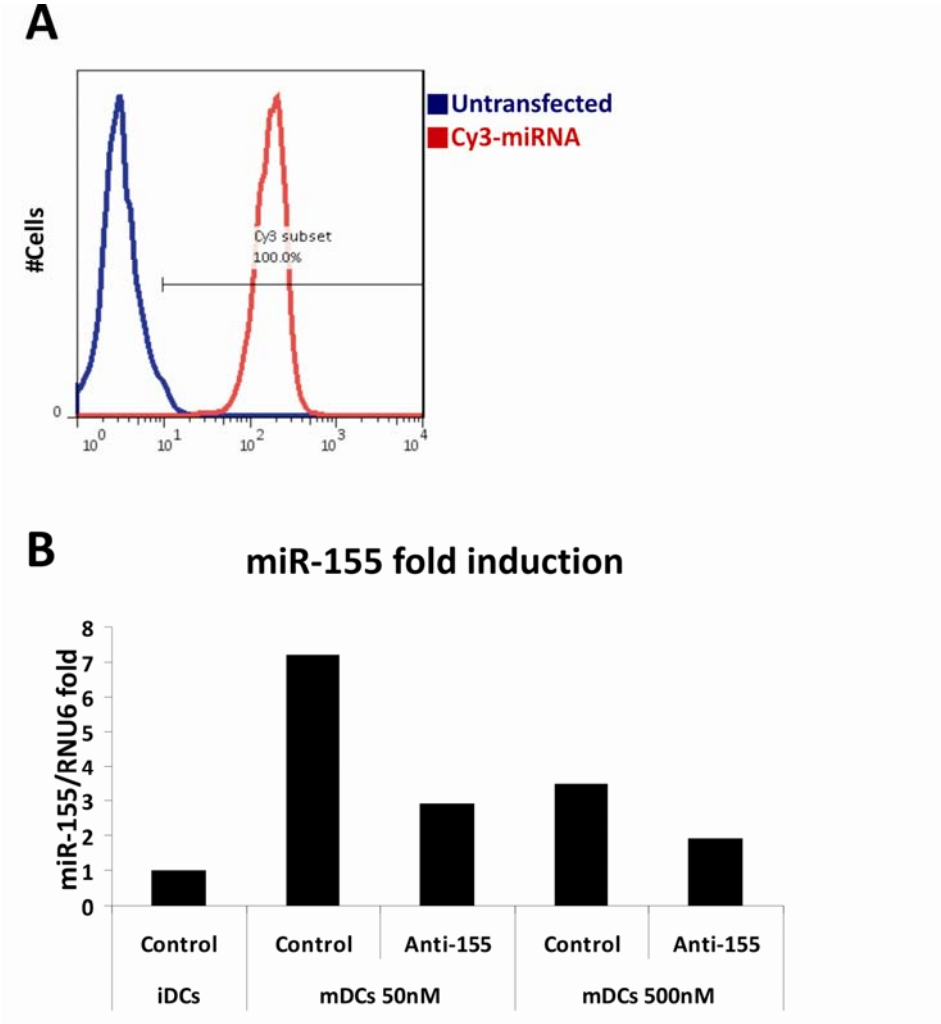

Figure 31 Transfection of Anti-microRNA in DCs. *A*: Flow cytometry overlay of DCs transfected (red) or not (blue) with a labelled Cy3-miRNA probe. All cells were transfected *B*: Blocking efficency of Anti-miR-155 oligonulceotides when transfecting 50nM or 500nM in mature dendritic cells (mDCs). Fold induction was calculated by comparing to immature dendritic cells (iDCs) and RNU6 was used as a normaliser.

3.7.2 MiR-155 effects on DC-SIGN surface expression and pathogen binding ability of dendritic cells

Once the transfection conditions were established, iDCs were transfected at day 5 with Anti-miR-155 or Anti-miR-Control oligonucleotides and maturation was induced with LPS (see 2.2.2). DC-SIGN surface expression was checked by flow cytometry (see 2.11.1) and binding experiments to FITC-gp120 protein and *C.albicans* conidia were performed 48h post transfection (see 2.11.2 for a detailed protocol). Fig. 32 shows the flow cytometry profiles (first and second columns) and overlays (third column) of transfected cells with Anti-miR-Control (in blue) or Anti-miR-155 (in red) oligonucleotides. As expected, Anti-miR-155 transfected DCs showed higher DC-SIGN membrane expression compared to Control transfected cells (Fig.32, first row). Concomitantly, DCs transfected with anti-miR-155 oligonucleotides showed greater binding to both *C.albicans* and gp120 in DCs (Fig.32, second and third rows, respectively) when compared to the binding observed in Anti-miR-Control transfected cells. Results shown correspond to one donor out of three replicates. These experiments were done with the help of Dr.Fethi Louafi.

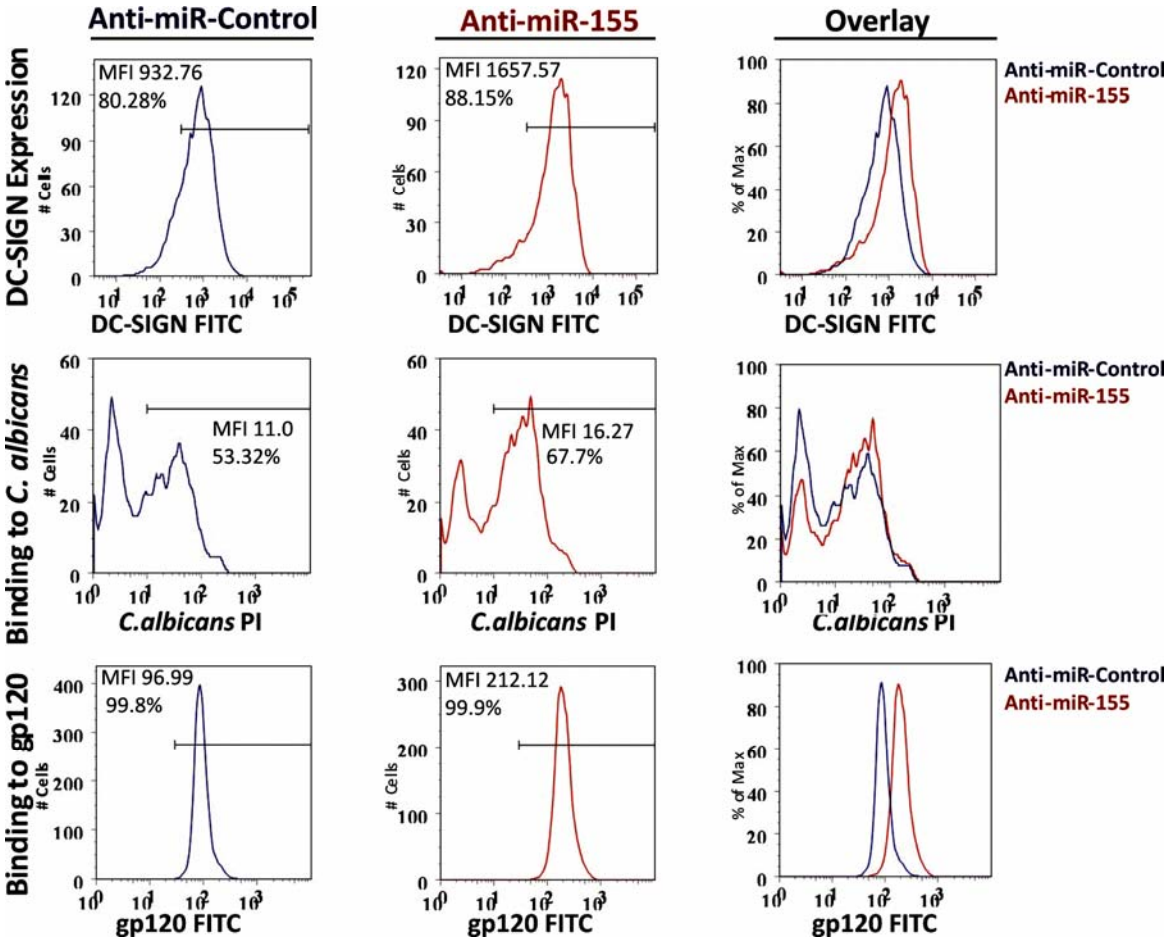

Figure 32 Dendritic cell pathogen binding modulation by miR-155. Flow cytometry profiles of mature DCs transfected with 50nM Anti-miR-155 (in red) or Anti-miRNA-Control (in blue) oligonucleotides. First row shows DC-SIGN membrane levels; second row shows binding to C.albicans and third row shows binding to gp120-FITC. Overlays in third column are the result of superposing blue and red plots. % shows the percentage of positively labelled cells; MFI: Mean Fluorescence Intensity. Experiments were performed in triplicates. It is shown one of the donors.

3.8 Discussion

In search of genes involved in inflammation, BIC (MIR155 HG) was found as a candidate up regulated by pro-Th_1 conditions in human macrophages; moreover, miR-155 was shown to be up regulated in murine macrophages by inflammatory stimuli (O'Connell et al., 2007). Employing *in silico* tools for the prediction of miR-155 targets PU.1 was found as a conserved candidate (Figs. 17 and 19) in which 3'UTR the only conserved site for miRNA action was that of miR-155 (Fig.18). PU.1 is an essential factor in dendritic cells (Bakri et al., 2005; Carotta et al., 2010) and an important regulator of hematopoiesis (Laslo et al., 2006; Scott et al., 1994) that has been linked to Th_2 responses (Brunner et al., 2007; Chang et al., 2005b). PU.1 is also a known transcriptional regulator of the pathogen binding receptor DC-SIGN (Dominguez-Soto et al., 2005), which is present in dendritic cells and it is regulated during DC maturation induced by inflammatory stimuli. Linking miR-155 and DC-SIGN regulation through PU.1targeting would prove a new role for this microRNA in DCs pathogen binding abilities. Moreover, it would establish a new role for miR-155 in the initial steps of the immune response.

LPS induced maturation of DCs triggered up regulation of miR-155 (Fig.15) concomitantly with DC-SIGN and PU.1 down regulation (Figs.14 and 16, respectively). *In vitro* assays demonstrated that miR-155 directly binds to the 3'UTR of PU.1 requiring nucleotides 45-51 of PU.1 3'UTR intact to exert its action (Fig.22). To isolate the effects of miR-155 over expression from those exerted by LPS signalling (which activates other pathways), a monocytic cell model was developed: THP1-155 cells. In THP1-155 cells, the over expression of miR-155 is controlled by the addition of tetracycline or a derivative, such as doxycycline. This inducibility allows testing the effects of miR-155 over expression in a more isolated manner. Importantly, these cells show basal levels of miR-155 comparable to those found in DCs and Mϕs and THP-1 cells have been previously reported as a cell model for the generation of DCs and Mϕs (Auwerx, 1991; Bocchietto et al., 2007; Park et al., 2007). These observations add value to the THP1-155 cell sytem as a good model for studying miR-155 effects in a DC/Mϕ-like environment. It is worth mentioning that non-specific effects of Doxycycline on PU.1 expression cannot be excluded in this system and the development of a control THP-1 cell line transfected with an empty vector is ongoing in the lab.

Up regulation of miR-155 in THP1-155 cells led to the down regulation of both DC-SIGN and PU.1 (Figs.26, 27 and 28). However, this down regulation was at different expression levels. Both PU.1 and DC-SIGN protein levels were shown to be down regulated and only DC-SIGN mRNA levels were diminished whilst PU.1 ones remained stable (Figs. 26 and 27). These results suggested a post-transcriptional mechanism for miR-155 regulation of PU.1 most likely through translation inhibition, one of the mechanisms exerted by microRNAs (Bartel, 2004; Eulalio et al., 2008; Filipowicz et al., 2008). Interestingly, PU.1 levels showed a down regulation in THP1-155 cells (up to 16%) similar to the down regulation observed by *in vitro* luciferase experiments (Figs. 26 and 22, respectively). These observations support the *in vitro* assays results, obtained with artificial constructs in a different cell context. It is likely that miR-155 is targeting PU.1 in different cell types like B cells, where miR-155 has been shown to regulate PU.1 and immunoglobulin switch in mice (Vigorito et al., 2007). Moreover, both miR-155 and PU.1 have shown to be oncogenic (leukemogenic) factors (Clurman and Hayward, 1989; Eis et al., 2005; Kluiver et al., 2005; Scott et al., 1994), and it is possible that an imbalance of miR-155/PU.1 levels might lead to aberrant cell proliferation with leukemogenic implications.

PU.1 is a known transcriptional activator of DC-SIGN (Dominguez-Soto et al., 2005) and miR-155 over expression led to a down regulation of DC-SIGN protein and mRNA levels (Fig. 27). These data suggested a role for miR-155 in the transcriptional activity of DC-SIGN likely to be meditaed via direct targeting of PU.1. Promoter assays were therefore performed to test the hypothesis that miR-155 modulates DC-SIGN transcriptional activity through regulation of PU.1 levels. Fig.30 shows that miR-155 over expression led to a diminished DC-SIGN transcriptional activity by modulating the amounts of PU.1. These results proved the link between miR-155 and DC-SIGN during DC maturation, in which miR-155 is up regulated and both PU.1 and DC-SIGN levels are diminished (Figs. 15, 16 and 14, respectively). To assay the possible role of miR-155 in the pathogen binding ability of dendritic cells by DC-SIGN modulation, DCs were transfected with Anti-miR-155 oligonucleotides (Fig.31). These cells were then analyzed in pathogen binding experiments which showed that miR-155 levels modulate both DC-SIGN membrane levels and dendritic cell binding to *C.albicans* and gp120 (Fig. 32). The

effects on *C.albicans* were milder when compared to those on DC-SIGN expression and gp120 binding. It is possible that assaying miR-155 effects in *C.albicans* binding might require more sensitive techniques that allow single cell monitoring. This can be achieved by microfluidic cell trapping systems such as the one presented in Chapter 5.

MiR-155 modulation of dendritic cell binding ability establishes a new role for miR-155 in immunity. Pathogen recognition is one of the first steps in the immune response, in which a correct sensing and binding of pathogens is essential to exert a balanced and effective response. It results in the development of different T cell populations (Th_1, Th_2, Th_{17} or T_{regs}) that prime the adaptive immune response. An equilibrium between these phenotypes is necessary for a healthy immune system and its unbalance leads to diseases such as asthma or inflammatory bowel disease (Fuss and Strober, 2008; O'Shea and Murray, 2008; Wills-Karp, 2004). Thus, by modulating DC-SIGN levels miR-155 contributes to the initial processes and effectiveness of the immune response. In this regard, PU.1 is a known Th_2 regulator (Brunner et al., 2007; Chang et al., 2005b) and DC-SIGN has been shown to be controlled by Th_2 stimuli and involved in the modulation of Th responses (Bergman et al., 2004; Geijtenbeek et al., 2003; Relloso et al., 2002; van Kooyk, 2008). Mice lacking miR-155 show a skew towards Th_2 development (Rodriguez et al., 2007), suggesting that miR-155 might act as an inhibitor of "pro-Th_2" responses.

DC-SIGN is a lectin that binds to both foreign and self-glycans -reviewed in (Geijtenbeek et al., 2004)- and it is localized in immune-tolerance sites like placenta (Soilleux et al., 2002). Thus, it needs to be tightly regulated: ectopic expression of DC-SIGN might trigger the binding of self structures and in turn lead to autorreactiviy. By modulating DC-SIGN and PU.1, miR-155 not only contributes to the Th balance, it also contributes to an effective and localized antigen presentation for the development of a healthy immunity.

In conclusion, miR-155 contributes to the pathogen binding ability of dendritic cells by down regulating DC-SIGN through the direct targeting of PU.1. This proves a new role for miR-155 (and in fact for any microRNA as yet) during the initial steps of the

immune response where adequate pathogen recognition will determine the efficency and balance of the immune system, making miR-155 a small director in a big orchestra.

4 Chapter 4. Results: MiR-155 modulates the IL-13 pathway in macrophages by direct targeting IL13RA1

4.1 Introduction

Mϕs act as a first barrier of defence in the immune response; they promote inflammation and its resolution and can differentiate into a broad spectrum of phenotypes depending on the microenvironment and pathogens they encounter (Kindt et al., 2007; Murphy et al., 2008). Activation of Mϕs results in a broad spectrum of phenotypes which are represented in Fig. 3: M1 (classically activated, pro-Th_1) and M2 (alternatively activated, pro-Th_2). Whilst M1 macrophages are triggered by pro-inflammatory stimuli, M2 macrophages depend on Th_2-type cytokines such as IL-4 and IL-13 (Gordon and Taylor, 2005; Mantovani et al., 2005; Mosser and Edwards, 2008).

Interleukin 4 and 13 are classical Th_2 cytokines that bind mainly to IL-4 Type I and II Receptors. Type I receptors consist of dimers of the common gamma chain (γ_c) and IL-4 receptor alpha chain (IL4Rα), and Type II receptors consist of dimers of IL4Rα and IL-13 receptor alpha 1 chain (IL13Rα1). IL-4 and IL-13 exert their effects mainly through phosphorylation of the transcription factor STAT6 (Signal Transducer and Activator of Transcription 6) (Jiang et al., 2000; Palmer-Crocker et al., 1996; Takeda et al., 1996). While IL-4 can bind to both Type I and II receptors, IL-13 only binds to Type II receptors. IL-13 can also bind to IL13Rα2, considered as a decoy receptor; however, this receptor has been shown to signal in a STAT6 independent manner (Fichtner-Feigl et al., 2006; Hershey, 2003). Binding of IL-13 to the Type II receptor depends on the presence of IL13Rα1 (Jiang et al., 2000); therefore, this chain accounts for the IL-13 dependent activation of STAT6.

Binding to the IL- 4 Type I and II receptors leads to the phosphorylation and activation of Janus Tyrosine Kinases (JAKs), which are believed to be bound to these receptors in unstimulated cells. The functional phospho-JAK proteins then phosphorylate

the IL4Rα chain, providing docking sites for STAT6. When STAT6 is bound to the receptor, it is also phosphorylated by JAKs, becoming active, dimerizing and translocating to the the nucleus, where it acts as a transcription factor (Hebenstreit et al., 2006).

M2 Mϕs are specialised in the defence against extracellular pathogens; they promote tissue repair and inflammation resolution and are also involved in pathologies characterized by exacerbated Th_2 responses, such as asthma or ulcerative colitis (Fuss and Strober, 2008; Martinez et al., 2009; Wills-Karp, 2004). Mϕs can be reprogrammed between M1 and M2 phenotypes depending on the stimuli sensed (Stout and Suttles, 2004). Previous work in Sanchez-Elsner's lab suggested that miR-155 might be involved in the pro-inflammatory profile of human M1 Mϕs; in addition, it was shown that inflammatory stimuli lead to up regulation of miR-155 in murine macrophages (O'Connell et al., 2007). Interestingly, bioinformatics analysis predicted IL13RA1 as a putative target of miR-155. IL13RA1 is a key component of the Type II IL-4 receptors (LaPorte et al., 2008) and it is essential for IL-13 function (Ramalingam et al., 2008). IL-13 is one of the main Th_2 cytokines that trigger alternative (M2) Mϕ activation through the STAT6 (Signalling Transducer and Activator of Transcription 6) signalling cascade, a typical Th_2/M2 signalling pathway (Hebenstreit et al., 2006; Hershey, 2003; Martinez et al., 2009; Wynn, 2003).

4.2 Hypothesis and aims

4.2.1 Hypothesis

MiR-155 targets IL13RA1 modulating the IL-13 response of macrophages and contributing to the M1/M2 macrophage differentiation system.

4.2.2 Aims

- To assay miR-155 direct targeting of IL13RA1 3'UTR.

- To determine miR-155 over expression effects on IL13RA1 expression and STAT6 activation in THP1-155 cells.

- To determine miR-155 over expression effects on IL13RA1 expression and STAT6 activation in primary macrophages.

- To assay miR-155 regulation of IL-13/STAT6 targets in primary macrophages.

To avoid confussion, the term "IL13RA1" will be used when referring to the gene/mRNA and "IL13Rα1" to the protein henceforth.

4.3 MiR-155 targets the 3'UTR of IL13RA1

BIC (MIR155 HG) was shown to be involved the expression profile of human M1 Mϕs and miR-155 was demonstrated to be up regulated by pro-inflammatory stimuli in mice (O'Connell et al., 2007). *In silico* analysis was performed to identify pro-Th_2 (pro-M2) factors putatively targeted by miR-155. Amongst the targets predicted for miR-155, IL13RA1 was considered as a good candidate due to its role and high expression in alternatively activated macrophages and where the levels of miR-155 were shown to be lower. Therefore the potentital for direct interaction between miR-155 and the 3'UTR of IL13RA1 was investigated.

In order to do this, two main objectives were proposed:

- Objective 1: *In silico* analysis of miR-155::IL13RA1 3'UTR interaction

- Objective 2: Cloning and mutation of the 3'UTR of IL13RA1 in pRLTK reporter vector. *In vitro* assay of the direct targeting of IL13RA1 3'UTR by miR-155 using the Dual Luciferase Assay system.

4.3.1 *In silico* analysis of miR-155 directly targeting IL13RA1 3'UTR

Using an *in silico* approach IL13RA1 was predicted as a putative target of miR-155. Table 4 shows a list of the predictions for mir-155 directly targeting IL13RA1 by different databases. The discrepancie between database predictions may be attributed to databases and algorithms differentially relying on the conservation of IL13RA1 3'UTR amongst several species (e.g., *D.melanogaster* or *C.elgans* have no ortholog for IL13RA1, and both rat and mouse 3'UTRs differ from humans).

Database	miR-155 targets IL13RA1
TargetScan 5.1.	No
microRNA.org (January 2008)	Yes (2 sites)
microRNA.org (September 2008)	Yes (1 site)
microCosm Targets	No
PITA	Yes
PicTar	No
Diana-microT	No

Table 4 Predictions for miR-155 targeting IL13RA1 3'UTR in the list of databases used

4.3.1.1 microRNA.org

microRNA.org is a microRNA::target prediction tool and database available on line at (http://www.microrna.org/microrna/home.do). It employs miRanda algorithm, which uses a method based on the conservation of evolutionary relationships between microRNAs and their targets (Enright et al., 2003). miRanda searches for sequence complementary (this includes Watson and Crick base pairing and G:U wobbles) rather than sequence similarity (alignment of sequences). It also evaluates the thermodynamic stability of the predicted alignments between target-microRNA using the RNAlib library included in the Vienna package, a compilation of RNA folding algorithms and tools (Hofacker et al., 1994; McCaskill, 1990; Zuker and Stiegler, 1981).

microRNA.org was released in January 2008; in this version miR-155 was predicted to target the 3'UTR of IL13RA1 in two different sites shown in Figure 33 that map to nucleotides 1049-1071 (named as Site 1) and 1399-1424 (named Site 2) of the 3'UTR of IL13RA1. microRNA.org September 2008 version does not include the contribution of the terminal nucleotides (first and last two) to the alignment score, in accordance to (Wang et al., 2008), and only Site 2 was predicted in this version.

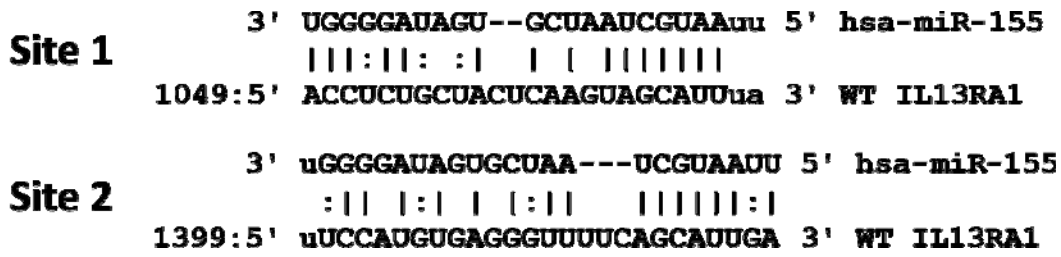

Figure 33 Sites for IL13RA1 as prediced by microRNA.org January 2008 version. In the 2008 September release, miR-155 was only predicted to bind to site 2.

4.3.1.2 PITA

The PITA (Probability of Interaction by Target Accesibility) algorithm was one of the first prediction methods to incorporate microRNA site accessibility (Kertesz et al., 2007a) and it models the thermodynamic stability of microRNA target interaction based on the folding of RNA structures. PITA software can be downloaded and is also a web interface (http://genie.weizmann.ac.il/pubs/mir07/mir07_prediction.html).

IL13RA1 3'UTR sequence was loaded from Ensembl Genome Browser and run on the PITA web interface. IL13RA1 3'UTR was predicted to have 5 different binding sites for miR-155. These are annotated in the form of X:Y:Z which corresponds to nucleotides:mismatches:GUwobbles. Sites were: 8:1:0 in position 1038; 8:1:1 in position 1389; 8:1:1 in position 2847; 8:1:1 in position 2946 and 8:1:0 in position 2275 of the 3'UTR of IL13RA1. Despite prediciting 5 different sites for miR-155, only the first two listed binding sites (which correspond to Site1 and 2, respectively, in agreement with Figure 33) were the only ones with a negative $\Delta\Delta G$ value, the free energy released in the microRNA::target interaction. Thus, negative values are those that are energetically favourable. Predicted energies were $\Delta\Delta G$= -5.36 for Site 1 and $\Delta\Delta G$= -2.12 for Site 2, which indicates a putative more stable binding to Site 1 for miR-155.

4.3.1.3 RNAHybrid

As shown for PU.1::miR-155 interaction (Fig.20), the secondary structure of IL13RA1 3'UTR and miR-155 interaction was sought using RNAHybrid. Fig. 34 shows the RNA structures of each one of miR-155 binding sites predicted in the 3'UTR of IL13RA1.

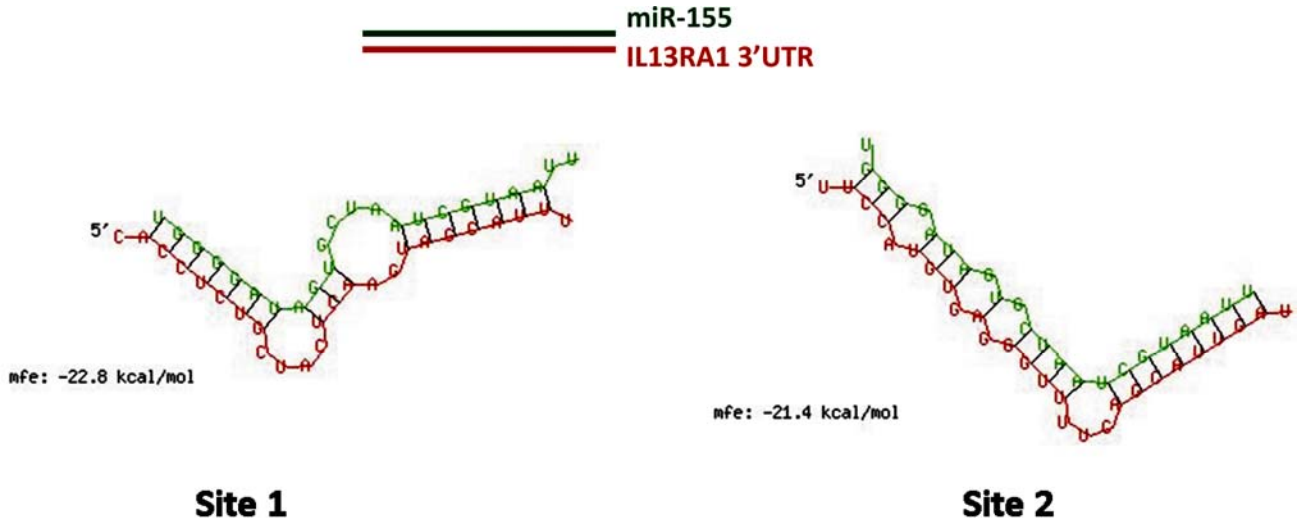

Figure 34 Predicted structures for miR-155::IL13RA1 3'UTR binding sites. Red indicates the 3'UTR sequence that is predicted to interact with miR-155 (in green). Energies indicated are the predicted energy values released in each one of sites. Site 1 maps to nucleotides 1049-1071 and Site 2 to 1399-1424 in the 3'UTR of IL13RA1. Downloaded from RNAHybrid (http://bibiserv.techfak.uni-bielefeld.de/rnahybrid/submission.html)

4.3.2 Cloning of pRLTK_3'UTR_PU.1 and mutagenesis of miR-155 binding sites.

The protocol for cloning the IL13RA1 3'UTR fragment harbouring the predicted binding sites for miR-155 (Sites 1 and 2) is detailed in section 2.3.1. This led to the construction of the reporter vector **pRLTK_WT_3'UTR_IL13RA1** (Fig.10). Site directed mutagenesis was performed in each one of the predicted binding sites: **pRLTK_MUT1_3'UTR_IL13RA1** contains a mutation in Site 1 and **pRLTK__MUT2_3´UTR_IL13RA1** contains a mutation in Site 2. As a preliminary screening, RNAHybrid was used to predict the structures of the binding sites for miR-155 in sire 1 and site 2 mutants. Figures 35 and 36 show these predicted binding structures. When mutating Site 1 neither the structure or energy of Site 2::miR-155 binding showed a change while that of Site 1 did (Fig.35, right and left columns, respectively). Similarly, mutation of Site 2 did not alter the structure or energy of Site 1 whilst those of Site 2 did (Fig.36 left and right columns, respectively).

Fig.37A shows the predicted nucleotide interactions between the 3'UTR of IL13RA1 with miR-155 in each one of the sites, for the wild type version (WT) and each one of the mutants: MUT1 (mutant in Site1) and MUT2 (mutant in Site 2).

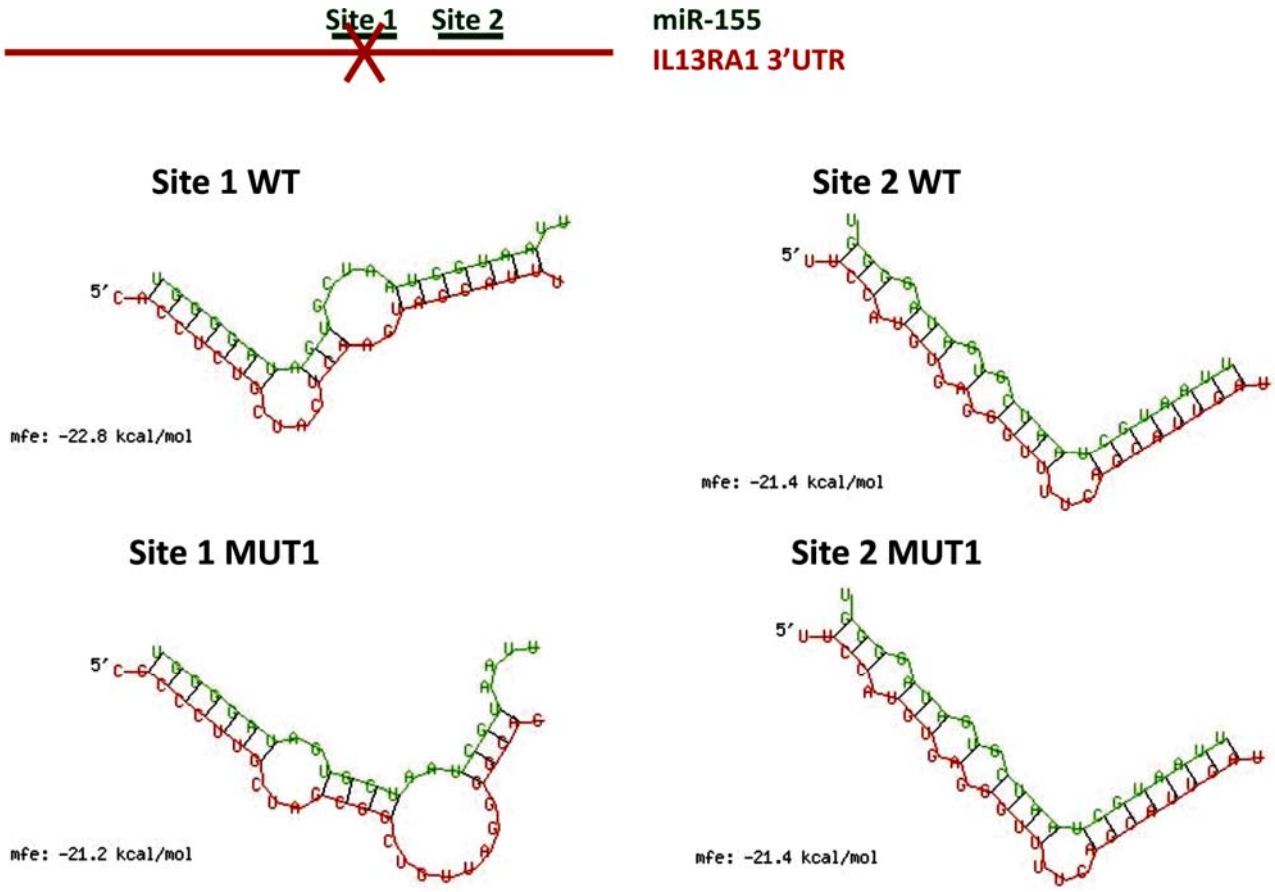

Figure 35 Predicted structures and energy released in each predicted binding site for miR-155 in the MUT1 IL13RA1 3'UTR. It is shown the comparison between the wild type (WT) and mutant for Site 1 (MUT1). Site 1 was predicted to change structure and energy while Site 2 did not show any predicted modification. Predictions were made using the web interface of RNAHybrid using as input the sequence of the cloned 3'UTR and mutant for Site 1 versions. MiR-155 sequence was downloaded from MiRBase release 15-April 2010.

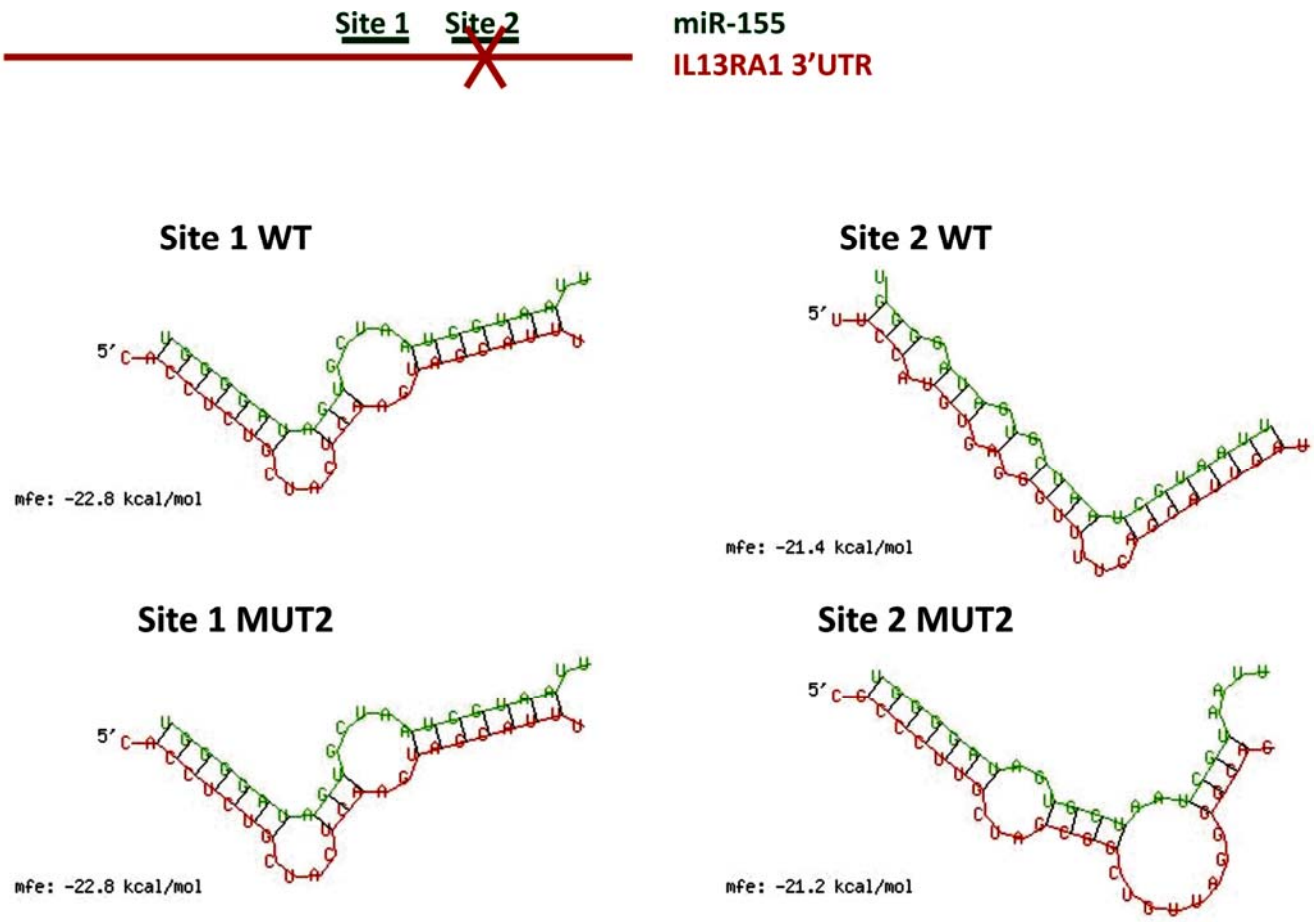

Figure 36 Predicted structures and energy released in each predicted binding site for miR-155 in the MUT2 IL13RA1 3'UTR. It is shown the comparison between the wild type (WT) and mutant for Site 2(MUT2). Site 2 was predicted to change structure and energy while Site 1 did not show any predicted modification. Predictions were made using the web interface of RNAHybrid using as input the sequence of the cloned 3'UTR and mutant for Site 2 versions. MiR-155 sequence was downloaded from MiRBase release 15-April 2010.

4.3.3 MiR-155 directly binds to the 3'UTR of IL13RA1

The targeting of IL13RA1 3'UTR by miR-155 was analyzed transfecting the wild type, MUT1 and MUT2 reporter constructs in HeLa cells and employing Dual Luciferase Assay (see 2.5 for Dual Luciferase Assay and 2.6.2 for the transfection protocol). Fig.37A shows the predicted pairings between each site in the 3'UTR of IL13RA1 in the wild type (WT) and mutant (MUT1 and MUT2) versions.

Co transfection of these constructs with pCDNA BIC (expression vector for miR-155, "miR-155", black bars in Fig.37B) or control vector ("Control" white bars in Fig.37B) allowed testing direct binding of miR-155 to each predicted site in the 3'UTR of IL13Rα1. Figure 37B shows the results of the luciferase assays performed. Co transfection of miR-155 with the wild type construct led to a significant reduction of the renilla luciferase activity by 50% (Fig.37B, WT). Mutation of either of the predicted binding sites for miR-155 abolished miR-155 effects (Fig.37B, MUT1 and MUT2, respectively). Experiments were performed in triplicates and it is shown one of them. Statistical analysis was performed using t-test with GraphPad Prism version 5.00 for Windows.

These data indicarte that miR-155 directly binds to the 3'UTR of IL13RA1 and that it requires both binding sites for its action, as mutation of either site rendered the construct unaffected by miR-155 over expression.

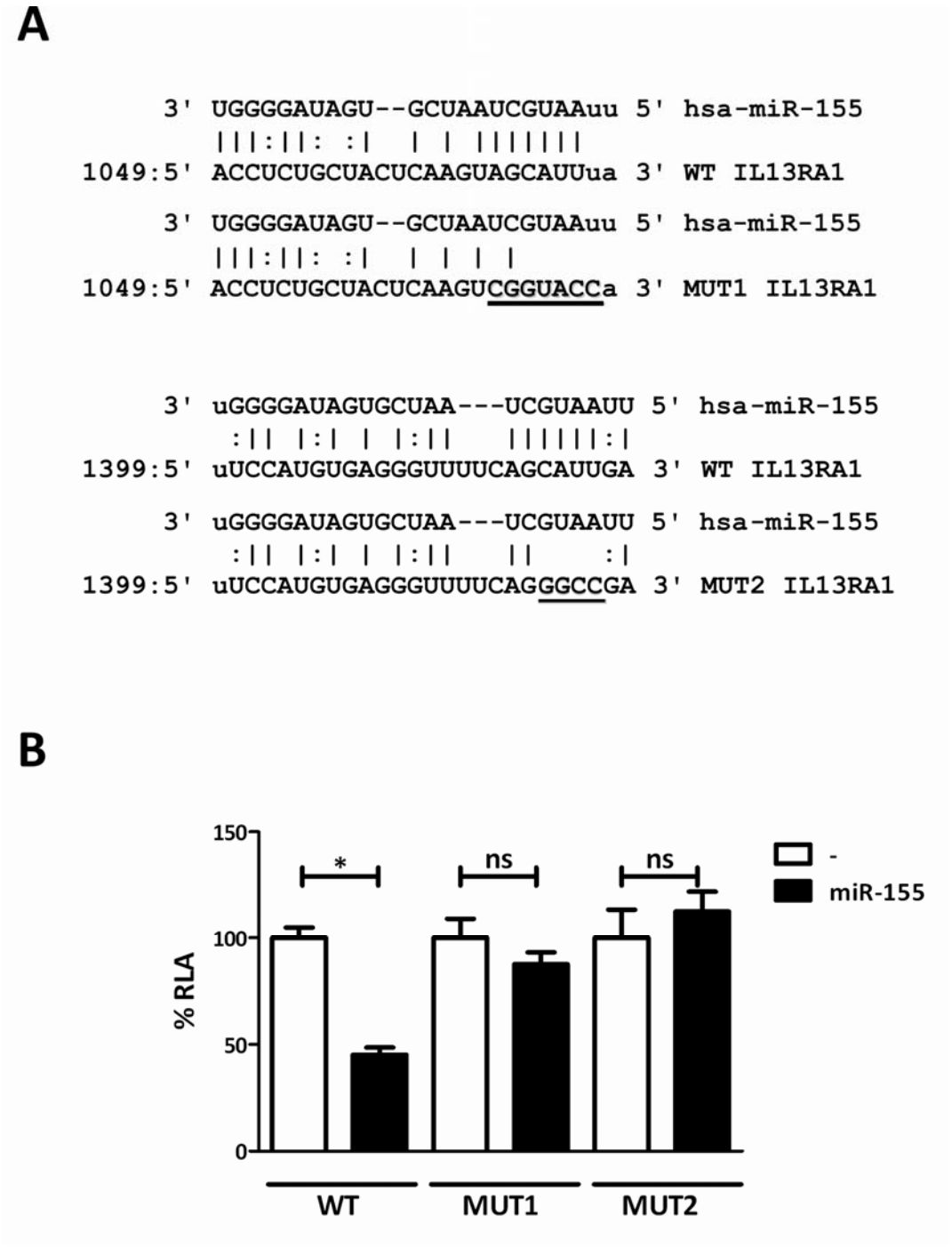

Figure 37 MiR-155 directly binds to the 3'UTR of IL13RA1. A: Predicted binding sites for miR-155 in the 3'UTR. MUT1 is the mutant version for Site 1 (nucleotides 1049-1071) and MUT2 is the mutant version of Site 2 (nucleotides 1399-1424) of the 3'UTR of IL13RA1. B: Reporter constructs were co transfected with empty pCDNA3.1 (white bars, -) or pCDNA3.1_BIC (black bars, miR-155). When mutating any of the predicted sites (MUT1 and MUT2) the over expression of miR-155 (black bars) showed no effect. It is shown one experiment of three replicates. *: P-value≤0.05

4.4 MiR-155 effects on IL13RA1 levels and STAT6 signalling in THP1-155 cells

After confirming *in vitro* the predicted targeting of IL13RA1 3'UTR by miR-155 (Fig.37), the next step investigated whether this occurred for endogenous expression of IL13RA1 in THP1-155 cells. This cell line provides a good model to study miR-155 over expression within a monocytic cell context and had been previously validated (section 3.5). These cells over express miR-155 under the control of tetracycline or a tetracycline derivative as doxycycline; this isolates the effects of miR-155 over expression from other pathways activated by pro-inflammatory stimuli that trigger miR-155 up regulation (O'Connell et al., 2007) and Fig.15. Moreover, THP-1 cells are commonly used to study macrophage biology (Auwerx, 1991; Park et al., 2007) and therefore provide a macrophage-like environment to study miR-155 effects.

The aim was to determine miR-155 over expression effects on endogenous IL13RA1 expression. IL13RA1 is part of the Type II IL-4 receptors and triggers STAT6 signalling, a transcription factor related to Th_2 responses (Hebenstreit et al., 2006; Hershey, 2003). Therefore, IL13RA1 expressiona and and STAT6 activation in THP1-155 cells was investigated following these objectives:

Objective 1: Determining IL13RA1 protein and mRNA levels in THP-1 155 cells by western blotting and RT-qPCR, respectively.

Objective 2: Analysis of STAT6 phosphorylation in THP-1 155 cells following IL-4 and IL-13 stimulation by western blotting.

4.4.1 The effects of miR-155 over expression on IL13RA1 in THP1-155 cells

THP1-155 cells were cultured in the presence or absence of doxycycline over 96h which had proven efficient to induce miR-155 over expression (Fig. 25; an example of Ct values is shown in Appendix 5). Cell extracts (see 2.10) were collected every 24h and protein and mRNA was analyzed by western blotting and RT-qPCR, respectively (see 2.8, 2.9.1.1, 2.9.2.1, 2.9.2.3 and 2.10). Fig.38 shows the results obtained of one time course experiment that was performed three times. β-tubulin was used as loading control. Figure 38A shows that upon addition of doxycycline, IL13Rα1 protein levels dropped to 4% of its original value (start of the treatment). Fig.38B shows the results of the RT-qPCR analysis for IL13RA1 mRNA; actin (ACTB1) was used as housekeeping (normaliser) control. mRNA levels of IL13RA1 did not show significant fold change suggesting a post transcriptional mechanism for the action of miR-155 over expression on the regulation of IL13RA1.

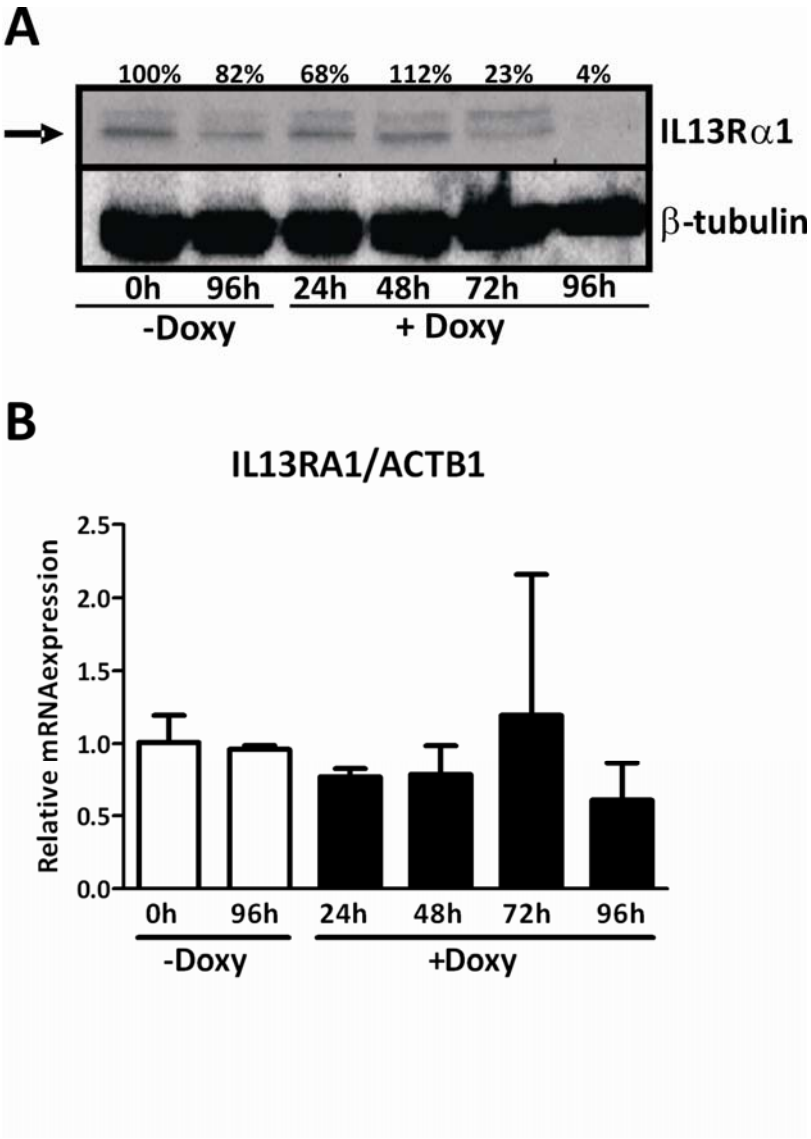

Figure 38 IL13RA1 regulation by miR-155 over expression in THP1-155 cells. *A*: western blot analysis of IL13Rα1 in THP1-155 cells over expressing (+Doxy) or not (-Doxy) miR-155 over the course of 96h of treatment with doxycycline. Densitometry values are %numbers on top of each lane, compared to time 0 and normalized with β-tubulin. B: RT-qPCR of IL13RA1 mRNA expression in cells treated over 96h with doxycycline. Actin (ACTB1) was used as normalizing control. It is shown one experiment of a triplicate.

4.4.2 MiR-155 effects on STAT6 activation in THP1-155 cells

IL13Rα1 is an essential component of Type II IL-4 receptors and signals through STAT6 phosphorylation(Hebenstreit et al., 2006; Hershey, 2003). While IL-4 can bind to both Type I IL-4 and Type II recptors, IL-13 binds solely to IL13Rα1 promoting STAT6 phosphorylation and has been shown to promote different actions than those of IL-4 (Jiang et al., 2000; Morimoto et al., 2009; Ramalingam et al., 2008; Wynn, 2003).

To dissect the effects of miR-155 over expression on both IL-4 and IL-13 signalling via STAT6, miR-155 was induced or not in THP1-155 cells which were then treated with IL-4 or IL-13. Results are shown in the next sections.

4.4.2.1 MiR-155 effects on IL-4 and IL-13 induced phosphorylation of STAT6 in THP1-155 cells

MiR-155 over expression effects were first tested on both IL-4 and IL-13 dependent activation of STAT6. Cells were incubated in the presence of doxycycline for a minimum period of 96h (which leads to miR-155 up regulation, Fig.25); after over night starvation (see 2.2.1) they were stimulated with IL-4, IL-13 or left untreated during 30 min. Cells were then collected and analyzed by western blotting (see 2.10). Figure 39 shows that in the presence of doxycycline (**+Doxy**) the phosphorylation of STAT6 (P-STAT6) was reduced following IL-4 or IL-13 stimulation. β-tubulin was used as loading control. Importantly, cells unstimulated showed no basal activation regardless of doxycycline treatment. P-STAT6 down regulation by IL-4 was less than that by IL-13 treatment in cells over expressing miR-155, which was attributed to signalling from IL-4 Type I receptors.

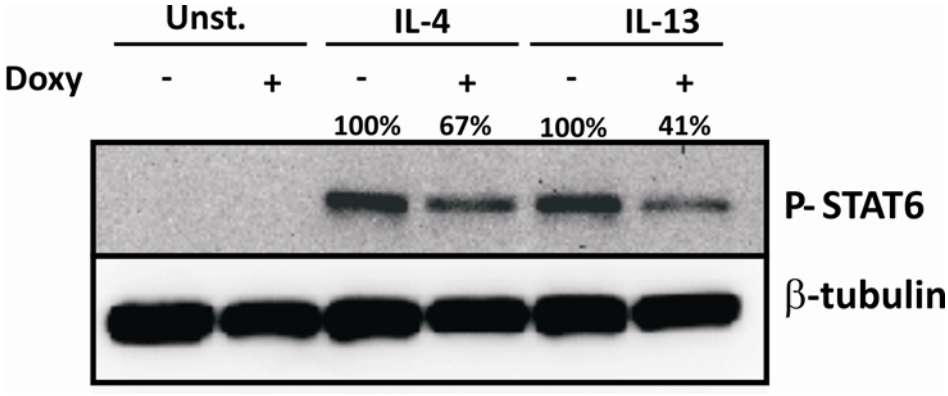

Figure 39. MiR-155 effects on IL-4 and IL-13 induced phosphorylation of STAT6. THP1-155 cells were treated with doxycycline (+ and – Doxy, respectively) during a minimum of 96h; after over night starvation cells were left unstimulated (Unst.) or treated with IL-4 or IL-13 during 30 min. Cell extracts were analyzed by western blot for phosphorylation of STAT6 (P-STAT6). It is shown one experiment of 3 replicates.

Once observed miR-155 effects on both IL-4 and IL-13 dependent phosphorylation of STAT6, and since IL-13-dependent phosphorylation of STAT6 solely depends on the presence of IL13RA1 (Hershey, 2003; Morimoto et al., 2009), the following experiments were only performed with IL-13 stimulation. This was done to avoid misinterpretation of results following IL-4 treatment because this cytokine can also bind to IL-4 Type I receptors and signal via STAT6 phosphorylation, which would make the results interpretation more complex or even misleading.

4.4.2.2 MiR-155 effects on total STAT6 levels in THP1-155 cells

In order to determine that miR-155 is not down regulating total STAT6 levels, THP1-155 cells were treated as before (section 4.4.2.1) and total STAT6 protein expression measured by western blot (see 2.10). Fig. 40 shows that STAT6 protein levels are not altered by miR-155 over expression (**+ Doxy**) or IL-13 stimulation. Thus, the lower P-STAT6 levels when miR-155 is up regulated (Fig. 39) do not depend on the total amount of STAT6 protein. These results suggested that miR-155 effects on the phosphorylation of STAT6 are due to impairment in the signalling cascade.

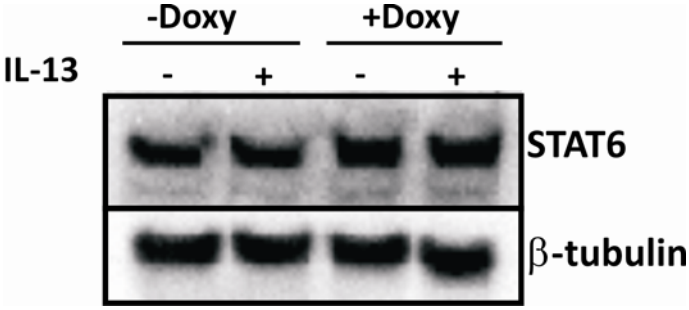

Figure 40. MiR-155 and IL-13 effects on total STAT6 protein expression. THP1-155 cells were treated with doxycycline (+Doxy and –Doxy, respectively) during 96h and cells were treated or not with IL-13 (+ and -, respectively). The western blot shows that miR-155 over expression did not alter total STAT6 levels. It is shown one experiment which was performed in triplicates.

4.4.2.3 MiR-155 lifetime effects on IL-13 signalling in THP1-155 cells

In order to further assay the effects of miR-155 on IL-13 signalling, THP1-155 cells were stimulated with IL-13 and analyzed at different time points. THP1-155 cells were cultured in the presence of doxycycline (**+Doxy**) or not (**-Doxy**) for 96h, starved over night (see 2.2.1) and then stimulated with IL-13. Cells were collected 30min, 1h and 2h post stimulation and P-STAT6 analyzed by western blotting. β-tubulin was used as loading control. Fig.41 shows the kinetics of IL-13 dependent phosphorylation of STAT6 in a doxycycline (miR-155 over expression) (**+/-Doxy**) dependent manner. Doxycycline treated cells (**+Doxy**) showed less STAT6 phosphorylation; under basal expression of mir-155 (**-Doxy**, in blue), in which the phosphorylation peak was at 30min and diminished over 2h. In the case of doxycycline treated cells (**+Doxy**, in red), phosphorylation peaked at 1h and reached 50% of the P-STAT6 levels when compared with no doxycycline treated cells (**-Doxy**, in blue). These experiments showed that miR-155 over expression diminished STAT6 phosphorylation and that these effects were maintained over the time.

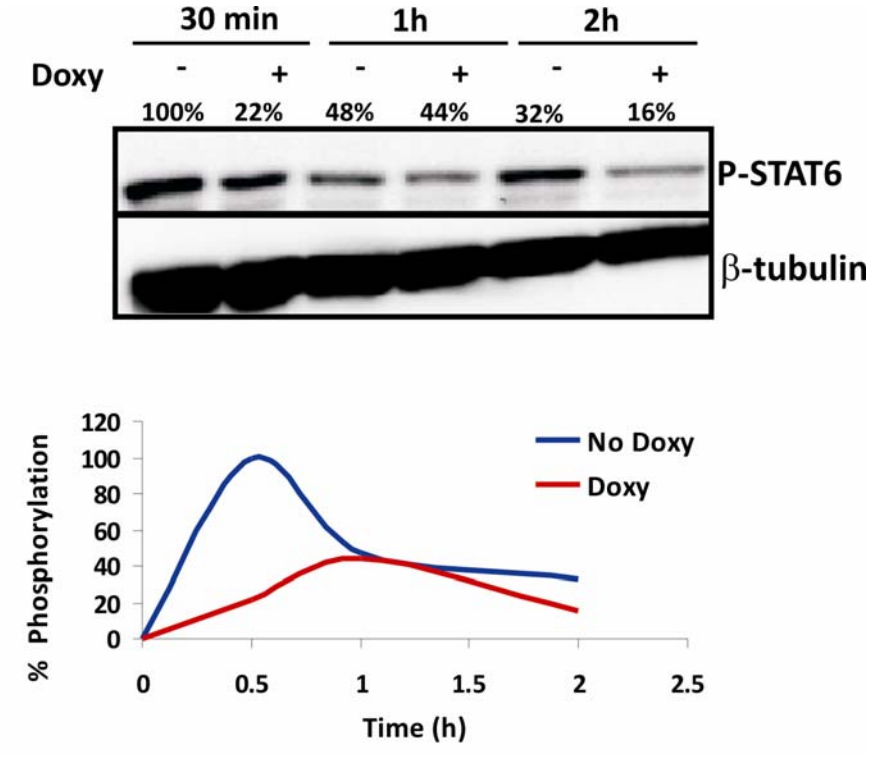

Figure 41 MiR-155 over expression effects on IL-13 induced phosphorylation of STAT6 over the time. THP1-155 cells were treated or not with doxycycline (+ or – Doxy, respectively) during a minimum of 96h; starved over night and stimulated with IL-13. Cells were collected at different times (30min, 1h and 2h) and phosphorylation of STAT6 (P-STAT6) was checked by western blotting (upper). The graph bellow plots the kinetics of STAT6 phosphorylation comparing % P-STAT6 in doxycycline treated (Doxy, in red) or not (No Doxy, in blue).

4.5 MiR-155 effects on IL13RA1 expression and STAT6 phosphorylation in primary macrophages

MiR-155 over expression was found to down regulate IL13Rα1 in THP1-155 cells (Fig.38); and also to lead to a diminished phosphorylation of STAT6 upon IL-4 and IL-13 treatments (Figs.39 and 41) without affecting STAT6 protein (Fig.40).

It was hypothesised that these effects might be similar in primary macrophages. THP1-155 cells are an excellent system to test myeloid target genes but it has the limitations of a cell line. In order to more closely match physiological conditions, Mϕs were analyzed employing Anti-miR-155 transfections. The objectives established were:

- Objective 1: Transfection of primary Mϕs with Anti-miR-155/Control oligonucleotides.

- Objective 2: Determine the expression of IL13RA1 and STAT6 phsophorylation in human macrophages transfected with Anti-miR-155.

4.5.1 Anti-miR-155 transfections in primary macrophages

4.5.1.1 Transfection efficency check by flow cytometry

Human blood monocytes were extracted from buffy coats (see 2.2.1). Monocytes were plated and stimulated with GM-CSF to allow macrophage differentiation. These cells show high phagocytic capability, and it was proposed that the method previously used with dendritic cells could be used: transfection by natural uptake. To assay this, monocytes were incubated in the presence of 50nM Cy3-labelled Control microRNA (Ambion) oligonucleotides and transfection efficency was checked by flow cytometry 3 days later. Section 2.7.3 details the transfection conditions. Before checking the cells in the cytometer, these were washed with 10 times their volume to reduce unspecific labelling. Fig. 42 shows a cytometry profile of macrophages at day 3 post transfection. The blue line shows the fluorescence of untransfected cells and the red line shows the shift in fluorescence of the cells transfected with the Cy3 labelled probe; 100% of the cells were positive. It is shown one of four independent donors.

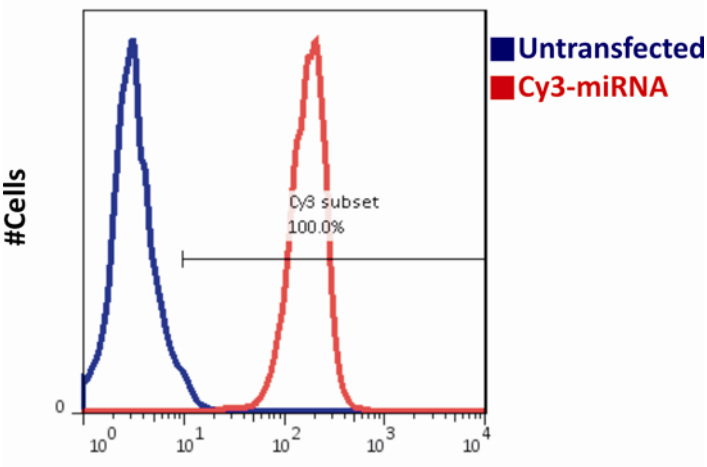

Figure 42 Transfection efficency in human macrophages checked by flow cytometry. Human monocytes transfected with Cy3 labelled Control-microRNA (Ambion) and checked 3 days post transfection by flow cytometry. An overlay of cells transfected and non transfected is shown. Blue: Untransfected cells. Red: cells transfected with Cy3-labelled probe. All cells were positive for Cy3. It is shown one of 4 independent donors.

4.5.1.2 Anti-miR-155 dose titration

After checking transfection efficency, monocytes were transfected with Anti-miR-155 oligonucleotides. Two Anti-miR-155 doses were assayed: a single dose ("**Normal dose**" in Fig.43) at day 0 and stimulated/unstimulated with IL-13 72h later, and a double dose (Fig.43, "**Extra dose**") which consisted on transfecting at day 0, re-transfect 50h later and stimulate with IL-13 or not at 72h. Anti-miR-155 or Anti-Negative Control #1 (Anti-miRNA Control hence foth) (both from Ambion) were employed. Cells were collected at day 5 and miR-155 expression analyzed by RT-qPCR (see 2.8, 2.9.1.2, 2.9.2.2 and 2.9.2.3) normalising with RNU44. Values shown in Fig.43 are the relative fold induction of miR-155 compared to day 0.

Both doses showed miR-155 knock down (Fig.43, black bars in both graphs). However, the double dose ("**Extra dose**"in Fig.43) showed to alter cells response to IL-13: this cytokine led to up regulation of miR-155 in the control transfection more than 30 times when compared to the single dose ("**Normal dose**"in Fig.43). Monocyte to macrophage differentiation up regulates miR-155 expression (personal communication of Dr. T. Sanchez-Elsner); however, this up regulation was around 3 times lower when Anti-miR-155 oligonucleotides were retransfected twice. This proved some instability under these conditions and it was therefore decided to use the single ("**Normal dose**" in Fig.43) in the following experiments for investigating miR-155 effects on IL13RA1 expression and signalling.

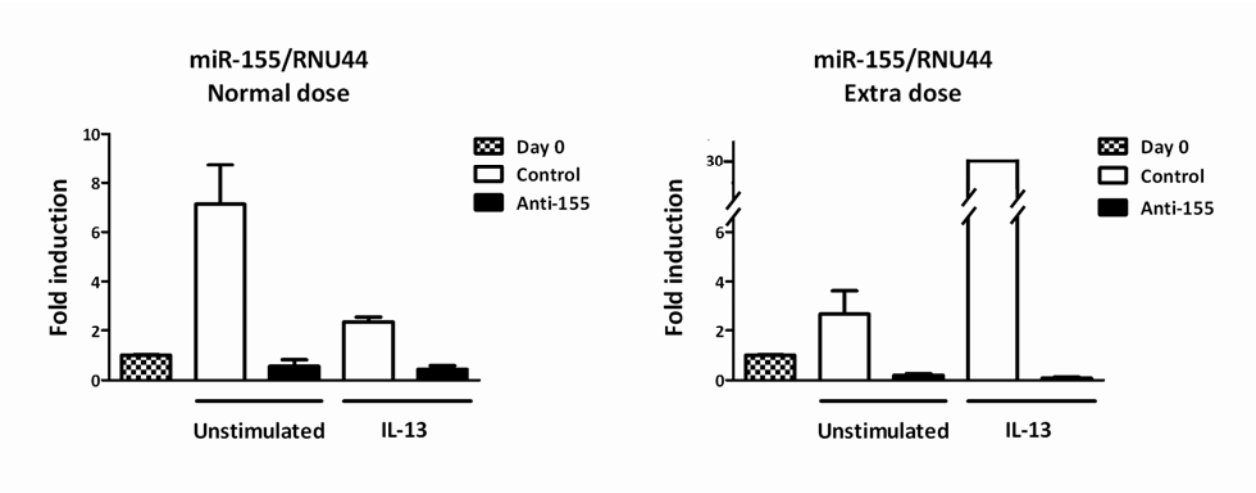

Figure 43 Anti-miR-155 (or Anti-miRNA Control) dose dependent effects. Normal dose: cells were transfected with 50nM on day day 0, stimulated or not with IL-13 on day 3 and collected 48h later. Extra dose: cells were transfected on day 0 with 50nM of Anti-155 or Control, re-transfected again using the same amounts 50h later, stimulated or not with IL-13 at day 3 and collected 48h post stimulation. This was a first experiment to test transfection conditions.

4.5.2 MiR-155 effects on IL13Rα1 expression and STAT6 phoshorylation in macrophages

It has been shown that miR-155 directly targets IL13Rα1 rendering lower STAT6 phosphorylation in THP-1 155 cells (Figs. 37, 38 and 39). It has also been shown that macrophages transfected with Anti-miR-155 have less miR-155 levels even 5 days post transfection (Fig. 43). To further test miR-155 effects in human primary macrophages in the expression of IL13RA1 and in IL-13 signalling, human macrophages were transfected with Anti-miR-155 oligonucleotides or Anti-miRNA Control (4.5.1.2, 2.8, 2.9.1.2., 2.9.2.2 and 2.9.2.3). Macrophages were stimulated or not with IL-13 on day 3 post transfection and cells were collected 2h post stimulation to check IL13Rα1 and phospho-STAT6 proteins by western blotting. In both experiments β-tubulin was used as loading control.

Figure 44A shows the results for IL13Rα1 protein expression by western blot analysis: when Anti-miR-155 was transfected IL13Rα1 protein showed up regulation. Fig.44B shows a bar graph representing the mRNA fold induction of IL13RA1 after Anti-miR-155 transfection: IL13RA1 mRNA showed no significant regulation by Anti-miR-155 (black bars). These results suggest a post transcriptional mechanism for miR-155 effects on IL13RA1 expression in macrophages. An experiment of a triplicate is shown. Statistics were performed using t-test with GraphPad Prism version 5.00 for Windows.

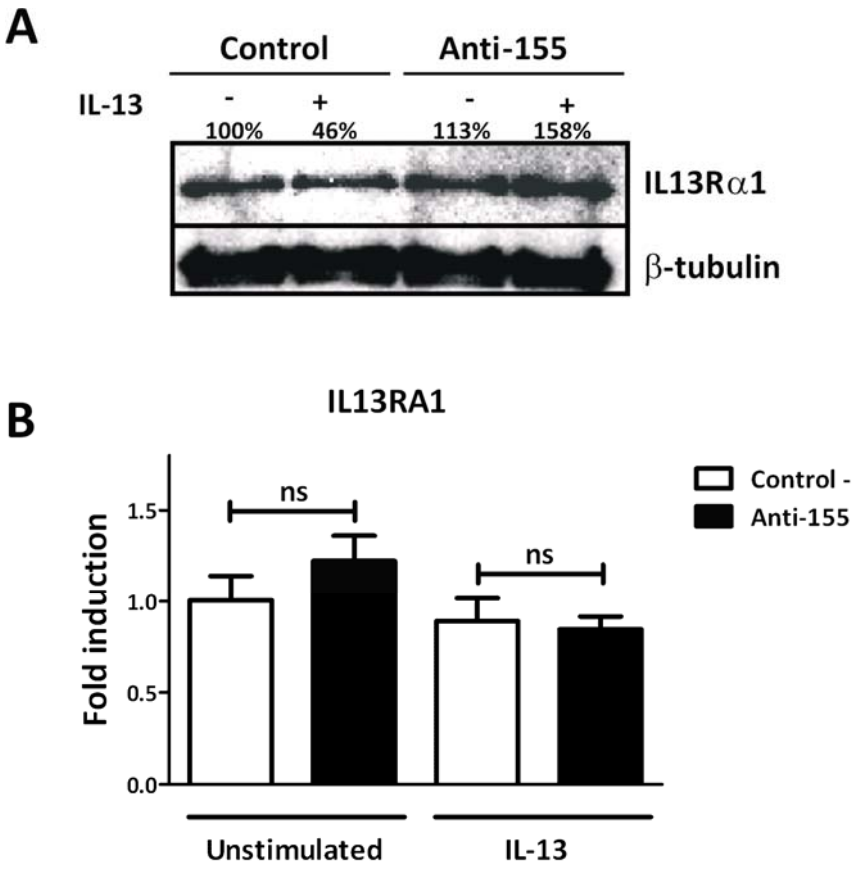

Figure 44 MiR-155 effects on IL13RA1 expression in primary macrophages. Monocytes were transfected with Anti-miR-155 (Anti-155) or Anti-miRNA Control (Control) and stimulated (+) or not (-) with IL-13. *A*: western blotting for IL13RA1; densitometry values compared to unstimulated Control transfected cells are shown above each lane. *B*: mRNA fold induction of IL13RA1 (ACTB1 used as normalizer) compared to unstimulated Control transfected cells. It is shown one experiment of three independent donors. ns: non significant

The effects of miR-155 levels on STAT6 phosphorylation were also investigated in these cells. Figure 45 shows that transfecting Anti-miR-155 increased IL-13 dependent phosphorylation of STAT6 in macrophages. No basal STAT6 activation was detected in unstimulated cells.

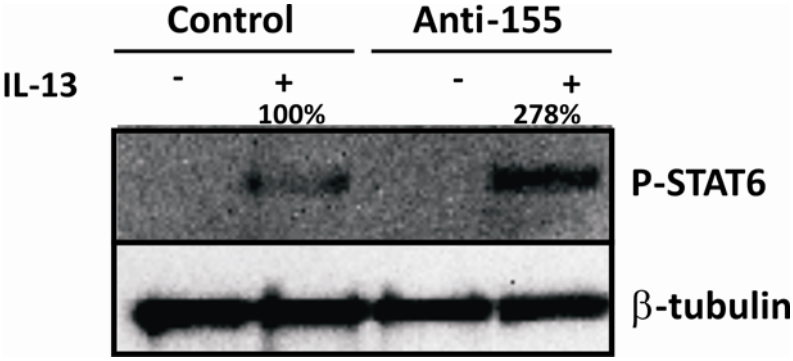

Figure 45 IL-13 dependent phosphorylation of STAT6 in primary macrophages transfected with Anti-miR-155 (Anti-155) or Anti-miRNA Control (Control). Western blotting for phosphorylated STAT6 (P-STAT6); densitometry values compared to unstimulated Control are shown above each lane. It is shown one experiment of three independent donors.

4.6 MiR-155 affects the expression of IL-13/STAT6 target genes in macrophages

It has been demonstrated that miR-155:

- directly targets IL13RA1 (Fig.37);

- regulates the expression of IL13Rα1 in THP1-155 cells (Fig.38) and primary macrophages (Fig.44);

- and that it modulates IL-13-dependent STAT6 phosphorylation in both THP1-155 cells and Mϕs (Figs.39 and 45, respectively).

It was therefore important to establish whether miR-155 could modulate target genes of the IL-13/STAT6 signalling cascade in primary Mϕs based on previous observations (Hebenstreit et al., 2006; Mantovani et al., 2004; Martinez et al., 2006; Martinez et al., 2009). Anti-miR-155 or Anti-miR Control oligonucleotides were transfected in human monocytes as previously described (see section 4.5.1.2). Three days post transfection cells were stimulated or not with IL-13 for 24h and then collected for RNA extraction and analysis by RT-qPCR (see 2.8, 2.9.1.1, 2.9.2.1, 2.9.2.3). Genes analyzed are shown in Fig.46 and included CCL18, SOCS1, CD23, SOCS1, DC-SIGN and SERPINE. Other genes were also assayed that did not show significant change such as IL-10 and TFGβ (IL-10 and TGFB1 in Fig.47). Results shown in Figs.46 and 47 correspond to one out of three independent donors. Statistics were performed using t-test with GraphPad Prism version 5.00 for Windows.

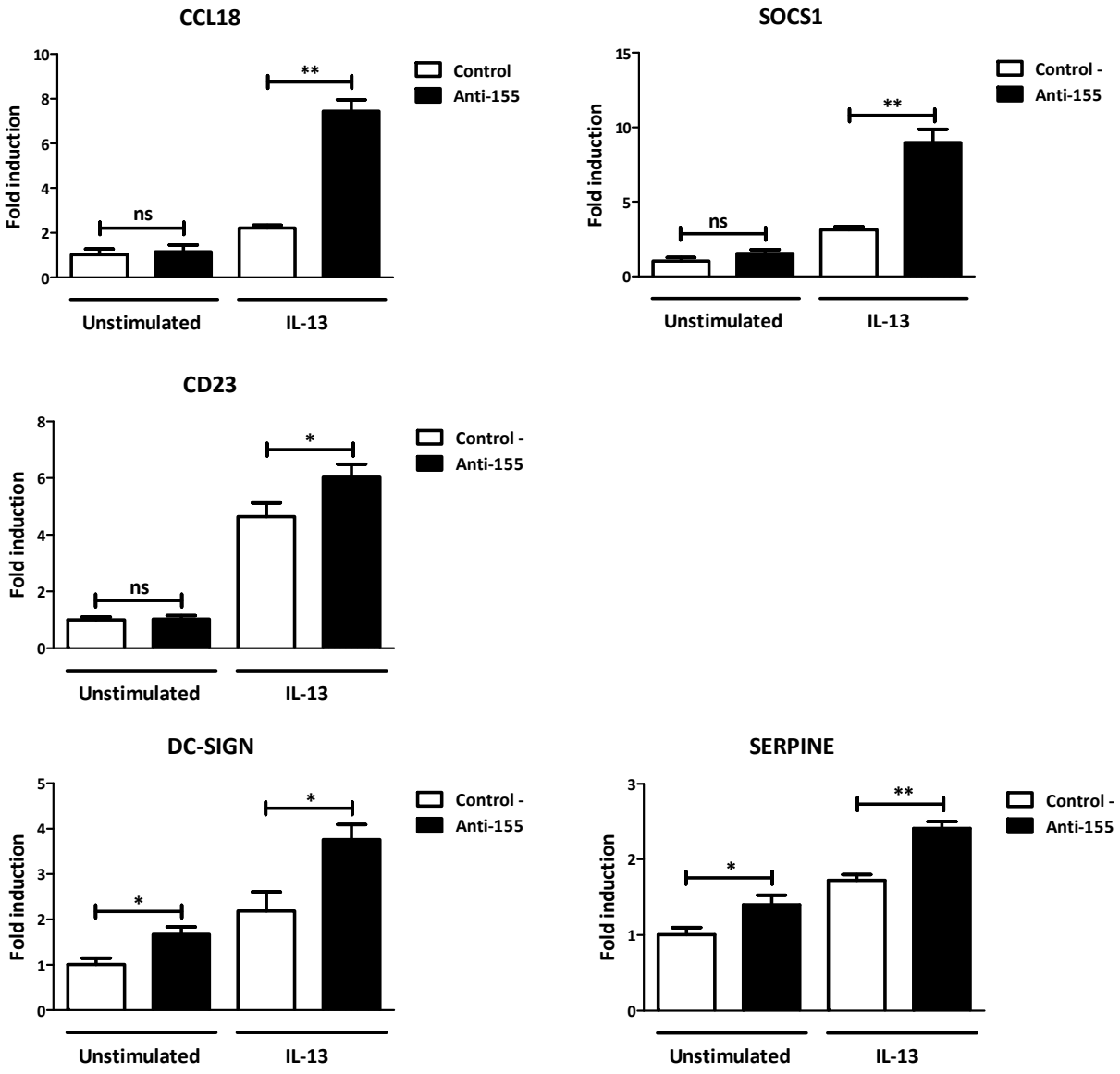

Figure 46 MiR-155 affects the expression of IL-13 dependent genes. Macrophages transfected with Anti-miR-155 (Anti-155, black bars) or Anti-miRNA Control (Control, white bars) were stimulated or not with IL-13 during 24h (IL-13 and Unstimulated, respectively). It is shown the results of the RT-qPCR of IL-13/STAT6 dependent genes as fold induction compared to Unstimulated Control cells. ACTB1 was used as normalizer. Results are from one out of three independent donors. *, P-value<0.05, **, P-value<0.01.

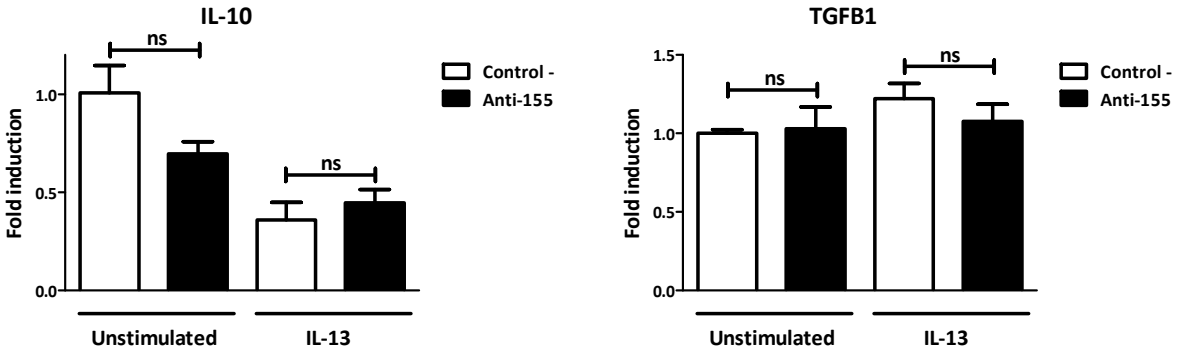

Figure 47 Control genes in macrophages transfected with Anti-miR-155 (Anti-155, black bars) or Anti-miRNA Control (Control, white bars) stimulated or not with IL-13 (IL-13 and Unstimulated, respectively) during 24h. It is shown the results of the RT-qPCR of IL-10 and TGF (TGFB1) genes as fold induction compared to Unstimulated Control cells. ACTB1 was used as normalizer Results shown are from one out of three independent donors. ns: non significant

CCL18, SOCS1 and CD23 genes showed a similar trend: IL-13 up regulated their expression (Fig. 46, **Control** cells) which was significantly higher in Anti-155 transfected cells (Fig.46, **IL-13**). Anti-miR-155 transfection showed no significant effect in unstimulated cells (Fig.46, **Unstimulated**). These results followed the previous observations: blocking miR-155 up regulated IL13Rα1 protein expression and consequently increased IL-13 dependent STAT6 phosphorylation (Figs. 44 and 45, respectively). Enhanced STAT6 transcriptional activity would therefore lead to the up regulation P-STAT6 dependent genes, as shown in Fig.46.

Fig.46 also shows that IL-13 dependent up regulation of DC-SIGN and SERPINE genes was significantly higher when miR-155 was inhibited (Fig.46, **IL-13**). Interestingly, Anti-miR-155 transfection also altered DC-SIGN and SERPINE levels in unstimulated cells (Fig.46, **Unstimulated**). These results suggested an additional action of miR-155 levels on DC-SIGN and SERPINE expression despite the absence of IL-13.

Fig.47 shows genes that were not significantly affected by miR-155 levels in unstimulated or IL-13 treated Mϕs. These genes were considered as a control of the specifity of miR-155 effects.

All these results proved the initial hypothesis: miR-155 directly targets IL13RA1 down regulating STAT6 activation and modulating the response of macrophages to IL-13.

4.7 Discussion

MiR-155 was involved in the gene expression profile of M1 (CAMϕs) when compared to M2 (AAMϕs) macrophages (data from Sanchez-Elsner's lab). Shortly after, miR-155 was involved in murine inflammatory responses (O'Connell et al., 2007). While M1 macrophages are specialized in the defence against intracellular pathogens and are triggered by pro-inflammatory stimuli, M2 Mϕs show a more pro-tolerogenic profile, being specialists in the defence against extracellular pathogens like protozoa, nematodes or helminths, promoting tissue repair and angiogenesis and depending on Th_2 cytokines such as IL-4 and IL-13 (Mantovani et al., 2005; Mantovani et al., 2004; Martinez et al., 2006; Stout and Suttles, 2004).

M1 and M2 macrophages are considered to be at the two ends of a continuum of reprogramming and activation and miR-155 was involved in M1 profiling. It was hypothesised that if miR-155 targetted pro-M2 factors the Mϕ profile would be skewed towards a M1 phenotype. Using *in silico* tools in search of pro-M2 factors, IL13RA1 was predicted as a putative target for miR-155 showing two different binding sites that mapped to positions 1049-1071 (Site 1) and 1399-1424 (Site 2) of the 3'UTR of IL13RA1 (Figs.33 and 34*). In vitro* dual luciferase assays demonstrated that both sites are required for miR-155 action (Fig.37). This could be a case of microRNA cooperativity, in which microRNA action relies on the presence of more than one binding site (Vella et al., 2004). Other sites present in the fragment cloned or in the remaining sequence of the 3'UTR of IL13RA1 cannot be excluded, although no favourable predictions were identified (discussed in section 4.3.1.2).

Using THP1-155 cells, which provide a myeloid environment and model a macrophage-like cell system (Auwerx, 1991; Park et al., 2007), it was shown that miR-155 over expression led to IL13Rα1 protein down regulation while its mRNA levels remained constant (Fig.38). This suggested a post transcriptional mechanism for miR-155 action on IL13RA1 expression. It is of note that the down regulation detected by the luciferase reporter assay *in vitro* was 50% whereas IL13Rα1 protein levels were reduced to 4% in THP1-155 cells. It has been shown that the context of the 3'UTR may play a key role in microRNA regulation (Didiano and Hobert, 2008), and this seems the case for miR-

155 in IL13RA1 regulation. IL13RA1 mRNA levels remained more or less constant in THP1-155 cells making it unlikely that transcriptional factors are involved in the down regulation observed.

IL13RA1 is an essential component of the IL-4 Type II receptors, composed of dimers of IL4Rα and IL13Rα1. Type II receptors can bind to both IL-13 and IL-4 cytokines triggering STAT6 phosphorylation and activation (Palmer-Crocker et al., 1996). IL-4 can also signal through the Type I receptors (dimmers of the common gamma chain (γc) and IL4Rα) via STAT6 phosphorylation (Junttila et al., 2008). However, IL-13 only binds to the Type II receptor and it depends on the presence of IL13Rα1 (Hershey, 2003; Morimoto et al., 2009; Ramalingam et al., 2008).

To test the role of miR-155 in IL13RA1 downstream signalling, STAT6 phosphorylation was checked in THP1-155 cells over expressing or not miR-155. Mir-155 over expression led to a diminished IL-4 and IL-13 dependent STAT6 phosphorylation without affecting total STAT6 protein levels (Fig.39 and 40 respectively). Moreover, miR-155 effects on IL-13 signalling seemed sustainable over the time (Fig.41). Interestingly, IL-13 dependent STAT6 phosphorylation seemed more unpaired, possibly due to STAT6 phosphorylation from IL-4 triggering Type I receptors.

In order to determine the role of miR-155 in M1/M2 balance, miR-155 was down regulated in primary macrophages using Anti-miR-155 specific oligonucleotides. It was shown that blocking miR-155 up regulated IL13Rα1 protein expression while IL13RA1 mRNA remained stable (Fig.44A and 44B, respectively). This suggested a post transcriptional role for miR-155 in IL13RA1 regulation. IL-13-dependent STAT6 phosphorylation was also enhanced upon inhibition of miR-155 (Fig.45), confirming that miR-155 affects the IL-13 signalling pathway in primary macrophages.

To further test the role of miR-155 in the IL-13 pathway of Mϕs, Anti-miR-155 (or Control) transfected macrophages were stimulated with IL-13 and assayed for IL-13/STAT6 dependent genes expression (Hebenstreit et al., 2006; Mantovani et al., 2004; Martinez et al., 2006; Martinez et al., 2009). Fig.46 shows a panel of genes that were shown to be significantly regulated by miR-155 levels and Fig.47 shows control genes that were not affected by miR-155 levels. Blocking of miR-155 (Fig.46, **Anti-155**) led to a

significant enhancement of CCL18, CD23 and SOCS1 expression in an IL-13-dependent manner. SOCS1 has been reported as a direct target of miR-155 (Jiang et al., 2010; Lu et al., 2009) and miR-155 direct action on this gene cannot therefore be excluded in macrophages. However, SOCS1 mRNA expression did not show significant up regulation *per se* when only Anti-155 oligonucleotides were transfected, leaving open the hypothesis of miR-155 acting directly on SOCS1 and also through IL13RA1.

In addition to CCL18, CD23 and SOCS1 regulation, DC-SIGN and SERPINE showed modulation by miR-155 levels in unstimulated cells (Fig.46, **Unstimulated**). This could be explained by miR-155 direct targeting of factors that regulate these genes: PU.1 in the case of DC-SIGN (Martinez-Nunez et al., 2009; Vigorito et al., 2007) and SMAD2 (Louafi et al.manuscript under revision) for SERPINE. Importantly, there were also genes that showed no change such as IL-10 or TGFβ (Fig.47), serving as a control of miR-155/IL-13 specifity.

Although IL-4 and IL-13 both signal via STAT6 phosphorylation and share the Type II IL-4 receptors, the development of a knock out model for IL13RA1 allowed distinguishing the functions of the Type I and II receptors and dissecting more the differences between IL-4 and IL-13 cytokines (Ramalingam et al., 2008). Mice lacking IL13Rα1 showed impaired defence in models of Th_2 diseases, and an almost complete abrogation of allergen-induced airway hyperreactivity and mucus production. Moreover, mice lacking IL13RA1 have proved an important role for IL13RA1 in allergic lung pathology and lung homeostasis (Munitz et al., 2008). Interestingly, mice lacking miR-155 show lung remodelling (Rodriguez et al., 2007), linking miR-155 and IL13Rα1 in lung physiology. In this context, IL-13 has been shown to play a key role in allergy and asthma (Wills-Karp, 2004). One of the genes induced by IL-13 is CD23, the low-affinity immunoglobulin (Ig) E receptor (FcepsilonRII). CD23 in triggered by CD23 in Mϕs and binds to IgE complexes promoting an inflammatory response and has been shown to play an important role in allergy, asthma and antigen presentation amongst other functions (Rambert et al., 2009; Rosenwasser and Meng, 2005). Moreover, it is one of the markers of M2 macrophages. Anti-155 transfected macrophages showed a significant up regulation of CD23 expression only when treated with IL-13 as blocking of miR-155 did not show any effect on its own (Fig.46). In line with these data, CCL18 and

SOCS1 showed a similar modulation to that of CD23 pattern by miR-155 (Fig.46). CCL18 is related to asthma and it is a typical M2 Mϕ marker (de Nadai et al., 2006; Gordon, 2003; Mantovani et al., 2004), and it has been shown that mice lacking SOCS1 gene have exacerbated Th_2 responses in lung (Lee et al., 2009). It might be possible that altered leveles of miR-155 contribute to the exacerbated immune response observed in asthmatic patients by skewing and unbalancing the Th_1/Th_2 reponses: less targeting IL13Rα1 would enhance IL-13 signalling, modulating CD23, CCL18, SOCS1 and other targets which in combination would promote a pro-Th_2 environment in the lung, as the one observed in asthma disease and related to IL-13 expression (Wills-Karp, 2004). Moreover, anti-STAT6 siRNA inhalation has been shown to diminish airway inflammation and hyperreactivity in lungs (Darcan-Nicolaisen et al., 2009). These data and assays open the possibility of using miR-155 as a therapeutical agent in asthma disease, or as a biomarker to assay the severity of exacerbated Th_2 pathologies.

Recent work in our group (Louafi et al., manuscript under revision), miR-155 is shown to directly target SMAD2 tuning the TGFβ pathway in human monocytes and regulating their fibrotic/remodeling capabilities. M2 macrophages show a more homeostatic profile than M1 macrophages; they promote angiogenesis, tissue repair (Mantovani et al., 2002) and scavenge functions. Importantly, TFG-β also promotes M2 differentiation (Martinez et al., 2009). SERPINE was demonstrated to be regulated by miR-155 levels (Fig.46), and this regulation significally enhanced when IL-13 was added, concomitantly with the SMAD2 targeting seen in our lab (Louafi et.al, manuscript under revision) and the pro-Th_2 roles of TFGβ.

Together, all these data indicate that miR-155 is positioned at the core of immune regulation. By direct targeting of IL13Rα1, miR-155 modulates IL-13 pathway in macrophages, a typical cytokine that triggers alternative activation of Mϕs. MiR-155 seems to play a center role in the plasticity displayed by macrophages, constituing an excellent example of microRNA function: a fine regulator in a system that requires constant balance and plasticity, key facts of microRNA biology.

5 Chapter 5. Results: Microfluidic trapping system to monitor cell to cell interactions

5.1 Introduction

DCs and Mϕs are key components of the immune system acting at the interface between innate (unspecific) and adaptive (pathogen specific) immunity (Kindt et al., 2007; Murphy et al., 2008). Both cells show high phagocytic abilities: whilst DCs mature upon binding to pathogens (see Fig.2) (Banchereau and Steinman, 1998; Kindt et al., 2007; Murphy et al., 2008; Steinman, 2001), Mϕs act as a first barrier of defence using different mechanisms such as Reactive Oxygen Species (ROS) production (Geissmann et al., 2010). Depending on the pathogen encountered and the cytokine milieu, Mϕs and DCs will drive the immune profile between pro-Th_1 and pro-Th_2 responses (Fig.1) which requires tight control and regulation.

Therefore, different cell types need to communicate and coordinate to develop an efficient immune response. Cell to cell communication is one of the most studied aspects of biology and it is key to understand the overall behaviour of a biological system. One of the major problems is studying and monitoring single cell interactions individually over the time. Bulk studies do not allow discriminating single events within a population or testing the microsurroundings of each element in the population. They also show limitations in terms of uniformly controlling the conditions and microenvironment of single cells. Moreover, studying specific cell types in bulk assays presents limitations when monitoring rare events in large populations. As an example, flow cytometry allows discriminating and sorting populations of cells but does not allow monitoring interaction between events or real time event-measurements. Biological processes can take from seconds to days; studying these time lapses has shown great difficulties due to the technical limitations of bulk systems.

Microscopy is the technique most commonly used for single cell event and live monitoring studies. However, it presents technical difficulties in changing and controlling the environment and free diffusion of cells while monitoring them.

Microfabrication technology allows building objects in a micro or milimeter scale, this is, in the range of mammalian cell dimensions. Microdevices can be patterned so that they include channels, pillars, valves, etc. allowing manipulating and controlling the environment in a microscale (Voldman et al., 1999). They have been more and more used in biology and medicine since the 80s and are now available commercially as devices for blood analysis and other applications (Toner and Irimia, 2005).

Microfluidics is a multidisciplinary field that studies the behaviour of fluids in a microscale, which differs from the properties that fluids have on a macroscale (Beebe et al., 2002). By combining microfluidics and microfabrication it is possible to analyze and monitor the behaviour of fluids (and cell suspensions); control their flow, dynamics and processes.

Microfluidic cell trapping devices are a useful tool for analysing single cell events. They have been used in stem cell biology, antibody production and immunology (Faley et al., 2008; Gao et al., 2009; Kobel et al., 2010). Cell trapping systems allow monitoring single cell events, control changes in the microenvironment and perform real time analysis. All are done in a microscale with low volumes and the inherent low cost advantage. These devices are called “Lab on a Chip” because it is possible to perform several analytical steps using a microdevice in which the experimental conditions can be changed and measured. In addition, the material analyzed can be recovered for further analysis. Generally they are made of gas-permeable and biocompatible materials such as PolyDiMethylSyloxane (PDMS) allowing experimental work that require culture conditions.

Our current understanding of DC and Mϕ biology is based on *in vivo* experiments using mice, bulk studies with primary cells and/or cell lines. These are valuable tools and models that are analyzed in the lab using molecular and *in vitro* approaches. An example is the work by (Mempel et al., 2004) which measured cell to cell contacts between murine DCs and lymphocytes *in vivo* using microscopy. Nevertheless, there are still questions and processes which study is limited by current lab techniques and animal models. Examples are measuring minimal cell distances required for cell to cell communication, determining requirements for cell to cell contact and especially real

time monitoring of single cell changes. These are essential processes that allow the orchestration of several cell types and responses (like DCs and Mϕs do) which will result in an overall behaviour, in health or disease. Performing this type of assays and measures in a controlled microscale allows monitoring and quantitating them in real time, and also monitoring cell behaviour by changing the microenvironment.

Many attempts have been made to design microdevices for cell trapping systems; they sometimes incorporate different tools like electrodes for cell fusion assays or antibody-covered pillars to discriminate and isolate small cell populations (Faley et al., 2008; Gao et al., 2009; Sequist et al., 2009; Skelley et al., 2009). All these devices proved to be a valuable tool for isolating and monitoring single cell events and changes in real time. Nevertheless, a device that allow single cell trapping with controlled distances has not been designed so far. This tool would prove of important use to understand the distance requirements, type of communication and cellular behaviour between different cell populations.

Antigen presenting cell (such as DCs and Mϕs) to lymphocyte interactions are well known and established (Mempel et al., 2004); however, little is known about the intercellular communications between antigen presenting cells themselves, if any exist.

5.2 Aims and objectives

In collaboration with the Nanogroup in Electronic and Computer Science in Southampton University, it was aimed *to design a new microfluidic device to monitor and measure the distance requirements for real time cell to cell communication* in order to further understand DC and Mϕ biology.

The main goal was *to assay real time exchange of antigens or pathogens between antigen presenting cells and measure the distance requirements* which was divided into several objectives as follows:

- Objective 1: *In silico* design of the device masks using CleWin 4.0

- Objective 2: To pattern the silicon mold using photolithography

- Objective 3: To make the devices in PDMS by soft lithography

- Objective 4: To test the device flow workout using THP-1 cells

- Objective 5: To test antigen/pathogen exchange between DCs and Mϕs and monitor them by fluorescent microscopy.

5.3 Design of the masks

Two different designs were required for the device: one design for “cell traps” and the other for a chamber that would contain the “cell traps” together with a branched system of pipes to flow in and out the cells.

The cell traps and chambers were designed using CleWin 4.0 (made by WieWeb software, the MESA+ Research Institute at the University of Twente and Deltamask). This program is a layout editor and mask design program that runs under Windows operating system. The output files are CIF (Caltech Intermediate Format) and Calma GDS-II files; these file formats are supported by all major layout editors. CleWin 4.0 generates other files in formats that be easily exported. It is therefore a useful tool that generates files compatible and readable by most mask manufacturers. Figure 48 shows a picture of the interface of CleWin 4.0 program. CleWin works with XY coordinates and allows precise design in different superimposable layers that can be fused to fit in different substrate dimensions. Mask manufacturers will then fabricate masks of different dimensions following the coordinates and dimensions of the *in silico* designed devices.

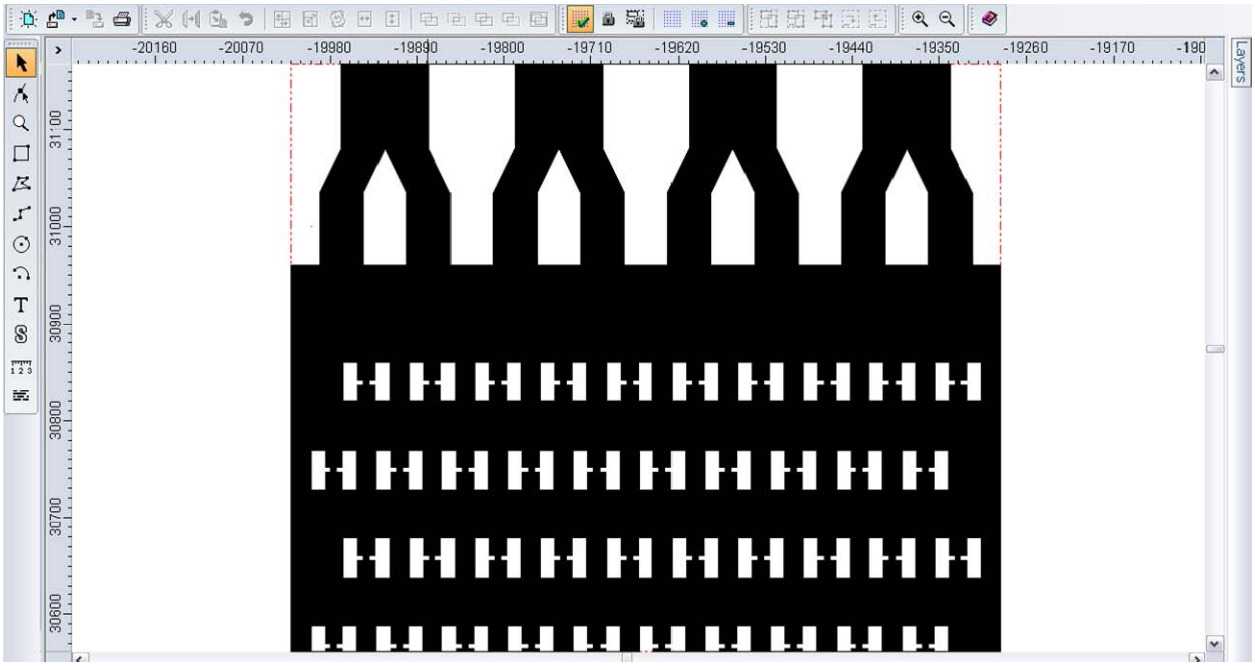

Figure 48 CleWin program interface. A mask design is shown.

Each device was designed to contain ten rows and ten columns of cell traps as an initial prototyping. Figure 49 shows an overview of the device. Each chamber had a system of branched micro pipes at both ends to flow the cells in and out (inlet/outlet). Trap rows were 100μm distance from the inlet/outlet and 20μm from the edges of the chamber.

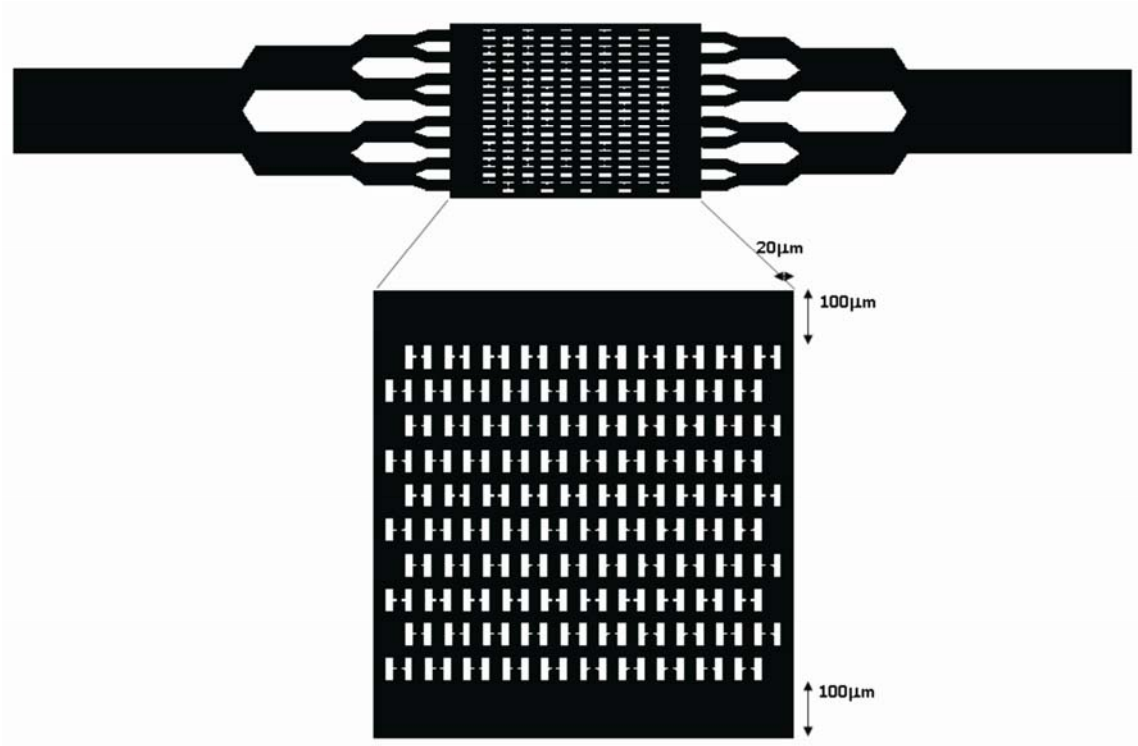

Figure 49 General view of the device. Separation distances between the rows of traps and the edge of the chamber are shown.

5.3.1 Traps design

Each trap was designed in an "H" shape: two hollows separated by a gap with varying distances (Fig.50A). Each hollow was designed with such dimensions that a single cell would fit in; given that the same cell type was going to be loaded in each hollow of the trap these were designed symmetrically. The gap width was designed to be 6μm, potentially big enough to allow cells to pass through and small enough to avoid cells reflux. This distance was determined based on previous studies related to the deformation properties of these cells (Kitagawa et al., 1997; Kurosaka et al., 1998).

Traps were designed with three different separation lengths between the two hollows: 5, 10 and 15 μm (Fig. 50A) to test different distance requirements for cell to cell communication.

To test the efficiency in cell trapping and determine whether there was clogging of the device, two distances were chosen to separate the rows of traps. The distances chosen were 20 and 50 μm (Fig. 50B) based on previous studies (Skelley et al., 2009). The spacing between columns was 20 μm, corresponding to 1-1.5 mm cell diameters approximately as previously suggested (Skelley et al., 2009).

The dimensions of the hollows in the H traps were designed to be 18 μm: theoretically big enough to fit a single cell and small enough not to trap two cells. This hollow size was decided by comparison of THP-1 cells distortion studies and HeLa cell dimensions (Kurosaka et al., 1998; Skelley et al., 2009) to DCs and Mϕs under the microscope. Included in these calculations was the fact that photolithography, development and etching processes would minimally diminish the dimensions of the devices and traps.

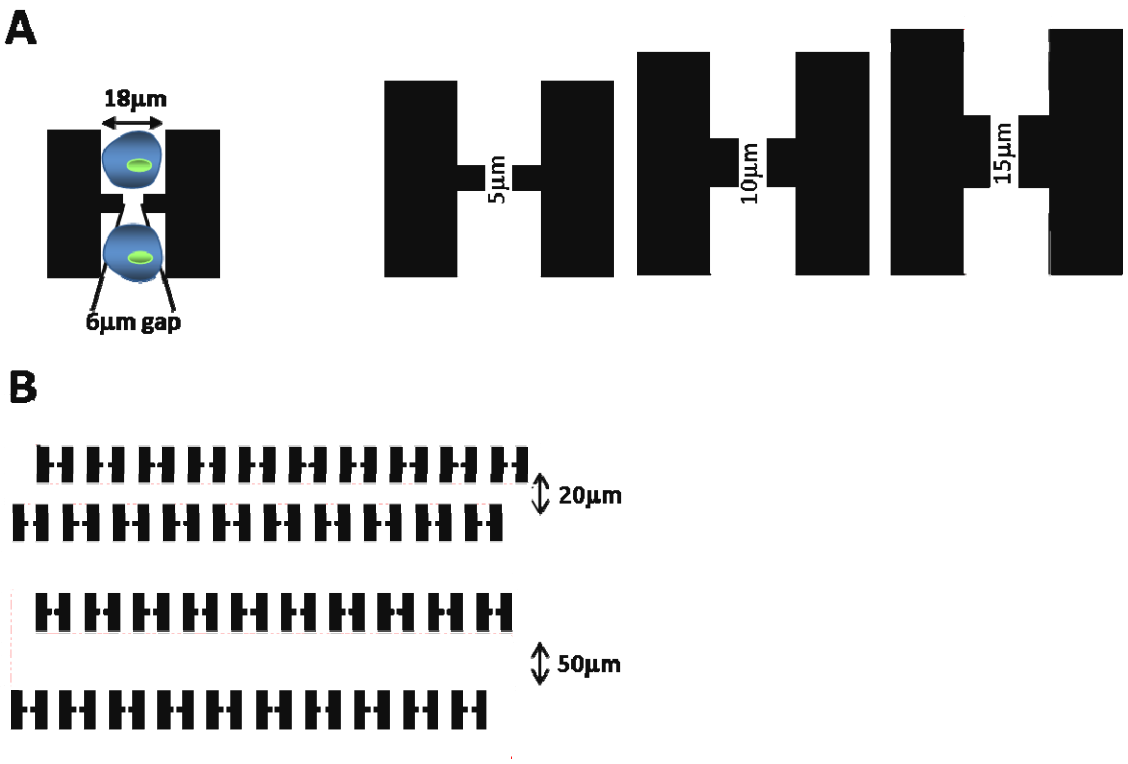

Figure 50 Dimensions of the different designed traps. *A*: Each trap has two hollows of 18µm2, 6µm gap of separation between the hollows. Drawn in blue are trapped cells. Three different distances between the 2 hollows were also tested: 5µm, 10µm and 15µm. *B*: Two different distances between the trap rows were also tested: 20µm and 50µm.

5.3.2 Chamber and channel design

The chambers were designed to fit the arrays of 10x10 cell traps adding 20 μm at both sides and 100 μm at both ends of the array of traps (Fig.49).

The channels that flow in the cell suspension were designed by Dr. Sam Birtwell according to previous data (Birtwell and Morgan, 2009). The number of pipes to irrigate the device had to be a power of two because of the branching of the channels, which number expanded from one into two and so forth to distribute the flow homogeneously (see Fig.51). The width of the pipes in contact with the device was 45μm (2 cell diameters approximately) so each chamber fitted eight pipes to flow the cells in and out (Fig.51). The branched pipes were centered at each edge of the chamber leaving a gap of 29.5μm at both sides of the device (Fig.51).

The length of the main branch of each system of pipes was designed to be 1.5mm to minimize the risk of piercing the whole device when trying to flow in the cells. Modelling of the flow dynamics was done by Dr. S. Birtwell using the dimensions of a device with 5μm gap and 50 μm between the rows of traps, taken as an average measure amongst the 6 different designed combinations.

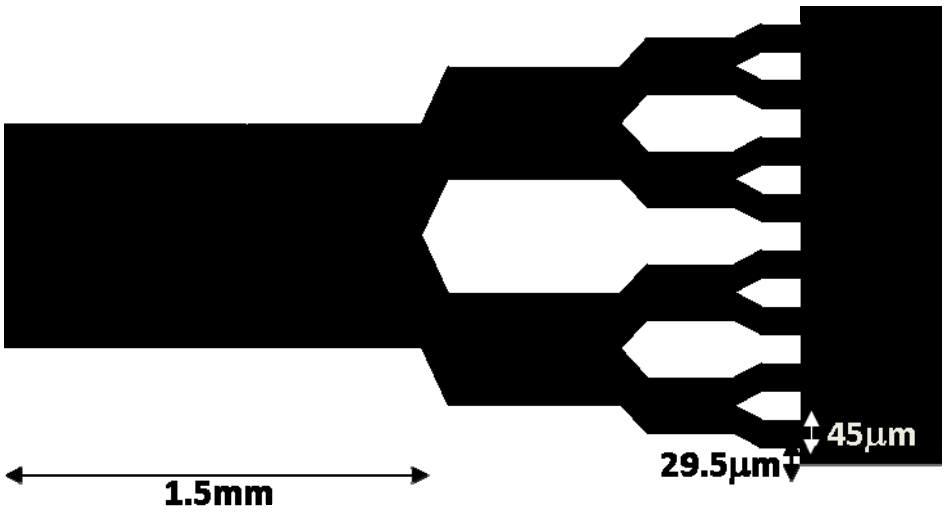

Figure 51 Schematic representation of the pipes design. The distance between the pipes and edges of the chamber was 29.5 μm and the width of the pipes was 45μm. The length of the main branch was 1.5mm.

5.4 Photolitography of the silicon substrate with the designed masks

In silico designed mask files were sent to a mask manufacturer (Swiss MicroLitho, Lausanne, Switzerland) that patterned two glass masks: one with the designed traps and another with the chambers. The masks drawing was done in chrome because an opaque material is required for the litography process afterwards (explained below). Litography is the process that define regions and patterns on a wafer from which materials are deposited or removed.

Figure 52 shows a schematic representation of the photolitographic procedure. Firstly, the masks were designed *in silico* using CleWin 4.0 program (see 5.3) and chrome-patterned on glass masks by a manufacturer. A layer of positive photoresist material was spun on a silicon disk (substrate) to reach a desired thickness. A photoresist is a material that is sensitive to light exposure: after exposure to light a positive photoresist (like the one used) becomes soluble in the developer and a negative photoresist insoluble. The pattern was therefore transferred to the photoresist layer by UV irradiation. Developing of the UV-patterned photoresist defined the features of the masks on the photoresist. Etching and an additional development steps patterned the designs on the silicon substrate and removed the remaining photoresist, respectively. After these steps, the silicon mold was ready to use for soft lithography with PDMS.

All these steps were carried out inside a clean room by Dr. S. Birtwell whose participation has been essential in the manufacturing process. Dr. S. Birtwell had already established many parameters and protocols of this process. The main parameters of the protocol are detailed below and more detailed in Appendix 6.

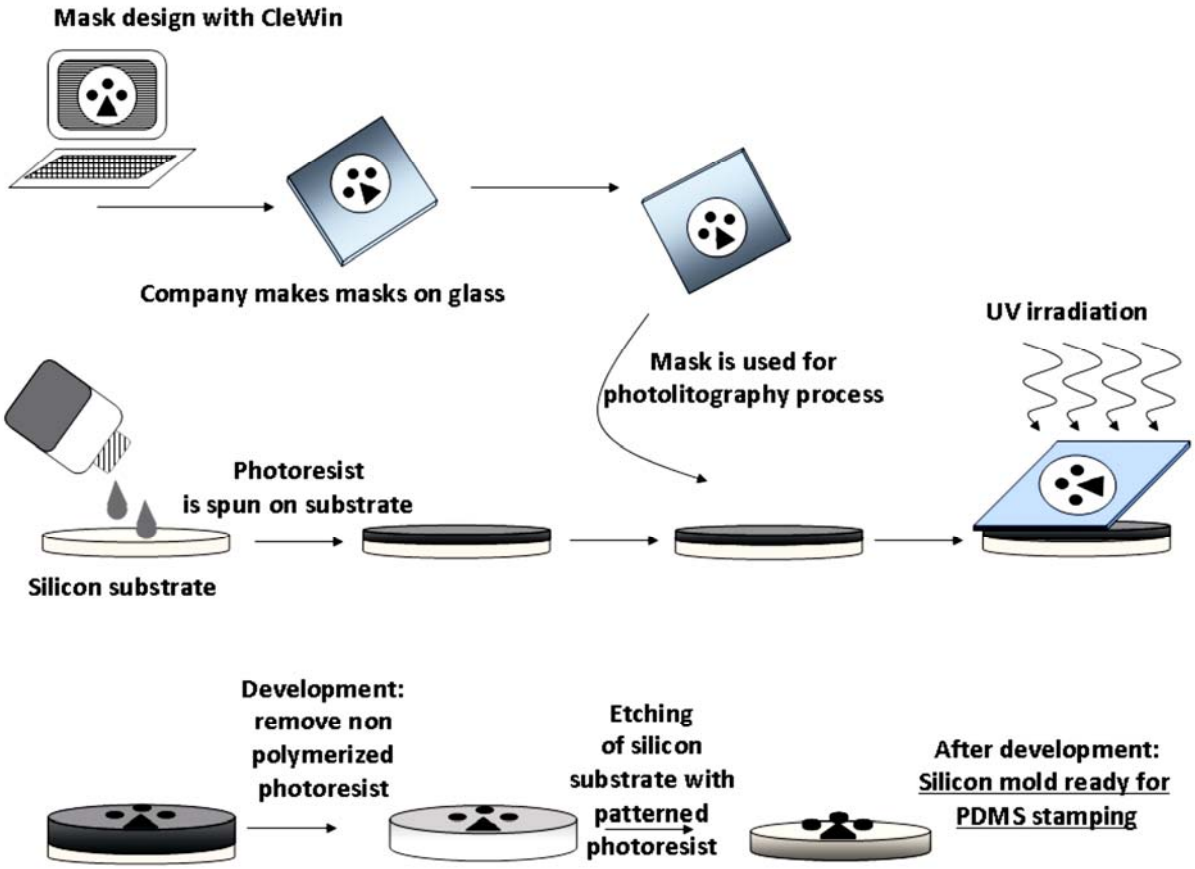

Figure 52 Overview of the photolitography procedure. Masks designed with CleWin were patterned with chrome by a mask manufacturer onto glass masks. A silicon disk was used as substrate on which a negative photoresist was spun to a desired thickness. Masks patterns were then transferred to the photoresist by UV irradiation and developed afterwards. Patterns were then etched in the substrate and an additional development step removed possible remaining photoresist. The silicon disk was then ready to use for PDMS stamping. Dr. Sam Birtwell (University of Southampton) performed the photolithographic process.

To pattern the silicon wafer that will be used as the mold for the PDMS devices a photoresist layer was firstly spun on the wafer. The silicon wafer was dehydrated by baking to remove any moisture that would cause problems during the photoresist processing. After cleaning and drying out, a layer of positive photoresist (AZ® 9260) was spun at 400rpm on the surface of the wafer. After spinning, the wafer was left 20 min at room temperature to relieve stress in the wafer and the thickness of the photoresist layer was checked.

After the coating process, soft baking was performed at 100°C for 3 min on a heating plate. This step is required to dry away the solvent from the spun resist, enhance the adhesion of the resist to the wafer and to anneal shear stress introduced during the spin coating. The wafer was then left 30 min at room temperature to rehydrate the resist.

The coated wafer was then aligned with the mask containing the chambers and irradiated with UV light to pattern the photoresist. This was performed in an EVG620 mask aligner during 33 seconds.

After this step the photoresist was developed using AZ® 400K Developer in a dilution 1:3 in water during 90 secs. This step removed the photoresist not exposed to light, this is, the chromed patterns in the glass mask. The definition of the patterned shapes was checked under the microscope and re-immersion in the developer was performed if necessary until the features were defined. After this developing step the wafer was rinsed in distilled water and blown dried with nitrogen.

The patterned wafer was then etched using a plasma etcher. The etching process removes layers from a surface with a depth and angles that depend on the plasma used and the parameters set for the etching such as time of exposure. The wafer was etched during 1min and 52secs in a STS Pegasus DRIE alternating C_4F_8/SF_6 plasma. After this etching process the resist was stripped by sonication in AZ100 remover; the remaining resist residue which would create problems in the next steps was removed by a 10 min immersion in fuming nitric acid.

These processes of spin, exposure and development were repeated using the mask of traps on the same wafer. This was done to etch and pattern the features that would define the different traps inside the chambers. The etching was shorter (37secs) to get small height gaps (~6μm) above traps; putatively these would stop cells from exiting from the traps once flowed in. An additional step after stripping of the resist was performed: coating with C_4F_8 in the STS Pegasus DRIE. This layer prevents PDMS (PolyDiMethylSiloxane) to adhere onto the silicon wafer during the curing process afterwards.

Figure 53 shows a schematic representation of a section of the device. The silicon wafer substrate is shown in grey.

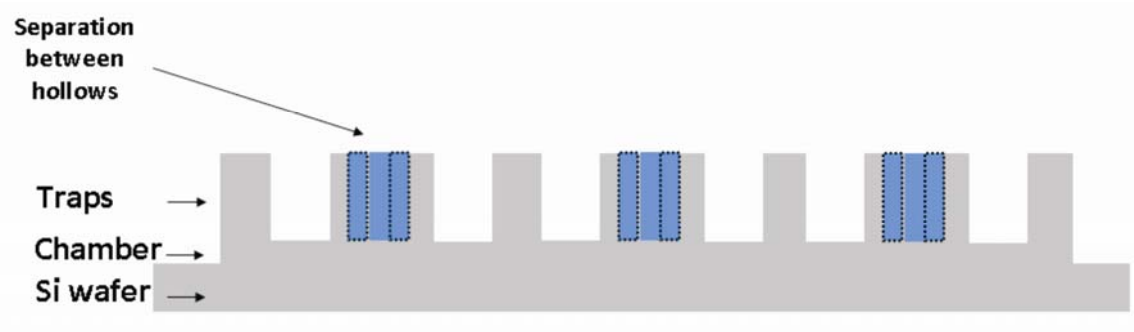

Figure 53 Section of the device showing the etched silicon wafer. Rows of traps were not parallels (see Fig. 50B) and this is indicated by the dotted lines. This patterned mold was used afterwards for PDMS molding and device making.

5.5 Soft lithography: making devices in PDMS

For the following steps (soft lithography and device tests), Dr. Marta Lombardini helped and fully collaborated especially regarding the flow workout and loading conditions.

Soft lithography consisted on the patterning of elastomeric stamps in PDMS (PolyDiMethylSiloxane) using the photolitographied silicon wafer as mold (see 5.4). PDMS is an elastic material broadly used for microdevice manufacturing. Some of its advantages are: low price and commercial availability, ideal for rapid prototyping and disposables; although hydrophobic, it can be easily made onto a hydrophilic material by plasma treatment; its elasticity allows building of valves, pumps and pipes that are deformable; it is biocompatible and permeable to O_2 and CO_2, gases needed when culturing mammalian cells; transparency and low autofluorescence allowing microscopy monitoring; and it can be coated to diminish cell attachment, for example, using BSA (Beebe et al., 2002; Mata et al., 2005; Whitesides et al., 2001).

PDMS is an elastomer that cures and polymerizes upon mixing with a curing agent in a 10:1 ratio. Figure 54 shows a diagram of the PDMS curing process. The mixture was poured on the patterned wafer and degassed during 1h in a vacuum manifold to disrupt the bubbles formed during the mixing of PDMS+curing agent. Then, PDMS was baked inside an oven at 80 degrees for 1h approx until it became cured.

Cured PDMS was sliced from the mold using a scalpel; PDMS devices were then pierced in the main pipes enabling the cells to be loaded afterwards. To bond the cured PDMS onto microscopy glass slides both PDMS and glass slides were exposed to O_2 plasma. This procedure allowed exposure of reactive groups in both the glass slide and the PDMS that reacted and bonded when pressed against each other.

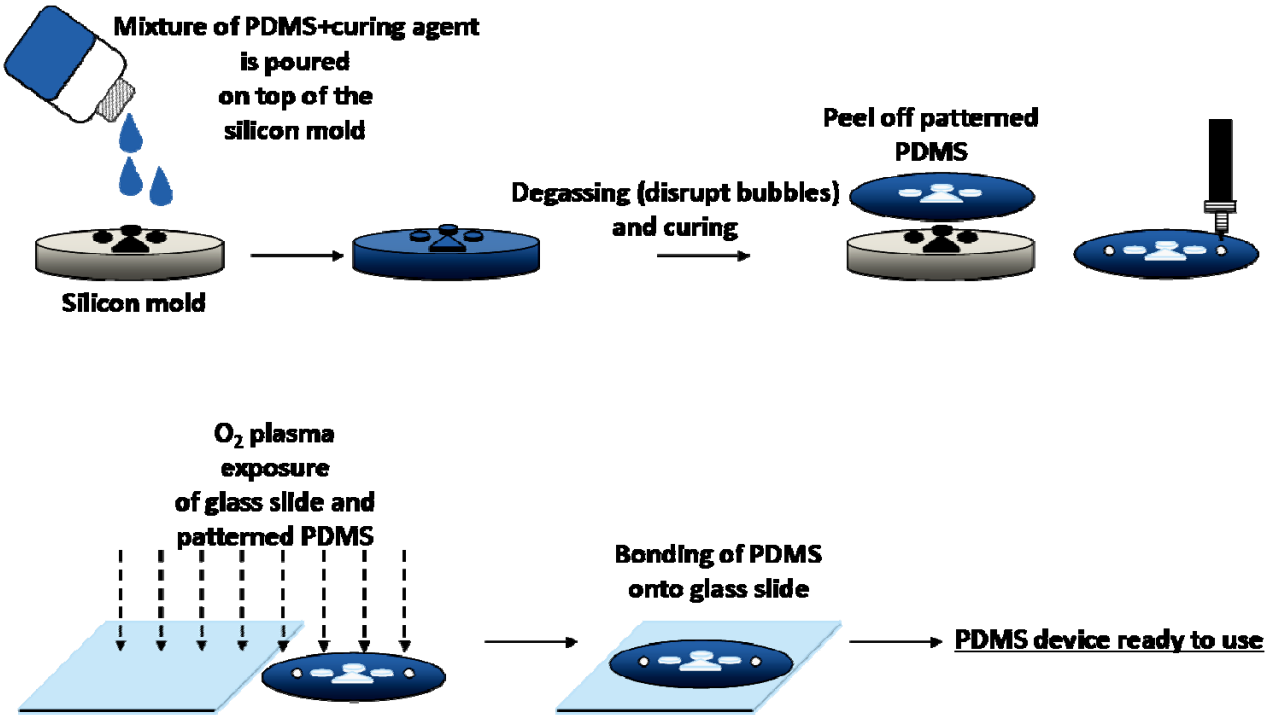

Figure 54 PDMS processing. A mixture of PDMS+curing agent is poured onto the silicon mask. After degassing and curing, the patterned PDMS is peeled off the mold. Microscopy glass slides and PDMS are then treated with O_2 plasma which exposes reactive groups that will allow bonding of their surfaces. Exposed PDMS and glass are then pressed against each other allowing bonding. Devices are then ready to use. Dr. Marta Lombardini (University of Southampton) assisted in the soft lithography process.

Once the PDMS was bond to the glass slides, it was ready to be loaded and tested. Fig.55 shows an example of the view of one of the PDMS devices under a light microscope. Devices contained arrays of 10x10 H-shaped traps within a chamber. Chamber dimensions were approximately 1mmx600μm

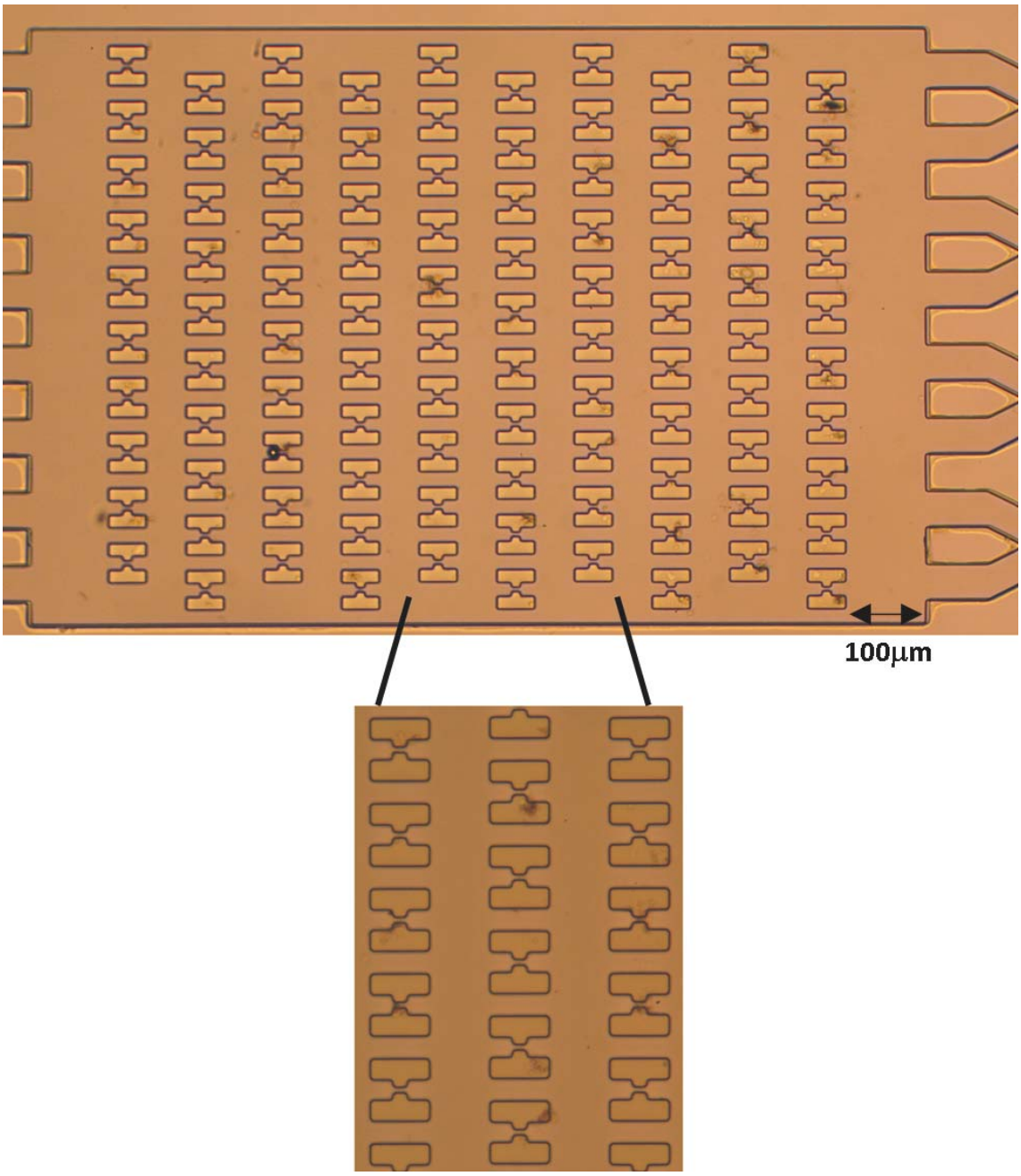

Figure 55 Picture of one of the devices in PDMS under the microscope. A zoom of a device is shown. The device shown corresponds to the design of 5μm gap and 50μm of separation between rows.

5.6 Flow workout using THP-1 cells

5.6.1 Loading overview

THP-1 cells were initially used to test the device as these are easily cultured and are of a similar size to dendritic cells and macrophages; moreover, they can be differentiated into DCs and Mϕs-like cells (Auwerx, 1991; Bocchietto et al., 2007; Park et al., 2007). Therefore, they are a good model to test myeloid cell to cell interaction and loading of the device.

The chamber was filled by means of two set of channels as shown in Figure 56. The aim was to set up the cell concentration and flow rate to fill both hollows (side A and side B in Fig.56) without cells flowing out on the other side of the trap. The two sets of channels were designed to achieve a homogeneous distribution of cells within the chamber.

A unique feature of this device is the bi-directional flow of the channels. Both channels are considered inlet or outlet depending on the side of the H-shaped trap that is loaded. Cell loading was done using two syringe pumps (one for each side of the chamber) that allowed changing the flow rate by controlling the pressure on the syringe plungers. Each one of the two syringes was attached to a plastic pipe; these pipes converged in a set of valves that allowed manual control of the opening and closing of the pipes, in order to alternate the selection of inlet and outlet.

The flow rate used was determined by controlling the fluid coming out of the syringes using the syringe pumps. During the loading process it was important that the fluid flow rate was maintained in a biocompatible range. Too high speeds disrupted the cells and very low speeds did not exert enough pressure. The minimum flow rate to prevent cell-sedimentation was found to be 2μl/min which corresponded to 0.2μl/min within the chamber. The maximum biocompatible flow rate of the syringe pump was 20μl/min, corresponding to 2μl/min within the chamber.

In addition, two different row distances were assayed: 50 and 20μm (Fig.50B). Devices with 20μm separation between the rows of traps were not efficient in trapping

cells: trapping efficiency, measured as cells present in both sides of a trap, was around 5%. Therefore, only the devices with 50μm separation between the rows of traps were further used.

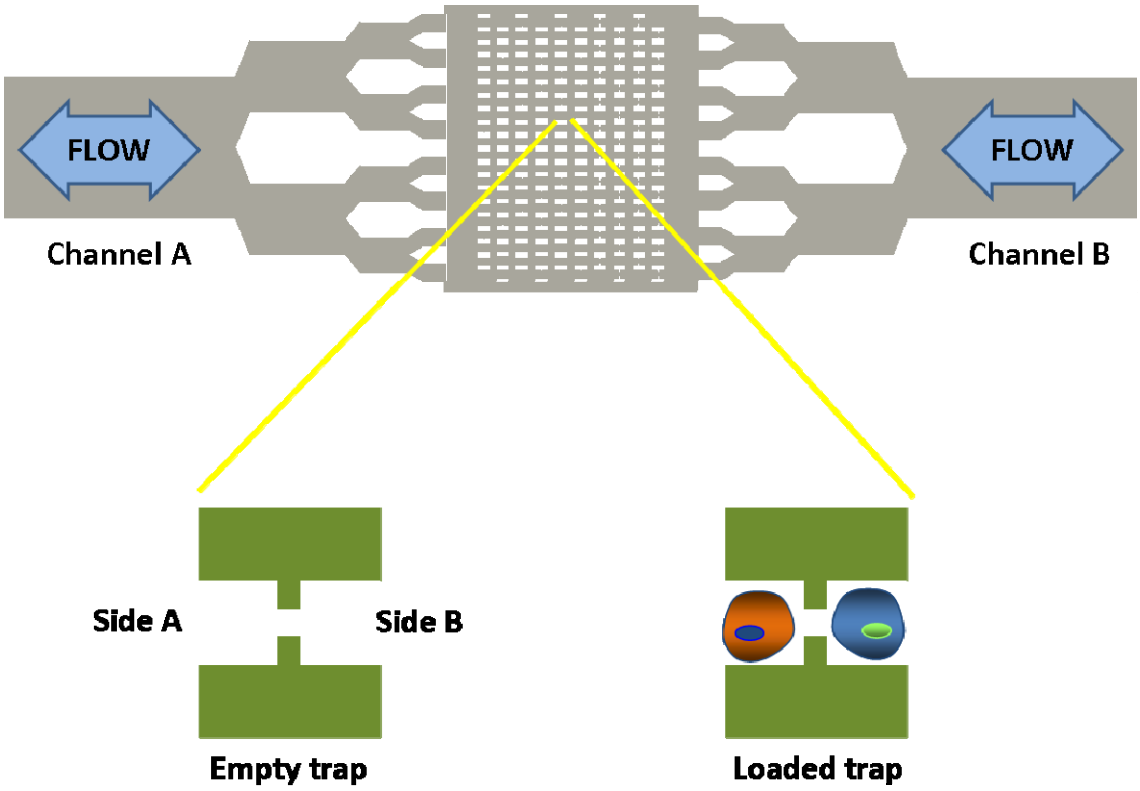

Figure 56 Flow representation in the devices. The chamber was filled first from the channel of one side and then from the one on the other side, represented as "A" and "B". These channels were alternatively used as inlet and outlet.

5.6.2 Loading parameters and factors

Loading of the device was done in two steps. Figure 57 shows two pictures of each one of these steps. Following the terminology used in Fig.56, cells were first loaded in side A of the trap (left picture in Fig.57); in this case channel-A was set as inlet and channel-B as outlet. After this and using the set of valves previously mentioned, channel-B was turned into inlet and channel-A into outlet. By doing so, the side-B of the traps was loaded (right picture in Fig.57).

A cell concentration of 10^6cells/mL was chosen and achieved an adequate loading time of approximately 1 minute, avoiding; the clogging of the device. An important requirement of this device was that the second loading step had to be done using a flow-rate that did not free the cells firstly trapped. Considering all these aspects, 1μl/min flow rate was found to be the right choice to fulfil the loading requirements.

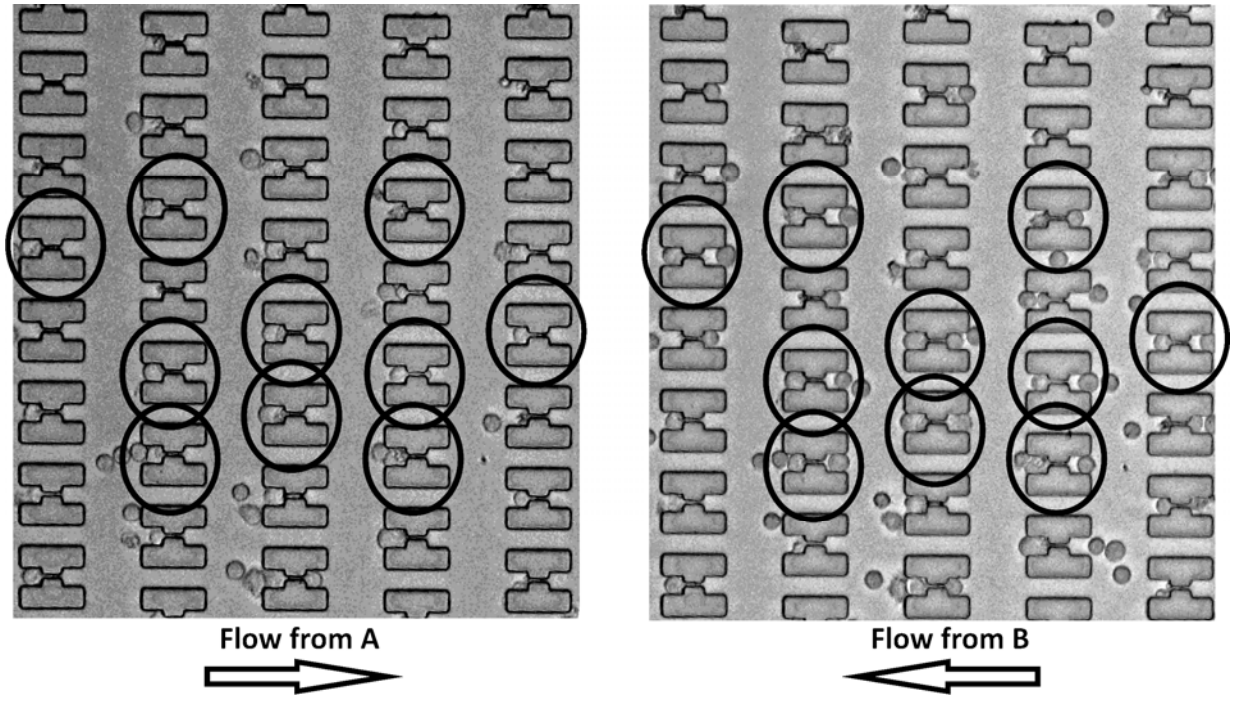

Figure 57 Flow workout of the device in two steps. A and B correspond to terminology used in Fig.56. Left picture shows the flow in of cells from channel A; channel B served as outlet. Right picture shows the filling of the device from channel B and thus, channel A served as outlet.

One of the main problems in microfluidics is the presence of air bubbles in the devices. Bubbles disrupt cell membranes when they blow and do not allow homogeneous flow of the liquid. An example is shown in Fig.58: left shows a trap with a cell on top, middle trap is empty (probably it contains cell debris) and right trap shows an air bubble on top and a disrupted cell below.

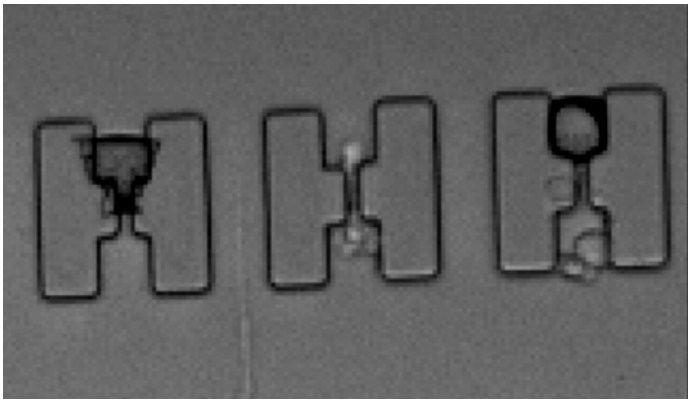

Figure 58 Bubbles in microfluidic devices. A set of traps is shown; from left to right: a cell trapped (upper side), empty trap (with cell debris) and an air bubble with a disrupted cell (upper and lower sides, respectively).

The problem was solved by pre-filling the devices with PBS and confirming the absence of air bubbles using a microscope before cells were introduced in the chamber. This allowed a regular and homogeneous flow of cells and no air bubbles inside the device. Loading efficiency (number of traps loaded in both sides) was measured to be 60%.This loading procedure was performed more than 10 times and Fig.59 shows an example.

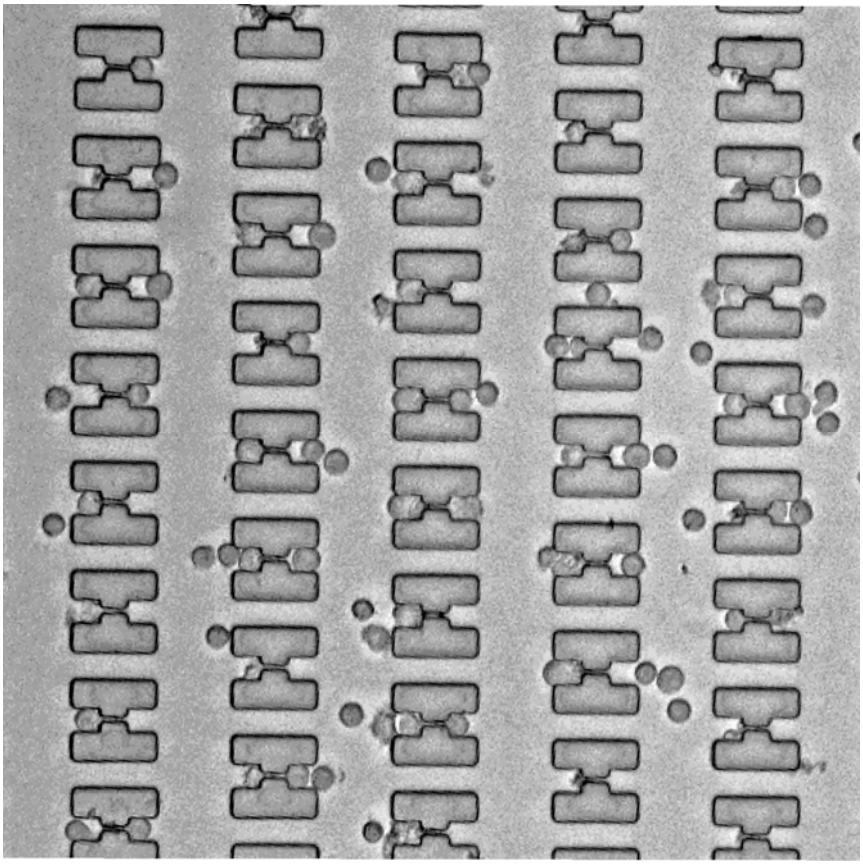

Figure 59 Loading efficiency of the devices. An example of one of the devices with cells loaded in both sides of the traps is shown. Efficiency (traps with both sides containing one cell) was estimated in 60% approximately.

5.6.3 Fluorescence labelling and biocompatibility test

The main goal of the device is to test cell to cell interaction and communication by the exchange of antigens or pathogens while real time monitoring by fluorescent microscopy. Therefore, the fluorescence labelling, monitoring and biocompatibility of the system were first checked.

THP-1 cells were labelled using a Reactive Oxygen Species (ROS) detector (Invitrogen) (see 2.11.3). This molecule is a fluorescein derivate that is non fluorescent and permeable to the cell membrane in its acetylated and reduced form. Once inside the cells it is de-acetylated by cellular esterases and oxidized becoming fluorescent and non permeable to the cell membrane. The fluorescence is detector using excitation sources and filters appropriate for FITC, and it serves as an indicator of the cellular oxidative state and ROS production. ROS production is induced by stimuli such as cellular stress, DNA damage or pathogen responses (Yamada et al., 2006). As a positive control cells were incubated with tert-butyl hydroperoxide (TBHP) which induces oxidative stress (Garcia-Cohen et al., 2000), conditions that induce H_2DCFDA to fluoresce. TBHP was used instead of H_2O_2 (commonly used for ROS assays) as it is more stable and biocompatible.

This experiment was also a measure of the biocompatibility of the system (device, pumps, pipes, etc): cells under stress would produce ROS and appear fluorescent under the microscope. This was useful as cellular stress modify cell responses and behaviour, which would be important for future applications of this device.

H_2DCFDA harbouring cells did not become fluorescent as they passed through the microfluidic system when compared with cells engaged in ROS production by incubation with TBHP. This test was performed 3 times and was reproducible; Figure 60 shows an example of a picture of one of the traps in which one cell fluoresces (left trap) and the other does not (right hollow). Both cells contained the probe but only the one incubated with TBHP was fluorescent.

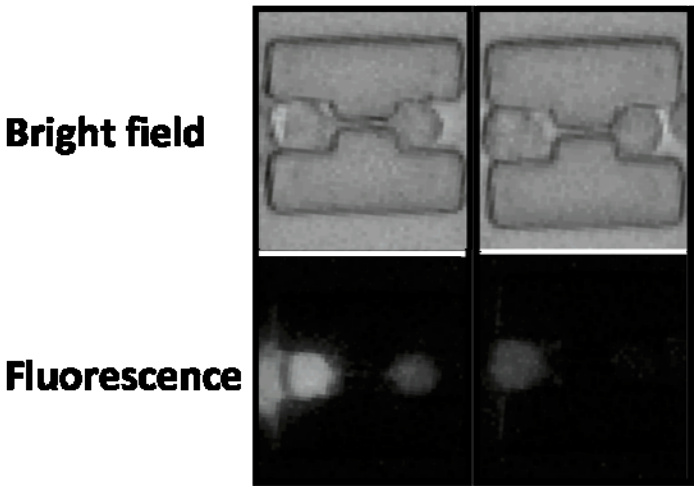

Figure 60 ROS production imaged by fluorescence microscopy. First row shows cells under white light and second row show the same cells under fluorescent light. THP-1 cells harbouring H_2DCFDA were loaded in the device; H_2DCFDA becomes fluorescent when de-acetylated and oxidized. Cells on the left hand side were incubated with TBHP (which produces ROS) as positive control. Cells not incubated with THBP were not fluorescent (right side of the trap). It is shown one experiment of 3 replicates.

5.7 Testing dendritic cell to pathogen communication

Interrogating DC to DC communication via exchange of antigens or pathogens was the main aim of the microfluidic device. A first step towards reaching that goal was assaying DC to pathogen interaction in order to measure the distance requirements and cell behaviour inside the designed device. DCs had already been shown to bind to pathogens (see 3.7.2) and performing binding assay inside the device would give insight into the distance requirements for such interaction to occur, and measure the cell responses in those conditions. The second step, DC to DC communication, is on going work (see 6.2.2)

Experiments were done with dendritic cells and *Candida albicans* conidia, known to bind to DCs (Cambi et al., 2003) and already tested in bulk experiments (see 3.7.2). As LPS induces ROS production by dendritic cells (Matsue et al., 2003; Yamada et al., 2006), DCs sensing pathogens will produce ROS. It was therefore aimed *to test DC to C.albicans interactions monitoring the distance requirements and ROS production in real time.*

First, monocyte derived DCs (prepared as described in 2.2.2) were incubated with H_2DCFDA (see 2.11.3) and loaded into the device. At this stage, DCs showed no fluorescence emission indicating that levels of oxidative stress were not raised. It also indicated that the fluidic stress inherent to the loading procedure did not seem to induce cellular stress in DCs. When TBHP was flowed in from the other side of the chamber, ROS were instantly produced and fluorescence decreased afterwards taking approximately 20min to fade away. It was only possible to perform this experiment once (data not shown).

Unlabelled DCs were loaded from one side of the device and propidium iodide labelled *C.albicans* conidia (see 2.11.2.1.) were then loaded from the other side (Fig.61A). Real time monitoring of phagocytosis was observed in traps with a separation of 10μm between sides A and B: Fig.61A shows a sequence of images taken at different times that captured the movement of a labelled *C.albicans* conidium from one side of a trap to the other (indicated with an arrow). This trap contained a dendritic cell on the side towards which the conidium moved, and this process took 20min approximately. It is noticeable that the shape of the trap was efficient for trapping these pathogens, which

are smaller than 2 μm in diameter. Events were monitored over 3h using a fluorescence microscope within an environmentally controlled chamber (37°C and 5%CO_2) which allowed mimicking physiological conditions. Images were captured 1min intervals, minimising the fluorescence exposure to reduce photobleaching.

Devices containing traps with a separation of 15μm between the two hollows (see Fig. 50A) did not show any phagocytosis event. This type of devices were tested twice and suggested that 15μm was a too long distance for DC and *C.albicans* to communicate under the assayed conditions. The devices that worked best were the ones containing traps with gaps of 5μm or 10μm (see Fig.50A) and these devices were the ones assayed further.

DC to pathogen interaction was then interrogated employing DCs containing the ROS detector probe H_2DCFDA (see 2.11.3). If DCs contacting pathogens produced ROS they would show green fluorescence due to the de-acetylation and oxidation of the probe.

DCs harbouring H_2DCFDA were loaded from one side of the device and labelled *C.albicans* from the other side. Phagocytosis with simultaneous production of ROS was observed: Fig.61B shows a series of images that captured the process by which a ROS producing DC captured *C.albicans* conidia. This event took 20 min approximately to occur. Interestingly, DCs were able to sense and phagocytose dead *C.albicans*, as conidia were heat inactivated and then stained with propidium iodide (see 2.11.2.1). Propidium iodide is a fluorescent dye that binds to DNA; it is membrane impermeable and it therefore penetrates cell membranes that are disrupted (like it happens in dead cells), being generally excluded by live cells (Darzynkiewicz et al., 1992). Thus, despite conidia being dead, DCs were able to sense and phagocytose them.

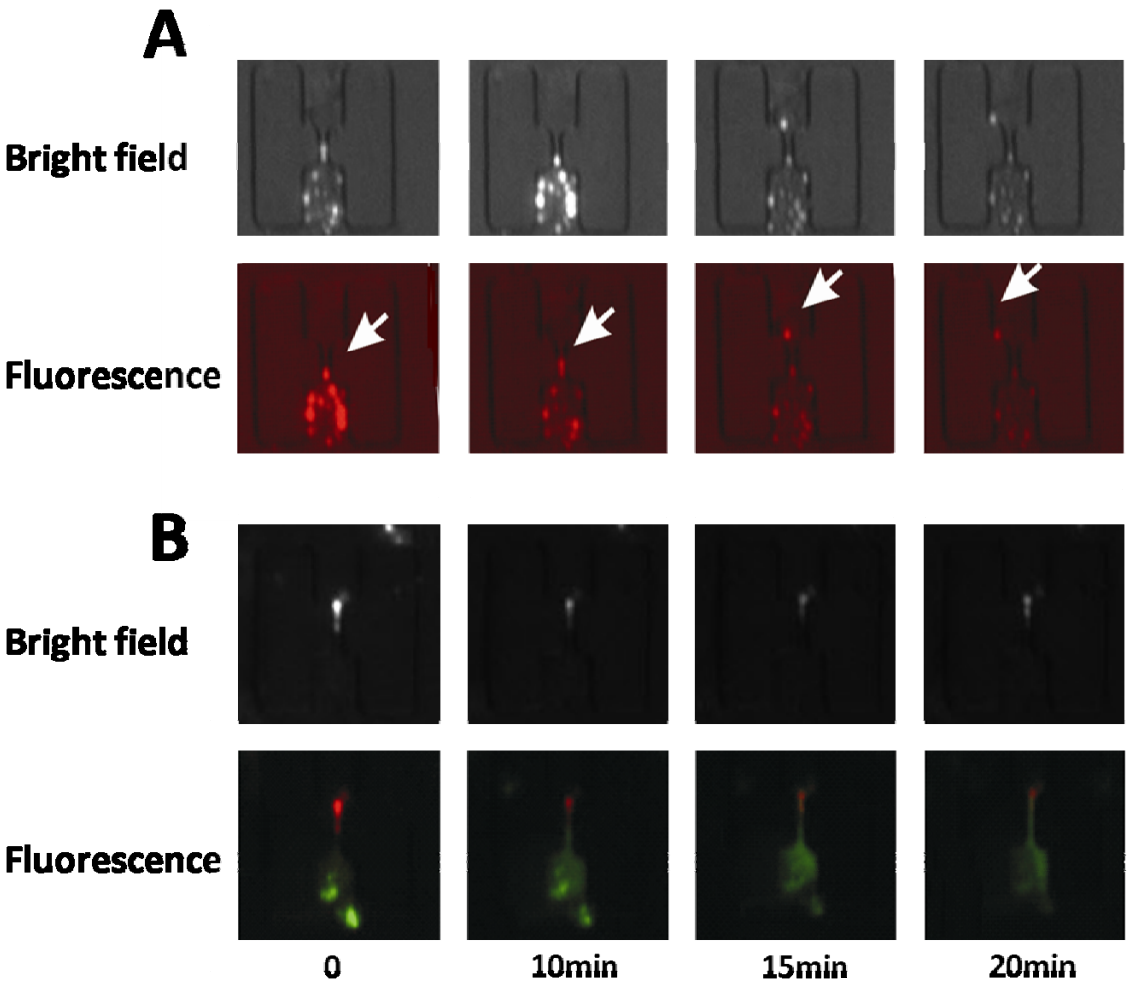

Figure 61 Real time monitoring of phagocytosis. Two sequences of pictures of two independent phagocytosis events taken at time intervals of 10, 15 and 20 min (below pictures) by fluorescence microscopy are shown. *A*: A propidium iodide labelled *C.albicans* conidium (indicated with a white arrow) moves from one side of the trap to the other side which harboured a DC. *B*: A ROS producing DC (in green) phagocytosed *C.albicans* conidia labelled with propidium iodide (in red) is shown.

5.8 Discussion

Cell to cell communication has proved difficult to investigate and observe in a one to one basis. Developing a single cell trapping system to monitor events in single cells would be a useful tool; moreover, testing different distances for intercellular communication to occur would be of interest to further understand such requirements. Pathogen to DC interaction is known to occur but it has mostly been monitored in bulk experiments (see 3.7.2.1). A microfluidic device was therefore designed in order to assay DC to pathogen interaction and for future use to observe DC to DC communication (see 6.2.2).

In this microfluidic device cells were trapped in H shaped traps and kept at a defined fixed distance of 5, 10 or 15 μm (Fig.50). Thus, cells can be placed in defined close proximity but with no contact, therefore allowing the monitoring of intercellular communication requirements and intracellular changes. Trap dimensions were designed based on previous studies (Skelley et al., 2009) and considering the mechanically-induced deformation of THP-1 cells as a DC and Mϕ-like cell model (Auwerx, 1991; Bocchietto et al., 2007; Kitagawa et al., 1997; Kurosaka et al., 1998). This device had a novel design that positioned cells by a bi-directional flow (Fig.56) without the need of other mechanical, electrical or magnetical forces (Fig.57).

Devices for trapping cells were etched on a silicon wafer that served as mold for patterning the devices in PDMS (Figs.53 an 55). PDMS is an elastomer whose properties make it biocompatible; it allows gas exchange (necessary for cell culture) and easy monitoring under visible and fluorescent light microscopy due to its transparency and low auto fluorescence. PDMS is a material that can be coated (e.g. with BSA) to reduce cell attachment; this offers the possibility of using it for cell sorting by coating with antibodies against cell surface markers. As PDMS is elastic, microfluidic devices made in this material can also contain electrodes and other microtools that allow moving cells, fusing them, stimulating them, monitoring cell membrane properties and/or changes; all possibilities that makes this type of microdevices a superb tool for biological work. Importantly, PDMS is a low cost material that is commercially available which makes it of value for developing disposable devices.

Microfluidic devices were first tested employing THP-1 cells. Devices trapped single cells and efficiency, measured as % of traps loaded in both sides, was estimated in 60% approximately (Fig.59). THP-1 cells were also employed to test the possible cellular stress induced by the loading procedure; these cells were labelled using a ROS detector probe that fluoresces upon oxidation (see 2.11.3) and they showed no fluorescence when compared to cells engaged in ROS production (Fig.60).

One of the advantages of the bi-directional flow design is that it allows stimulating trapped cells and monitor inter and intracellular changes. This was assayed measuring ROS production when DCs harbouring H_2DCFDA (a ROS detector probe that fluoresces when oxidized) were loaded in one side of the device and TBHP (an oxidative stress inducer (Garcia-Cohen et al., 2000) was flowed in from the other side. ROS were instantly produced measured as fluorescence that decreased afterwards, taking approximately 20min to fade away. However, it was only possible to perform this experiment once (data not shown) and needs further testing (see 6.2.2).

Cell to cell communication was observed in the form of DC to pathogen interaction (Fig.61). *C. albicans* conidia were loaded from one side of the device and DCs from the other side. It was possible to observe the movement of *C.albicans* from one to the other side of a trap (Fig.61A). Following the results presented in Chapter 3 (Fig.32) and the ability to monitor phagocytosis events (Fig.61), it would be of interest to use this device to measure the effect of miR-155 over-expression on the ability of cells to interact with *C.albicans* conidia at the single cell level. This approach could reveal differences in individual or subsets of cells complementing or enhancing the observations from the previous bulk experiments (Fig.32). To further assay the effect of DC to *C.albicans* interaction on the oxidative status of DCs, which would also facilitate their monitoring by fluorescence microscopy, DCs labelled with H_2DCFDA were loaded from one side of the device a labelled *C.albicans* conidia from the other side. Fig.61B shows a sequence of images of an experiment in which it was observed that a ROS producing DC phagocytosed labelled conidia. It is remarkable that DCs phagocytosed dead *C.albicans*, as conidia had been previously heat inactivated and propidium iodide is generally excluded from living cells. This event did not require close contact, as it was observed inside a trap in which both sides were separated by 10μm, so close contact was

not required to trigger phagocytosis. This is an interesting finding that will be further assayed; moreover, when using traps with a gap distance of it 15μm no phagocytosis was ever observed. Therefore, it suggests that DCs are able to sense pathogens up to a maximum distance and that this sensing does not require direct contact. One possibility is that "pathogen detection" might be due to the diffusion of molecules not monitorable by microscopy. Another possibility is that as DCs naturally behave like sensors, once on a substrate (even *in vitro*) they emit prolongations to sample their surroundings.

In conclusion, the designed device allows assaying live cell to cell communication and monitoring of intra and extracellular changes by fluorescence microscopy, as well as the distance requirements for these events to occur. It can be easily redesigned on a cell dependent manner according to cell size and shape. It is economic and reusable, good qualities for clinical application. As an example, clinical samples could be loaded and exposed to different drugs, monitoring real time changes in single cells and measuring the exact conditions required for these events to occur. In theory, these devices could be used as a tool to determine patient-specific treatments. The microfluidic design and the use of PDMS as substrate would also allow recovering the material once assayed for further testing. All in all, the designed chamber is a good example of a Lab on Chip that can be of use in both the lab and the clinic, to understand both health and disease.

6 Chapter 6: Discussion and future work

6.1 General discussion

The immune response is accomplished by the interplay of different structures and cells that communicate with each other to achieve a balanced behaviour. To develop an effective response, the immune system regulates and coordinates its two main branches, innate and adaptive immunity: “general troops” (innate response) and “specialized killers” (adaptive response) in analogy with a war against a given pathogen.

In this interplay, both dendritic cells and macrophages play a key role and connect both branches of immunity. Immature DCs reside in peripheral tissues working as sentinels; they sense and sample their surroundings in search of PAMPs using a broad range of receptors such as DC-SIGN, also present in alternatively activated macrophages (Banchereau and Steinman, 1998; Janeway and Medzhitov, 2002). Mϕs derive from monocytes recruited from blood to tissues under inflammatory conditions, or they reside in tissues as homeostatic cells (Gordon and Taylor, 2005; Kindt et al., 2007). Thus, both DCs and Mϕs activate under inflammatory conditions to exert their immune roles.

Upon binding to pathogens, DCs mature and migrate to lymphoid organs in which they will present those antigens to T cells (see Figs.1 and 2); T cells will then proliferate and differentiate either into a Th_1 or Th_2 profile, related to inflammation and tolerogenicity, respectively. Similarly, Mϕs activate upon sensing of inflammatory signals such as LPS into a pro-Th_1 profile (CAMϕs or M1 Mϕs) or towards a pro-Th_2 profile (AAMϕs or M2 Mϕs) by cytokines such as IL-4 or IL-13 (see Fig.3). Therefore, a correct sensing of such stimuli is key in order to exert an appropriate and effective immune response.

In search of genes differentially expressed under pro- or anti-inflammatory conditions, BIC (MIR155 HG) had been found to be involved in the inflammatory profile of human macrophages; coincidentally, microRNA-155 was found up regulated by inflammatory conditions in murine Mϕs (O'Connell et al., 2007). MicroRNAs are small non-coding RNAs of ~22nt in length that inhibit gene expression upon pairing to the

3'UTR of their target genes mRNA (Bartel, 2004). MiRNAs can exert their inhibitory functions on a wide range of target genes upon binding to sites in their 3'UTRs (summarized in Fig.5), putatively regulating hundreds of targets (Bartel, 2009).

Thus, microRNAs are ideal candidates in the context of Th_1/Th_2 responses, in which they may potentially act as regulators between these two profiles. It was therefore proposed that ***miR-155 is involved in the pro-Th_1 response of macrophages by down regulating pro-Th_2 factors***.

In silico analysis of Th_2 factors bound by miR-155 predicted both PU.1 and IL13RA1 as targets (see 3.4.1 and Table 3, and 4.3.1 and Table 4, respectively). PU.1 is a known Th_2 factor, essential in myelopoiesis and required for acquiring a dendritic cell fate versus a macrophagic one (Bakri et al., 2005; Brunner et al., 2007; Chang et al., 2005; Laslo et al., 2006; Scott et al., 1994). Importantly, PU.1 has been shown to be the main transcriptional activator of DC-SIGN in myeloid cells (Dominguez-Soto et al., 2005). Moreover, DC-SIGN expression has been shown to be triggered by the Th_2 cytokine IL-4 in DCs (Relloso et al., 2002) relating DC-SIGN with a Th_2 environment. IL13RA1 is the main receptor for the Th_2 cytokine IL-13 which has been shown to exert different effects to those of IL-4 and it is a known trigger of alternative macrophage activation (Martinez et al., 2009; Ramalingam et al., 2008).

Pro-inflammatory stimuli trigger maturation of iDCs; iDCs undergo a series of changes (see Fig.2) that include the down regulation of DC-SIGN with the concomitant decrease in the binding of pathogens by mature DCs (Steinman, 2001). It was therefore hypothesized that ***miR-155 is induced during dendritic cell maturation modulating the pathogen binding ability of DCs by down regulating DC-SIGN through the direct targeting of PU.1***.

In addition, BIC involvement in CAMϕs expression profile opposed to AAMϕs and the *in silico* prediction of IL13RA1 as a miR-155 target suggested that ***miR-155 directly targets IL13RA1 modulating IL-13 pathway in macrophages***.

MiR-155 was shown to be up regulated by LPS-maturation of DCs (Fig. 15) in which both DC-SIGN and PU.1 were shown to be down regulated (Figs. 14 and 16,

respectively). This experiment established the link between miR-155, PU.1 levels and DC-SIGN in dendritic cell maturation and settled the basis of the first hypothesis.

To further analyze the direct relationship predicted *in silico* between miR-155 and PU.1, *in vitro* luciferase assays were performed. Fig.22 shows that PU.1 is directly bound by miR-155 and that nucleotides 45-51 of the 3'UTR of PU.1 (NM_001080547.1) are essential for miR-155 action. PU.1 has also been demonstrated as a direct target of miR-155 in mice, where it is involved in the immunoglobulin class switch of B-cells (Vigorito et al., 2007) and as a miR-155 target (O'Connell et al., 2008) related to pathological myeloproliferation. Despite miR-155 binding sites being conserved between mouse and human species (Fig. 18) and miR-155 shown to target PU.1 in murine cells (Vigorito et al., 2007) the secondary structure of miR-155::PU.1 interaction *in silico* is different between both species (Fig. 20). This observation adds importance to the results obtained and indicates their novelty.

In a similar experiment, IL13RA1 was shown to be directly targeted by miR-155 (Fig.37) at two different binding sites mapping to positions 1049-1071 (named as Site 1) and 1399-1424 (named Site 2) of the 3'UTR of IL13RA1 (NM_001560.2). Abrogation of either of these sites abolished miR-155 action suggesting that both sites are required for miR-155 to down regulate IL13RA1 expression. This could be a case of microRNA cooperativity (Vella et al., 2004) in which miR-155 binding to one site facilitates access to the other and *vice versa*, with both sites required to exert inhibitory function. An alternative possibility is that the *in vitro* assay performed only partially measures the action of miR-155 on IL13RA1 in their natural cell environment.

Therefore, in order to investigate the role of miR-155 in a myeloid context on both PU.1 and IL13RA1 expression, a cell system was developed in which miR-155 over expression could be induced and titrated. Pro-inflammatory stimuli such as LPS lead to the up regulation of miR-155 (Fig. 15) and (O'Connell et al., 2007), but these stimuli trigger several pathways that may mask (or mimic) miR-155 action. Developing a cell line in which the over expression of miR-155 could be controlled allowed the effects of miR-155 over expression to be isolated from other inflammatory events. THP-1 cells are a promyeloid cell line that can be differentiated and stimulated into macrophage-like and

dendritic cell like- cells (Auwerx, 1991; Bocchietto et al., 2007; Park et al., 2007; Tsuchiya et al., 1980). Importantly, these cells express both PU.1 and IL13RA1 so they were ideal candidates to test miR-155 over expression effects in a myeloid context and test those predicted targets.

THP-1 cells were doubly transduced with a lentivirus containing miR-155 (see 2.3.1) and a lentivirus that controlled the expression of miR-155 transgene by a Tet-On system (section 3.5. and Fig. 23). The established cell line was named THP1-155 cells, which showed up regulation of miR-155 upon doxycycline treatment (Fig. 25).

THP1-155 cells were then cultured in the presence of doxycycline and miR-155, PU.1 and DC-SIGN levels were determined. MiR-155 over expression led to a down regulation of both PU.1 and DC-SIGN at the protein level; PU.1 mRNA levels remained stable while DC-SIGN mRNA expression was down regulated (Figs. 26, 27 and 28). Similarly, IL13RA1 protein levels showed down regulation upon miR-155 over expression whilst its mRNA levels remained steady (Fig. 38). These results suggested a post transcriptional role for miR-155 in PU.1 and IL13RA1 regulation most likely by inhibiting mRNA translation, one of the most described mechanisms of microRNA action (Eulalio et al., 2008; Filipowicz et al., 2008).

Interestingly, it has been recently suggested that microRNA action leads to mRNA levels down regulation (Guo et al., 2010). Nevertheless, microRNAs can exert their inhibitory functions in two ways: inhibiting the mRNA translation or promoting the mRNA degradation of their target genes (Bartel, 2009). These effects may not be mutually exclusive and it is possible that a given microRNA may lead to different effects on different targets or different effects in a time and/or dose dependent manner. These may be addressed by further investigating miR-155 action on the transcription (e.g. by PU.1 and IL13RA1 promoter assays) and translation of IL13RA1 and PU.1 (e.g. by polyribosome profiling) in miR-155 titrated cells.

It is also possible that the lack of other factors promoted by pro-inflammatory stimuli that trigger miR-155 over expression influence these observations. It would be interesting to check longer effects in the over expression of miR-155 in THP1-155 cells

for PU.1 and IL13RA1 regulation (and possibly, other targets) to test the efficiency/timing or dose dependency of miR-155 on target regulation (see 6.2.1).

It is worth noting that DCs showed down regulation of PU.1 at both protein and mRNA levels (Fig.16); together with the results obtained in THP1-155 cells (Fig.26) suggests several possibilities: i) miR-155 regulates PU.1 by different mechanisms depending on the cell environment (in a dose/time dependent manner, promoting PU.1 degradation in DCs and PU.1 mRNA translation blockage in THP1-155 cells); ii) miR-155 regulates PU.1 in DCs but PU.1 is also regulated at a pre transcriptional level; iii) a combination of both. Further studies might address these possibilities (see 6.2.1).

Alternatively, levels of both protein and mRNA of DC-SIGN showed down regulation upon miR-155 over expression in THP1-155 cells (Figs. 27 and 28) suggesting a pre transcriptional role for miR-155 in the regulation of DC-SIGN. PU.1 is a known transcriptional regulator of DC-SIGN in myeloid cells (Dominguez-Soto et al., 2005) and it was therefore hypothesised that miR-155 triggered down regulation of DC-SIGN by directly targeting PU.1. This possibility was further tested employing promoter assays in THP1-155 cells (Fig.30). It was shown that miR-155 modulates the transcriptional activity of a DC-SIGN promoter reporter previously shown to be bound by PU.1 (Dominguez-Soto et al., 2005) depending on PU.1 levels. Moreover, this regulation required the presence of PU.1 with its 3'UTR intact in line with the previous results employing Renilla luciferase assay (Fig. 22).

THP1-155 cells were also used to check miR-155 effects on the Th_2 signalling cascade through STAT6. Upon binding to their receptors both IL-4 and IL-13 lead to the phosphorylation and activation of STAT6 transcription factor (Hebenstreit et al., 2006). IL-4 can bind also to IL-4 Type I receptors (Junttila et al., 2008) but IL-13 triggering phosphorylation of STAT6 depends solely on the presence of IL13Rα1 (Hershey, 2003). THP1-155 cells over expressing miR-155 showed diminished STAT6 phosphorylation when stimulated with both IL-4 and IL-13 (Figs.39 and 41). Interestingly, STAT6 phosphorylation showed an increased down regulation when cells were stimulated with IL-13 in comparison to IL-4 stimulation possibly due to IL-4 signalling through Type I receptors. STAT6 total protein content showed no regulation by miR-155 levels (Fig. 40)

determining that the role of miR-155 in STAT6 phosphorylation is due to modulation of an upstream factor in STAT6 signalling cascade shared by both IL-4 and IL-13 such as IL13RA1. As IL-4 can also signal through Type I receptors leading to STAT6 phosphorylation, only IL-13 was employed in further assays. IL-13 dependent phosphorylation of STAT6 was lower in cells over expressing miR-155 and this effect was shown to be maintained over the time (Fig. 41). The phosphorylation of STAT6 when comparing miR-155 over expression or not showed a similar pattern to previous studies aimed to dissect IL-13/IL-4 signalling through differential expression of their receptors (LaPorte et al., 2008) supporting the results obtained.

In order to further assay the described miR-155 effects in THP1-155 cells in an *in vivo* context more closely related to physiological conditions, monocyte-derived DCs and Mϕs were transfected with Anti-miR-155 oligonucleotides (or Anti-miR-Negative Control) (Figs. 31, 42 and 43).

Anti-miR-155 transfected DCs showed increased DC-SIGN surface expression (Fig. 32). It is known that the pathogens *Candida albicans* and the HIV glycoprotein gp120 are bound by DC-SIGN (Cambi et al., 2003; Hong et al., 2007) and, accordingly, Anti-mir-155 transfected DCs showed increased binding to *C.albicans* conidia and gp120 (Fig. 32). Together, these and previous experiments demonstrated that miR-155 levels modulate the pathogen binding ability of DCs by modulating DC-SIGN expression through the direct targeting of PU.1

Employing a similar approach to that in DCs, Mϕs were transfected with Anti-miR-155 oligonucleotides and stimulated with IL-13 to determine the role of miR-155 in the IL-13/STAT6 pathway. Mϕs showed increased IL13Rα1 protein while its mRNA levels remained stable (Fig. 44); this suggested a post transcriptional mechanism for miR-155 action in the regulation of IL13RA1in Mϕs similar to that observed in THP1-155 cells (Fig.38). Consequently, Anti-miR-155 transfected Mϕs showed enhanced IL-13 dependent phosphorylation of STAT6 (Fig. 45). Moreover, these cells showed over expression of IL-13/STAT6 dependent genes: CCL18, CD23 and SOCS1 showed significant up regulation in Anti-miR-155 transfected cells in an IL-13 dependent manner (Fig.46). SERPINE and DC-SIGN showed a significant up regulation when miR-155 was blocked and

these effects to be enhanced upon IL-13 stimulation (Fig.46). Both DC-SIGN and SERPINE are regulated by direct targets of miR-155: PU.1 in the case of DC-SIGN, corroborating the results previously observed in DCs (Martinez-Nunez et al., 2009; Vigorito et al., 2007) and SMAD2 for SERPINE (Louafi et al. under revision). It is very likely that blocking of miR-155 in Mϕs led to increased levels of these miR-155 targets leading to DC-SIGN and SERPINE up regulation, respectively.

Pathogen binding of DCs was assayed by flow cytometry, the most common technique used in these type of studies, e.g. (Cambi et al., 2003; Colmenares et al., 2004; Geijtenbeek et al., 2003; Koppel et al., 2004; Serrano-Gomez et al., 2007). Nevertheless, this technique shows limitations common to bulk studies: they do not allow real time monitoring or analysis of single cell events. Moreover, flow cytometry does not allow determining the requirements for cell to cell communication such as direct contact or cell to cell distance requirements.

In order to assay these parameters in DC to pathogen interaction, a microfluidic device was designed (see 5.3). This type of Lab on a Chip devices allow single cell discrimination, working with small volumes and real time monitoring (Chang and Sretavan, 2007; Faley et al., 2008). Moreover, the devices were patterned in PDMS (see 5.5 and Fig.55), a polymer that is biocompatible, gas permeable, elastic and transparent that shows low autofluorescence, making it ideal for live cell microscopy imaging (Mata et al., 2005; Voldman et al., 1999; Whitesides et al., 2001). Cell trap arrays of 10x10 H-shaped traps were designed with three different gap lengths between both sides of the trap (Fig.50A) inside a chamber with a novel design of a bi-directional flow (Fig.56). This bi-directional flow proved to be sufficient to trap cells with no need of additional electrical or mechanical forces (Fig. 59). Moreover, the device did not induced cellular stress as measured by the absence of ROS production (Fig.60). It was possible to observe real time phagocytosis of *C.albicans* conidia by DCs and this interaction to lead to ROS production (Fig.61). Both these events took 20 min approximately and further assays are currently under development. Interestingly, out of the three distances assayed (see Fig.50A), 15µm seemed too far for the cells to interact. Interestingly, DCs showed phagocytosis despite the fact that *C.albicans* conidia were dead. These results show the need of further developing this type of assays in which parameters can be controlled,

cells can be monitored individually and both inter and intracellular events measured. On going experiments assaying Mϕs (with high phagocytic abilities), are under development to measure distance requirements for these cells to interact with pathogens, DCs and other Mϕs (see 6.2.2). This combined approach of cell biology and microfluidics attempts to understand myeloid cell to cell communication, essential in the development of a balanced immunity, in which pathogen recognition is the first and key step to exert an adequate and efficient immune response.

In this regard, pathogen recognition and DC-SIGN expression are an interesting link between DCs and Mϕs, between both PU.1 and IL13RA1 targeting by miR-155. DC-SIGN is present in both DCs and M2 Mϕs (Geijtenbeek et al., 2000; Martinez et al., 2009) and it is induced by Th_2 stimuli (Puig-Kroger et al., 2004; Relloso et al., 2002). Interestingly, mice lacking IL13RA1 show lack of hyper reactivity and mucus hypersecretion in the lungs (Ramalingam et al., 2008) and the same murine model has shown the role of IL13RA1 in allergen induced lung pathology (Munitz et al., 2008). Moreover, mice treated with siRNA against STAT6 show diminished airway hyper reactivity and inflammation in a model of Th_2 lung response (Darcan-Nicolaisen et al., 2009), which opens the possibility of siRNA (or Anti-miRNA)-based therapies in the treatment of certain Th_2 pathologies. DCs and Mϕs were transfected by natural uptake (Figs. 31 42 and 43) supporting the feasibility and efficiency of this type of reagents in human cells. Further analysis of systemic effects and cell-specific delivery technologies are needed; however this is a first step towards that goal.

DC-SIGN has been involved in the modulation of T cell responses by biasing them mainly towards a more anti inflammatory and pro-Th_2 phenotype with little exceptions (Bergman et al., 2004; Geijtenbeek et al., 2003; Gringhuis et al., 2007; Smits et al., 2005; Steeghs et al., 2006). Moreover, several studies in mice have shown that DC-SIGN is required for an effective response to the pulmonary bacterial pathogen *M.tuberculosis* (Schaefer et al., 2008; Tanne et al., 2009) and DC-SIGN deficient mice (without the DC-SIGN ortholog SIGNR1) show a skewed Th_1 response to this pathogen (Wieland et al., 2007). Interestingly, Th_2 cytokines induce DC-SIGN expression in myeloid cells (Puig-Kroger et al., 2004; Relloso et al., 2002) placing DC-SIGN in a pro-Th_2 immune context, which has been shown to be promoted by miR-155 targets such as PU.1 and SHIP

(Brunner et al., 2007; Chang et al., 2005b; Martinez-Nunez et al., 2009; O'Connell et al., 2009; Vigorito et al., 2007) and in which IL-13 is a main mediator (Wynn, 2003).

These observations converge in the fact that miR-155 deficient mice show a Th_2 skewed phenotype (Rodriguez et al., 2007), positioning miR-155 centrally in the Th_1/Th_2 balance by targeting different factors. This is of importance not only in health but also in disease, as exacerbated immune responses lead to pathologies such as asthma or ulcerative colitis (de Nadai et al., 2006; Fuss and Strober, 2008; Umetsu et al., 2003; Wills-Karp, 2004).

It is very tempting to suggest a model in which de regulated miR-155 levels and a pro-pathological environment may contribute to the development of these "multifactorial" diseases, in which several genes are candidates that contribute to the development of a given phenotype. As an example, CCL18, IL-13, STAT6 or SOCS1 (direct or indirect targets of miR-155, see Figs.44 and 46) have been involved in asthma pathogenesis (Borowski et al., 2008; Darcan-Nicolaisen et al., 2009; de Nadai et al., 2006; Lee et al., 2009; Wills-Karp, 2004), a typical Th_2 exacerbated lung pathology. Interestingly, miR-155 deficient mice show lung remodelling (Rodriguez et al., 2007). As microRNAs can exert their regulatory effects on putatively hundreds of targets (Bartel, 2009), they are ideal candidates for such multigenic-linked pathologies.

In conclusion, the data presented together with other studies suggest that under inflammatory conditions miR-155 is up regulated and exerts its pro-Th_1/anti-Th_2 role by down regulating pro-Th_2 factors such as PU.1 and IL13RA1. It may be possible that miR-155 also contributes to the restore of the immune balance when required, functioning as pro-Th_2 microRNA by targeting known Th_1 mediators (Ceppi et al., 2009); this makes miR-155 an excellent example of microRNA regulation. Does size matter? Not in this case: big effects in a small mediator.

6.2 Future work

6.2.1 MiR-155 dose-dependent regulation of PU.1

PU.1 was shown to be down regulated at both protein and mRNA levels in DCs (Fig. 16) whilst in THP1-155 cells only PU.1 protein was down regulated (Fig.26). This different regulation might be due to different levels of miR-155 over expression: whilst mature DCs showed an up regulation of miR-155 of more than 130 times (Fig.15), in THP1-155 the up regulation upon doxycycline treatment reached an eight fold (Fig. 25). Investigating longer times of miR-155 over expression in THP1-155 cells might show different effects for PU.1 (and maybe IL13RA1) regulation, with the possibility of assaying other known targets. Putatively, THP1-155 cells might provide a molecular tool to develop a mathematical model. Protein quantification by western blotting limits these types of assays because it is influenced by antibody affinity, which might vary between different proteins. qPCR analysis would reveal mRNA regulation and this is also a possibility to explore employing longer miR-155 over expression times than those employed (96h, Figs. 24 and 25). In addition, polyribosome profiling would reveal the translational state of any target and it might be used as a measure of translational efficiency depending on miR-155 levels.

Another possibility is that the differences observed in PU.1 regulation between DCs and THP1-155 cells are due to miR-155 modulating PU.1 promoter. Further studies employing PU.1 promoter assays dependent on miR-155 levels similar to those presented for DC-SIGN regulation (Fig. 30) could reveal and give insight to this hypothesis.

6.2.2 Microfluidic device

Current and further work is being carried out using an improved design for the flowing system. The new devices include more chambers and more traps within each chamber as done by others (Sequist et al., 2009; Skelley et al., 2009; Toner and Irimia, 2005; Valero et al., 2005).

Little is known about the interaction and communication between antigen presenting cells, or regarding the intercellular distances required. This may be of importance as it has been shown that the time and frequency of contact between cells determines cellular responses in the immune system (Krummel, 2010). Experiments employing Mϕs in addition to DCs are under development in order to assay the main aim of the device: communication between these antigen presenting cells via pathogen or antigen exchange. This combined approach of cell biology and microfluidics attempts to understand myeloid cell to cell communication, essential in the development of a balanced immunity, in which pathogen recognition is the first and key step to exert an adequate and efficient immune response.

It was possible to monitor phagocytosis of *C.albicans* conidia by DCs (Fig.61). Intriguingly, conidia were dead, suggesting that DCs are able to sense them even if not in direct contact or that DCs act like natural samplers once on a substrate. Further assays are on going employing primary macrophages also: Mϕs show high phagocytic ability and it might be possible that these cells behave differently and require close proximity to sense pathogens. ROS production will be also monitored, not only as an indicator of the cellular oxidative stress but also because M1 and M2 Mϕs differ in their ROS production, which has been shown higher in M1 Mϕs (Brys et al., 2005; Mantovani et al., 2004; Mytar et al., 1999; Mytar et al., 2004). It would be interesting to monitor how M1 and M2 macrophages respond to different stimuli; moreover, it would be important to observe if the close proximity of these cells modulate their responses. This might show how M1 and M2 interact and modulate each other's behavior, which might give insight into the biology of this system and the plasticity observed for these cells.

An ideal application of this device would be assaying cells from patients suffering from pathologies with exacerbated immune responses (e.g. asthma, ulcerative colitis or

allergies). The arrays of traps under development are of 100x100 traps; this increases the number of cell pairs and the possibility of monitor rare events in larger cell populations, whilst still using small volumes and samples. Potentially, individual cells could be isolated from the traps and further analyzed, opening the opportunity of creating expression profiles, comparing different samples and searching similarities or differences amongst them.

In conclusion, new devices are under development and testing which hopefully will give insight to intercellular communication between DCs and Mϕs during antigen presentation. This will be of use not only to understand DC and Mϕ biology, but also to use as a therapeutic tool, in which pathological cells could be “re-educated” or even serve as auto-vaccines. Combining microfluidics and biology broadens our current knowledge and will most likely change the way biology is analyzed towards becoming a more precise and, possibly, mathematical science.

7 Appendices

Appendix 1

BIC sequence

The genomic region encompassing miR-155 was cloned into pCDNA3.1 vector; the resulting construct was named pCDNA_BIC and the cloned sequence is detailed bellow. According to BLAST it maps to locus NT_011512.11 (GRCh37). Blue sequence corresponds to MIR155 HG; underlined nucleotides shaded in grey correspond to microRNA-155 stem loop (NR_030784.1 and MirBase Accession MI0000681) and red nucleotides to pri-miR-155.

…..CAGAATTCGCC**CTTTATGCCTCATCCTCTGAGTGCTGAAGGCTTGCTGTAGGCTGTA TGCTGTTAATGCTAATCGTGATAGGGGTTTTTGCCTCCAACTGACTCCTACATATTAGCATTAAC AGTGTATGATGCCTGTTACTAGCATTCACATGGAACAAATTGCTGCCGTGGGAGGATGACAAA GAAGCATGAGTCACCCCGCTGGATAAACTTAGACTTCAGGCTTTATCATTTTTCAATCTGTTAAT CATAATCTGGTCACTGGGATGTTCAACCTTAA**GGGCGAATTCC….

Appendix 2

3’UTR of PU.1 sequence

The sequenced clone of PU.1 3’UTR is shown bellow. Blue case in bold corresponds to the fragment cloned in **pRLTK_3’UTR_PU.1**. It maps to NCBI Reference Sequence NM_001080547.1, gene ID 6688, official symbol SPI1. Red case shows the binding site for miR-155.

…CTTTCTAGATACCAG**TTCAGCGGCGAAGTGCTGGGCCGCGGGGGCCTGGCCGAGCG**
GCGCCACCCGCCCCACTGAGCCCGCAGCCCCCGCCGGGCCCCGCCAGGCCTCCCCGCTGGCCAT
AGCATTAA**GCCCTCGCCCGGCCCGGACACAGGGAGGACGCTCCCGGGGCCCAGAGGCAGGAC**
TGTGGCGGGCCGGGCCTCGCCTCACCCGCCCCCTCCCCCCACTCCAGGCCCCCTCCACATCCCGC
TTCGCCTCCCTCCAGGACTCCACCCCGGCTCCCGGACGCCAGCTGGGCGTCAGACCCCACCGGG
GCAACCTTGCAGAGGACGACCCGGGGTACTGCCTTGGGAGTCTCAAGTCCGTATGTAAATCAG
ATCTCCCCTCTCACCCCTCCCACCCATTAACCTCCTCCCAAAAAACAAGTAAAGTTATTCTCAATC
CGGATCCAAGGG…

Appendix 3

3’UTR of IL13RA1 sequence

The sequenced clone of PU.1 is shown bellow. Blue case in bold corresponds to the fragment cloned in **pRLTK_3’UTR_PU.1**. It maps to NCBI Reference Sequence NM_001080547.1, gene ID 6688, official symbol SPI1. Red case shows the binding sites for miR-155.

…CGTTCGTTGAGCGAGTTCTCAAAATGAACAATAATTCTAGAGCGGCCTCGAGCGGCC
GCCAGTGTGATGGATATCTGCAGAATTCGCCCTTGCTAGC**GGCTGTTAGGGGCAGTGGAGGTA**
GAATGACTCCTTGGGTATTAGAGTTTCAACCATGAAGTCTCTAACAATGTATTTTCTTCACCTCT
GCTACTCAAGTAGCATTTACTGTGTCTTTGGTTTGTGCTAGGCCCCCGGGTGTGAAGCACAGAC
CCCTTCCAGGGGTTTACAGTCTATTTGAGACTCCTCAGTTCTTGCCACTTTTTTTTTTAATCTCCA
CCAGTCATTTTTCAGACCTTTTAACTCCTCAATTCCAACACTGATTTCCCCTTTTGCATTCTCCCTC
CTTCCCTTCCTTGTAGCCTTTTGACTTTCATTGGAAATTAGGATGTAAATCTGCTCAGGAGACCT
GGAGGAGCAGAGGATAATTAGCATCTCAGGTTAAGTGTGAGTAATCTGAGAAACAATGACTA
ATTCTTGCATATTTTGTAACTTCCATGTGAGGGTTTTCAGCATTGATATTTGTGCATTTTCTAAA
CAGAGATGAGGTGGTATCTTCACGTAGAACATTGGTATTCGCTTGAGAAAAAAAGAATAGTT
GAACCTATTTCTCTTTCTTTACAAGATGGGTCCAGGATTCCTCTTTTCTCTGCCATAAATGATTA
ATTAAATAGCTTTTGTGTCTTACATTGGTAGCCAGCCAGCCAAGGCTCTGAAGGGCGAATTCCA
GCACACTGGCGGCCGTTACTAGTGGATCGGCCGCTTCGAGCAGACATGATAAGATACATTGATG
AGTTTGGACAAACCACAACTAGAATGCAGTGAAAAAAATGCTTTATTTGTGAAATTTGTGATGCT
ATTGCTTTATTTGTAACCATTATAAGCTGCAATAAACAAGTTAACAACAACAATTGCATTCATTTT
ATGTTTCNNNTTCAGGGGGANGTGTGGGNGGTTTTTTAAAGCAAGTAAAACCTCTACAAATGTN
NAAATCGATAANNATNCAGGTGGCACTTTTCGGGGAATGTGCG…

Appendix 4

Cycle threshold values of maturing DCs

DCs were matured in the presence of 1mg/mL of LPS (see 2.2.2) and miR-155 was detected employing RT-qPCR (see 2.8, 2.9.1.2, 2.9.2.2 and 2.9.2.3.). Threshold values (Ct values) are shown in the table below. Each time point was measured in triplicates and RNU6 was used as normaliser.

		RNU6	miR-155
Immature DCs	0h	28.2	27.5
		28	27.3
		28.1	27.4
	4h	28.8	28.1
		28.8	28.1
		28.8	28
	12h iDC	28.1	27.6
		28.3	27.6
		28	27.6
	24h iDC	28.6	27.4
		29.2	27.3
		28.7	27.5
	48h	26.6	28.1
		27	28
		26.7	27.8
Mature DCs	4h	28.7	24.8
		28.3	24.9
		28.2	24.9
	12h	28.7	22.4
		28.7	22.4
		28.7	22.5
	24h	28.6	21
		28.5	21
		28.9	21.1
	48h	28	20.4
		28	20.35
		28.50	20.4

Appendix 5

Cycle threshold values of THP1-155 cells

THP1-155 cells were treated or nor with doxycycline and subjected to analysis to detect miR-155 levels by RT-qPCR (see 2.8, 2.9.1.2, 2.9.2.2 and 2.9.2.3.). Threshold values (Ct values) are shown in the table below. MiR-155 induction shown in the table corresponds to one experiment of more than three independent ones. Each time point was measured in duplicates and RNU44 was used as normaliser.

		RNU44	**miR-155**
No Doxy	0h	23.50	22.67
		23.73	23.24
	96h	25.37	25.78
		24.03	25.49
Doxy	24h	25.36	25.12
		25.47	25.17
	48h	24.93	25.27
		25.71	25.74
	72h	24.71	23.99
		25.26	24.19
	96h	25.90	23.90
		26.65	24.13

Appendix 6

Etching protocol

- Spin AZ9260 resist at 4000rpm.

- Leave for 20min at room temperature to relieve the stress induced in the wafer.

- Bake at 100°C 3min.

- Leave for 30min at room temperature to rehydrate the resist.

- Expose 33s in an EVG620 mask aligner to pattern the chamber mask.

- Develop 90s in a 3:1 mixture AZ400K developer:water.

- Rinse in water and blow dry with nitrogen.

- Etch for 1min 52s in STS Pegasus DRIE using alternating C_4F_8/SF_6 plasma.

- Strip resist by sonicating in AZ100 remover.

- Remove remaining residue by 10min immersion in fuming nitric acid.

- Repeat the spin/expose/develop steps with the trap mask.

- Etch 37s to get small height (~6um) above traps.

- Strip resist as before.

- Etch to STS Pegasus for coating with C_4F_8 to prevent PDMS adhesion to Si wafer during curing process afterwards.

8 References

Acosta-Rodriguez, E.V., Napolitani, G., Lanzavecchia, A., and Sallusto, F. (2007). Interleukins 1[beta] and 6 but not transforming growth factor-[beta] are essential for the differentiation of interleukin 17-producing human T helper cells. Nat Immunol *8*, 942-949.

Anthony, R.M., Urban, J.F., Jr., Alem, F., Hamed, H.A., Rozo, C.T., Boucher, J.L., Van Rooijen, N., and Gause, W.C. (2006). Memory T(H)2 cells induce alternatively activated macrophages to mediate protection against nematode parasites. Nat Med *12*, 955-960.

Auwerx, J. (1991). The human leukemia cell line, THP-1: a multifacetted model for the study of monocyte-macrophage differentiation. Experientia *47*, 22-31.

Back, J., Allman, D., Chan, S., and Kastner, P. (2005). Visualizing PU.1 activity during hematopoiesis. Exp Hematol *33*, 395-402.

Baek, D., Villen, J., Shin, C., Camargo, F.D., Gygi, S.P., and Bartel, D.P. (2008). The impact of microRNAs on protein output. Nature *455*, 64-71.

Bagga, S., Bracht, J., Hunter, S., Massirer, K., Holtz, J., Eachus, R., and Pasquinelli, A.E. (2005). Regulation by let-7 and lin-4 miRNAs results in target mRNA degradation. Cell *122*, 553-563.

Bakri, Y., Sarrazin, S., Mayer, U.P., Tillmanns, S., Nerlov, C., Boned, A., and Sieweke, M.H. (2005). Balance of MafB and PU.1 specifies alternative macrophage or dendritic cell fate. Blood *105*, 2707-2716.

Banchereau, J., and Steinman, R.M. (1998). Dendritic cells and the control of immunity. Nature *392*, 245-252.

Bartel, D.P. (2004). MicroRNAs: genomics, biogenesis, mechanism, and function. Cell *116*, 281-297.

Bartel, D.P. (2009). MicroRNAs: target recognition and regulatory functions. Cell *136*, 215-233.

Beebe, D.J., Mensing, G.A., and Walker, G.M. (2002). Physics and applications of microfluidics in biology. Annu Rev Biomed Eng *4*, 261-286.

Berges, C., Naujokat, C., Tinapp, S., Wieczorek, H., Hoh, A., Sadeghi, M., Opelz, G., and Daniel, V. (2005). A cell line model for the differentiation of human dendritic cells. Biochem Biophys Res Commun *333*, 896-907.

Bergman, M.P., Engering, A., Smits, H.H., van Vliet, S.J., van Bodegraven, A.A., Wirth, H.P., Kapsenberg, M.L., Vandenbroucke-Grauls, C.M., van Kooyk, Y., and Appelmelk, B.J. (2004). Helicobacter pylori modulates the T helper cell 1/T helper cell 2 balance through phase-variable interaction between lipopolysaccharide and DC-SIGN. J Exp Med *200*, 979-990.

Bernstein, E., Caudy, A.A., Hammond, S.M., and Hannon, G.J. (2001). Role for a bidentate ribonuclease in the initiation step of RNA interference. Nature *409*, 363-366.

Birtwell, S., and Morgan, H. (2009). Microparticle encoding technologies for high-throughput multiplexed suspension assays. Integrative Biology *1*, 345-362.

Bocchietto, E., Paolucci, C., Breda, D., Sabbioni, E., and Burastero, S.E. (2007). Human monocytoid THP-1 cell line versus monocyte-derived human immature dendritic cells as in vitro models for predicting the sensitising potential of chemicals. Int J Immunopathol Pharmacol *20*, 259-265.

Bohnsack, M.T., Czaplinski, K., and Gorlich, D. (2004). Exportin 5 is a RanGTP-dependent dsRNA-binding protein that mediates nuclear export of pre-miRNAs. RNA *10*, 185-191.

Borowski, A., Kuepper, M., Horn, U., Knüpfer, U., Zissel, G., Höhne, K., Luttmann, W., Krause, S., Jr, J.C.V., and Friedrich, K. (2008). Interleukin-13 acts as an apoptotic effector on lung epithelial cells and induces pro-fibrotic gene expression in lung fibroblasts. Clinical & Experimental Allergy *38*, 619-628.

Brunner, C., Sindrilaru, A., Girkontaite, I., Fischer, K.D., Sunderkotter, C., and Wirth, T. (2007). BOB.1/OBF.1 controls the balance of TH1 and TH2 immune responses. EMBO J *26*, 3191-3202.

Brys, L., Beschin, A., Raes, G., Ghassabeh, G.H., Noel, W., Brandt, J., Brombacher, F., and De Baetselier, P. (2005). Reactive oxygen species and 12/15-lipoxygenase contribute to the antiproliferative capacity of alternatively activated myeloid cells elicited during helminth infection. J Immunol *174*, 6095-6104.

Buchan, J.R., and Parker, R. (2007). Molecular biology. The two faces of miRNA. Science *318*, 1877-1878.

Buckwalter, M.R., and Albert, M.L. (2009a). Orchestration of the immune response by dendritic cells. Current Biology *19*, R355-R361.

Buckwalter, M.R., and Albert, M.L. (2009b). Orchestration of the immune response by dendritic cells. Curr Biol *19*, R355-361.

Cambi, A., Gijzen, K., de Vries, J.M., Torensma, R., Joosten, B., Adema, G.J., Netea, M.G., Kullberg, B.J., Romani, L., and Figdor, C.G. (2003). The C-type lectin DC-SIGN (CD209) is an antigen-uptake receptor for Candida albicans on dendritic cells. Eur J Immunol *33*, 532-538.

Carmell, M.A., and Hannon, G.J. (2004). RNase III enzymes and the initiation of gene silencing. Nat Struct Mol Biol *11*, 214-218.

Carotta, S., Dakic, A., D'Amico, A., Pang, S.H., Greig, K.T., Nutt, S.L., and Wu, L. (2010). The transcription factor PU.1 controls dendritic cell development and Flt3 cytokine receptor expression in a dose-dependent manner. Immunity *32*, 628-641.

Carthew, R.W., and Sontheimer, E.J. (2009). Origins and Mechanisms of miRNAs and siRNAs. Cell *136*, 642-655.

Cella, M., Sallusto, F., and Lanzavecchia, A. (1997). Origin, maturation and antigen presenting function of dendritic cells. Current Opinion in Immunology *9*, 10-16.

Ceppi, M., Pereira, P.M., Dunand-Sauthier, I., Barras, E., Reith, W., Santos, M.A., and Pierre, P. (2009). MicroRNA-155 modulates the interleukin-1 signaling pathway in activated human monocyte-derived dendritic cells. Proc Natl Acad Sci U S A *106*, 2735-2740.

Chang, H.-C., Zhang, S., Thieu, V.T., Slee, R.B., Bruns, H.A., Laribee, R.N., Klemsz, M.J., and Kaplan, M.H. (2005a). PU.1 Expression Delineates Heterogeneity in Primary Th2 Cells. Immunity *22*, 693-703.

Chang, H.C., Zhang, S., Thieu, V.T., Slee, R.B., Bruns, H.A., Laribee, R.N., Klemsz, M.J., and Kaplan, M.H. (2005b). PU.1 expression delineates heterogeneity in primary Th2 cells. Immunity *22*, 693-703.

Chang, W.C., and Sretavan, D.W. (2007). Microtechnology in medicine: the emergence of surgical microdevices. Clin Neurosurg *54*, 137-147.

Chendrimada, T.P., Gregory, R.I., Kumaraswamy, E., Norman, J., Cooch, N., Nishikura, K., and Shiekhattar, R. (2005). TRBP recruits the Dicer complex to Ago2 for microRNA processing and gene silencing. Nature *436*, 740-744.

Clurman, B.E., and Hayward, W.S. (1989). Multiple proto-oncogene activations in avian leukosis virus-induced lymphomas: evidence for stage-specific events. Mol Cell Biol *9*, 2657-2664.

Coelen, R.J., Jose, D.G., and May, J.T. (1983). The effect of hexadimethrine bromide (polybrene) on the infection of the primate retroviruses SSV 1/SSAV 1 and BaEV. Arch Virol *75*, 307-311.

Colmenares, M., Corbi, A.L., Turco, S.J., and Rivas, L. (2004). The dendritic cell receptor DC-SIGN discriminates among species and life cycle forms of Leishmania. J Immunol *172*, 1186-1190.

Darcan-Nicolaisen, Y., Meinicke, H., Fels, G., Hegend, O., Haberland, A., Kuhl, A., Loddenkemper, C., Witzenrath, M., Kube, S., Henke, W.*, et al.* (2009). Small interfering RNA against transcription factor STAT6 inhibits allergic airway inflammation and hyperreactivity in mice. J Immunol *182*, 7501-7508.

Dardalhon, V., Awasthi, A., Kwon, H., Galileos, G., Gao, W., Sobel, R.A., Mitsdoerffer, M., Strom, T.B., Elyaman, W., Ho, I.C.*, et al.* (2008). IL-4 inhibits TGF-beta-induced Foxp3+ T

cells and, together with TGF-beta, generates IL-9+ IL-10+ Foxp3(-) effector T cells. Nat Immunol *9*, 1347-1355.

Darzynkiewicz, Z., Bruno, S., Del Bino, G., Gorczyca, W., Hotz, M.A., Lassota, P., and Traganos, F. (1992). Features of apoptotic cells measured by flow cytometry. Cytometry *13*, 795-808.

de Nadai, P., Charbonnier, A.S., Chenivesse, C., Senechal, S., Fournier, C., Gilet, J., Vorng, H., Chang, Y., Gosset, P., Wallaert, B*., et al.* (2006). Involvement of CCL18 in allergic asthma. J Immunol *176*, 6286-6293.

DeKoter, R.P., and Singh, H. (2000). Regulation of B Lymphocyte and Macrophage Development by Graded Expression of PU.1. Science *288*, 1439-1441.

Deuschle, U., Meyer, W.K., and Thiesen, H.J. (1995). Tetracycline-reversible silencing of eukaryotic promoters. Mol Cell Biol *15*, 1907-1914.

Didiano, D., and Hobert, O. (2008). Molecular architecture of a miRNA-regulated 3' UTR. RNA *14*, 1297-1317.

Dominguez-Soto, A., Puig-Kroger, A., Vega, M.A., and Corbi, A.L. (2005). PU.1 regulates the tissue-specific expression of dendritic cell-specific intercellular adhesion molecule (ICAM)-3-grabbing nonintegrin. J Biol Chem *280*, 33123-33131.

Doulatov, S., Notta, F., Eppert, K., Nguyen, L.T., Ohashi, P.S., and Dick, J.E. (2010). Revised map of the human progenitor hierarchy shows the origin of macrophages and dendritic cells in early lymphoid development. Nat Immunol *11*, 585-593.

Eis, P.S., Tam, W., Sun, L., Chadburn, A., Li, Z., Gomez, M.F., Lund, E., and Dahlberg, J.E. (2005). Accumulation of miR-155 and BIC RNA in human B cell lymphomas. Proc Natl Acad Sci U S A *102*, 3627-3632.

Enright, A.J., John, B., Gaul, U., Tuschl, T., Sander, C., and Marks, D.S. (2003). MicroRNA targets in Drosophila. Genome Biol *5*, R1.

Eulalio, A., Behm-Ansmant, I., and Izaurralde, E. (2007). P bodies: at the crossroads of post-transcriptional pathways. Nat Rev Mol Cell Biol *8*, 9-22.

Eulalio, A., Huntzinger, E., and Izaurralde, E. (2008). Getting to the root of miRNA-mediated gene silencing. Cell *132*, 9-14.

Faley, S., Seale, K., Hughey, J., Schaffer, D.K., VanCompernolle, S., McKinney, B., Baudenbacher, F., Unutmaz, D., and Wikswo, J.P. (2008). Microfluidic platform for real-time signaling analysis of multiple single T cells in parallel. Lab Chip *8*, 1700-1712.

Filipowicz, W., Bhattacharyya, S.N., and Sonenberg, N. (2008). Mechanisms of post-transcriptional regulation by microRNAs: are the answers in sight? Nat Rev Genet *9*, 102-114.

Friedman, A.D. (2007). Transcriptional control of granulocyte and monocyte development. Oncogene *26*, 6816-6828.

Fuss, I.J., and Strober, W. (2008). The role of IL-13 and NK T cells in experimental and human ulcerative colitis. Mucosal Immunol *1*, S31-S33.

Gao, Y., Bhattacharya, S., Chen, X., Barizuddin, S., Gangopadhyay, S., and Gillis, K.D. (2009). A microfluidic cell trap device for automated measurement of quantal catecholamine release from cells. Lab Chip *9*, 3442-3446.

Garcia-Cohen, E.C., Marin, J., Diez-Picazo, L.D., Baena, A.B., Salaices, M., and Rodriguez-Martinez, M.A. (2000). Oxidative stress induced by tert-butyl hydroperoxide causes vasoconstriction in the aorta from hypertensive and aged rats: role of cyclooxygenase-2 isoform. J Pharmacol Exp Ther *293*, 75-81.

Geijtenbeek, T.B., and Gringhuis, S.I. (2009). Signalling through C-type lectin receptors: shaping immune responses. Nat Rev Immunol *9*, 465-479.

Geijtenbeek, T.B., Torensma, R., van Vliet, S.J., van Duijnhoven, G.C., Adema, G.J., van Kooyk, Y., and Figdor, C.G. (2000). Identification of DC-SIGN, a novel dendritic cell-specific ICAM-3 receptor that supports primary immune responses. Cell *100*, 575-585.

Geijtenbeek, T.B., and van Kooyk, Y. (2003). DC-SIGN: a novel HIV receptor on DCs that mediates HIV-1 transmission. Curr Top Microbiol Immunol *276*, 31-54.

Geijtenbeek, T.B., van Vliet, S.J., Engering, A., t Hart, B.A., and van Kooyk, Y. (2004). Self- and nonself-recognition by C-type lectins on dendritic cells. Annu Rev Immunol *22*, 33-54.

Geijtenbeek, T.B., Van Vliet, S.J., Koppel, E.A., Sanchez-Hernandez, M., Vandenbroucke-Grauls, C.M., Appelmelk, B., and Van Kooyk, Y. (2003). Mycobacteria target DC-SIGN to suppress dendritic cell function. J Exp Med *197*, 7-17.

Geissmann, F., Manz, M.G., Jung, S., Sieweke, M.H., Merad, M., and Ley, K. (2010). Development of monocytes, macrophages, and dendritic cells. Science *327*, 656-661.

Gordon, S. (2003). Alternative activation of macrophages. Nat Rev Immunol *3*, 23-35.

Gordon, S., and Taylor, P.R. (2005). Monocyte and macrophage heterogeneity. Nat Rev Immunol *5*, 953-964.

Grimson, A., Farh, K.K., Johnston, W.K., Garrett-Engele, P., Lim, L.P., and Bartel, D.P. (2007). MicroRNA targeting specificity in mammals: determinants beyond seed pairing. Mol Cell *27*, 91-105.

Guo, H., Ingolia, N.T., Weissman, J.S., and Bartel, D.P. (2010). Mammalian microRNAs predominantly act to decrease target mRNA levels. Nature *466*, 835-840.

Hamilton, A.J., and Baulcombe, D.C. (1999). A species of small antisense RNA in posttranscriptional gene silencing in plants. Science *286*, 950-952.

Harrington, L.E., Hatton, R.D., Mangan, P.R., Turner, H., Murphy, T.L., Murphy, K.M., and Weaver, C.T. (2005). Interleukin 17-producing CD4+ effector T cells develop via a lineage distinct from the T helper type 1 and 2 lineages. Nat Immunol *6*, 1123-1132.

He, S., Su, H., Liu, C., Skogerbo, G., He, H., He, D., Zhu, X., Liu, T., Zhao, Y., and Chen, R. (2008). MicroRNA-encoding long non-coding RNAs. BMC Genomics *9*, 236.

Hebenstreit, D., Wirnsberger, G., Horejs-Hoeck, J., and Duschl, A. (2006). Signaling mechanisms, interaction partners, and target genes of STAT6. Cytokine & Growth Factor Reviews *17*, 173-188.

Hershey, G.K.K. (2003). IL-13 receptors and signaling pathways: An evolving web. Journal of Allergy and Clinical Immunology *111*, 677-690.

Hofacker, I.L., Fontana, W., Stadler, P.F., Bonhoeffer, L.S., Tacker, M., and Schuster, P. (1994). Fast folding and comparison of RNA secondary structures. Monatshefte für Chemie / Chemical Monthly *125*, 167-188.

Hutvagner, G., and Simard, M.J. (2008). Argonaute proteins: key players in RNA silencing. Nat Rev Mol Cell Biol *9*, 22-32.

Janeway, C.A., Jr., and Medzhitov, R. (2002). Innate immune recognition. Annu Rev Immunol *20*, 197-216.

Jiang, H., Harris, M.B., and Rothman, P. (2000). IL-4/IL-13 signaling beyond JAK/STAT. J Allergy Clin Immunol *105*, 1063-1070.

Jiang, S., Zhang, H.-W., Lu, M.-H., He, X.-H., Li, Y., Gu, H., Liu, M.-F., and Wang, E.-D. (2010). MicroRNA-155 Functions as an OncomiR in Breast Cancer by Targeting the Suppressor of Cytokine Signaling 1 Gene. Cancer Res *70*, 3119-3127.

John, B., Sander, C., and Marks, D.S. (2006). Prediction of human microRNA targets. Methods Mol Biol *342*, 101-113.

Junttila, I.S., Mizukami, K., Dickensheets, H., Meier-Schellersheim, M., Yamane, H., Donnelly, R.P., and Paul, W.E. (2008). Tuning sensitivity to IL-4 and IL-13: differential expression of IL-4Ralpha, IL-13Ralpha1, and gammac regulates relative cytokine sensitivity. J Exp Med *205*, 2595-2608.

Kertesz, M., Iovino, N., Unnerstall, U., Gaul, U., and Segal, E. (2007a). The role of site accessibility in microRNA target recognition. Nat Genet *39*, 1278-1284.

Kertesz, M., Iovino, N., Unnerstall, U., Gaul, U., and Segal, E. (2007b). The role of site accessibility in microRNA target recognition. Nat Genet *39*, 1278-1284.

Kindt, T.J., Goldsby, R.A., Osborne, B.A., and Kuby, J. (2007). Kuby immunology, 6th edn (New York, W.H. Freeman).

Kitagawa, Y., Van Eeden, S.F., Redenbach, D.M., Daya, M., Walker, B.A., Klut, M.E., Wiggs, B.R., and Hogg, J.C. (1997). Effect of mechanical deformation on structure and function of polymorphonuclear leukocytes. J Appl Physiol *82*, 1397-1405.

Kluiver, J., Poppema, S., de Jong, D., Blokzijl, T., Harms, G., Jacobs, S., Kroesen, B.J., and van den Berg, A. (2005). BIC and miR-155 are highly expressed in Hodgkin, primary mediastinal and diffuse large B cell lymphomas. J Pathol *207*, 243-249.

Kluiver, J., van den Berg, A., de Jong, D., Blokzijl, T., Harms, G., Bouwman, E., Jacobs, S., Poppema, S., and Kroesen, B.J. (2007). Regulation of pri-microRNA BIC transcription and processing in Burkitt lymphoma. Oncogene *26*, 3769-3776.

Kobel, S., Valero, A., Latt, J., Renaud, P., and Lutolf, M. (2010). Optimization of microfluidic single cell trapping for long-term on-chip culture. Lab Chip *10*, 857-863.

Kohlhaas, S., Garden, O.A., Scudamore, C., Turner, M., Okkenhaug, K., and Vigorito, E. (2009). Cutting edge: the Foxp3 target miR-155 contributes to the development of regulatory T cells. J Immunol *182*, 2578-2582.

Koppel, E.A., Ludwig, I.S., Hernandez, M.S., Lowary, T.L., Gadikota, R.R., Tuzikov, A.B., Vandenbroucke-Grauls, C.M., van Kooyk, Y., Appelmelk, B.J., and Geijtenbeek, T.B. (2004). Identification of the mycobacterial carbohydrate structure that binds the C-type lectins DC-SIGN, L-SIGN and SIGNR1. Immunobiology *209*, 117-127.

Krummel, M.F. (2010). Illuminating emergent activity in the immune system by real-time imaging. Nat Immunol *11*, 554-557.

Kurosaka, K., Watanabe, N., and Kobayashi, Y. (1998). Production of Proinflammatory Cytokines by Phorbol Myristate Acetate-Treated THP-1 Cells and Monocyte-Derived

Macrophages After Phagocytosis of Apoptotic CTLL-2 Cells. The Journal of Immunology *161*, 6245-6249.

Langerhans, P. (1868). Ueber die Nerven der menschlichen Haut. Virchows Archiv *44*, 325-337.

Langrish, C.L., Chen, Y., Blumenschein, W.M., Mattson, J., Basham, B., Sedgwick, J.D., McClanahan, T., Kastelein, R.A., and Cua, D.J. (2005). IL-23 drives a pathogenic T cell population that induces autoimmune inflammation. J Exp Med *201*, 233-240.

Lanzavecchia, A., and Sallusto, F. (2001). Regulation of T cell immunity by dendritic cells. Cell *106*, 263-266.

LaPorte, S.L., Juo, Z.S., Vaclavikova, J., Colf, L.A., Qi, X., Heller, N.M., Keegan, A.D., and Garcia, K.C. (2008). Molecular and Structural Basis of Cytokine Receptor Pleiotropy in the Interleukin-4/13 System. Cell *132*, 259-272.

Lee, C., Kolesnik, T.B., Caminschi, I., Chakravorty, A., Carter, W., Alexander, W.S., Jones, J., Anderson, G.P., and Nicholson, S.E. (2009). Suppressor of cytokine signalling 1 (SOCS1) is a physiological regulator of the asthma response. Clin Exp Allergy *39*, 897-907.

Lee, R.C., Feinbaum, R.L., and Ambros, V. (1993). The C. elegans heterochronic gene lin-4 encodes small RNAs with antisense complementarity to lin-14. Cell *75*, 843-854.

Lee, Y., Jeon, K., Lee, J.T., Kim, S., and Kim, V.N. (2002). MicroRNA maturation: stepwise processing and subcellular localization. EMBO J *21*, 4663-4670.

Lombardi, V., Van Overtvelt, L., Horiot, S., and Moingeon, P. (2009). Human dendritic cells stimulated via TLR7 and/or TLR8 induce the sequential production of Il-10, IFN-gamma, and IL-17A by naive CD4+ T cells. J Immunol *182*, 3372-3379.

Lu, L.F., Thai, T.H., Calado, D.P., Chaudhry, A., Kubo, M., Tanaka, K., Loeb, G.B., Lee, H., Yoshimura, A., Rajewsky, K.*, et al.* (2009). Foxp3-dependent microRNA155 confers competitive fitness to regulatory T cells by targeting SOCS1 protein. Immunity *30*, 80-91.

Mantovani, A., Sica, A., Sozzani, S., Allavena, P., Vecchi, A., and Locati, M. (2004). The chemokine system in diverse forms of macrophage activation and polarization. Trends in Immunology *25*, 677-686.

Mantovani, A., Sozzani, S., Locati, M., Allavena, P., and Sica, A. (2002). Macrophage polarization: tumor-associated macrophages as a paradigm for polarized M2 mononuclear phagocytes. Trends in Immunology *23*, 549-555.

Maragkakis, M., Reczko, M., Simossis, V.A., Alexiou, P., Papadopoulos, G.L., Dalamagas, T., Giannopoulos, G., Goumas, G., Koukis, E., Kourtis, K.*, et al.* (2009). DIANA-microT web server: elucidating microRNA functions through target prediction. Nucleic Acids Res *37*, W273-276.

Martin, M.M., Lee, E.J., Buckenberger, J.A., Schmittgen, T.D., and Elton, T.S. (2006). MicroRNA-155 regulates human angiotensin II type 1 receptor expression in fibroblasts. J Biol Chem *281*, 18277-18284.

Martinez-Nunez, R.T., Louafi, F., Friedmann, P.S., and Sanchez-Elsner, T. (2009). MicroRNA-155 modulates the pathogen binding ability of dendritic cells (DCs) by down-regulation of DC-specific intercellular adhesion molecule-3 grabbing non-integrin (DC-SIGN). J Biol Chem *284*, 16334-16342.

Martinez, F.O., Gordon, S., Locati, M., and Mantovani, A. (2006). Transcriptional Profiling of the Human Monocyte-to-Macrophage Differentiation and Polarization: New Molecules and Patterns of Gene Expression. J Immunol *177*, 7303-7311.

Martinez, F.O., Helming, L., and Gordon, S. (2009). Alternative activation of macrophages: an immunologic functional perspective. Annu Rev Immunol *27*, 451-483.

Mata, A., Fleischman, A.J., and Roy, S. (2005). Characterization of polydimethylsiloxane (PDMS) properties for biomedical micro/nanosystems. Biomed Microdevices *7*, 281-293.

Matsue, H., Edelbaum, D., Shalhevet, D., Mizumoto, N., Yang, C., Mummert, M.E., Oeda, J., Masayasu, H., and Takashima, A. (2003). Generation and function of reactive oxygen species in dendritic cells during antigen presentation. J Immunol *171*, 3010-3018.

McCaskill, J.S. (1990). The equilibrium partition function and base pair binding probabilities for RNA secondary structure. Biopolymers *29*, 1105-1119.

Mempel, T.R., Henrickson, S.E., and Von Andrian, U.H. (2004). T-cell priming by dendritic cells in lymph nodes occurs in three distinct phases. Nature *427*, 154-159.

Minty, A., Chalon, P., Derocq, J.M., Dumont, X., Guillemot, J.C., Kaghad, M., Labit, C., Leplatois, P., Liauzun, P., Miloux, B.*, et al.* (1993). Interleukin-13 is a new human lymphokine regulating inflammatory and immune responses. Nature *362*, 248-250.

Morimoto, M., Zhao, A., Sun, R., Stiltz, J., Madden, K.B., Mentink-Kane, M., Ramalingam, T., Wynn, T.A., Urban, J.F., Jr., and Shea-Donohue, T. (2009). IL-13 receptor alpha2 regulates the immune and functional response to Nippostrongylus brasiliensis infection. J Immunol *183*, 1934-1939.

Mosser, D.M., and Edwards, J.P. (2008). Exploring the full spectrum of macrophage activation. Nat Rev Immunol *8*, 958-969.

Munitz, A., Brandt, E.B., Mingler, M., Finkelman, F.D., and Rothenberg, M.E. (2008). Distinct roles for IL-13 and IL-4 via IL-13 receptor alpha1 and the type II IL-4 receptor in asthma pathogenesis. Proc Natl Acad Sci U S A *105*, 7240-7245.

Murphy, K., Travers, P., Walport, M., and Janeway, C. (2008). Janeway's immunobiology, 7th edn (New York, Garland Science).

Mytar, B., Siedlar, M., Woloszyn, M., Ruggiero, I., Pryjma, J., and Zembala, M. (1999). Induction of reactive oxygen intermediates in human monocytes by tumour cells and their role in spontaneous monocyte cytotoxicity. Br J Cancer *79*, 737-743.

Mytar, B., Woloszyn, M., Macura-Biegun, A., Hajto, B., Ruggiero, I., Piekarska, B., and Zembala, M. (2004). Involvement of pattern recognition receptors in the induction of cytokines and reactive oxygen intermediates production by human monocytes/macrophages stimulated with tumour cells. Anticancer Res *24*, 2287-2293.

Nottrott, S., Simard, M.J., and Richter, J.D. (2006). Human let-7a miRNA blocks protein production on actively translating polyribosomes. Nat Struct Mol Biol *13*, 1108-1114.

Nutt, S.L., Metcalf, D., D'Amico, A., Polli, M., and Wu, L. (2005). Dynamic regulation of PU.1 expression in multipotent hematopoietic progenitors. J Exp Med *201*, 221-231.

O'Connell, R.M., Chaudhuri, A.A., Rao, D.S., and Baltimore, D. (2009). Inositol phosphatase SHIP1 is a primary target of miR-155. Proc Natl Acad Sci U S A *106*, 7113-7118.

O'Connell, R.M., Rao, D.S., Chaudhuri, A.A., Boldin, M.P., Taganov, K.D., Nicoll, J., Paquette, R.L., and Baltimore, D. (2008). Sustained expression of microRNA-155 in hematopoietic stem cells causes a myeloproliferative disorder. J Exp Med *205*, 585-594.

O'Connell, R.M., Taganov, K.D., Boldin, M.P., Cheng, G., and Baltimore, D. (2007). MicroRNA-155 is induced during the macrophage inflammatory response. Proc Natl Acad Sci U S A *104*, 1604-1609.

O'Shea, J.J., and Murray, P.J. (2008). Cytokine signaling modules in inflammatory responses. Immunity *28*, 477-487.

Orom, U.A., Nielsen, F.C., and Lund, A.H. (2008). MicroRNA-10a binds the 5'UTR of ribosomal protein mRNAs and enhances their translation. Mol Cell *30*, 460-471.

Park, E., Jung, H., Yang, H., Yoo, M., Kim, C., and Kim, K. (2007). Optimized THP-1 differentiation is required for the detection of responses to weak stimuli. Inflammation Research *56*, 45-50.

Parker, R., and Sheth, U. (2007). P Bodies and the Control of mRNA Translation and Degradation. Molecular Cell *25*, 635-646.

Peck, A., and Mellins, E.D. (2010). Plasticity of T-cell phenotype and function: the T helper type 17 example. Immunology *129*, 147-153.

Pedersen, I.M., Cheng, G., Wieland, S., Volinia, S., Croce, C.M., Chisari, F.V., and David, M. (2007). Interferon modulation of cellular microRNAs as an antiviral mechanism. Nature *449*, 919-922.

Place, R.F., Li, L.C., Pookot, D., Noonan, E.J., and Dahiya, R. (2008). MicroRNA-373 induces expression of genes with complementary promoter sequences. Proc Natl Acad Sci U S A *105*, 1608-1613.

Polisky, B. (1988). ColE1 replication control circuitry: sense from antisense. Cell *55*, 929-932.

Porcheray, F., Viaud, S., Rimaniol, A.C., Leone, C., Samah, B., Dereuddre-Bosquet, N., Dormont, D., and Gras, G. (2005). Macrophage activation switching: an asset for the resolution of inflammation. Clin Exp Immunol *142*, 481-489.

Puig-Kroger, A., Serrano-Gomez, D., Caparros, E., Dominguez-Soto, A., Relloso, M., Colmenares, M., Martinez-Munoz, L., Longo, N., Sanchez-Sanchez, N., Rincon, M.*, et al.* (2004). Regulated expression of the pathogen receptor dendritic cell-specific intercellular adhesion molecule 3 (ICAM-3)-grabbing nonintegrin in THP-1 human leukemic cells, monocytes, and macrophages. J Biol Chem *279*, 25680-25688.

Punnonen, J., Aversa, G., Cocks, B.G., McKenzie, A.N., Menon, S., Zurawski, G., de Waal Malefyt, R., and de Vries, J.E. (1993). Interleukin 13 induces interleukin 4-independent IgG4 and IgE synthesis and CD23 expression by human B cells. Proc Natl Acad Sci U S A *90*, 3730-3734.

Ralser, M., Querfurth, R., Warnatz, H.J., Lehrach, H., Yaspo, M.L., and Krobitsch, S. (2006). An efficient and economic enhancer mix for PCR. Biochem Biophys Res Commun *347*, 747-751.

Ramalingam, T.R., Pesce, J.T., Sheikh, F., Cheever, A.W., Mentink-Kane, M.M., Wilson, M.S., Stevens, S., Valenzuela, D.M., Murphy, A.J., Yancopoulos, G.D.*, et al.* (2008). Unique functions of the type II interleukin 4 receptor identified in mice lacking the interleukin 13 receptor alpha1 chain. Nat Immunol *9*, 25-33.

Rambert, J.r.m., Mamani-Matsuda, M., Moynet, D., Dubus, P., Desplat, V., Kauss, T., Dehais, J.l., Schaeverbeke, T., Ezzedine, K., Malvy, D.*, et al.* (2009). Molecular Blocking of CD23 Supports Its Role in the Pathogenesis of Arthritis. PLoS One *4*, e4834.

Rehmsmeier, M., Steffen, P., Hochsmann, M., and Giegerich, R. (2004). Fast and effective prediction of microRNA/target duplexes. RNA *10*, 1507-1517.

Relloso, M., Puig-Kroger, A., Pello, O.M., Rodriguez-Fernandez, J.L., de la Rosa, G., Longo, N., Navarro, J., Munoz-Fernandez, M.A., Sanchez-Mateos, P., and Corbi, A.L. (2002). DC-SIGN (CD209) expression is IL-4 dependent and is negatively regulated by IFN, TGF-beta, and anti-inflammatory agents. J Immunol *168*, 2634-2643.

Rodriguez, A., Vigorito, E., Clare, S., Warren, M.V., Couttet, P., Soond, D.R., van Dongen, S., Grocock, R.J., Das, P.P., Miska, E.A.*, et al.* (2007). Requirement of bic/microRNA-155 for normal immune function. Science *316*, 608-611.

Romano, N., and Macino, G. (1992). Quelling: transient inactivation of gene expression in Neurospora crassa by transformation with homologous sequences. Molecular Microbiology *6*, 3343-3353.

Rosenwasser, L., and Meng, J. (2005). Anti-CD23. Clinical Reviews in Allergy and Immunology *29*, 61-72.

Ruby, J.G., Jan, C.H., and Bartel, D.P. (2007). Intronic microRNA precursors that bypass Drosha processing. Nature *448*, 83-86.

Ruggiero, T., Trabucchi, M., De Santa, F., Zupo, S., Harfe, B.D., McManus, M.T., Rosenfeld, M.G., Briata, P., and Gherzi, R. (2009). LPS induces KH-type splicing regulatory protein-dependent processing of microRNA-155 precursors in macrophages. FASEB J.

Saraiya, A.A., and Wang, C.C. (2008). snoRNA, a novel precursor of microRNA in Giardia lamblia. PLoS Pathog *4*, e1000224.

Schaefer, M., Reiling, N., Fessler, C., Stephani, J., Taniuchi, I., Hatam, F., Yildirim, A.O., Fehrenbach, H., Walter, K., Ruland, J.*, et al.* (2008). Decreased pathology and prolonged survival of human DC-SIGN transgenic mice during mycobacterial infection. J Immunol *180*, 6836-6845.

Seggerson, K., Tang, L., and Moss, E.G. (2002). Two genetic circuits repress the Caenorhabditis elegans heterochronic gene lin-28 after translation initiation. Dev Biol *243*, 215-225.

Selbach, M., Schwanhausser, B., Thierfelder, N., Fang, Z., Khanin, R., and Rajewsky, N. (2008). Widespread changes in protein synthesis induced by microRNAs. Nature *455*, 58-63.

Sequist, L.V., Nagrath, S., Toner, M., Haber, D.A., and Lynch, T.J. (2009). The CTC-chip: an exciting new tool to detect circulating tumor cells in lung cancer patients. J Thorac Oncol *4*, 281-283.

Serrano-Gomez, D., Martinez-Nunez, R.T., Sierra-Filardi, E., Izquierdo, N., Colmenares, M., Pla, J., Rivas, L., Martinez-Picado, J., Jimenez-Barbero, J., Alonso-Lebrero, J.L.*, et al.* (2007). AM3 modulates dendritic cell pathogen recognition capabilities by targeting DC-SIGN. Antimicrob Agents Chemother *51*, 2313-2323.

Serrano-Gomez, D., Sierra-Filardi, E., Martinez-Nunez, R.T., Caparros, E., Delgado, R., Munoz-Fernandez, M.A., Abad, M.A., Jimenez-Barbero, J., Leal, M., and Corbi, A.L. (2008). Structural requirements for multimerization of the pathogen receptor dendritic cell-specific ICAM3-grabbing non-integrin (CD209) on the cell surface. J Biol Chem *283*, 3889-3903.

Shin, C., Nam, J.W., Farh, K.K., Chiang, H.R., Shkumatava, A., and Bartel, D.P. (2010). Expanding the microRNA targeting code: functional sites with centered pairing. Mol Cell *38*, 789-802.

Skelley, A.M., Kirak, O., Suh, H., Jaenisch, R., and Voldman, J. (2009). Microfluidic control of cell pairing and fusion. Nat Methods *6*, 147-152.

Soilleux, E.J., Morris, L.S., Leslie, G., Chehimi, J., Luo, Q., Levroney, E., Trowsdale, J., Montaner, L.J., Doms, R.W., Weissman, D.*, et al.* (2002). Constitutive and induced expression of DC-SIGN on dendritic cell and macrophage subpopulations in situ and in vitro. J Leukoc Biol *71*, 445-457.

Soroosh, P., and Doherty, T.A. (2009). Th9 and allergic disease. Immunology *127*, 450-458.

Steinman, R.M. (2001). Dendritic cells and the control of immunity: enhancing the efficiency of antigen presentation. Mt Sinai J Med *68*, 160-166.

Steinman, R.M., and Cohn, Z.A. (1973). IDENTIFICATION OF A NOVEL CELL TYPE IN PERIPHERAL LYMPHOID ORGANS OF MICE: I. MORPHOLOGY, QUANTITATION, TISSUE DISTRIBUTION. J Exp Med *137*, 1142-1162.

Stout, R.D., and Suttles, J. (2004). Functional plasticity of macrophages: reversible adaptation to changing microenvironments. J Leukoc Biol *76*, 509-513.

Tam, W. (2001). Identification and characterization of human BIC, a gene on chromosome 21 that encodes a noncoding RNA. Gene *274*, 157-167.

Tanne, A., Ma, B., Boudou, F., Tailleux, L., Botella, H., Badell, E., Levillain, F., Taylor, M.E., Drickamer, K., Nigou, J.*, et al.* (2009). A murine DC-SIGN homologue contributes to early host defense against Mycobacterium tuberculosis. J Exp Med *206*, 2205-2220.

Toner, M., and Irimia, D. (2005). Blood-on-a-chip. Annu Rev Biomed Eng *7*, 77-103.

Trinchieri, G. (2003). Interleukin-12 and the regulation of innate resistance and adaptive immunity. Nat Rev Immunol *3*, 133-146.

Tsuchiya, S., Yamabe, M., Yamaguchi, Y., Kobayashi, Y., Konno, T., and Tada, K. (1980). Establishment and characterization of a human acute monocytic leukemia cell line (THP-1). Int J Cancer *26*, 171-176.

Umetsu, D.T., Akbari, O., and Dekruyff, R.H. (2003). Regulatory T cells control the development of allergic disease and asthma. J Allergy Clin Immunol *112*, 480-487; quiz 488.

Valero, A., Merino, F., Wolbers, F., Luttge, R., Vermes, I., Andersson, H., and van den Berg, A. (2005). Apoptotic cell death dynamics of HL60 cells studied using a microfluidic cell trap device. Lab Chip *5*, 49-55.

van Kooyk, Y. (2008). C-type lectins on dendritic cells: key modulators for the induction of immune responses. Biochem Soc Trans *36*, 1478-1481.

Vasudevan, S., and Steitz, J.A. (2007). AU-rich-element-mediated upregulation of translation by FXR1 and Argonaute 2. Cell *128*, 1105-1118.

Veldhoen, M., Uyttenhove, C., van Snick, J., Helmby, H., Westendorf, A., Buer, J., Martin, B., Wilhelm, C., and Stockinger, B. (2008). Transforming growth factor-beta 'reprograms' the differentiation of T helper 2 cells and promotes an interleukin 9-producing subset. Nat Immunol *9*, 1341-1346.

Vella, M.C., Choi, E.Y., Lin, S.Y., Reinert, K., and Slack, F.J. (2004). The C. elegans microRNA let-7 binds to imperfect let-7 complementary sites from the lin-41 3'UTR. Genes Dev *18*, 132-137.

Vigorito, E., Perks, K.L., Abreu-Goodger, C., Bunting, S., Xiang, Z., Kohlhaas, S., Das, P.P., Miska, E.A., Rodriguez, A., Bradley, A.*, et al.* (2007). microRNA-155 regulates the generation of immunoglobulin class-switched plasma cells. Immunity *27*, 847-859.

Voldman, J., Gray, M.L., and Schmidt, M.A. (1999). Microfabrication in biology and medicine. Annu Rev Biomed Eng *1*, 401-425.

Wallet, M.A., Sen, P., and Tisch, R. (2005). Immunoregulation of dendritic cells. Clin Med Res *3*, 166-175.

Wan, Y.Y. (2010). Multi-tasking of helper T cells. Immunology *130*, 166-171.

Wang, Y., Sheng, G., Juranek, S., Tuschl, T., and Patel, D.J. (2008). Structure of the guide-strand-containing argonaute silencing complex. Nature *456*, 209-213.

Whitesides, G.M., Ostuni, E., Takayama, S., Jiang, X., and Ingber, D.E. (2001). Soft lithography in biology and biochemistry. Annu Rev Biomed Eng *3*, 335-373.

Wieland, C.W., Koppel, E.A., den Dunnen, J., Florquin, S., McKenzie, A.N., van Kooyk, Y., van der Poll, T., and Geijtenbeek, T.B. (2007). Mice lacking SIGNR1 have stronger T helper 1 responses to Mycobacterium tuberculosis. Microbes Infect *9*, 134-141.

Wills-Karp, M. (2004). Interleukin-13 in asthma pathogenesis. Immunol Rev *202*, 175-190.

Wiznerowicz, M., and Trono, D. (2003). Conditional suppression of cellular genes: lentivirus vector-mediated drug-inducible RNA interference. J Virol *77*, 8957-8961.

Worm, J., Stenvang, J., Petri, A., Frederiksen, K.S., Obad, S., Elmen, J., Hedtjarn, M., Straarup, E.M., Hansen, J.B., and Kauppinen, S. (2009). Silencing of microRNA-155 in mice during acute inflammatory response leads to derepression of c/ebp Beta and down-regulation of G-CSF. Nucleic Acids Res.

Wynn, T.A. (2003). IL-13 EFFECTOR FUNCTIONS*. Annual Review of Immunology *21*, 425-456.

Xiao, B., Liu, Z., Li, B.S., Tang, B., Li, W., Guo, G., Shi, Y., Wang, F., Wu, Y., Tong, W.D.*, et al.* (2009). Induction of microRNA-155 during Helicobacter pylori infection and Its Negative Regulatory Role in the Inflammatory Response. J Infect Dis.

Yamada, H., Arai, T., Endo, N., Yamashita, K., Fukuda, K., Sasada, M., and Uchiyama, T. (2006). LPS-induced ROS generation and changes in glutathione level and their relation to the maturation of human monocyte-derived dendritic cells. Life Sci *78*, 926-933.

Yi, R., Qin, Y., Macara, I.G., and Cullen, B.R. (2003). Exportin-5 mediates the nuclear export of pre-microRNAs and short hairpin RNAs. Genes Dev *17*, 3011-3016.

Zeng, Y., Cai, X., Cullen, B.R., David, R.E., and John, J.R. (2005). Use of RNA Polymerase II to Transcribe Artificial MicroRNAs. In Methods in Enzymology (Academic Press), pp. 371-380.

Zhang, T., Nie, K., and Tam, W. (2008). BIC is processed efficiently to microRNA-155 in Burkitt lymphoma cells. Leukemia *22*, 1795-1797.

Zhao, A., Urban, J.F., Jr., Anthony, R.M., Sun, R., Stiltz, J., van Rooijen, N., Wynn, T.A., Gause, W.C., and Shea-Donohue, T. (2008). Th2 cytokine-induced alterations in intestinal smooth muscle function depend on alternatively activated macrophages. Gastroenterology *135*, 217-225 e211.

Zuker, M., and Stiegler, P. (1981). Optimal computer folding of large RNA sequences using thermodynamics and auxiliary information. Nucleic Acids Res *9*, 133-148.

Supplemental Material can be found at:
http://www.jbc.org/content/suppl/2009/04/22/M109.011601.DC1.html

THE JOURNAL OF BIOLOGICAL CHEMISTRY VOL. 284, NO. 24, pp. 16334–16342, June 12, 2009
© 2009 by The American Society for Biochemistry and Molecular Biology, Inc. Printed in the U.S.A.

MicroRNA-155 Modulates the Pathogen Binding Ability of Dendritic Cells (DCs) by Down-regulation of DC-specific Intercellular Adhesion Molecule-3 Grabbing Non-integrin (DC-SIGN)*[S]

Received for publication, October 14, 2008, and in revised form, April 22, 2009 Published, JBC Papers in Press, April 22, 2009, DOI 10.1074/jbc.M109.011601

Rocio T. Martinez-Nunez[‡1], Fethi Louafi[‡1], Peter S. Friedmann[‡], and Tilman Sanchez-Elsner[‡2]

From the [‡]Division of Infection, Inflammation and Repair, University of Southampton School of Medicine, and [§]Southampton General Hospital, Southampton SO16 6YD, United Kingdom

MicroRNA-155 (miR-155) has been involved in the response to inflammation in macrophages and lymphocytes. Here we show how miR-155 participates in the maturation of human dendritic cells (DC) and modulates pathogen binding by down-regulating DC-specific intercellular adhesion molecule-3 grabbing non-integrin (DC-SIGN), after directly targeting the transcription factor PU.1. During the maturation of DCs, miR-155 increases up to 130-fold, whereas PU.1 protein levels decrease accordingly. We establish that human PU.1 is a direct target for miR-155 and localize the target sequence for miR-155 in the 3′-untranslated region of PU.1. Also, overexpression of miR-155 in the THP1 monocytic cell line decreases PU.1 protein levels and DC-SIGN at both the mRNA and protein levels. We prove a link between the down-regulation of PU.1 and reduced transcriptional activity of the DC-SIGN promoter, which is likely to be the basis for its reduced mRNA expression, after miR-155 overexpression. Finally, we show that, by reducing DC-SIGN in the cellular membrane, miR-155 is involved in regulating pathogen binding as dendritic cells exhibited the lower binding capacity for fungi and HIV protein gp-120 when the levels of miR-155 were higher. Thus, our results suggest a mechanism by which miR-155 regulates proteins involved in the cellular immune response against pathogens that could have clinical implications in the way pathogens enter the human organism.

MicroRNAs have emerged as important regulators of key cellular processes. They consist of endogenous small, non-coding RNA molecules of about 19–22 nucleotides in length (1), which regulate mRNAs in a post-transcriptional manner. They bind to the 3′-untranslated regions of their target mRNAs and exert their function in two ways: mainly blocking the translation and also inducing their cleavage in a similar fashion to small interfering RNAs (2). MicroRNAs are initially expressed as long immature pri-microRNAs, which are processed in the nucleus into the precursor pre-microRNAs and finally matured by Dicer in the cytoplasm into the functional 19–22-nucleotide long microRNAs, which are then incorporated into the RNA-induced silencing complex (1).

The role of microRNAs is being intensively studied in many different fields such as fetal development and the immune system. One of the miRNAs that appears to play a particularly important role in the immune system is microRNA-155 (miR-155),[3] the expression of which is induced by inflammatory signals such as exposure to antigen, Toll-like receptor ligands, or interferon γ stimulation in T-cells, B-cells, and macrophages, respectively (3, 4).

miR-155 knock-out mice show aberrant immune functions including defective B and T cell immunity and abnormal function of antigen-presenting cells (4, 5). These mutant mice exhibit an imbalance in the immune Th1/Th2 response, with the CD4+ T cells biased toward Th2 differentiation (4). A lack of miR-155 also leads to a failure in production of high-affinity IgG_1 antibodies by murine B-cells (28). This effect has been related to its ability to target the transcription factor PU.1, a key transcription factor in human hematopoiesis, restricted to B lymphoid, granulocytic, and monocytic cells (6).

So far, the role of miR-155 in dendritic cell biology has not been studied in depth. Dendritic cells (DCs) are professional antigen presenting cells that have a pivotal role in controlling immune responses, directing them toward immune activation or tolerance (7), orchestrating an efficient and protective immune response. DCs are present as sentinels in peripheral tissues where they capture antigens that will be presented to CD4+ and CD8+ T cells in lymphoid organs. They arise either from myeloid- or lymphoid-derived precursors and exhibit an immature phenotype characterized by a high phagocytic capacity and low expression of co-stimulatory molecules (8). DCs undergo a maturation process after "sensing" pathogen-derived structures through pattern recognition receptors such as Toll-like receptors, exposure to pro-inflammatory cytokines, or after ligation of the surface receptor CD40. Upon maturation, DCs stop taking up antigens and change their pattern of homing receptors, acquiring a phenotype that allows them to migrate into the T cell compartments, where they perform their antigen

* This work was supported by Wessex Medical Research Grant M14.
[S] The on-line version of this article (available at http://www.jbc.org) contains supplemental Figs. S1–S6.
[1] Both authors contributed equally to this work.
[2] To whom correspondence should be addressed: General Hospital MP 813, Tremona Rd., Southampton SO16 6YD, United Kingdom. E-mail: T.Sanchez-Elsner@soton.ac.uk.

[3] The abbreviations used are: miR-155, microRNA-155; UTR, untranslated region; DC-SIGN, dendritic cell-specific intercellular adhesion molecule-3-grabbing non-integrin; DC, dendritic cell; HIV-1, human immunodeficiency virus, type 1; LPS, lipopolysaccharide; WT, wild type; RT, reverse transcriptase; qPCR, quantitative PCR.

Downloaded from www.jbc.org at University of Southampton Libraries, on December 17, 2010

presenting function. Many transcription factors such as NF-κB and PU.1 are involved in this process, although no microRNA has been implicated so far.

In addition to its role in DC maturation, PU.1 has been implicated in the differentiation of DCs from myeloid precursors. In this process, the balance between PU.1 and MafB determines the phenotype as being a dendritic cell or a macrophage (9). PU.1 controls a number of myeloid genes, and it has been shown to contribute to transcriptional expression of DC-SIGN (CD209) (10). DC-SIGN is a C-type lectin, present in myeloid dendritic cells, that binds a large array of pathogens via mannan- and Lewis oligosaccharides-dependent interactions (11–15). For example, it has been proposed that DC-SIGN binds to HIV-1, facilitating transport of the virus by DCs' migrating into the lymph nodes, thus promoting transinfection of CD4+ lymphocytes (16). Moreover, CD209 mediates transient adhesion contact with T cells through intercellular adhesion molecule 3 recognition, (17), DC transmigration across endothelium via intercellular adhesion molecule 2 interactions (18), and interaction with neutrophils via Mac-1 (19). DC-SIGN is mainly expressed in DCs and macrophages activated by interleukin-4, and is down-regulated together with PU.1 during maturation of human DCs (10).

In this report, we demonstrate that miR-155 levels increase during maturation of human monocyte-derived dendritic cells after exposure to lipopolysaccharide (LPS). We show that human miR-155 directly targets the 3′-untranslated region (3′-UTR) of PU.1 mRNA and we map the target sequence for miR-155 binding. We also present a stably transfected, inducible cell system using the THP-1 monocytic cell line. This cell line, hence forth named THP1–155, was able to overexpress miR-155 in a regulated fashion, after treatment with doxycycline. In this system, we prove that overexpression of miR-155 elicits protein level down-regulation of PU.1 and subsequently of DC-SIGN mRNA and protein. Furthermore, we demonstrate that miR-155 reduction increased DC-SIGN levels in the membrane of DCs resulting in impaired pathogen binding capacity. Thus, inhibition of miR-155 by synthetic oligonucleotides increased the binding of DCs to both *Candida albicans* and HIV-1 protein (gp120). Our results show how DC-SIGN, a protein of functional importance in the immune system, is regulated indirectly by miR-155 by direct targeting of the transcription factor PU.1. This has an important physiological role in the pathogen binding ability of dendritic cells, with potentially important effects on the entry and interaction of pathogens such as HIV-1.

EXPERIMENTAL PROCEDURES

Cell Culture

Dendritic cells were generated from human peripheral blood mononuclear cells as previously described (20). Monocytes were cultured for 5–7 days in complete medium (RPMI 1640 medium supplemented with 10% fetal calf serum) with 1000 units/ml granulocyte macrophage-colony stimulating factor and 1000 units/ml interleukin-4 (Immunotools) to obtain immature DCs. To mature these DCs, ultrapure LPS from *Escherichia coli* 0111:B4 (1 μg/ml) was used. The cell line THP1–155 was cultured in RPMI complete medium. HEK293T and HeLa cells were cultured in Dulbecco's modified Eagle's medium plus 10% fetal calf serum.

Vectors Generated

pCDNA3.1.BIC—The genomic region encompassing miR-155 was amplified and cloned into HindIII/XhoI of the pCDNA3.1 multicloning site. Primers employed were BIC-FOR, AAGCTTTATGCCTCATCCTCTGAGTGC and BIC-REV, CTCGAGACGAAGGTTGAACATCCCAGTGACC.

pLVTHM_BIC—The same fragment as above was first cloned in pSUPER in the HindIII/XhoI sites, from where it was removed using EcoRI and MluI sites, and then subcloned into pLVTHM. pRLTK_WT_3′UTR_PU1 was generated by cloning the 3′-UTR of human PU.1 into XbaI and NotI sites of the pRLTK vector (Promega). PU.1 3′UTR was amplified from genomic DNA by PCR amplification following the protocol established by Ralser *et al.* (21) using the following primers: 3′-UTR PU.1 FOR2 (TCT AGA TAC GAC TTC AGC GGC GAA GTG CTG) and 3′-UTR PU.1 REV BamHI (GGA TCC GGA TTG AGA ATA ACT TTA CTT G). pRLTK_MUT_3′UTR_PU1 was generated by site-directed mutagenesis on pRLTK_WT_3′UTR_PU1. This vector was mutated in the putative miR-155 binding site, using the following primers: 3′UTR_Mut_PU.1 FOR (GCC TCC CCG CTG GCC TGA ATT CGA AGC CCT CGC CCG GCC CGG) and 3′UTR_Mut_PU.1 REV (CCG GGC CGG GCG AGG GCT TCG AAT TCA GGC CAG CGG GGA GGC). Mutagenesis was done using the QuikChange® Site-directed Mutagenesis Kit (Stratagene) and following the manufacturer's instructions.

Transfections

To generate the THP1–155 cell line, HEK293 T cells were transfected with Superfect (Qiagen) following the manufacturer's protocol with 5 μg of pLVTHM_BIC (or pLV/tTR_KRAB_Red in the case of generating the repressor lentiviral particles), 3.75 μg of pPAX2 and 1.5 μg of pMD2G. Supernatant from these cells, containing lentiviral particles, was added to THP-1 cells that were preincubated in the presence of 8 μg/ml of Polybrene (Sigma) for 30 min at 37 °C. Infection was checked 4 days after infection, and positive cells were sorted. All the vectors used in the lentiviral system were kindly provided by Prof. Didier Trono (Ecole Polytechnique Fédérale de Lausanne, Switzerland).

For the luciferase promoter assays, we used the pCD209–468 pXP2 reporter plasmid, which contains the proximal region of the DC-SIGN promoter and pCDNA3.1-PU.1 encoding for full-length PU.1 (10). These plasmids were kindly provided by Prof. A. L. Corbi (Centro de Investigaciones Biologicas, CSIC, Spain). pCDNA3.1_PU.1_3UTR was generated by inserting the 3′-UTR of PU.1 after the coding region of pCDNA3.1 employing a blunt end ligation strategy. THP1–155 cells were electroporated following standard procedures. Electroporation results were normalized by co-transfection with the pRLTK-*Renilla* luciferase plasmid. To assess direct targeting of miR-155, pRLTK, pRLTK_WT_3′UTR_PU1, or pRLTK_MUT_3′UTR_PU1 were transfected into HeLa cells employing Superfect (Qiagen) following the manufacturer's instructions. pCDNA3.1.BIC or pCDNA3.1 empty vector was co-trans-

Downloaded from www.jbc.org at University of Southampton Libraries, on December 17, 2010

fected. Normalization was achieved with co-transfection of pGL3 (Promega). All luciferase/*Renilla* luciferase assays were measured employing the Dual-Glo kit from Promega. The experiments were performed three times in triplicates. Statistical differences were determined using Student's *t* test.

Flow Cytometry

For the pathogen binding experiments, mature DCs were transfected with 100 nM of oligonucleotides anti-miR-155 or anti-miR-Control, and 50 nM Cy3-premiR-control-1 (Ambion) at day 5 of culture. Cy3 fluorescence was used both to assess transfection efficiency and to specifically select the transfected population of DCs. DC-SIGN surface expression was checked by flow cytometry, using 0.3 ng/μl APC-anti-human DC-SIGN antibody or APC Rat IgG2a as Isotype Control (eBiosciences). To perform the binding assays, *C. albicans* was resuspended in phosphate-buffered saline, inactivated at 90 °C for 20 min, and stained using propidium iodide (1 mg/ml) for 1 h at 4 °C with shaking. Blocking of DC-SIGN was done using 20 μg/ml of AZND1 (Beckman Coulter) or a matched isotype, incubating cells for 20 min at room temperature. Cells were then fixed with CellFix (BD Bioscience) for 30 min at 4 °C, and labeled *Candida* conidia or gp120-fluorescein isothiocyanate (Trinity Biotech) were added. Binding was performed in binding buffer (20 mM Tris, pH 7.5, 150 mM NaCl, 1 mM $CaCl_2$, 2 mM $MgCl_2$, and 1% bovine serum albumin), after which cells were washed and analyzed by flow cytometry (FACSAria, BD Biosciences). Data were processed with the program FlowJo.

RT and qPCR Analysis

RNA samples were obtained using the TRIzol isolation (Invitrogen) method. Real time PCR using Applied Biosystems TaqMan® MicroRNA Assays was used to detect both mature miR-155 and the housekeeping RNU6B, which was used as normalizing control. These assays were performed following the manufacturer's instructions. Briefly, a stem loop primer was used for reverse transcription of 2 ng of total RNA in two steps (30 min, 16 °C; 30 min, 37 °C), followed by qPCR employing the FAM-TaqMan probe and primers provided. Perfectprobe, from PrimerDesign (Southampton SO15 0DJ), was employed to detect DC-SIGN (For, TGTAGGAATGGTCTGGACTAGG; Rev, CAAGGGGAGAGAGAGGATGG) and PU.1 (For, TGCCCTATGACACGGATCTATA; Rev, GTAATGGTCGCTATGGCTCTC) mRNA.

Western Blotting

Cells were lysed in Nonidet P-40 (1%), 2 mM Pefablock, and 2 μg/ml aprotinin, leupeptin, and pepstatin, at 4 °C for 10 min. 30 μg of cell lysates were subjected to SDS-PAGE under reducing conditions and transferred onto an Immobilon polyvinylidene difluoride membrane (Millipore Corp., Bedford, MA). Protein detection was performed using the SuperSignal West Pico chemiluminescent system (Pierce). Antibodies employed were from Santa Cruz Biotechnology, Inc.: α-PU.1 (sc-352); α-DC-SIGN (sc-20081), and α-tubulin (sc-58667). Quantity One program was used to quantify PU.1 in Fig. 3.

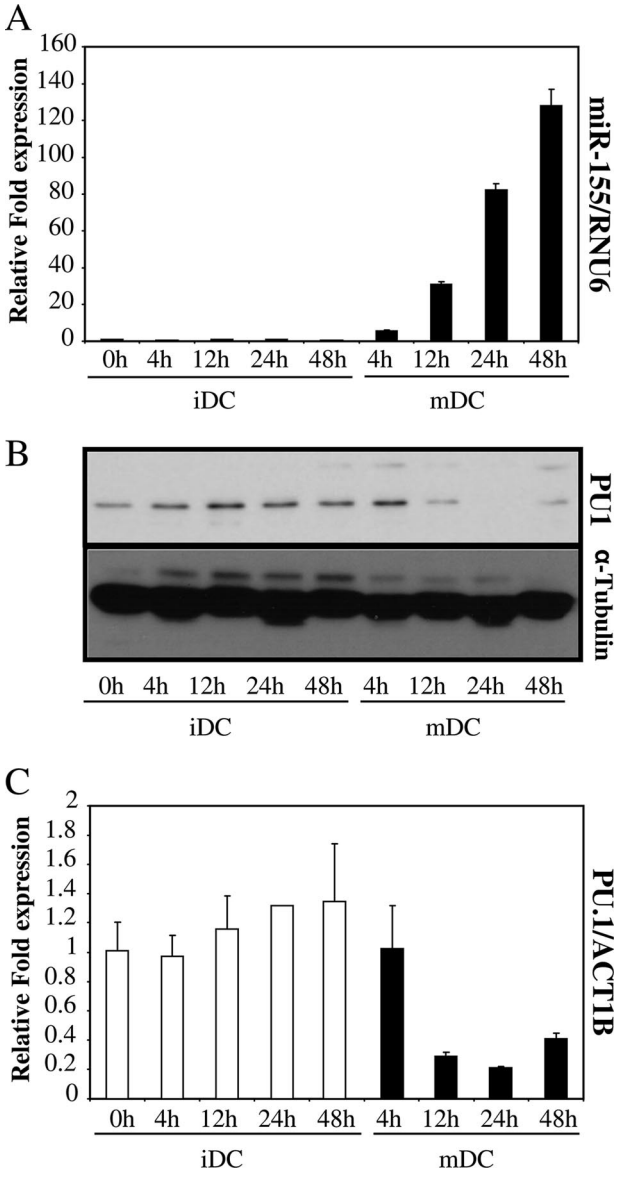

FIGURE 1. **miR-155 increases during maturation of DCs.** *A*, RNA from LPS matured dendritic cells (*mDC*) and untreated DCs (*iDC*) was collected at different time points and mature miR-155 was determined by microRNA-specific RT qPCR. Data were normalized with RNU6B. *B*, protein extracts of the same samples were subjected to Western blot. PU.1 expression was determined and protein concentration controlled with α-tubulin. *C*, RNA extracted for *A* was also subjected to standard RT qPCR and PU.1 mRNA levels were quantified, normalizing with ACT1B. Data in *A* and *C* represent mean ± S.D. (*error bars*). These experiments were done on cells from three different donors, with similar results. A representative one is shown.

RESULTS

MiR-155 Increases during Maturation of DCs—DC maturation can be induced by several stimuli such as components of bacteria, viruses, parasites, and cytokines. Lipopolysaccharides, peptidoglycans, flagellin, CpG motifs, and viral nucleic acids induce Toll-like receptor signaling, which triggers dendritic cell maturation. It has been shown previously that most of these inflammatory stimuli up-regulate miR-155 levels in macrophages by activating the NF-κB signaling pathway (3, 22). To determine whether this up-regulation occurs during dendritic cell maturation, we exposed monocyte-derived DC to LPS, which is widely reported to drive DC maturation (23)

Downloaded from www.jbc.org at University of Southampton Libraries, on December 17, 2010

(supplemental Fig. S1). We then followed the changes in miR-155 levels over time in these cells, by use of reverse transcription followed by stem loop-specific quantitative PCR. During LPS-induced maturation, we could detect increased differential expression of miR-155 by 6 h, whereas a maximum value of 136-fold increase was reached by 48 h; no significant change occurred in the immature DCs over that time (Fig. 1*A*).

It has been described that PU.1 protein levels decrease during DC maturation (10). From computer analyses using different programs that predicted PU.1 as a putative target of miR-155 (24, 25), we wondered whether there was a correlation between the increase in miR-155 levels and the pattern of expression of PU.1 over the maturation process. PU.1 protein expression in maturing DCs was assessed by Western blotting, and we observed that PU.1 levels decreased over time; levels were reduced at 12 h, whereas they remained constant in immature DCs over this time (Fig. 1*B*). Also, the levels of PU.1 mRNA in these cells were determined by qPCR. LPS stimulation also reduced the levels of PU.1 mRNA (Fig. 1*C*). Thus, miR-155 levels increased during DC maturation, whereas PU.1 protein and mRNA levels decreased. These data suggested that miR-155 might play a role during DC maturation, and it raised the possibility that PU.1 might be targeted by miR-155 during this process.

miR-155 Directly Targets Human PU.1—Using bioinformatic databases, miR-155 was predicted to target human PU.1 (24–26). The core binding sequence (seeding region) for this microRNA in the 3′-UTR of PU.1 has a perfect 9-base Watson-Crick match, above the usual target-microRNA matches, and is also widely conserved across several species. To date, there have been several reports unveiling direct targets of miR-155: angiotensin II, several NF-κB pathway gene transcripts (Ripk1, IKKε, and FADD), MAF and, more recently, miR-155 was demonstrated to target the 3′-UTR of murine PU.1 (4, 22, 27, 28).

To prove, for the first time, a direct link between miR-155 and human PU.1, we performed luciferase reporter assays in HeLa cells. For this assay, we generated a reporter construct that expressed a fusion protein between the *Renilla* luciferase mRNA and the 3′-UTR of PU.1 (pRLTK-WT-PU.1). Also, we generated an alternative construct in which the predicted seeding region for miR-155 in the 3′-UTR of PU.1 was mutated (pRLTK-MUT-PU.1) (shown in Fig. 2*B*). This mutation was decided upon by the abrogation of the match between miR-155 and the 3′-UTR of PU.1, as predicted by the RNA-Hybrid program (29). HeLa cells were co-transfected with a plasmid that expressed miR-155 and one of the *Renilla* luciferase fusion plasmids described, or the empty vector. It was found that co-transfection of the plasmid expressing miR-155 reduced the activity of the wild type 3′-UTR of the PU.1 reporter by ~85%. The reporters that did not contain the seeding sequence for miR-155, both control and mutant exhibited no significant reduction in their *Renilla* luciferase activity, when co-transfected with the miR-155 expressing vector (Fig. 2*A*).

As a conclusion, our experimental results confirm the target prediction given by different bioinformatic databases and establish that human PU.1 is indeed a direct functional target of miR-155. We also localized the binding region for miR-155 on

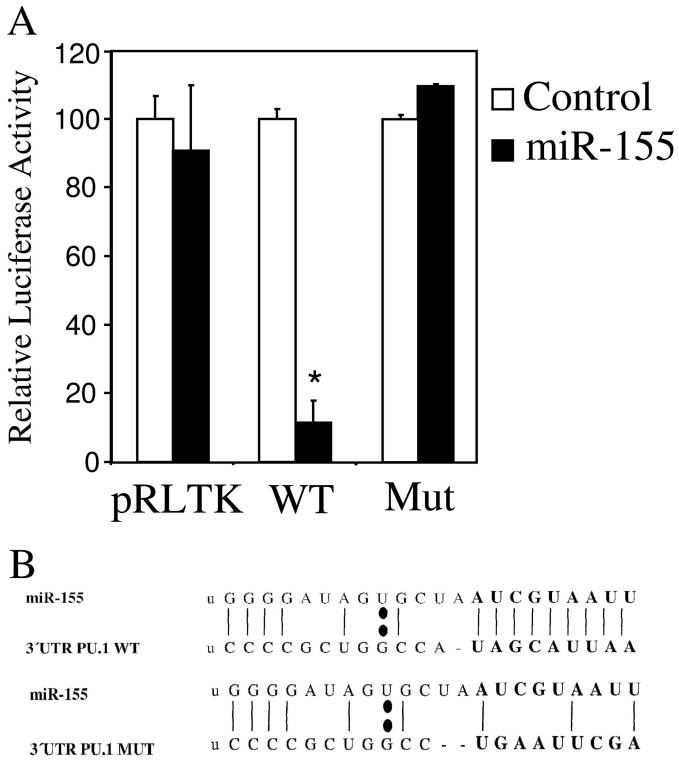

FIGURE 2. **MiR-155 targets PU.1 3′-UTR.** Dual luciferase assay was performed on HeLa cells transfected with pGL3 (normalizing control) and pRLTK (*Control*), pRLTK_WT_3′UTR_PU1 (*WT*), or pRLTK_MUT_3′UTR_PU1 (*Mut*). These plasmids were co-transfected with pCDNA3.1 (Control) or pCDNA3.1-BIC (*miR-155*). Normalized *Renilla* luciferase values were represented relative to the control in each case. Data represent mean ± S.D. (*error bars*). *, statistically significant, ≤0.05.

the 3′-UTR of PU.1, because mutation of the predicted seeding region abrogated the down-regulation exerted by miR-155.

miR-155-induced Overexpression Down-regulates PU.1 Protein Levels—During DC maturation, after LPS stimulation, there is a correlation between the increase in miR-155 levels and the decrease in PU.1 (Fig. 1). Because of the profound influence of pro-inflammatory stimuli on gene expression, LPS may trigger a number of direct or indirect cellular responses that could lead to a decrease of PU.1 during DC maturation. To dissect whether there is a link between the presence of increased levels of miR-155 and the down-regulation of PU.1, we generated a cellular system in which we could rule out an effect due to other signaling pathways activated by LPS. To achieve this, we employed lentiviral vectors containing a sequence that could be processed into mature miR-155, under the transcriptional control of the Tetracycline TeT repressor motif, based on a Tet-on system (30). We stably transduced THP-1 monocytic cells, thus generating a cell line in which the expression of miR-155 is induced after addition of doxycycline, a tetracycline derivative, to the culture medium. Therefore, this cell line, THP1–155, is able to express miR-155 in the absence of LPS or other inflammatory stimuli. This allowed us to elucidate more clearly the effect of miR-155 on the regulation of PU.1 in a myeloid cell line.

We compared THP1–155 cells treated or untreated with doxycycline over the course of 96 h. Then, we determined the levels of miR-155 during this period, using RT qPCR, as

Downloaded from www.jbc.org at University of Southampton Libraries, on December 17, 2010

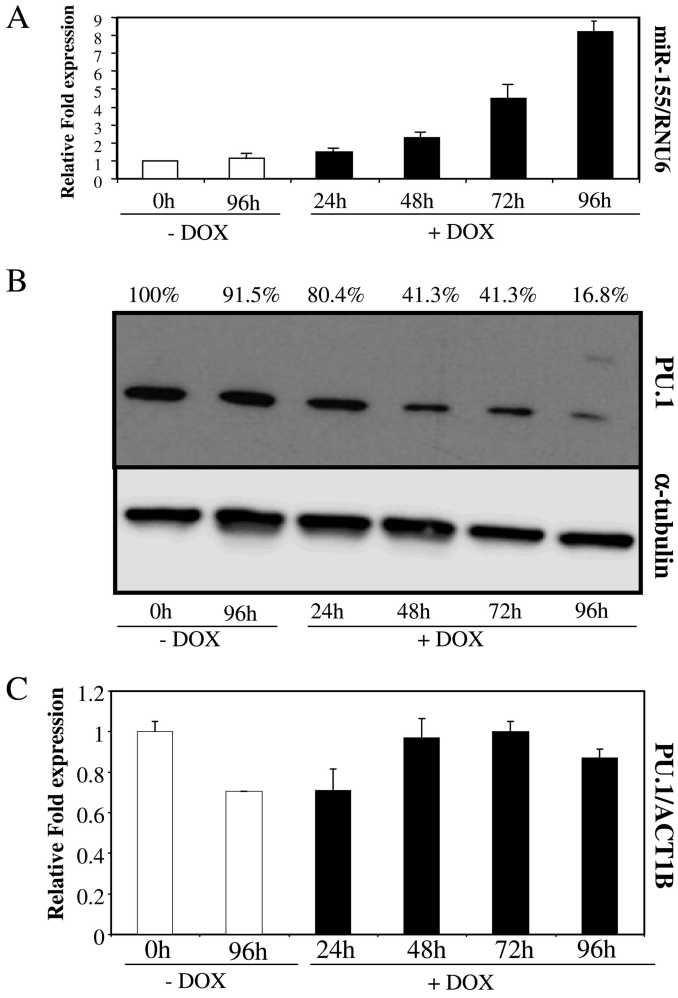

FIGURE 3. **THP1–155 cells overexpressing miR-155 showed down-regulation of PU.1 protein expression.** *A*, THP1–155 cells were treated or not with doxycycline (*DOX*) to de-repress or not the expression of the miR-155 transgene, respectively. Cells were collected at different time points, and subjected to RNA extraction. RNA from these samples was subjected to specific microRNA RT qPCR, and miR-155 levels were quantified. RNU6B was employed for normalization purposes. *B*, protein extracts from the same samples were subjected to Western blotting, and PU.1 levels were determined. As a control, α-tubulin was also detected in the same blot. Values represent percentage of PU.1 normalized against α-tubulin and compared with control. *C*, the same RNA extracts were also used to perform standard RT qPCR, to detect PU.1 mRNA levels. Values were normalized against ACT1B. This figure shows one representative experiment of three. Data in *A* and *C* represent mean ± S.D. (*error bars*). Differences in *B* (+Dox *versus* −Dox), not significant.

described above. The results showed an increase in the levels of miR-155 (Fig. 3*A*) over time, reaching a maximum of 8-fold induction 96 h after transgene induction, when compared with the doxycycline untreated, non-induced control.

We then interrogated the system for the expression of PU.1 to establish a link between the expression of miR-155 and the previously observed reduction in PU.1 protein and mRNA levels in DCs (Fig. 1). We performed PU.1 protein detection by Western blot and, as expected, when miR-155 was overexpressed following doxycycline treatment, the levels of PU.1 were clearly reduced, reaching the minimum expression in the doxycycline-treated THP1–155 after 96 h (Fig. 3*B*). PU.1 protein levels were reduced by approximately 85% at this time point, which correlated with the maximum value of miR-155, an 8-fold induction, both compared with time 0 h. To learn more about the mechanism of action of miR-155 on the regulation of PU.1, we determined the mRNA levels of PU.1 over the same time course. We quantified the expression of PU.1 mRNA by RT qPCR, comparing doxycycline-treated with untreated THP1–155 cells. Fig. 3*C* shows that the increase of miR-155 in THP1–155 cells does not affect the expression levels of PU.1 mRNA. This result suggests that miR-155 might be blocking the translation of PU.1 mRNA, a common mechanism of action of microRNAs.

Thus, aspects of DC maturation that are related to miR-155 are mimicked by THP1–155 cells. In this regard, an increase of miR-155 over time results in a decrease in PU.1 protein levels. These data demonstrate a direct link between the expression of miR-155 and the protein expression levels of the transcription factor PU.1.

miR-155 Expression Down-regulates DC-SIGN Levels in THP1–155 Cells—DC-SIGN is a C-type lectin that mediates binding and internalization of viral, bacterial, and fungal pathogens by myeloid dendritic cells. This is an important role of immature DCs, as they act as immune sentinels sampling their surroundings in search for pathogen antigens. Also, it has been reported that DC-SIGN triggers intracellular signals that modulate dendritic cell maturation (31). DC-SIGN is reported to be down-regulated during the maturation of dendritic cells (10). After phagocytosis and activation, mature dendritic cells show a significantly reduced capacity to detect and ingest antigens, which is reflected by down-regulation of DC-SIGN. The transcriptional down-regulation of DC-SIGN in DC maturation seems to depend on the concurrent decrease of PU.1 (10). Taking these previous studies into consideration, we investigated whether miR-155 could be regulating DC-SIGN levels during the maturation process by targeting PU.1.

We used THP1–155 in which we could control miR-155 expression and down-regulate PU.1. It has already been reported that THP-1 cells could be differentiated into dendritic-like cells, sharing some inherent functions such as pathogen binding, T cell stimulation, and DC-SIGN down-regulation after LPS treatment (32). Also, THP1 cells have been shown to overexpress miR-155 in response to LPS treatment (3). To determine whether the presence of miR-155 and the subsequent down-regulation of PU.1 could affect the expression of DC-SIGN, we cultured THP1–155 cells, in the presence or absence of doxycycline, and determined the levels of DC-SIGN protein by Western blot after 24 and 48 h. In concordance with the expected outcome, the induction of miR-155 by doxycycline reduced the levels of DC-SIGN to ~50% when compared with untreated cells (Fig. 4*A*, *upper panel*). This result was further confirmed by flow cytometry, where the membrane expression of DC-SIGN was similarly reduced when cells overexpressed miR-155 (Fig. 4*B*). DC-SIGN mRNA levels were quantified to elucidate whether the effect of miR-155 was taking place at the mRNA expression level. Cells overexpressing miR-155 expressed lower levels of DC-SIGN mRNA than the untreated control (Fig. 4*C*). A control experiment was performed to show that this effect was indeed due to miR-155. THP1–155 cells were transfected with oligonucleotide anti-miR-155 (or an irrelevant anti-miR control). This was expected to block the effects of miR-155 overexpression, which would

Downloaded from www.jbc.org at University of Southampton Libraries, on December 17, 2010

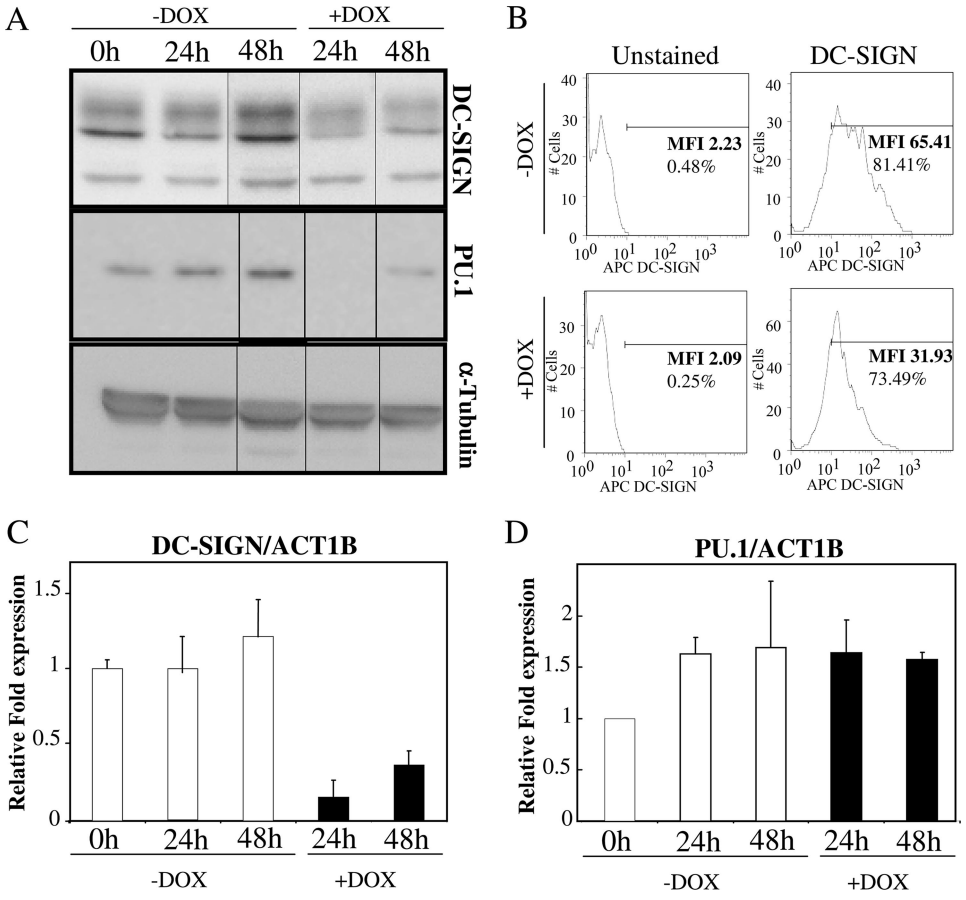

FIGURE 4. **DC-SIGN levels are down-regulated by miR-155 expression in THP1–155 cells.** *A*, THP1–155 cells were treated or not with doxycycline (*DOX*), to de-repress miR-155 inducible expression, respectively. Cells were collected at different time points and protein extracts subjected to Western blot. DC-SIGN and PU.1 protein expression was determined, as well as α-tubulin, as control. *B*, these cells were subjected to flow cytometry and DC-SIGN and graphs show percentage of positive population (%) and mean fluorescence intensity (*MFI*). *C* and *D*, RNA from the same samples was subjected to standard RT qPCR. DC-SIGN (*C*) and PU.1 (*D*) mRNA levels were quantified and normalized against ACT1B. Shown is one representative experiment of three. Data in *C* and *D* represent mean ± S.D. (*error bars*). Differences in *D* (+Dox *versus* −Dox), not significant.

establish that they were due solely to the presence of miR-155. In this experiment (supplemental Fig. S1) we confirmed that we could rescue the expression of DC-SIGN with an antagonist to miR-155. We confirmed in THP-155 cells that when miR-155 was overexpressed PU.1 protein levels were down-regulated, and that PU.1 expression was not affected at the mRNA level (Fig. 4, *A, lower panel*, and *D*).

Overall, we have demonstrated that THP1–155 cells are a good model in which to investigate the effect of miR-155 on DC-SIGN and PU.1 regulation. We have shown that, as in maturation of monocyte-derived DCs (10), so in THP-155 cells, an increase in miR-155 correlates with down-regulation of DC-SIGN, at both the mRNA and protein levels.

The Transcriptional Activation of DC-SIGN Promoter Is Regulated by miR-155 via PU.1—Both PU.1 and DC-SIGN appear to be regulated by miR-155 in THP1–155 cells. However, DC-SIGN mRNA is down-regulated by the presence of miR-155, whereas PU.1 mRNA remains unaltered. These results suggest a different regulatory mechanism for both proteins; whereas DC-SIGN could be affected at the transcriptional level, PU.1 seems to be regulated by miR-155 at the translational level. Interestingly, PU.1 has been shown to regulate DC-SIGN expression through binding of two motifs in its promoter region, both in dendritic cells and THP1 cells (10). Based on this finding, we hypothesized that miR-155 was affecting DC-SIGN levels indirectly through down-regulation of PU.1 and the subsequent decrease in the transcriptional activity of the DC-SIGN promoter. To test this, we employed a luciferase-based reporter construct in which transcriptional activity is controlled by the proximal DC-SIGN promoter (10). We transfected this construct into THP1–155 cells, which overexpressed miR-155 when treated with doxycycline. The results showed that overexpression of miR-155 reduced the activity of the DC-SIGN-luciferase reporter; the decrease was similar to that found in previous assays of DC-SIGN protein and mRNA levels (Fig. 5). To investigate the role of PU.1, we co-transfected the cells with expression vectors coding for PU.1. In both doxycycline-treated and untreated cells, overexpression of PU.1 induced a similar relative luciferase activity in the DC-SIGN reporters, which was clearly independent of the presence of miR-155. Thus, the miR-155-mediated suppression of the DC-SIGN promoter was effectively rescued by the presence of PU.1. Of note, the PU.1 cDNA sequence cloned into the expression vector does not contain the 3′-UTR of PU.1 and therefore does not contain the target seeding region for miR-155 (Fig. 2). This presumably renders the expressed PU.1 mRNA resistant to the blocking activity of miR-155. Interestingly, co-transfection of a PU.1 construct containing the 3′-UTR was not able to efficiently rescue expression of the DC-SIGN promoter. Altogether, these results indicate that miR-155 regulates the expression of DC-SIGN at the transcriptional level, and that this regulation is related to the 3′-UTR-dependent down-regulation of PU.1.

Pathogen Binding Capacity Is Affected by miR-155 Overexpression—Finally, the functional consequences of the expression of miR-155 and subsequent down-regulation of DC-SIGN were investigated. DC-SIGN recognizes pathogens by binding to pathogen-specific carbohydrate residues and is mainly expressed in DCs and alternatively activated macrophages (32). Importantly, the binding activity of DC-SIGN seems to be involved in determining the immune response triggered by the presence of certain pathogens (33, 34). To determine the effect of miR-155 on the expression of DC-SIGN in the membrane of DCs, we transfected mature DCs with anti-miR-155 to inhibit

Downloaded from www.jbc.org at University of Southampton Libraries, on December 17, 2010

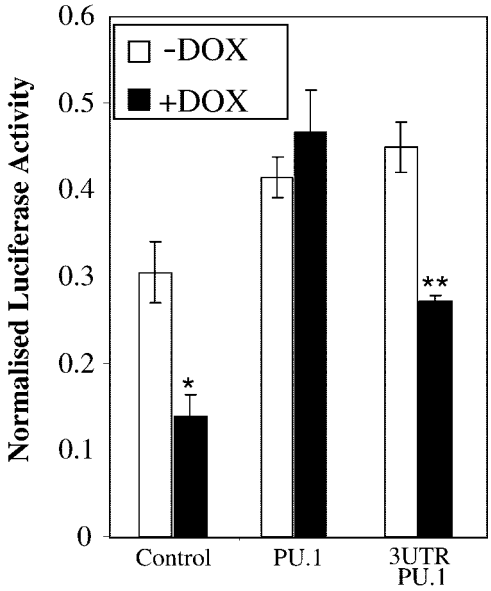

FIGURE 5. **The transcriptional activity of DC-SIGN promoter decreases when miR-155 is overexpressed.** THP1–155 cells were treated or not with doxycycline (*DOX*) for 96 h, to allow for miR-155 to be expressed or to maintain the repression, respectively. Cells were then transfected with pRLTK-*Renilla*, as control for transfection, and a reporter containing the proximal promoter of DC-SIGN (pCD209–468 pXP2). These cells were co-transfected with expression vectors pCDNA3.1 (*Control*), pCDNA3.1_PU.1 (*PU.1*), or pCDNA3.1_PU.1_3UTR. Luciferase values were determined and normalized against *Renilla* luciferase. Data represent mean ± S.D. (*error bars*). *, statistically significant ≤0.05 compared with −Dox control. **, statistically significant (≤0.05) when compared with −Dox/pCDNA3,1_PU.1_3UTR-transfected.

the activity of miR-155. Then, we incubated the DCs transfected with anti-miR-155 or anti-miR-Control with a specific anti-DC-SIGN antibody and analyzed the cells by flow cytometry. Fig. 6*A* shows that the expression of DC-SIGN on DCs increases when miR-155 is inhibited by anti-miR-155. This result is in accordance with the decrease in total and membrane-expressed protein as well as in the mRNA expression observed previously in THP1–155 cells, when miR-155 was overexpressed (Fig. 4). A parallel control experiment revealed that transfection with anti-miR-155 significantly reduced the level of miR-155 in LPS-treated DCs (supplemental Fig. S3).

We then hypothesized that the increase in DC-SIGN observed in the membrane of DCs when miR-155 levels were reduced, could affect their capacity to bind pathogens. To test this hypothesis, we employed *C. albicans* as a model pathogen bound by DC-SIGN (13), and performed a pathogen binding assay. The fungi were heat inactivated, labeled with propidium iodide as described under "Experimental Procedures," and co-incubated with DCs (transfected with anti-miR-155 or anti-miR-Control). After several washes, cells binding labeled *C. albicans* were analyzed using flow cytometry. DCs transfected with anti-miR-155 showed an increased binding capacity for *C. albicans* (Fig. 6*B*) when compared with anti-miR-Control-transfected DCs. Furthermore, blocking DC-SIGN with a specific anti-DC-SIGN antibody reduced binding to *C. albicans*, suggesting the participation of DC-SIGN in this process (supplemental Fig. S4). We then performed binding experiments with labeled HIV-1 protein gp120. gp120 protein has been shown to bind DC-SIGN, which is crucial in the trans-infection of HIV-1 (16). As expected, the anti-miR-155 augmented the binding capacity of mature DCs for gp120 (Fig. 6*C*). Taken together, these data show that the increase of miR-155 during DC maturation reduces the capacity of the cells to bind pathogens by DC-SIGN down-regulation.

DISCUSSION

In their normal peripheral location, the main function of DCs is to sample their surroundings, detecting pathogens and foreign molecules. They express a variety of pathogen binding molecules such as DC-SIGN and are actively endocytic. After activation, the DC migrates to the lymph nodes to present the foreign antigen to T cells. During this migration the DC undergoes maturation, down-regulating endocytic activity and pathogen binding molecules, whereas up-regulating molecules such as major histocompatibility complex class II that will be involved in antigen presentation. In this study we have shown that miR-155 regulates the levels of DC-SIGN at the transcriptional level, indirectly, through direct targeting of transcription factor PU.1.

The reciprocal relationship between increased miR-155 levels and reduced PU.1 expression during LPS induced DC maturation (Fig. 1) suggested a link or interaction between miR-155 and PU.1. Searches of computer databases predicted that the recognition sequence for miR-155 was present in the 3′-UTR of PU.1. By use of a reporter assay in which expression of *Renilla* luciferase was driven by the 3′-UTR of PU.1 (Fig. 2) we have shown that human PU.1 is indeed a direct target for miR-155. A similar observation has been made in murine systems although the sequences differ between the species. Moreover, employing the program RNA Hybrid (29), we show a difference in the predicted secondary structure of the complex of miR-155:PU.1 (supplemental Fig. S5), which is known to be key in microRNA targeting. We also mapped the binding region for miR-155, which coincides with the one predicted using several bioinformatic tools. It consists of a seeding region of 9 bases, which is stronger than those of other targets studied so far, which are in the range of 6–8 bases (4, 27). This region is likely to play an important role in PU.1 regulation in different contexts such as hematopoietic development and myeloid disorders (9, 35–37). Intriguingly, it has recently been demonstrated that miR-155 overexpression is linked to a myeloid disorder (38), which could be related to the ability of miR-155 to target PU.1.

Apart from its role in hematopoietic development, PU.1 plays an important role in dendritic cells, as described in several reports (9, 10, 39). Furthermore, it is well established that PU.1 is able to regulate the levels of DC-SIGN (10). PU.1 is down-regulated during maturation of DCs, and this is associated with reduced levels of DC-SIGN. To investigate a possible link between miR-155 and the maturation-related decrease in DC-SIGN expression, we generated a system in which THP1 cells were able to express miR-155 in an inducible way, isolating its effect from other pathways activated during DC maturation. We chose THP1 cells as they can regulate DC-SIGN and miR-155 in a similar way to DCs (3, 32), and it has been described as a cellular model that shares characteristics with DCs (32). In the newly established cell line, THP1–155, increased levels of miR-155 lead to reduced expression of the PU.1 protein (Fig. 3). This result mimics that in DCs, where PU.1 decreased during matu-

Downloaded from www.jbc.org at University of Southampton Libraries, on December 17, 2010

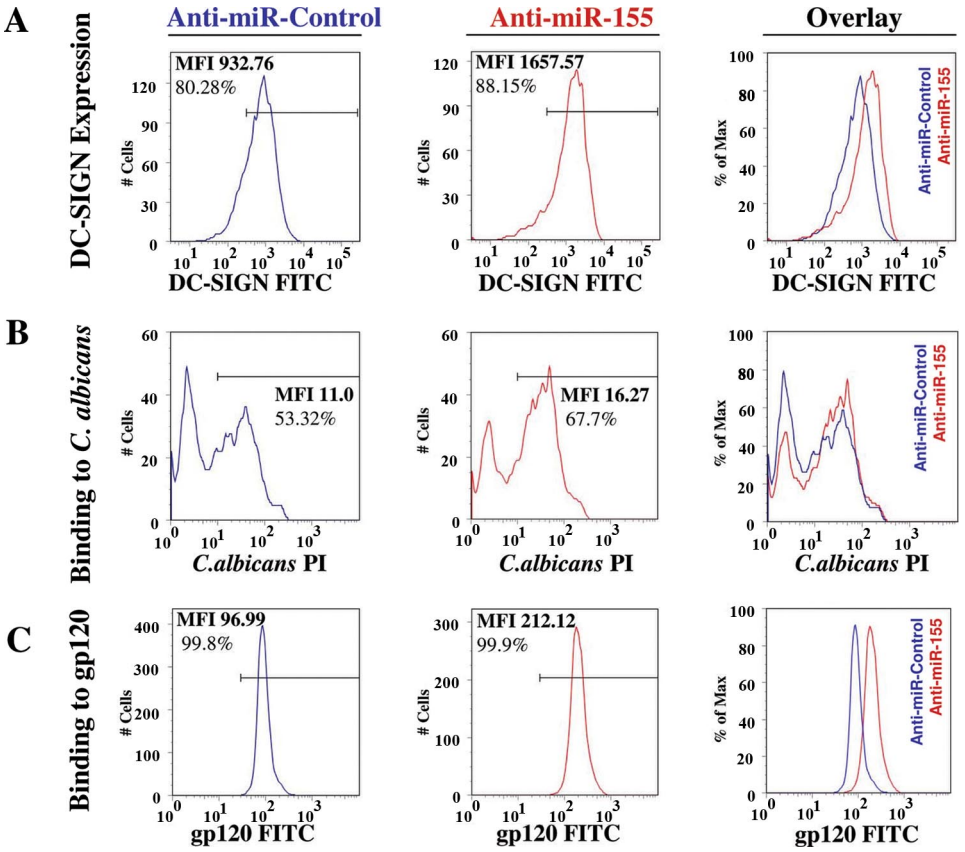

FIGURE 6. **Pathogen binding capacity of DCs is affected by miR-155.** DCs were transfected with either oligonucleotide anti-miR-155 or anti-miR-Control, and Cy3 labeled pre-miR-Control. *A,* DC-SIGN membrane expression in transfected cells was assessed by flow cytometry and presented as graphs showing percentage of positive population (%) and mean fluorescence intensity (*MFI*). Overlay of both graphs is also shown. Cell number is normalized as percentage of maximum (FlowJo). *B,* these cells were assayed for their binding capacity to labeled *C. albicans* conidia. The binding ability of the cells was determined by flow cytometry and presented as in *A*. *C,* DCs transfected as previously described were subjected to binding assays employing HIV-1 recombinant gp120-fluorescein isothiocyanate (*FITC*). Binding capacity was determined through flow cytometry and expressed as in *A*. The flow cytometry data in this figure correspond to a representative experiment out of three independent repeats. *PI*, propidium iodide.

ration, whereas miR-155 increased (Fig. 1). However, there appears to be a difference in the regulation of PU.1 mRNA in maturing DCs and induced THP1–155 cells. In THP1–155, PU.1 mRNA levels are stable (Fig. 3), which suggests that miR-155 is blocking PU.1 mRNA translation, rather than promoting its cleavage. During DC maturation, however, PU.1 mRNA is down-regulated (Fig. 1). A possible explanation could lie in the different levels of miR-155 expression attained by the two cell types (with a similar basal expression of miR-155); the expression of miR-155 in THP1–155 reaches a maximum of 8-fold over the basal levels, whereas mature DCs have ~130 times more miR-155 than the immature ones. Thus, it is conceivable that when miR-155 reaches certain levels of overexpression, it could promote cleavage of PU.1 mRNA as well as blocking its translation. Other explanations, not exclusive of the previous one, could involve either other microRNAs, or possibly, yet to be described pathways triggered by LPS, which might affect PU.1 mRNA expression at the transcriptional level.

We found that the levels of DC-SIGN mRNA and protein were down-regulated in THP1–155 cells that overexpressed miR-155 (Fig. 4). These results were consistent with our initial hypothesis that DC-SIGN is regulated at the transcriptional level by PU.1, and that down-regulation of PU.1 by miR-155 would lead to a decrease in the transcriptional expression of DC-SIGN. By using a reporter containing the DC-SIGN promoter fused to the luciferase gene, we showed that the promoter activity of DC-SIGN is down-regulated when miR-155 is overexpressed. Furthermore, this down-regulation is rescued when a vector encoding for PU.1 but lacking the 3′-UTR, is co-transfected into the cells (Fig. 5). The experiments shown in Figs. 4 and 5 demonstrate the indirect effect of miR-155 on the transcriptional regulation of DC-SIGN, through targeting PU.1.

Having shown how, as DCs mature, miR-155 down-regulates expression of PU.1, which in turn results in reduced expression of DC-SIGN, we then predicted that this should result in impaired recognition and binding of pathogens by DCs. Our data (Fig. 6) show that miR-155 levels are correlated with the ability of the cell to bind pathogens (*C. albicans* and HIV-1 gp120 protein). To test this hypothesis we employed mature DCs and showed that blocking the activity of miR-155 by transfecting an anti-miR-155 oligonucleotide, levels of DC-SIGN were increased and there was augmented binding of pathogens by DCs. Thus, the increase in miR-155 levels has a functional consequence, with an important physiological role in DCs.

The link between miR-155 and the pathogen binding ability of DC-SIGN could have a role in determining the immune response against certain pathogens or in the ability of certain pathogens to infect the humans. It has been reported that SIGNR1 (human DC-SIGN orthologue in mouse) knock-out mice have a more Th1-dominated immune response against *Mycobacterium tuberculosis* when compared with WT mice, suggesting a role for SIGNR1 in the Th1/Th2 balance of the immune response. In agreement with this, there is also reported evidence for an important role of DC-SIGN during tuberculosis in humans (40). Thus, DC-SIGN-mediated pathogen binding may have important consequences on the immune responses against the tubercle bacilli in the infected host.

The dramatic increase of the levels of miR-155 (up to 130-fold, Fig. 1) during DC maturation, not previously described, adds this process to others regulated by miR-155 (4, 5). Importantly, DCs are implicated in the delicate balance of T cell polarization and the maturing DC in response to different microbial products could have a decisive influence (41). It is tantalizing to

Downloaded from www.jbc.org at University of Southampton Libraries, on December 17, 2010

hypothesize that the effect of miR-155 on DC-SIGN and the PU.1 expression described here could affect the balance of the immune response against pathogens. Thus, miR-155 in DCs could contribute to driving Th1 polarization, hence playing an important role in the initial steps of infection. In addition to effects on the immune response, miR-155 could have a more obvious impact on the infection process of certain pathogens. Our results could have important consequences in infection by HIV-1, and might suggest a role for miR-155 in making subjects more or less susceptible to infection. Interestingly, there are several studies reporting the possible use of DC-SIGN blocking agents that aim to stop HIV-1 infection (42–45). Thus, miR-155 could be a new therapeutic target that could help prevent entrance of HIV-1 through binding of DC-SIGN.

In conclusion, our study reveals that miR-155 has an important role during DC maturation, inhibiting the expression of the transcription factor PU.1 and thus decreasing the levels of DC-SIGN and the pathogen binding ability of the cells. miR-155 could be of importance in several infectious diseases, and may contribute to susceptibility to infection and invasion by a range of pathogens. Furthermore, our findings suggest an additional explanation for how miR-155 is involved in modulating the Th1/Th2 balance, namely through controlling the maturation of DCs.

Acknowledgments—We thank Prof. Angel L. Corbi for being the most helpful critic and Dr. Chris Pickard for reviewing the manuscript.

REFERENCES

1. Bartel, D. P. (2004) *Cell* **116,** 281–297
2. Stefani, G., and Slack, F. J. (2008) *Nat. Rev. Mol. Cell Biol.* **9,** 219–230
3. O'Connell, R. M., Taganov, K. D., Boldin, M. P., Cheng, G., and Baltimore, D. (2007) *Proc. Natl. Acad. Sci. U. S. A.* **104,** 1604–1609
4. Rodriguez, A., Vigorito, E., Clare, S., Warren, M. V., Couttet, P., Soond, D. R., van Dongen, S., Grocock, R. J., Das, P. P., Miska, E. A., Vetrie, D., Okkenhaug, K., Enright, A. J., Dougan, G., Turner, M., and Bradley, A. (2007) *Science* **316,** 608–611
5. Thai, T. H., Calado, D. P., Casola, S., Ansel, K. M., Xiao, C., Xue, Y., Murphy, A., Frendewey, D., Valenzuela, D., Kutok, J. L., Schmidt-Supprian, M., Rajewsky, N., Yancopoulos, G., Rao, A., and Rajewsky, K. (2007) *Science* **316,** 604–608
6. Fisher, R. C., and Scott, E. W. (1998) *Stem Cells* **16,** 25–37
7. Banchereau, J., and Steinman, R. M. (1998) *Nature* **392,** 245–252
8. Wallet, M. A., Sen, P., and Tisch, R. (2005) *Clin. Med. Res.* **3,** 166–175
9. Bakri, Y., Sarrazin, S., Mayer, U. P., Tillmanns, S., Nerlov, C., Boned, A., and Sieweke, M. H. (2005) *Blood* **105,** 2707–2716
10. Domínguez-Soto, A., Puig-Kröger, A., Vega, M. A., and Corbí, A. L. (2005) *J. Biol. Chem.* **280,** 33123–33131
11. Serrano-Gómez, D., Sierra-Filardi, E., Martínez-Nuñez, R. T., Caparrós, E., Delgado, R., Muñoz-Fernández, M. A., Abad, M. A., Jimenez-Barbero, J., Leal, M., and Corbí, A. L. (2008) *J. Biol. Chem.* **283,** 3889–3903
12. Arrighi, J. F., Pion, M., Garcia, E., Escola, J. M., van Kooyk, Y., Geijtenbeek, T. B., and Piguet, V. (2004) *J. Exp. Med.* **200,** 1279–1288
13. Cambi, A., Gijzen, K., de Vries, J. M., Torensma, R., Joosten, B., Adema, G. J., Netea, M. G., Kullberg, B. J., Romani, L., and Figdor, C. G. (2003) *Eur. J. Immunol.* **33,** 532–538
14. Alvarez, C. P., Lasala, F., Carrillo, J., Muñiz, O., Corbí, A. L., and Delgado, R. (2002) *J. Virol.* **76,** 6841–6844
15. Colmenares, M., Puig-Kröger, A., Pello, O. M., Corbí, A. L., and Rivas, L. (2002) *J. Biol. Chem.* **277,** 36766–36769
16. Geijtenbeek, T. B., Kwon, D. S., Torensma, R., van Vliet, S. J., van Duijnhoven, G. C., Middel, J., Cornelissen, I. L., Nottet, H. S., KewalRamani, V. N., Littman, D. R., Figdor, C. G., and van Kooyk, Y. (2000) *Cell* **100,** 587–597
17. Geijtenbeek, T. B., Torensma, R., van Vliet, S. J., van Duijnhoven, G. C., Adema, G. J., van Kooyk, Y., and Figdor, C. G. (2000) *Cell* **100,** 575–585
18. Geijtenbeek, T. B., Krooshoop, D. J., Bleijs, D. A., van Vliet, S. J., van Duijnhoven, G. C., Grabovsky, V., Alon, R., Figdor, C. G., and van Kooyk, Y. (2000) *Nat. Immunol.* **1,** 353–357
19. van Gisbergen, K. P., Sanchez-Hernandez, M., Geijtenbeek, T. B., and van Kooyk, Y. (2005) *J. Exp. Med.* **201,** 1281–1292
20. Sallusto, F., and Lanzavecchia, A. (1994) *J. Exp. Med.* **179,** 1109–1118
21. Ralser, M., Querfurth, R., Warnatz, H. J., Lehrach, H., Yaspo, M. L., and Krobitsch, S. (2006) *Biochem. Biophys. Res. Commun.* **347,** 747–751
22. Tili, E., Michaille, J. J., Cimino, A., Costinean, S., Dumitru, C. D., Adair, B., Fabbri, M., Alder, H., Liu, C. G., Calin, G. A., and Croce, C. M. (2007) *J. Immunol.* **179,** 5082–5089
23. Cella, M., Sallusto, F., and Lanzavecchia, A. (1997) *Curr. Opin. Immunol.* **9,** 10–16
24. Griffiths-Jones, S., Saini, H. K., van Dongen S., and Enright, A. J. (2008) *Nucleic Acids Res.* **36,** D154–D158
25. Lewis, B. P., Shih, I. H., Jones-Rhoades, M. W., Bartel, D. P., and Burge, C. B. (2003) *Cell* **115,** 787–798
26. Kertesz, M., Iovino, N., Unnerstall, U., Gaul, U., and Segal, E. (2007) *Nat. Genet.* **39,** 1278–1284
27. Martin, M. M., Lee, E. J., Buckenberger, J. A., Schmittgen, T. D., and Elton, T. S. (2006) *J. Biol. Chem.* **281,** 18277–18284
28. Vigorito, E., Perks, K. L., Abreu-Goodger, C., Bunting, S., Xiang, Z., Kohlhaas, S., Das, P. P., Miska, E. A., Rodriguez, A., Bradley, A., Smith, K. G., Rada, C., Enright, A. J., Toellner, K. M., Maclennan, I. C., and Turner, M. (2007) *Immunity* **27,** 847–859
29. Krüger, J., and Rehmsmeier, M. (2006) *Nucleic Acids Res.* **34,** W451–454
30. Bulliard, Y., Wiznerowicz, M., Barde, I., and Trono, D. (2006) *J. Biol. Chem.* **281,** 35742–35746
31. Caparrós, E., Munoz, P., Sierra-Filardi, E., Serrano-Gómez, D., Puig-Kröger, A., Rodríguez-Fernández, J. L., Mellado, M., Sancho, J., Zubiaur, M., and Corbí, A. L. (2006) *Blood* **107,** 3950–3958
32. Puig-Kröger, A., Serrano-Gómez, D., Caparrós, E., Domínguez-Soto, A., Relloso, M., Colmenares, M., Martínez-Muñoz, L., Longo, N., Sánchez-Sánchez, N., Rincon, M., Rivas, L., Sánchez-Mateos, P., Fernández-Ruiz, E., and Corbí, A. L. (2004) *J. Biol. Chem.* **279,** 25680–25688
33. Lanoue, A., Clatworthy, M. R., Smith, P., Green, S., Townsend, M. J., Jolin, H. E., Smith, K. G., Fallon, P. G., and McKenzie, A. N. (2004) *J. Exp. Med.* **200,** 1383–1393
34. Wieland, C. W., Koppel, E. A., den Dunnen, J., Florquin, S., McKenzie, A. N., van Kooyk, Y., van der Poll, T., and Geijtenbeek, T. B. (2007) *Microbes Infect.* **9,** 134–141
35. Dahl, R., Walsh, J. C., Lancki, D., Laslo, P., Iyer, S. R., Singh, H., and Simon, M. C. (2003) *Nat. Immunol.* **4,** 1029–1036
36. Anderson, K. L., Smith, K. A., Conners, K., McKercher, S. R., Maki, R. A., and Torbett, B. E. (1998) *Blood* **91,** 3702–3710
37. Rosenbauer, F., Wagner, K., Kutok, J. L., Iwasaki, H., Le Beau, M. M., Okuno, Y., Akashi, K., Fiering, S., and Tenen, D. G. (2004) *Nat. Genet.* **36,** 624–630
38. O'Connell, R. M., Rao, D. S., Chaudhuri, A. A., Boldin, M. P., Taganov, K. D., Nicoll, J., Paquette, R. L., and Baltimore, D. (2008) *J. Exp. Med.* **205,** 585–594
39. Laiosa, C. V., Stadtfeld, M., Xie, H., de Andres-Aguayo, L., and Graf, T. (2006) *Immunity.* **25,** 731–744
40. Tailleux, L., Pham-Thi, N., Bergeron-Lafaurie, A., Herrmann, J. L., Charles, P., Schwartz, O., Scheinmann, P., Lagrange, P. H., de Blic, J., Tazi, A., Gicquel, B., and Neyrolles, O. (2005) *PLoS Med.* **2,** e381
41. Kapsenberg, M. L. (2003) *Nat. Rev. Immunol.* **3,** 984–993
42. Spear, G. T., Zariffard, M. R., Xin, J., and Saifuddin, M. (2003) *Immunology* **110,** 80–85
43. Deiva, K., Khiati, A., Hery, C., Salim, H., Leclerc, P., Horellou, P., and Tardieu, M. (2006) *AIDS Res. Hum. Retroviruses* **22,** 1152–1161
44. Rappocciolo, G., Piazza, P., Fuller, C. L., Reinhart, T. A., Watkins, S. C., Rowe, D. T., Jais, M., Gupta, P., and Rinaldo, C. R. (2006) *PLoS Pathog.* **2,** e70
45. Wang, S. K., Liang, P. H., Astronomo, R. D., Hsu, T. L., Hsieh, S. L., Burton, D. R., and Wong, C. H. (2008) *Proc. Natl. Acad. Sci. U. S. A.* **105,** 3690–3695

Downloaded from www.jbc.org at University of Southampton Libraries, on December 17, 2010

JBC Papers in Press. Published on November 19, 2010 as Manuscript M110.169367
The latest version is at http://www.jbc.org/cgi/doi/10.1074/jbc.M110.169367

THE INTERLEUKIN 13 (IL-13) PATHWAY IN HUMAN MACROPHAGES IS MODULATED BY MICRORNA-155 VIA DIRECT TARGETING OF INTERLEUKIN 13 RECEPTOR ALPHA 1 (IL13Rα1)

Rocio T. Martinez-Nunez[1], Fethi Louafi[1], Tilman Sanchez-Elsner[1]

[1] JunkRNA Lab, Division of Infection, Inflammation and Immunity, University of Southampton School of Medicine, Southampton General Hospital, SO16 6YD UK

Running Title: microRNA-155 targets IL13Rα1

Address correspondence to: Sanchez-Elsner, T, General Hospital MP 813, Tremona Road Southampton SO16 6YD, UK; e-mail: T.Sanchez-Elsner@soton.ac.uk

Macrophages play a central role in the balance and efficiency of the immune response and are at the interface between innate and adaptive immunity. Their phenotype is a delicate equilibrium between the M1 (classical, pro-Th_1) and M2 (alternative, pro-Th_2) profiles. This balance is regulated by cytokines such as interleukin 13 (IL-13), a typical pro-M2-Th_2 cytokine that has been related to allergic disease and asthma. IL-13 binds to IL-13 Receptor α1 (IL13Rα1), a component of the Type II IL- 4Receptor, and exerts its effects by activating the transcription factor Signal Transducer and Activator of Transcription 6 (STAT6) through phosphorylation. MicroRNAs are short (~22nt) inhibitory non-coding RNAs that block the translation or promote the degradation of their specific mRNA targets. By bioinformatics' analysis we found that microRNA 155 (miR-155) is predicted to target IL13Rα1. This suggested that miR-155 might be involved in the regulation of the M1/M2 balance in macrophages by modulating IL-13 effects. Mir-155 has been implicated in the development of a healthy immune system and function as well as in the inflammatory pro-Th_1/M1 immune profile. Here we have shown that in human macrophages miR-155 directly targets IL13Rα1 and reduces the levels of IL13Rα1 protein leading to diminished activation of STAT6. Finally we also demonstrate that miR-155 affects the IL13-dependent regulation of several genes (SOCS1, DC-SIGN, CCL18, CD23 and SERPINE) involved in the establishment of a M2/pro-Th_2 phenotype in macrophages. Our work shows a central role for miR-155 in determining the M2 phenotype in human macrophages.

Macrophages are key players at the interface between innate and adaptive immunity. They arise from circulating monocytes that are recruited to tissues by different stimuli. They work as phagocytes and antigen presenting cells, promoting inflammation and its resolution. Macrophages present a wide range of phenotypic profiles and defence mechanisms depending on the tissue context and the stimuli present (pathogens, cytokines, apoptotic cells…). They are generally classified into two main types: M1 (classically activated) and M2 (alternatively activated) macrophages. Classically activated (M1) macrophages are a result of an exposure to pro-Th_1 cytokines, while alternatively activated (M2) macrophages are generated in a pro-Th_2 environment (1). Classically activated macrophages are specialised in defence against intracellular pathogens and upon stimulation with pro-inflammatory stimuli (interferon-γ or LPS), they promote inflammation, causing tissue damage. By contrast, alternative activation of macrophages is induced by a broader range of stimuli including interleukin 4 (IL-4), interleukin 13 (IL-13), interleukin 10 (IL-10) or glucocorticoids and are specialised in defence against extracellular pathogens, promoting tissue repair and the resolution of the inflammatory process (2). Regardless of this classification, one of the most remarkable characteristics of macrophages is their plasticity and heterogeneity, depending on the specific task carried out. This is reflected by their ability to reverse their phenotype and reprogram their M1/pro-Th_1 and M2/pro-Th_2 gene expression profiles, presenting in-between phenotypic profiles and a constituting a heterogeneous population (1). The present study has focused on alternatively activated macrophages generated by IL-4 and IL-13 (2).

Interleukin 13 (IL-13) is a typical Th_2 type cytokine which, together with IL-4, drives and

Copyright 2010 by The American Society for Biochemistry and Molecular Biology, Inc.

Downloaded from www.jbc.org at University of Southampton Libraries, on December 17, 2010

modulates the immune response. First described as a Th_1 down-regulator (3), its role as an active immune mediator has been described and distinguished from those of IL-4 by several studies (4-7). Interleukin 13 is a key cytokine in the defence against gastrointestinal nematodes (8) and plays a central role in some chronic inflammatory diseases such as asthma and ulcerative colitis (9,10). Interestingly, and underscoring the role of IL-13 in asthma, mice lacking the IL-13 receptor alpha 1 chain (IL13Rα1), showed a complete absence of allergen-induced airway hyper-reactivity and mucus hypersecretion (6). IL13Rα1 is an essential component of the Type II IL-4 receptor, which consists of heterodimers of IL4Rα and IL13Rα1 chains. Both IL-4 and IL-13 bind to the Type II receptor, but only IL-4 can bind to the Type I receptor. Therefore, the binding of IL-13 depends solely on the presence of IL13Rα1 (11,12). Engagement of these receptors leads to phosphorylation and activation of Janus Tyrosine Kinases (JAK) proteins, believed to be bound to these cytokines receptors in unstimulated cells. The active phospho-JAK proteins phosphorylate the IL4Rα chain, providing docking sites for STAT6. Once bound to the receptor, STAT6 is also phosphorylated by JAKs, which causes its activation, dimerization and translocation to the nucleus, where it exerts its transcriptional roles (13).

Since their relatively recent discovery (14), miRNAs have been shown to play important biological roles in different contexts: during development, cell differentiation and immune regulation, and also in pathologies such as cancer (15-17). They are small non-coding RNAs of ~22 nt (nucleotides) that regulate gene expression upon binding to the 3'UTRs (UnTranslated Regions) of their target mRNAs (18). MicroRNAs are firstly transcribed as immature pri-miRNAs which are processed in the nucleus into ~70nt hairpin pre-miRNAs by Drosha proteins. Pre-miRNAs are then exported to the cytoplasm where Dicer proteins process them into mature miRNA*::miRNA complexes. The leading strand ,miRNA, is loaded into the RISC complex where it guides Argonaute proteins towards their target mRNAs (19). The selectivity of miRNA action is given by the nucleotides 2 to 7 at their 5' end (the "seed region") that pairs to its complementary site in the targeted 3'UTR by Watson-Crick interactions directing the RISC action (18). The inhibitory activity of microRNAs ensues by blocking the target mRNA translation into protein and/or the degradation of the mRNA (20).

MicroRNAs have proven to be key in modulating the immune system (21).The microRNA focus of this study, microRNA-155 (miR-155), has been extensively studied in immunology and inflammation (21-23). Two different knock out models have been generated showing that mice lacking miR-155 present an abnormal immune function with aberrant B and T cell repertoires and defective antigen presenting cells (16,24). Several reports present miR-155 as a key player in B cell responses (17) and in dendritic cell function (25,26). Moreover, miR-155 expression levels increase during inflammation in classically (pro-Th_1) activated macrophages (21,27) and has been clearly linked to a pro-Th_1 bias, since knockout mice for miR-155 have a pro-Th_2 unbalanced T cell repertoire (16). Therefore, it is well established that miR-155 plays a central role not only in the development of a healthy immune system but also as a pro-Th_1 microRNA.

Using *in silico* analysis (miRanda (28), RNAHybrid (29), PITA algorithm (30)) we identified IL13Rα1 as a putative target of miR-155. We have shown for the first time that indeed, miR-155 down regulates the effects of the Th_2 cytokines IL4 and IL13, providing a straightforward link between miR-155 and the Th_1/Th_2 balance. Our work shows that miR-155 directly targets IL13Rα1 3'UTR reducing the levels of IL13Rα1 protein. By doing so, miR-155 affects the IL-4 and IL-13 dependent phosphorylation of STAT6. We finally show that miR-155 levels modulate the response of human macrophages to IL-13 leading to a change in their genetic profile. Therefore, miR-155 contributes to the Th_1/Th_2 equilibrium, favouring a pro-Th_1/classical activation of macrophages by reducing the expression of several pro-Th_2/IL-13-dependent genes.

Experimental Procedures

Cell culture. THP1-155 cells. This cell line was generated as described before (26). Briefly, THP-1 cells were doubly transduced with a doxycycline-inducible (Tet-on) lentiviral system described

Downloaded from www.jbc.org at University of Southampton Libraries, on December 17, 2010

elsewhere (31), in which miR-155 transgene is under the control of a tetracycline response element. Lentiviral vectors were kindly provided by Prof. Didier Trono and cells were maintained in RPMI 10%FBS (GIBCO). To induce miR-155 expression 2.5 μg/ml doxycycline (SIGMA) was added or not to the medium and renewed daily over 96h of culture. Cytokine treatments were performed as following: firstly, cells were incubated or not with doxycycline for 96h and then they were starved for an extra 12h period and then stimulated or not with IL-4 (Immunotools) or IL-13 (R&D). Cell extracts were collected when indicated, after the treatment.

HeLa. Cells were maintained in DMEM 10% FBS.

Macrophages: Monocytes were obtained from buffy coats from healthy donors over a density gradient (Ficoll-Paque™ PLUS, GE Healthcare) following manufacturer's instructions. Briefly, PBMCs (Peripheral Blood Mononuclear Cells) were isolated by centrifugation over Ficoll-Paque and monocytes were isolated from the PBMC fraction using CD14 magnetic microbeads (Miltenyi). Cells were maintained in RPMI 10% FBS supplemented with 500U/ml GM-CSF (Immunotools) to allow differentiation.

Vector constructs. pCDNA BIC: the genomic region encompassing miR-155 was cloned into pCDNA 3.1 expression vector as previously described (26).

IL13Rα1 3'UTR was amplified using plasmid DNA (HmiT009700-MT01, gene Copoeia) as template and the following primers: IL13RA1_3'UTR_FOR GGC TGT TAG GGG CAG TGG AG and IL13RA1_3'UTR_REV CAG AGC CTT GGC TGG CTG G. The product was cloned in pCR2.1 TOPO TA (Invitrogen), from where it was removed using BamHI/NotI. After blunt ending with Klenow DNA polymerase, the product was cloned into NotI site in pRLTK (Promega), this construct named hence forth pRLTK__WT_3´UTR_IL13RA1.

Mutagenesis was performed on pRLTK__WT_3´UTR_IL13RA1 using QuickChange Site Directed Mutagenesis (Stratagene) following manufacturer's instructions. For pRLTK_MUT1_3´UTR_IL13RA1 we used the primers IL13RA1 3'UTR MUT1FOR: CTG CTA CTC AAG TCG GTA CCA CTG TGT CTT TGG TTT GTG CTA GGC CCC and IL13RA1 3'UTR MUT1REV: GGG GCC TAG CAC AAA CCA AAG ACA CAG TGG TAC CGA CTT GAG TAG CAG. In the case of pRLTK__MUT2_3´UTR_IL13RA1 the primers used were IL13RA1 3'UTR MUT2FOR CCA TGT GAG GGT TTT CAG GGC CGA TAT TTG TGC ATT TTC TAA ACA G and IL13RA1 3'UTR MUT2 REV CTG TTT AGA AAA TGC ACA AAT ATC GGC CCT GAA AAC CCT CAC ATG G. Normalization was performed using pGL3 (Promega).

RT-qPCR. Total RNA was extracted using TRI Reagent (Ambion). Reverse transcription was performed using High Capacity cDNA Reverse Transcription Kit (Applied Biosystems). MicroRNA detection was performed using TaqMan MicroRNA Assays (Applied Biosystems). For Real Time PCR (qPCR) we employed TaqMan® Universal PCR Master Mix, No AmpErase® UNG in a 7900HT Fast Real-Time PCR System machine (both from Applied Biosystems). IL13RA1 qPCR detection was performed using Perfect Probe from PrimerDesign (Southampton SO15 0DJ) and normalized against GAPDH from the same manufacturer. Genes assayed in the IL-13/STAT6 pathway were TaqMan® Gene Expression Assays (Applied Biosystems).

Western Blotting. Total protein lysates were subjected to SDS-PAGE under reducing conditions and transferred onto an Immobilon polyvinylidene difluoride membrane (Millipore Corp., Bedford, MA). Antibodies used were: anti IL13Rα1 (sc-27861, Santa Cruz Biotechnology); anti STAT6 (#9362, Cell Signalling Technology); anti Phospho-STAT6 (#9361, Cell Signalling Technology) and anti beta Actin antibody - Loading Control (ab8227, abcam).

Transfections. To determine direct targeting of IL13Rα1 by miR-155, constructs pRLTK_WT_3´UTR_IL13RA1, pRLTK_MUT1_3´UTR_IL13RA1 or pRLTK_MUT2_3´UTR_IL13RA1 were transfected into HeLa cells employing LT1 Reagent (Mirus) following manufacturer's instructions. pCDNA BIC or control pCDNA 3.1 empty vector were co-transfected to check miR-155 activity on the 3'UTR of IL13Rα1. pGL3

Downloaded from www.jbc.org at University of Southampton Libraries, on December 17, 2010

(Promega) was used as normalizing vector. Luminometry was performed using Dual-Glo kit (Promega). Experiments were performed three times in triplicates. Statistical differences were determined using Student's t test and GraphPad Prism software.

In order to reduce the levels of miR-155 in primary macrophages, 100nM Anti-miR-155 Inhibitor or Anti-miR Inhibitors—Negative Control # (Applied Biosystems) were transfected in human monocytes at day 0 as described previously (26). Briefly, cells were plated onto 96 well flat bottom plates at a cell density of 5 10^5 cells/ml with GM-CSF and oligos were added at a final concentration of 100nM and then kept in culture. On day 3, IL-13 was added or not with a renewal dose of GM-CSF, and 24h later RNA was collected and subjected to analysis.

RESULTS

MiR-155 directly targets IL13Rα1.

By performing bioinformatic analysis (miRanda, RNAHybrid, PITA algorithm) IL13Rα1 was found to have two putative binding sites for miR-155 in the 3'UTR and hence, was predicted to be a direct target for miR-155 (Fig.1). Both miR-155-IL13RA1-3'UTR pairs are shown in supplement Fig. S1 and their free energy is within the range of validated miRNA-target pairs (32). Site 1 is located between nucleotides 1049 and 1071 of the 3'UTR (seeding region is a 7mer) and site 2 between nucleotides 1399 and 1424 (seeding region is an 8mer that includes a G:U wobble pair). The direct targeting by miR-155 of IL13Rα1, a component of the Type II IL-4 receptor, could provide a crucial link between miR-155 and its role as "pro-Th_1 microRNA": by reducing signaling via the Type II IL-4 receptor miR-155 would reduce the ability of a cell to respond to the classical pro-Th_2 cytokines IL-4 and IL-13. In order to test IL13Rα1 as a direct target for miR-155 we employed a dual luciferase assay in HeLa cells. For this purpose the 3'UTR sequence of IL13Rα1 harbouring the predicted binding sites for miR-155 was cloned into the renilla-luciferase reporter vector pRLTK (named pRLTK_WT_3'UTR_IL13RA1). To test the contribution of the predicted binding sites for miR-155 action, each site was mutated by site directed mutagenesis. Mutations (shown in Fig.1) were designed according to the predicted abrogation of miR-155 binding using bioinformatics (RNAHybrid). The constructs were named pRLTK_MUT1_3'UTR_IL13RA1 (mutant in site 1) and pRLTK_MUT2_3'UTR_IL13RA1 (mutant in site 2). Co-transfection of each renilla-luciferase construct with an expression vector for miR-155 (pCDNA BIC) allowed determination of the effects of this microRNA on the 3'UTR of IL13Rα1 as well as mapping its binding. When miR-155 was co transfected with the reporter construct that harboured the wild type 3'UTR of IL13Rα1 (WT in Fig.1), the expression of the renilla-luciferase construct was reduced to less than 50% of its activity. When the putative sites for miR-155 binding were mutated individually, both mutants failed to be regulated by miR-155 (MUT1 and MUT2 in Fig.1). Thus, it was concluded that miR-155 directly targets IL13Rα1 and that it binds to the 3'UTR of IL13Rα1 in positions 1049-1071 and 1399-1424, and that both sites are necessary for miRNA action.

MiR-155 regulates the expression of IL13Rα 1 in human monocytes.

Having established that miR-155 directly targets the IL13Rα1 3'UTR, we aimed to determine the effects of miR-155 on the expression of this receptor chain in human monocytes. It is known that miR-155 is up regulated by several pro-Th_1 factors during the inflammatory response and that it plays a role in the Th_1 response in different cell types such as dendritic cells (25,26) and macrophages (21,27). We wondered whether miR-155 could modulate the M2/alternative activation of macrophages by decreasing IL13Rα1 expression. This would also suggest a role for miR-155 in the differentiation of a classically activated pro-Th_1 macrophage. For this purpose, we chose a previously established and validated monocytic cell line, THP1-155 (26). The THP1-155 cell line is a doubly transduced cell line in which a miR-155 transgene is under the control of a Tet-On response element, a regulatory system described elsewhere (31). Thus, miR-155 expression can be induced upon addition of tetracycline or a derivative, doxycycline. This system allows miR-155 up-regulation to be isolated from other events that are also triggered by inflammatory stimuli (e.g. LPS) that lead to

Downloaded from www.jbc.org at University of Southampton Libraries, on December 17, 2010

miR-155 over expression (21). In this cellular system we could determine whether increased levels of miR-155 have an effect on the expression of IL13Rα1 both at the protein and mRNA levels. Cells were treated with doxycycline for 96 h allowing miR-155 over expression to occur. Cells were collected at 24h intervals during the course of the treatment, for RNA and protein analysis. Mir-155 expression was checked by qPCR and showed a 3.5 fold increase (Fig.S4). MiR-155 effects on IL13Rα1 expression were examined at the protein level by Western blotting protein extracts (Fig 2A). The protein levels of IL13Rα1 (lower band) were down-regulated in parallel with the up-regulation observed for miR-155. Densitometric analysis determined that IL13Rα1 protein levels were reduced to 4% when cell extracts were compared at time 96 hrs and 0 hrs of treatment (Fig.2A). We also determined mRNA levels for IL13Rα1 by RT-qPCR and found that the levels did not vary significantly during the course of the treatment (Fig.2B).

Altogether, these findings show that miR-155 regulates the expression of IL13Rα1 in human monocytes. Up-regulation of MiR-155 led to a down-regulation of IL13Rα1 at the protein level whilst its mRNA levels remained stable. These findings suggest that miR-155 is acting by blocking the translation of IL13Rα1 mRNA rather than promoting its degradation in THP1-155 cells. These results, together with the molecular link previously shown between the 3'UTR of IL13Rα1 and miR-155, prove that IL13Rα1 is a direct target for miR-155 in human monocytes.

MiR-155 reduces the IL13 and IL-4-dependent phosphorylation of STAT-6.

Having shown that miR-155 directly targets IL13Rα1 in monocytes (Figs. 1 and 2) we expected that the miR-155 dependent reduction of IL13Rα1 would impair the ability of macrophages to respond to IL-13 and IL-4. Both cytokines bind to the Type II IL-4 receptor, composed of heterodimers of IL13Rα1 and IL4Rα, but only IL-4 can bind to Type I receptors (12). Upon binding to the Type II receptor, IL-4 and IL-13 initiate a signaling cascade that causes phosphorylation and activation of STAT6 which is then able to perform its transcriptional roles (13) . An impaired response to IL-13 and IL-4, cytokines that promote M2/alternative activation in macrophages, would bias the macrophages towards a more M1/classical activation. Hence, we predicted that by down-regulating the levels of IL13Rα1 miR-155 would modulate the downstream signaling cascade and reduce STAT6 phosphorylation.

In order to test the effects of miR-155 levels on STAT6 phosphorylation we used THP1-155 cells, in which miR-155 over-expression can be induced upon the addition of doxycycline. Moreover, STAT6 phosphorylation can be seen as an indicator of the status of the Th_2 pathway (13). THP-1-155 cells were treated (+Doxy) or not (- Doxy) with doxycycline for 5 days to allow miR-155 over-expression. Cells were then starved over night before stimulation with IL-13 (10ng/ml) or IL-4 (250U/ml). When miR-155 was up-regulated (+Doxy), IL-4 and IL-13-induced STAT6 phosphorylation was reduced below basal levels (- Doxy). In the case of IL-13 stimulation, the reduction in phospho-STAT6 levels was more pronounced (41% remaining) than in the case of IL-4 (67% phospho-STAT6 remaining). These data point to a more pronounced inhibitory effect by miR-155 on the IL-13 pathway than on the IL-4 one. This could be due to signaling from the Type I IL4 receptor in the case of IL-4, as IL-13-dependent STAT6 phosphorylation depends solely on its binding to IL13Rα1 (12). We therefore aimed to dissect the role of miR-155 on IL-13 signaling through STAT6 phosphorylation, as it relies on the presence of the direct target of miR-155 IL13Rα1.

We then assayed the duration and timing of the effects of miR-155 on IL-13 dependent STAT6 signaling. For this purpose, THP1-155 cells were treated or not with doxycycline over 96h, respectively allowing (or not) miR-155 over-expression to occur. After this, cells were starved over night before stimulation with IL-13. Cells were collected and lysed 30min, 1h and 2h post IL-13 stimulation, and protein extracts subjected to Western blotting in order to detect the course of STAT6 phosphorylation.

In cells with basal levels of miR-155 (- Doxy), IL-13-induced STAT6 phosphorylation reached a peak after 30 min and decreased over the course of 2h, (Fig 3B, upper panel). In cells over-expressing miR-155 (+ Doxy) STAT6 phosphorylation was reduced when compared to non-over-expressing cells (- Doxy), confirming the results shown in

Downloaded from www.jbc.org at University of Southampton Libraries, on December 17, 2010

Fig.3A. . Quantification of P-STAT6/β-Tubulin (Fig 3B, lower panel) showed that the peak of STAT6 phosphorylation was abrogated when miR-155 was over-expressed (+ Doxy) To determine whether this effect could reflect a direct targeting of STAT6 by miR-155, we analysed the levels of total STAT6 protein in Western blots of the same cell extracts. STAT6 protein levels were not affected by over-expression of miR-155 (Fig 3C); therefore, miR-155 is acting at an upstream step of the IL-13 signaling pathway, most likely by targeting IL13Rα1 as shown in Figs. 1 and 2. Our results suggest that miR-155 is reducing the STAT6 dependent alternative activation of macrophages.

MiR-155 regulates IL13Rα1 and STAT6 phosphorylation in human macrophages.

Having shown that miR-155 directly targets IL13Rα1 and that up-regulation of miR-155 in THP1-155 cells reduces the expression of IL13Rα1 with diminished downstream phosphorylation of STAT6, we next investigated in a "reverse" model whether down-regulation of miR-155 would increase IL13Rα1 levels and STAT6 activation in human primary macrophages. Human macrophages were transfected with either specific anti-miR-155 oligonucleotides or a negative control. Three days after transfection, cells were treated (or not) with IL-13 and collected after 2 hrs. Prior to this treatment, a group of cells was collected in order to determine expression of miR-155. Figure S9 shows that miR-155 was effectively knocked down. Cell lysates collected after 2hrs of treatment were subjected to Western blot detection in order to determine the levels of IL13Rα1 protein. Down-regulation of miR-155 resulted in increased expression of IL13Rα1 protein, both in IL-13 treated or unstimulated cells (Fig 4A), thus confirming that miR-155 regulates IL13Rα1 in primary macrophages. The presence of phospho-STAT6 was also assessed in Western blots of cell lysates. As expected, the IL-13 dependent phosphorylation of STAT6 was affected by miR-155 levels (Fig.4B); when miR-155 was blocked (anti-miR-155) the phosphorylated and active form of STAT6 showed a 2.7 fold increase compared to cells transfected with anti-miR-control. Interestingly, the levels of mRNA of IL13Rα1 remained constant (Fig.4C) suggesting that miR-155 targeting effects are due to the blocking of translation of IL13Rα1 mRNA into protein. These data show that miR-155 down-regulates the levels of IL13Rα1 in human macrophages, thereby reducing the phosphorylation of STAT6.

MiR-155 regulates the IL-13 cascade in human macrophages.

Importantly, IL13Rα1 is not only a key component in the IL-13 cascade but is also a marker for alternative activation of macrophages (2), suggesting a possible role for miR-155 in the "M type" or "Th" profile of these cells. MiR-155 has been shown to play an important role in the inflammatory profile of macrophages (21) and it is known that STAT6 is the main mediator in the Th_2 signaling cascade triggered by IL-13 (13). Our results show that miR-155 directly targets IL13Rα1 (Fig.1); that the levels of miR-155 regulate the expression of IL13Rα1 in macrophages (Figs. 2 and 4) with consequent effects on the phosphorylation of STAT6 (Figs. 3 & 4). We next aimed to test the influence of miR-155 levels on the transcriptional profile of macrophages stimulated with IL-13, i.e. M2 or alternatively activated macrophages (2).

Human primary monocytes were transfected with specific anti-miR-155 inhibitors or control anti-miR oligonucleotides. Three days post transfection cells were stimulated or not with IL-13 for 24h, lysed and RNA extracted and analyzed by RT-qPCR. Based on our previous results, we hypothesized that reducing the levels of miR-155 would lead to an increase in the IL-13 dependent expression of several target genes in the IL-13 cascade. To test this, we determined the expression of genes known to be involved in the STAT6 cascade and/or alternative activation of macrophages (2,13). Stimulation with IL-13 increased the levels of expression of SOCS1, DC-SIGN, CCL18, CD23 and SERPINE (Fig. 5A). This occurred both in cells transfected with control anti-miR and active anti-miR-155 although, as expected, the up-regulation was significantly greater in the cells in which miR-155 was knocked down (Fig.5). MiR-155 levels did not seem to affect significantly the basal expression of these genes with the exception of DC-SIGN and SERPINE. We also assayed other genes that showed no statistical difference, including TGFβ1and IL-10. (Fig.5B). Thus, we can

Downloaded from www.jbc.org at University of Southampton Libraries, on December 17, 2010

conclude that microRNA 155 directly targets IL13Rα1 in human macrophages, that it has an effect on the activation of STAT6 and that miR-155 levels play a key role in the IL-13 pathway, contributing to the expression profile and activation of macrophages.

DISCUSSION

In this work we have shown that microRNA-155 modulates the response of human macrophages to IL-13, a crucial cytokine in the programming of Th_2 responses (8), and we have shown that miR-155 regulates the IL-13 dependent expression profile of these cells. We also provide evidence regarding the mechanism underlying this role, showing that miR-155 directly targets IL13Rα1, a key component of the Type II IL-4 receptor (11). In order to study the role of miR-155 in the immune profile of monocytes/macrophages we used a previously generated cell line, THP1-155 cells (26) and primary human macrophages in which we blocked miR-155 expression. Thus, our study provides a molecular mechanism by which miR-155 regulates the response of human macrophages to IL-13.

From our bioinformatic analysis (miRanda, RNAHybrid, PITA algorithm) IL13Rα1 was predicted as a putative target of miR-155, with two binding sites mapped at positions 1049 –site 1- and 1399 –site2- in the 3'UTR of IL13Rα1 mRNA. To determine the role of these potential binding sites, we used a renilla luciferase reporter assay to show that miR-155 directly targets the 3'UTR of IL13Rα1 (Fig.1). Interestingly, both binding sites contributed to the inhibitory role of miR-155, since when either site was mutated the effect of mir-155 was almost completely abrogated. Both miRNA-target pairs present free energy values (S1) just below the -20 Kcal/mol cut-off suggested by Watanabe *et al* (32), and above other strong target sites for miR-155 studied by us (PU.1 and SMAD2, approx -26 Kcal/mol, (26) and manuscript under revision). Additionally, both sites are conserved across several species (Supplement Figs. S2 and S3) although the conservation is not as wide as in the previously mentioned examples PU.1 and SMAD2. Thus, this relatively weaker binding regions could explain why miR-155 needs both site 1 and site 2 intact in order to block expression of IL13Rα1 and points towards a possible co-operation between both sites, which has also been suggested to lead to translational repression of the target gene rather than mRNA degradation (33,34).

We next performed a series of experiments in a cell model, THP1-155 that allows experimental augmentation of miR-155 levels without use of inflammatory stimuli (such as LPS) that could affect other pathways (21). It was shown that miR-155 up-regulation led to a decrease of IL13Rα1 at the protein level, while its mRNA levels remained stable (Figs.2A and B). This suggested that miR-155 could be blocking the translation of IL13Rα1 mRNA in these cells.

We next aimed to establish the role of miR-155 in the IL-13 signaling pathway by determining the activation of STAT6. STAT6 is the main mediator in the IL-13/IL-4 signaling pathway, becoming phosphorylated and active upon stimulation with these cytokines (12). The over-expression of Mir-155 in THP1-155 led to diminished STAT6 phosphorylation without affecting total STAT6 protein levels (Figs.3A, B and C). Both IL-4 and IL-13 signaling cascades seemed to be affected, which can be explained by the fact that both cytokines share and can signal through the Type II IL-4 receptor, which consists of dimers of IL4Rα and IL13Rα1. Importantly, only IL-4 can also signal through the Type I IL-4 receptor, while IL-13 requires the presence of IL13Rα1 in order to exert its effects. The specific dependence on IL13Rα1 of the IL-13 pathway could explain the observation that IL-13 signaling appeared to be more affected than that induced by IL-4 (Fig.3A). After this experimental observation, we decided to focus on the effect of miR-155 on IL-13 signaling.

Having investigated the effects of mir-155 in the first series of experiments by augmenting its expression, we went on to confirm our results with a "reverse" experimental approach in which miR-155 was knocked down by transfection of anti-miR-155 oligonucleotides in human primary macrophages. As expected, the reduction of miR-155 led to an increase in IL13Rα1 protein (Fig.4A) and in the IL-13 dependent phosphorylation of STAT6 (Fig.4B). Since IL-13 triggers a M2 or pro-Th_2 phenotype (8), we next determined the impact of miR-155 on several

Downloaded from www.jbc.org at University of Southampton Libraries, on December 17, 2010

genes that are markers of alternative activation/pro-Th_2 profiling and/or phospho-STAT6 dependent genes (2,13). After reducing the levels of miR-155, IL-13 signaling was increased (Fig.4), so we hypothesized an increase in the IL-13 dependent expression of several target genes in the IL-13 cascade. Amongst the genes assayed when miR-155 was knocked down, SOCS1, DC-SIGN, CCL18, CD23 and SERPINE showed a significant increase in their IL-13 dependent gene expression (Fig. 5). DC-SIGN and SERPINE also showed a decrease in their basal expression levels probably due to a parallel effect of miR-155 on factors that control their expression, such as PU.1 and SMAD2, known to regulate DC-SIGN (35) and SERPINE (36) respectively, and directly targeted by miR-155 (26), Louafi et al. manuscript in revision]. DC-SIGN is a typical marker for alternatively activated macrophages (2) and it is involved in the binding and recognition of pathogens by the immune system. We have previously described the inhibitory effects of miR-155 on DC-SIGN expression in dendritic cells (26). Thus, the increased expression of DC-SIGN when miR-155 is down-regulated (Fig. 5) suggests that miR-155 is probably affecting pathogen binding ability also in macrophages.

Our results showed that miR-155 blockade leads to increased STAT6 signaling. Since STAT6 is a key transcription factor involved in the generation of Th_2 cells it could be supposed that the pro-Th2 biased phenotype of miR-155 deficient mice might involve STAT6 regulation. Moreover, signaling through STAT6 also involves SHIP-1 (12), a repressor of M2 macrophage differentiation, and SHIP-1 has been demonstrated to be a direct target of miR-155 (37). In addition to this, miR-155 was recently reported to be inhibited by IL-10 (22), an anti-inflammatory cytokine that also promotes alternative activation of macrophages (2). Together, all these data suggest a central role for miR-155 in the acquisition and modulation of the M1/M2 and Th_1/Th_2 profiles. By targeting IL13Rα1 and modulating the STAT6 cascade, miR-155 would shift the immune profile towards a more pro-Th_1 phenotype; thus, the regulation of miR-155 levels is key in order to exert and develop an appropriate and balanced immune response.

This central role seems to be confirmed by the fact that miR-155 affects several genes that are important to the human immune balance. CCL18 is a cytokine associated with Th_2 profiling and that has also been shown to be secreted by Tumor Associated Macrophages (TAMs) (38), macrophages that display an M2-like profile (39); CD23, which binds to IgE complexes promoting an inflammatory response and has been shown to play an important role in allergy and antigen presentation, also being a typical marker of M2 macrophages; SOCS1 a pro-Th_2 protein, that inhibits the Janus kinase/signal transducer, blocking the signaling of proTh_1 stimuli such as LPS (40,41). SOCS1 is reportedly affected by miR-155 by direct targeting (15,23) and our data suggest that miR-155 is also affecting SOCS1 indirectly, by reducing the ability of IL-13 to stimulate SOCS1 gene expression.

Importantly, several of the genes affected by miR-155, CCL18, CD23 and SOCS1, together with IL13, have been shown to play a key role in the pathogenesis of allergy and asthma (9,42,43), characterised by an exacerbated Th_2 profile and lung remodeling, features also shown by miR-155 deficient mice (16). Additionally, miR-155 mediated down-regulation of the IL-13 and TGF-β (Louafi et al. manuscript in revision) dependent regulation of SERPINE underscores the role of miR-155 in pro-fibrotic processes that could also explain the previously mentioned lung remodeling, an important feature in asthma and other lung diseases.

Together, all these data position miR-155 at the heart of immune regulation and with an important role in the pathogenesis of diseases such as asthma, with a pro-fibrotic remodeling component. This is in line with our previous observation that miR-155 can decrease the response of macrophages to TGF-β (Louafi et al. manuscript in revision), which indicated that this microRNA affects not only the immune functions of these cells, but also their role in repair and remodeling. The broad implications of these biological functions position miR-155 as a crucial molecule for the fine tuning of a healthy balance in the immune system and justify future research on the clinical implications that might link miR-155 with several pathologies.

Downloaded from www.jbc.org at University of Southampton Libraries, on December 17, 2010

REFERENCES

1. Mantovani, A., Sica, A., Sozzani, S., Allavena, P., Vecchi, A., and Locati, M. (2004) *Trends in Immunology* **25**, 677-686
2. Martinez, F. O., Helming, L., and Gordon, S. (2009) *Annu Rev Immunol* **27**, 451-483
3. Minty, A., Chalon, P., Derocq, J. M., Dumont, X., Guillemot, J. C., Kaghad, M., Labit, C., Leplatois, P., Liauzun, P., Miloux, B., and et al. (1993) *Nature* **362**, 248-250
4. Hogan, S. P., Mould, A., Kikutani, H., Ramsay, A. J., and Foster, P. S. (1997) *J Clin Invest* **99**, 1329-1339
5. Punnonen, J., Aversa, G., Cocks, B. G., McKenzie, A. N., Menon, S., Zurawski, G., de Waal Malefyt, R., and de Vries, J. E. (1993) *Proc Natl Acad Sci U S A* **90**, 3730-3734
6. Ramalingam, T. R., Pesce, J. T., Sheikh, F., Cheever, A. W., Mentink-Kane, M. M., Wilson, M. S., Stevens, S., Valenzuela, D. M., Murphy, A. J., Yancopoulos, G. D., Urban, J. F., Jr., Donnelly, R. P., and Wynn, T. A. (2008) *Nat Immunol* **9**, 25-33
7. Kolodsick, J. E., Toews, G. B., Jakubzick, C., Hogaboam, C., Moore, T. A., McKenzie, A., Wilke, C. A., Chrisman, C. J., and Moore, B. B. (2004) *J Immunol* **172**, 4068-4076
8. Wynn, T. A. (2003) *Annual Review of Immunology* **21**, 425-456
9. Wills-Karp, M. (2004) *Immunol Rev* **202**, 175-190
10. Fuss, I. J., and Strober, W. *Mucosal Immunol* **1**, S31-S33
11. Hershey, G. K. K. (2003) *Journal of Allergy and Clinical Immunology* **111**, 677-690
12. Jiang, H., Harris, M. B., and Rothman, P. (2000) *J Allergy Clin Immunol* **105**, 1063-1070
13. Hebenstreit, D., Wirnsberger, G., Horejs-Hoeck, J., and Duschl, A. (2006) *Cytokine & Growth Factor Reviews* **17**, 173-188
14. Lee, R. C., Feinbaum, R. L., and Ambros, V. (1993) *Cell* **75**, 843-854
15. Jiang, S., Zhang, H.-W., Lu, M.-H., He, X.-H., Li, Y., Gu, H., Liu, M.-F., and Wang, E.-D. *Cancer Res* **70**, 3119-3127
16. Rodriguez, A., Vigorito, E., Clare, S., Warren, M. V., Couttet, P., Soond, D. R., van Dongen, S., Grocock, R. J., Das, P. P., Miska, E. A., Vetrie, D., Okkenhaug, K., Enright, A. J., Dougan, G., Turner, M., and Bradley, A. (2007) *Science* **316**, 608-611
17. Vigorito, E., Perks, K. L., Abreu-Goodger, C., Bunting, S., Xiang, Z., Kohlhaas, S., Das, P. P., Miska, E. A., Rodriguez, A., Bradley, A., Smith, K. G., Rada, C., Enright, A. J., Toellner, K. M., Maclennan, I. C., and Turner, M. (2007) *Immunity* **27**, 847-859
18. Bartel, D. P. (2004) *Cell* **116**, 281-297
19. Eulalio, A., Huntzinger, E., and Izaurralde, E. (2008) *Cell* **132**, 9-14
20. Filipowicz, W., Bhattacharyya, S. N., and Sonenberg, N. (2008) *Nat Rev Genet* **9**, 102-114
21. O'Connell, R. M., Taganov, K. D., Boldin, M. P., Cheng, G., and Baltimore, D. (2007) *Proc Natl Acad Sci U S A* **104**, 1604-1609
22. McCoy, C. E., Sheedy, F. J., Qualls, J. E., Doyle, S. L., Quinn, S. R., Murray, P. J., and O'Neill, L. A. *J Biol Chem*
23. Lu, L. F., Thai, T. H., Calado, D. P., Chaudhry, A., Kubo, M., Tanaka, K., Loeb, G. B., Lee, H., Yoshimura, A., Rajewsky, K., and Rudensky, A. Y. (2009) *Immunity* **30**, 80-91
24. Thai, T. H., Calado, D. P., Casola, S., Ansel, K. M., Xiao, C., Xue, Y., Murphy, A., Frendewey, D., Valenzuela, D., Kutok, J. L., Schmidt-Supprian, M., Rajewsky, N., Yancopoulos, G., Rao, A., and Rajewsky, K. (2007) *Science* **316**, 604-608
25. Ceppi, M., Pereira, P. M., Dunand-Sauthier, I., Barras, E., Reith, W., Santos, M. A., and Pierre, P. (2009) *Proc Natl Acad Sci U S A* **106**, 2735-2740

Downloaded from www.jbc.org at University of Southampton Libraries, on December 17, 2010

26. Martinez-Nunez, R. T., Louafi, F., Friedmann, P. S., and Sanchez-Elsner, T. (2009) *J Biol Chem* **284**, 16334-16342
27. Worm, J., Stenvang, J., Petri, A., Frederiksen, K. S., Obad, S., Elmen, J., Hedtjarn, M., Straarup, E. M., Hansen, J. B., and Kauppinen, S. (2009) *Nucleic Acids Res* **37**, 5784-5792
28. Betel, D., Wilson, M., Gabow, A., Marks, D. S., and Sander, C. (2008) *Nucl. Acids Res.* **36**, D149-153
29. Rehmsmeier, M., Steffen, P., Hochsmann, M., and Giegerich, R. (2004) *RNA* **10**, 1507-1517
30. Kertesz, M., Iovino, N., Unnerstall, U., Gaul, U., and Segal, E. (2007) *Nat Genet* **39**, 1278-1284
31. Wiznerowicz, M., and Trono, D. (2003) *J Virol* **77**, 8957-8961
32. Watanabe, Y., Yachie, N., Numata, K., Saito, R., Kanai, A., and Tomita, M. (2006) *Gene* **365**, 2-10
33. Doench, J. G., and Sharp, P. A. (2004) *Genes Dev* **18**, 504-511
34. John, B., Enright, A. J., Aravin, A., Tuschl, T., Sander, C., and Marks, D. S. (2004) *PLoS Biol* **2**, e363
35. Dominguez-Soto, A., Puig-Kroger, A., Vega, M. A., and Corbi, A. L. (2005) *J Biol Chem* **280**, 33123-33131
36. Gaspar, N. J., Li, L., Kapoun, A. M., Medicherla, S., Reddy, M., Li, G., O'Young, G., Quon, D., Henson, M., Damm, D. L., Muiru, G. T., Murphy, A., Higgins, L. S., Chakravarty, S., and Wong, D. H. (2007) *Mol Pharmacol* **72**, 152-161
37. O'Connell, R. M., Chaudhuri, A. A., Rao, D. S., and Baltimore, D. (2009) *Proc Natl Acad Sci U S A* **106**, 7113-7118
38. Schutyser, E., Struyf, S., Proost, P., Opdenakker, G., Laureys, G., Verhasselt, B., Peperstraete, L., Van de Putte, I., Saccani, A., Allavena, P., Mantovani, A., and Van Damme, J. (2002) *J Biol Chem* **277**, 24584-24593
39. Mantovani, A., Sozzani, S., Locati, M., Allavena, P., and Sica, A. (2002) *Trends in Immunology* **23**, 549-555
40. Kinjyo, I., Hanada, T., Inagaki-Ohara, K., Mori, H., Aki, D., Ohishi, M., Yoshida, H., Kubo, M., and Yoshimura, A. (2002) *Immunity* **17**, 583-591
41. Nakagawa, R., Naka, T., Tsutsui, H., Fujimoto, M., Kimura, A., Abe, T., Seki, E., Sato, S., Takeuchi, O., Takeda, K., Akira, S., Yamanishi, K., Kawase, I., Nakanishi, K., and Kishimoto, T. (2002) *Immunity* **17**, 677-687
42. de Nadai, P., Charbonnier, A. S., Chenivesse, C., Senechal, S., Fournier, C., Gilet, J., Vorng, H., Chang, Y., Gosset, P., Wallaert, B., Tonnel, A. B., Lassalle, P., and Tsicopoulos, A. (2006) *J Immunol* **176**, 6286-6293
43. Lee, C., Kolesnik, T. B., Caminschi, I., Chakravorty, A., Carter, W., Alexander, W. S., Jones, J., Anderson, G. P., and Nicholson, S. E. (2009) *Clin Exp Allergy* **39**, 897-907

Downloaded from www.jbc.org at University of Southampton Libraries, on December 17, 2010

FOOTNOTES

We would like to thank Professor Peter Friedmann for critical review of the manuscript and for help in the discussion of the results.

1 This work was funded by grant G0801984 awarded to TS-E by the Medical Research Council (MRC). FL was supported by this grant.

Abbreviations used in this paper: UTR, untranslated region; DC-SIGN, dendritic cell-specific intercellular adhesion molecule-3-grabbing non-integrin; IL13Rα1, Interleukin 13 Receptor alpha 1.

Louafi, F, Martinez-Nunez, RT, Sanchez-Elsner, T. *MicroRNA-155 (miR-155) targets SMAD2 and modulates the response of macrophages to transforming growth factor-β (TGF-β).* Currently in revision in The Journal of Biological Chemistry.

Downloaded from www.jbc.org at University of Southampton Libraries, on December 17, 2010

FIGURE LEGENDS

Figure 1. MiR-155 directly targets the 3'UTR of IL13Rα1. HeLa cells were co-transfected with a Renilla luciferase construct harbouring an IL13Rα1 3'UTR fragment containing the predicted binding sites for miR-155 (Wild Type, WT) and either an empty expression vector ("-") or a miR-155 over-expressing vector (miR-155). MUT1 and MUT2 correspond to mutants in each one of the predicted sites, Site 1 and Site 2, respectively. One of three independent experiments is shown. . ns= not significant, * $p \leq 0.05$.

Figure 2. Over-expression of miR-155 reduces the levels of IL13Rα1 protein. THP1-155 cells were treated with doxycycline ("**miR-155**") or not ("**Control**") during the course of 96h to allow miR-155 over expression. Cells were collected in intervals of 24h and subjected to protein and RNA extraction. ***A.*** Cell lysates were subjected to Western blotting for IL13Rα1 protein detection (upper panel, lower band pointed by arrow) and normalised against β-tubulin (lower panel). ***B.*** Total RNA was extracted and mRNA levels of IL13Rα1 were determined by RT-qPCR. Shown is one experiment out of three independent ones. Statistical analysis of Western blots in S5.

Figure 3. Over-expression of miR-155 reduces STAT6 phosphorylation. THP1-155 cells were treated with doxycycline (+) or not (-) during 96h to over-express miR-155. Cells were then starved over night and stimulated with either IL-4 or IL-13 or not stimulated ("Control") and lysed at the indicated times. ***A.*** Analysis of STAT6 phosphorylation (P-STAT6) after 30 min of treatment was performed by Western blotting and normalised against β-tubulin. ***B.*** THP1-155 cells were stimulated with IL-13 or not, and collected after 30 min, 1 hr and 2 hr and subjected to Western Blotting. Lower panel shows % of P-STAT6 in ***B*** plotted against time of treatment as analyzed by densitometry (three independent experiments shown, * $p \leq 0.05$). ***C.*** THP1-155 cells treated or not with Doxycycline for 96 hrs (over-expressing or not miR-155, respectively) were subjected to analysis of total STAT6 content by Western blotting and normalised against β-tubulin expression. Shown is one experiment out of three independent ones. Statistical analysis of Western Blots in S6.

Figure 4. MiR-155 down-regulation increases IL13Rα1 protein expression and STAT6 phosphorylation. In a "reverse" model in human macrophages, cells were transfected with blocking oligonucleotides against miR-155 (Anti-155) or a negative control (Control). On day 3 of culture macrophages were stimulated with IL-13 or not and collected after 30 min. ***A*** Cell lysates were subjected to Western blotting in order to detect IL13Rα1 normalised against β-tubulin. ***B*** Cells lysates were used to determine P-STAT6 levels normalising against β-tubulin. ***C*** RNA was extracted from the same collected cells and mRNA of IL13Rα1 was determined by RT-qPCR. One of three independent experiments is shown. ns= not significant. Shown is one experiment out of three independent ones. Statistical analysis of Western blots in S7 and S8.

Figure 5. Down-regulation of miR-155 increases the transcription of several STAT6/IL-13-dependent genes. Human macrophages were transfected with Anti-miR-155 oligonucleotides (Anti-155) or a negative control (Control). On day 3 of culture cells were stimulated with or without IL-13 and collected 24h post stimulation to analyze mRNA expression by RT-qPCR analysis. The genes assayed were grouped in ***A*** Genes dependent on the IL-13/STAT6 signaling: CCL18, SOCS1, CD23, SERPINE and DC-SIGN and ***B***, genes not affected by IL-13 treatment: TGFB1 IL-10. One of three independent experiments is shown. ns= not significant, * $p \leq 0.05$, ** $p \leq 0.01$.

Downloaded from www.jbc.org at University of Southampton Libraries, on December 17, 2010

Figure 1

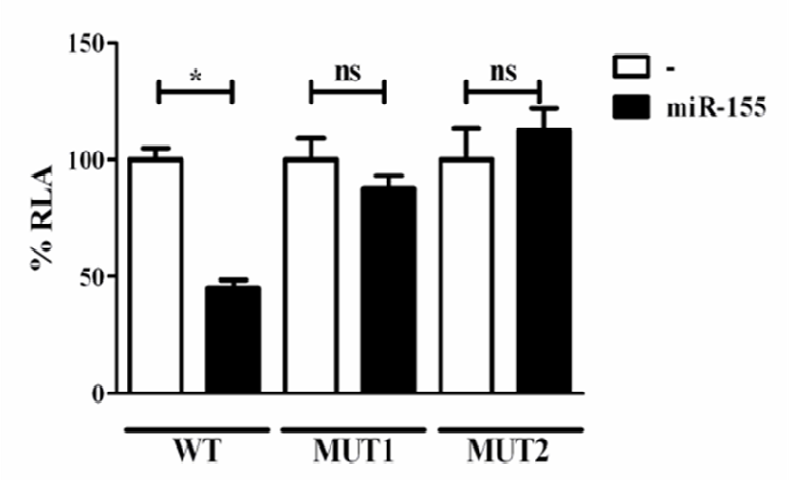

Site 1

```
          3' UGGGGAUAGU--GCUAAUCGUAAuu 5' hsa-miR-155
             |||:||: :|  | | |||||||
1049:5' ACCUCUGCUACUCAAGUAGCAUUua 3' WT IL13RA1

          3' UGGGGAUAGU--GCUAAUCGUAAuu 5' hsa-miR-155
             |||:||: :|  | | | |
1049:5' ACCUCUGCUACUCAAGUCGGUACCa 3' MUT1 IL13RA1
```

Site 2

```
          3' uGGGGAUAGUGCUAA---UCGUAAUU 5' hsa-miR-155
              :|| |:| | |:||   |||||:|
1399:5' uUCCAUGUGAGGGUUUUCAGCAUUGA 3' WT IL13RA1

          3' uGGGGAUAGUGCUAA---UCGUAAUU 5' hsa-miR-155
              :|| |:| | |:||   ||    :|
1399:5' uUCCAUGUGAGGGUUUUCAGGGCCGA 3' MUT2 IL13RA1
```

Downloaded from www.jbc.org at University of Southampton Libraries, on December 17, 2010

Figure 2

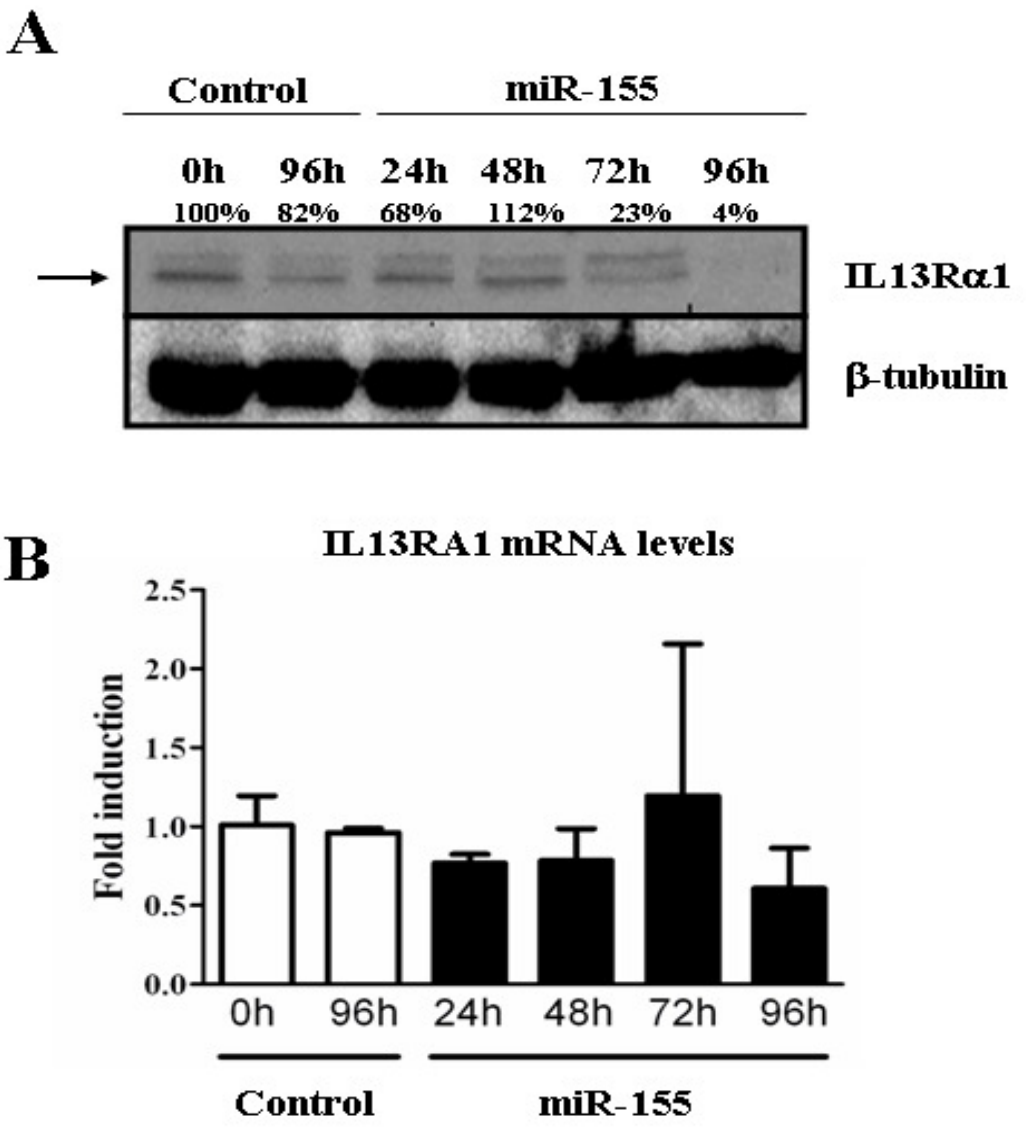

Downloaded from www.jbc.org at University of Southampton Libraries, on December 17, 2010

Figure 3

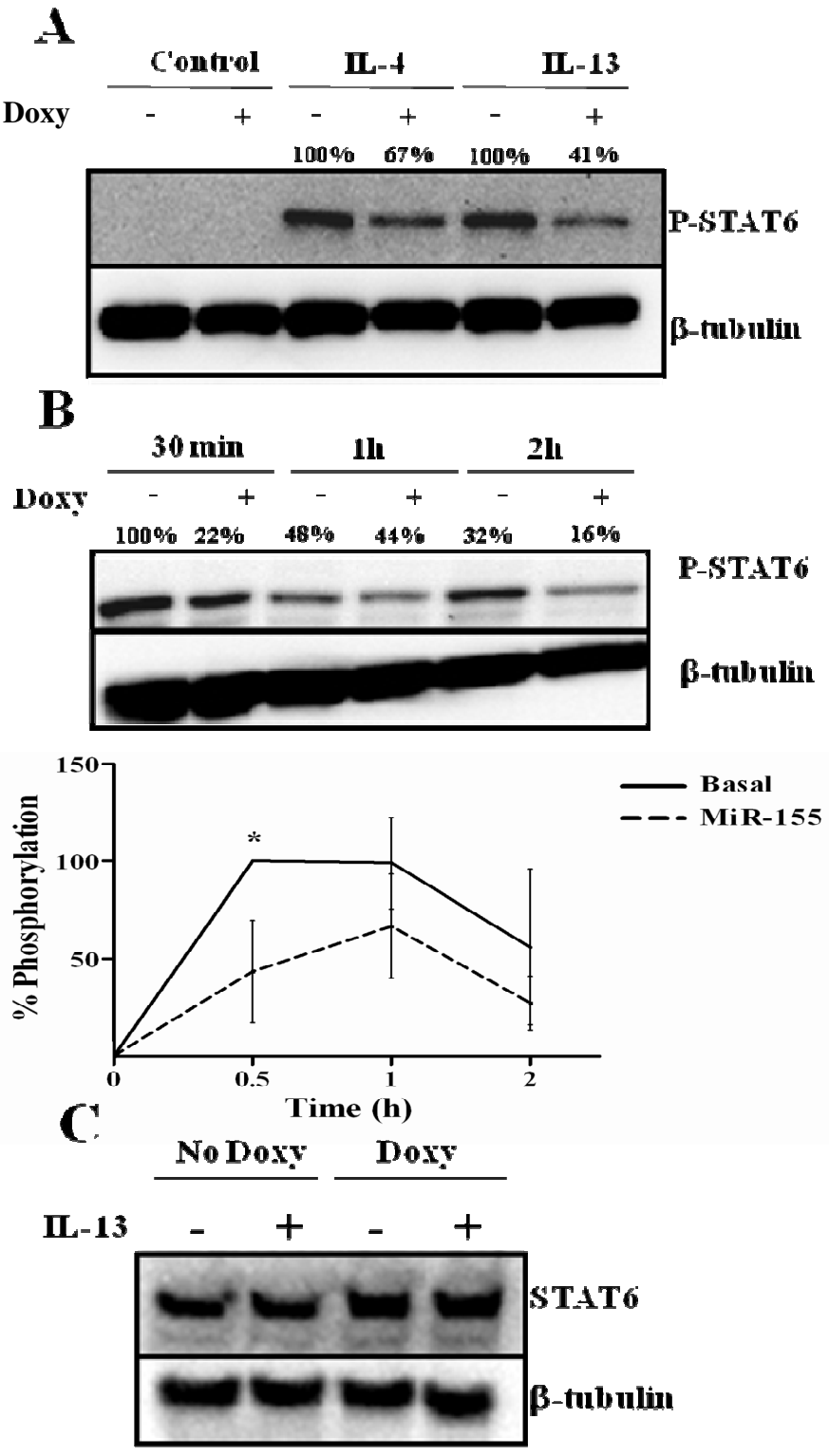

Downloaded from www.jbc.org at University of Southampton Libraries, on December 17, 2010

Figure 4

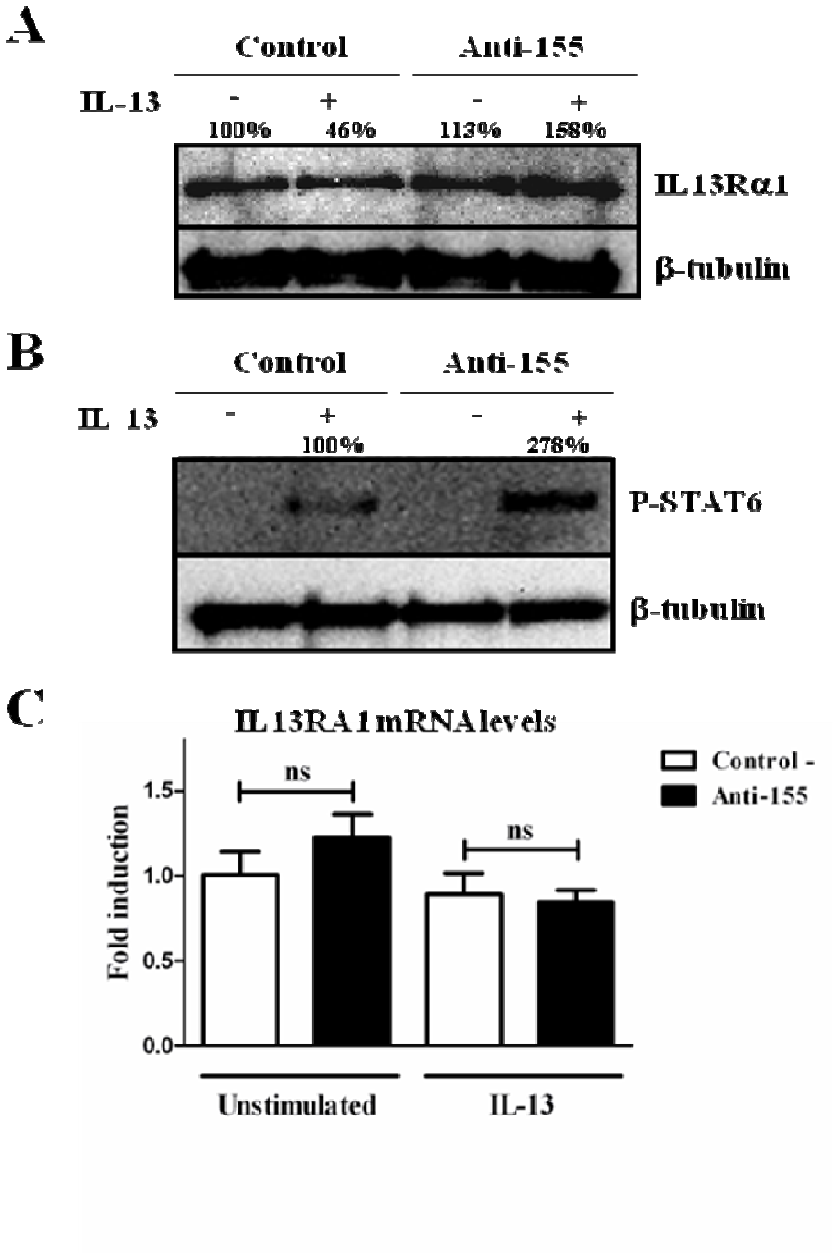

Downloaded from www.jbc.org at University of Southampton Libraries, on December 17, 2010

Figure 5

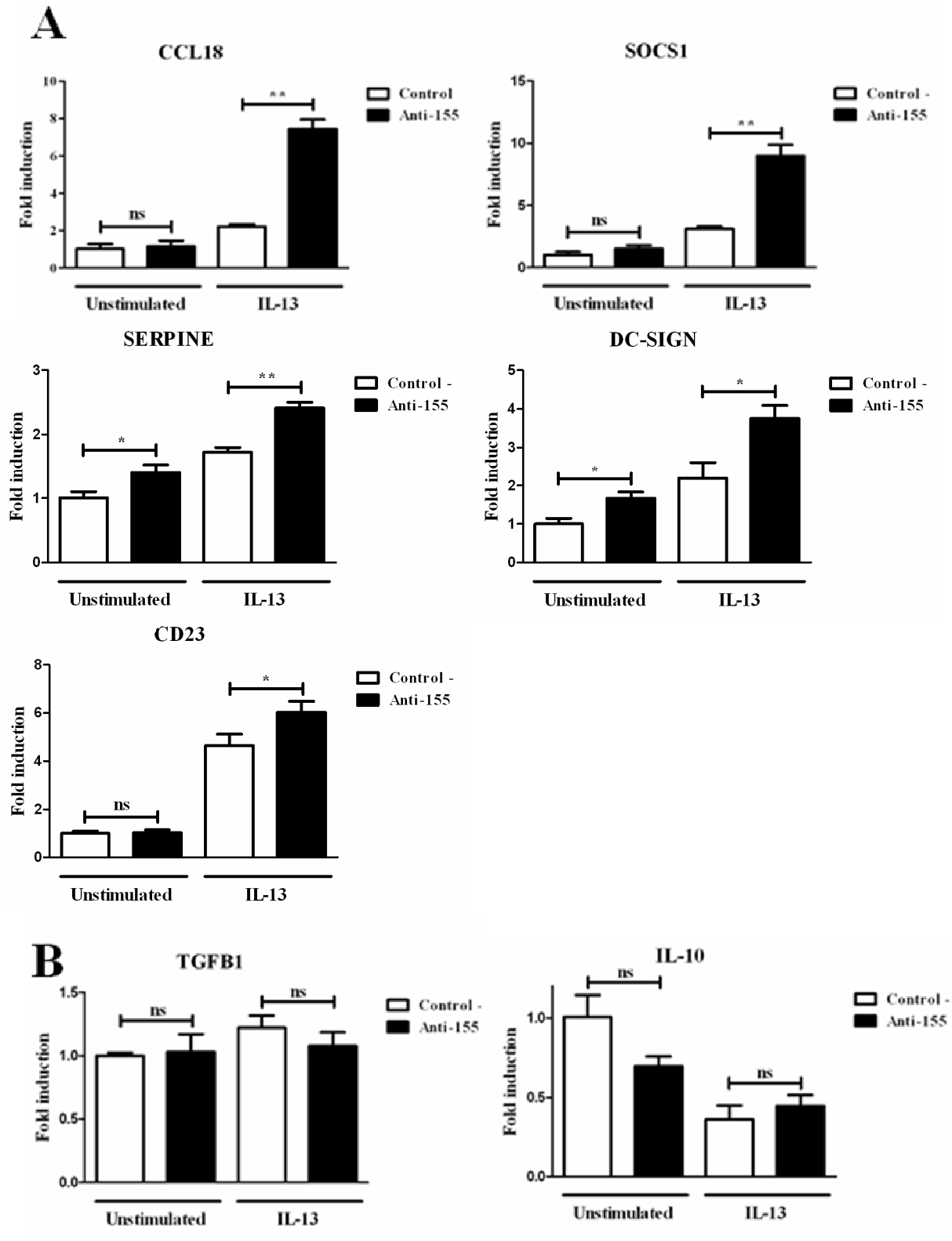

Downloaded from www.jbc.org at University of Southampton Libraries, on December 17, 2010